

---

Single cell biology of typhoidal *Salmonella*:  
heterogeneity of intracellular *Salmonella*  
and the unique cytosolic lifestyle  
of *S. Paratyphi A*

---

DISSERTATION

zur Erlangung des Grades  
„**Doctor rerum naturalium**“  
(**Dr. rer. nat.**)

des Fachbereichs Biologie/Chemie  
der Universität Osnabrück

vorgelegt von

**Felix Scharte**

aus Harsewinkel

Osnabrück, Juli 2022



Hauptberichterstatter:

Prof. Dr. Michael Hensel  
Universität Osnabrück  
Fachbereich Biologie/Chemie  
Abteilung Mikrobiologie  
CellNanOs - Center of Cellular Nanoanalytics Osnabrück

2. Berichterstatter:

Prof. Dr. Guntram Graßl  
Medizinische Hochschule Hannover  
Institut für Medizinische Mikrobiologie und Krankenhaushygiene  
Deutsches Zentrum für Infektionsforschung

Weitere Mitglieder der  
Prüfungskommission:

Prof. Dr. Joost Holthuis  
Universität Osnabrück  
Fachbereich Biologie/Chemie  
Abteilung Molekulare Zellbiologie  
CellNanOs - Center of Cellular Nanoanalytics Osnabrück

Dr. Rainer Kurre  
Universität Osnabrück  
Fachbereich Biologie/Chemie  
iBiOs - Integrated Bioimaging Facility Osnabrück  
CellNanOs - Center of Cellular Nanoanalytics Osnabrück



## Table of Contents

<b><u>I. Abstract .....</u></b>	<b><u>1</u></b>
<b><u>II. Zusammenfassung.....</u></b>	<b><u>2</u></b>
<b><u>III. Introduction .....</u></b>	<b><u>3</u></b>
<b>III.1. <i>Salmonella enterica</i> .....</b>	<b>3</b>
III.1.1. Pathogenesis of <i>Salmonella enterica</i> .....	3
III.1.2. Invasion: Breaking the barrier.....	4
III.1.3. Intracellular lifestyle: The life within.....	6
<b>III.2. Typhoidal <i>Salmonella</i> .....</b>	<b>9</b>
III.2.1. Adapted armory: Genetic equipment of typhoidal <i>Salmonella</i> .....	11
III.2.2. Host specificity & limitations of model systems.....	13
<b>III.3. Organoids, a game changer in life sciences? .....</b>	<b>13</b>
III.3.1. Organoids in infection biology research .....	13
<b>III.4. From vacuole to cytosol: Lifestyles of intracellular pathogens .....</b>	<b>15</b>
III.4.1. How pathogenic bacteria manipulate their host .....	15
<b><u>IV. Aims of this work.....</u></b>	<b><u>19</u></b>
<b><u>V. Results and Publications.....</u></b>	<b><u>20</u></b>
<b>V.1. Single cell analyses reveal distinct adaptation of typhoidal and non-typhoidal <i>Salmonella enterica</i> serovars to intracellular lifestyle.....</b>	<b>20</b>
<b>V.2. Intracellular <i>Salmonella</i> Paratyphi A is motile and differs in the expression of flagella-chemotaxis, SPI-1 and carbon utilization pathways in comparison to intracellular <i>S. Typhimurium</i>.....</b>	<b>49</b>
<b>V.3. Ca<sup>2+</sup>-activated sphingomyelin scrambling and turnover mediate ESCRT-independent lysosomal repair.....</b>	<b>85</b>
<b>V.4. From vacuole to cytosol – Disruptive invasion triggers cytosolic release of <i>Salmonella</i> Paratyphi A and subsequent cytosolic motility favors evasion of xenophagy.....</b>	<b>102</b>
<b>V.5. Establishment of a novel infection model for <i>Salmonella</i> adhesion and invasion - human intestinal organoids .....</b>	<b>138</b>
<b>V.6. Contributions of co-authors .....</b>	<b>193</b>

<b><u>VI.</u></b>	<b><u>Discussion.....</u></b>	<b><u>195</u></b>
<b>VI.1.</b>	<b>Differences in typhoidal and non-typhoidal <i>Salmonella</i> infection .....</b>	<b>196</b>
VI.1.1.	Deploying the needle – Role of SPI2-T3SS in typhoidal <i>Salmonella</i> .....	196
VI.1.2.	Choosing the right equipment –Host-restriction factors in typhoidal <i>Salmonella</i> .....	198
VI.1.3.	Regulation is key – Transcriptional adaptation to host environment .....	199
VI.1.4.	The many-faced pathogen – Intracellular heterogeneity of SPA .....	201
VI.1.5.	Catch me if you can – Xenophagic escape of cytosolic motile SPA.....	204
<b>VI.2.</b>	<b>Organoids – Biology’s next top model?.....</b>	<b>205</b>
<b>VI.3.</b>	<b>Concluding remarks.....</b>	<b>207</b>
<b><u>VII.</u></b>	<b><u>References .....</u></b>	<b><u>210</u></b>
<b><u>VIII.</u></b>	<b><u>List of Abbreviations .....</u></b>	<b><u>225</u></b>
<b><u>IX.</u></b>	<b><u>List of Publications.....</u></b>	<b><u>229</u></b>
<b><u>X.</u></b>	<b><u>Curriculum Vitae .....</u></b>	<b><u>230</u></b>
<b><u>XI.</u></b>	<b><u>Danksagung .....</u></b>	<b><u>233</u></b>
<b><u>XII.</u></b>	<b><u>Erklärung über die Eigenständigkeit der erbrachten wissenschaftlichen Leistungen.....</u></b>	<b><u>234</u></b>
<b><u>XIII.</u></b>	<b><u>Supplementary Information on DVD.....</u></b>	<b><u>235</u></b>

## I. Abstract

*Salmonella enterica* is a common foodborne, facultative intracellular enteropathogen. The typhoidal *S. enterica* serovars Paratyphi A (SPA) and Typhi (STY) are human-restricted, and cause severe systemic diseases, while many *S. enterica* serovars like Typhimurium (STM) have a broad host range and in human hosts usually lead to self-limiting gastroenteritis. There are key differences between typhoidal (TS) and non-typhoidal (NTS) *Salmonella* in pathogenesis, but research on TS is challenging due to host restriction. Since STM causes a typhoid-like disease in mice, it was widely used as model organism to mimic human TS infection. Although results gained by research on STM could provide major insights in *Salmonella* virulence in general, the specific virulence mechanisms of TS are far from being understood.

Both TS and NTS are able to invade mammalian cells and to replicate within host cells, including epithelial cells and macrophages. After invasion or phagocytic uptake, *Salmonella* resides in a membrane-bound compartment, the *Salmonella*-containing vacuole (SCV). The subsequent intracellular lifestyle is dependent on the translocation of effector proteins via a type 3 secretion system (T3SS) which is encoded by genes on *Salmonella* pathogenicity island 2 (SPI2). During the intracellular lifestyle, vesicular compartments of host cells are manipulated by effector proteins of the SPI2-T3SS and *Salmonella*-induced filaments (SIF) are formed. It is currently unknown if observations regarding the molecular pathogenesis made for STM are applicable to TS serovars SPA and STY.

In this work, the intracellular lifestyles of TS were investigated on single cell level. Analyses of intracellular activities of STY and SPA in various host cells showed that STY and SPA deploy SPI2-T3SS to actively manipulate their host cells, but with far lower frequency than STM. A role of SPI2-T3SS for proliferation of STY and SPA in epithelial cells was observed, but not for survival or proliferation in phagocytic host cells. Reduced intracellular activities and pronounced SCV integrity of STY and SPA might contribute to the stealth strategy of STY and SPA, facilitating systemic spread and persistence. Furthermore, by analyses of intracellular transcriptomic architecture during human epithelial cell infection of SPA and STM, different gene expression patterns in key virulence and metabolic pathways were identified. Elevated expression of SPI1 and flagella-chemotaxis genes by intracellular SPA results in cytosolic, flagella-mediated motility and increased invasiveness of SPA. Distinct gene expression patterns of carbon utilization pathways, flagella-chemotaxis and SPI1 genes might contribute to the invasive and systemic disease developed following SPA infection in humans. Live cell imaging revealed that SPA invades host cells in a cooperative manner with multiple bacteria per invasion site, leading to error-prone macropinocytosis with increased membrane damage of the early SCV. After release into the cytosol, motile bacteria showed reduced autophagosomal capture.

The results provide new insights into the virulence profile of STY and SPA by unravelling previously unknown intracellular phenotypes and virulence traits. The established 3D and 2D intestinal organoid models offer new tools for analyses of human-restricted pathogens in a more *in vivo* relevant context.

## II. Zusammenfassung

*Salmonella enterica* ist ein weitverbreiteter, fakultativ intrazellulärer Krankheitserreger. Viele *S. enterica* Serovare wie Typhimurium (STM) besitzen ein breites Wirtsspektrum und lösen im Menschen eine selbstlimitierende Gastroenteritis aus. Die typhoidalen *S. enterica* Serovare Paratyphi A (SPA) und Typhi (STY) sind human-spezialisiert und verursachen schwere systemische Erkrankungen. In der Pathogenese gibt es wesentliche Unterschiede zwischen typhoidalen (TS) und nicht-typhoidalen (NTS) Salmonellen, jedoch ist die Erforschung von TS aufgrund der Wirtsbeschränkung schwierig. Da STM Infektionen in Mäusen eine typhusähnliche Erkrankung hervorrufen, wurden diese häufig als Modell für TS Infektion verwendet. Obwohl Ergebnisse aus Studien mit STM wichtige Erkenntnisse über die allgemeine Virulenz von Salmonellen liefern konnten, sind die spezifischen Virulenzmechanismen von TS nicht vollständig geklärt.

Sowohl TS als auch NTS sind in der Lage, in Säugerzellen zu invadieren und sich in Wirtszellen, einschließlich Epithelzellen und Makrophagen, zu vermehren. Nach der Invasion oder phagozytischen Aufnahme befinden sich die Salmonellen in einem membrangebundenen Kompartiment, der *Salmonella*-containing vacuole (SCV). Die anschließende intrazelluläre Lebensweise hängt von der Translokation von Effektorproteinen über ein Typ-3-Sekretionssystem (T3SS) ab, das von Genen auf der *Salmonella*-Pathogenitätsinsel 2 (SPI2) kodiert wird. Während der intrazellulären Lebensweise werden vesikuläre Kompartimente der Wirtszellen durch Effektorproteine des SPI2-T3SS manipuliert und *Salmonella*-induced filaments (SIF) gebildet. Es ist derzeit nicht bekannt, ob die für STM gemachten Beobachtungen zur molekularen Pathogenese auch für die TS-Serovare SPA und STY gelten.

In dieser Arbeit wurden die intrazellulären Lebensweisen von TS auf Einzelzellebene untersucht. Analysen der intrazellulären Aktivitäten von STY und SPA in verschiedenen Wirtszellen zeigten, dass STY und SPA, im Vergleich zu STM, das SPI2-T3SS seltener einsetzen, um ihre Wirtszellen aktiv zu manipulieren. Es wurde eine Rolle des SPI2-T3SS für das Überleben und die Proliferation von STY und SPA in Epithelzellen, jedoch nicht in phagozytischen Wirtszellen beobachtet. Darüber hinaus wurden durch Transkriptomanalysen während der Infektion menschlicher Epithelzellen mit SPA und STM, unterschiedliche Genexpressionsmuster in wichtigen Virulenz- und Stoffwechselwegen identifiziert. Eine erhöhte Expression von SPI1-, sowie Flagellen- und Chemotaxis-Genen durch intrazelluläre SPA führt zu erhöhter Invasivität und flagellenvermittelter Motilität im Zytosol. Lebendzellmikroskopie zeigte, dass SPA kooperativ in Wirtszellen eindringt, was zu einer fehleranfälligen Makropinozytose mit erhöhter Membranschädigung der frühen SCV führt. Nach der Freisetzung in das Zytosol wiesen die beweglichen Bakterien eine reduzierte Dekoration mit autophagosomalen Markern auf.

Die Ergebnisse dieser Arbeit geben neue Einblicke in das Virulenzprofil von STY und SPA, indem sie bisher unbekannte intrazelluläre Phänotypen und Virulenzmerkmale entschlüsseln. Die etablierten 3D- und 2D-Intestinalorganoid-Modelle bieten neue Möglichkeiten für die Analyse, von auf den Menschen beschränkten Krankheitserregern, in einem *in vivo* relevanten Kontext.



### III. Introduction

Infectious diseases caused by organisms such as fungi, parasites, bacteria or viruses are a major health concern around the world. After cardiovascular diseases they are the second most common cause of death (WHO, 2008). Infections are often mediated by pathogens which can cause severe diseases with complicated progression or even lethal outcome. Rising infection rates and frequently emerging antimicrobial resistance in pathogenic bacteria are one of the top ten threats to global health issues (WHO, 2014). Antibiotic resistance is often referred to as silent pandemic which threatens our ability to treat common infectious diseases and may take over the number one cause of death globally already in 2050 (Antimicrobial Resistance, 2022). This illustrates the need for a better understanding of pathogenesis to develop strategies to counteract infections or for vaccine development. Many bacterial pathogens cause enteric infections, which are a major cause of disease, predominantly in developing countries. Enteric, diarrhea causing diseases can be severe, especially for infants, elderly, or immunocompromised persons. Approximately half a billion people suffer from diarrheal diseases every year (WHO, 2018a).

#### III.1. *Salmonella enterica*

One of the four most prevalent enteropathogens belongs to the genus *Salmonella* that can cause diseases ranging from self-limiting gastroenteritis to life-threatening systemic infections (typhoid fever) (Johnson *et al.*, 2018). The pathogenic, Gram-negative bacteria are rod-shaped and live facultative anaerobic. There are over 2,600 serovars within the species *Salmonella enterica* (*S. enterica*) which can be highly human adapted like *S. enterica* serovar Typhi (STY) or *S. enterica* serovar Paratyphi A (SPA), or with a broad host range like *S. enterica* serovar Typhimurium (STM) (Pui, 2011). *S. enterica* developed sophisticated strategies to invade mammalian host cells, and to survive and replicate within host cells (Haraga *et al.*, 2008). However, these host-pathogen interactions are still not understood in detail and further research with appropriate model systems is required.

##### III.1.1. Pathogenesis of *Salmonella enterica*

Infections with *Salmonella* are initiated by consumption of contaminated food or water. Once the bacteria reach the gastrointestinal tract, they are able to cross the epithelial barrier of the intestine, mainly through microfold-cells (M-cells) (Jepson and Clark, 2001). The invasion of and the subsequent intracellular lifestyle in epithelial cells and cells of the immune system are major characteristics of *Salmonella*. The pathogenesis is thereby mediated by virulence genes mainly encoded on *Salmonella* pathogenicity islands (SPI). SPIs are large genetic areas on the chromosome consisting of several virulence associated genes (Gerlach and Hensel, 2007; Hensel, 2004). SPI4 is crucial to initiate first contact and adherence to the brush boarder of polarized epithelial cells (PEC) with the giant adhesin SiiE secreted by the SPI4-encoded type I secretion system (SPI4-T1SS) (Lorkowski *et al.*, 2014; Wong *et al.*, 1998). SPI1 and SPI2 play a major role in efficient invasion of non-phagocytic cells (Mills *et al.*, 1995) and intracellular survival (Shea *et al.*, 1996), respectively. Both encode for type III secretion systems (T3SS)

with associated chaperones and effector proteins. T3SS act as molecular syringes spanning over both inner and outer bacterial membrane and inserting a translocation pore into the hosts membrane for efficient translocation of effector proteins (Galan and Wolf-Watz, 2006).

### III.1.2. Invasion: Breaking the barrier

*Salmonella* establishes initial contact with host cells by adhesive structures as the giant adhesin SiiE, or other adhesins such as fimbriae or flagella (Wagner and Hensel, 2011). While the SPI4-T1SS substrate SiiE is mandatory for invasion of PEC, the function of SPI1-T3SS alone is sufficient to invade non-PEC (Gerlach *et al.*, 2008). During the invasion process, the host actin cytoskeleton is dramatically reorganized to allow internalization of the pathogen in non-phagocytic cells. The process is mediated by translocated effector proteins of the SPI1-T3SS and is referred to as trigger invasion (Figure III.1). The vigorous membrane ruffling and the formation of large macropinosomes also allow non-invasive bacteria to be co-engulfed during the invasion process in a cooperative manner (Lorkowski *et al.*, 2014). Shortly after internalization, membrane ruffling subsides and the actin cytoskeleton restores its initial architecture (Cossart and Sansonetti, 2004) while *Salmonella* resides in nascent *Salmonella*-containing vacuole (SCV), preparing for an intracellular lifestyle (Krieger *et al.*, 2014).

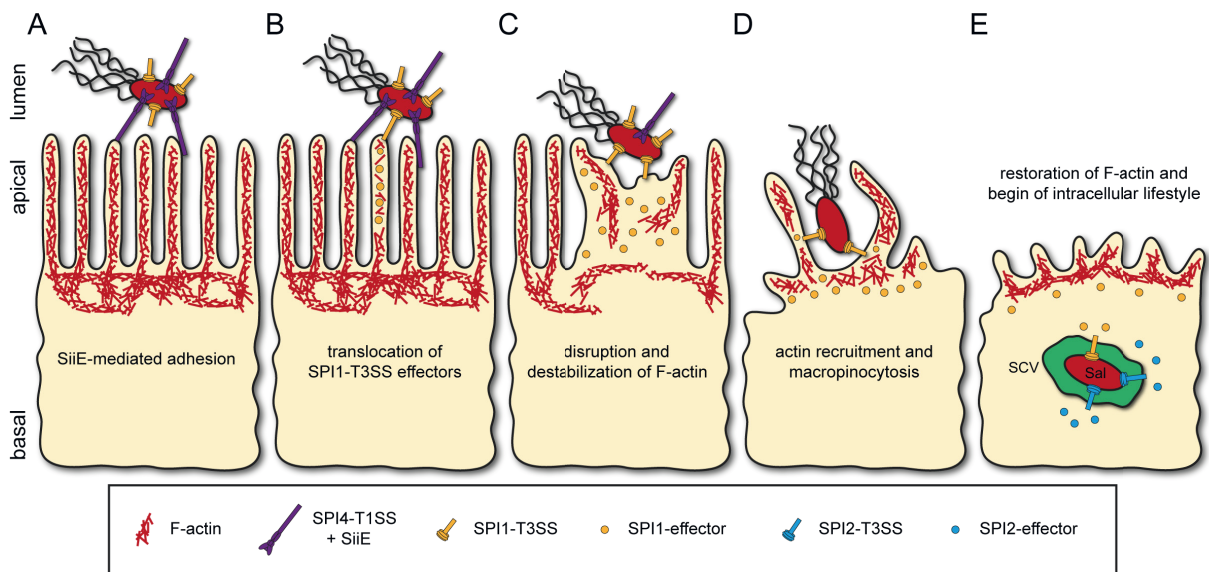


**Figure III.1. SPI4-T1SS dependent adhesion to and SPI1-T3SS-dependent trigger invasion of polarized epithelial cells by *Salmonella*.** (A) *Salmonella* (Sal) mediates adhesion to the brush border of polarized epithelial cells mediated by giant adhesin SiiE. (B) Tight adhesion allows translocation of SPI1-encoded effector proteins into the host cell through SPI1-T3SS. (C) SPI1-T3SS effector proteins lead to disruption of F-actin and thus to destabilization of microvilli. (D) Effector proteins manipulate host cell functions and lead to activate specific actin recruitment at the invasion site, leading to membrane ruffling and macropinocytosis. (E) Subsequent to internalization, restoration of actin cytoskeleton is induced and intracellular lifestyle of *Salmonella* begins within the early SCV.

Several genes encoding SPI1-T3SS effector proteins are located on SPI1, but others are located elsewhere in the genome and some originate from genomes of bacteriophages, hence the set of effector proteins can vary between *Salmonella* serovars (Galan, 2001; Johnson *et al.*, 2018). Besides mediating invasion of host cells, SPI1-genes also play a role in host immune response, apoptosis and biofilm

formation (Lou *et al.*, 2019). The expression of genes encoding SPII-T3SS effector proteins involves many environmental stimuli and genetic regulators in complex networks. The two-component systems BarA/SirA and PhoPQ regulate SPII gene expression dependent on pH, bile, Mg<sup>2+</sup> and phosphate concentration, as well as concentration and composition of short-chain fatty acids allowing adaptation to different host environments (Baxter and Jones, 2015; Lawhon *et al.*, 2002; Prouty and Gunn, 2000). Direct activators of SPII gene expression are the SPII-encoded transcription factors HilA and InvF (Ellermeier and Schlauch, 2007). Expression of *hilA* and *invF* is further positively regulated by e.g. HilD, HilC and FimZ (Altier *et al.*, 2000). Repression of SPII is mediated by H-NS, LeuO and Hile.

The SPII-T3SS consists of proteins forming the inner rod (PrgJ), the export apparatus (SpaPQRS/InvA), the base units inner ring (PrgHK) and outer ring (InvG), the needle filament (PrgI), the tip (SipD) and the translocon (SipBC) which is inserted in the host cell membrane (Cornelis, 2006; Galan and Wolf-Watz, 2006; Lou *et al.*, 2019). Other proteins are involved as chaperones (SicAP, InvB) required for loading effectors and translocases onto the sorting platform (SpaO, OrgAB, InvI, InvC) (Lara-Tejero *et al.*, 2011).

The cocktail of translocated SPII-T3SS effector proteins is responsible for hijacking of and interference with various host cell functions. AvrA plays a critical role in inhibiting activation of the key proinflammatory transcription factor NF- $\kappa$ B (Ye *et al.*, 2007). It is further involved in stabilization of tight junctions to prevent disruption by *Salmonella*-induced inflammation (Liao *et al.*, 2008). SipA and SipC are actin-binding proteins and act in different stages of infection by regulating concentration, polymerization and stability of actin molecules at the invasion site (Kaniga *et al.*, 1995; Zhou *et al.*, 1999). SopA, SopB, SopD, SopE and SopE2 target different host proteins to induce further actin rearrangement and immune modulation. SopE and SopE2 are major factors driving membrane ruffling and micropinocytosis. However, only few *Salmonella* strains possess the respective genes located on bacteriophage genomic regions (Miroid *et al.*, 1999). SopE and SopE2 are guanine exchange factors (GEF) for Cdc42 and Rac1 (only SopE) which activate Arp2/3-dependent actin nucleation (Friebel *et al.*, 2001; Guiney and Lesnick, 2005). Presence of *sopE* is linked to increased SCV damage and cytosolic release of bacteria (Roder *et al.*, 2021b). The role of SopA in efficient invasion process is still unclear but it stimulates immune signaling via members of the TRIM E3 ubiquitin ligases and also contributes to bacterial escape from the SCV to the cytosol inside epithelial cells (Fiskin *et al.*, 2017; Kamanova *et al.*, 2016; Wood *et al.*, 2000; Zhang *et al.*, 2006). SopB, located on SPI5, contributes in immune modulation by inhibition of apoptosis in early and late infection (Finn *et al.*, 2017; Knodler *et al.*, 2005) and cooperatively acts with SopD to promote membrane fission and macropinosome formation (Bakowski *et al.*, 2007; Raffatellu *et al.*, 2005). SptP consists out of three different functional domains: a binding site for chaperone SicP, a phosphorylation site for activation of GTPase proteins (GAP) and a tyrosine phosphatase domain (Johnson *et al.*, 2017). It is acting as antagonist to SopE/SopE2 by dephosphorylating Rho GTPases Rac1 and Cdc42 leading to rearrangement of pathogen-induced F-actin accumulation into

normal apical brush border architecture and is thereby directly responsible for reversal (Fu and Galan, 1999). Only recently, SopF was identified as SPI-T3SS effector protein promoting stability of the nascent SCV and replication within macrophages. (Cheng *et al.*, 2017; Lau *et al.*, 2019). Furthermore, SopF blocks V-ATPase recruitment of ATG16L1 to damaged SCV membranes and thereby specifically inhibits xenophagy without affecting canonical autophagy (Xu *et al.*, 2019). Altogether, the mentioned SPI1-T3SS effector proteins are key to orchestrate *Salmonella*-induced trigger invasion into host cells.

### **III.1.3. Intracellular lifestyle: The life within**

Following internalization, *Salmonella* is present in a membrane-bound compartment, the SCV. The SCV shares characteristics of a late endosomal compartment, yet allows *Salmonella* survival and proliferation. The manipulation of the host cell endosomal system mainly mediated by effector proteins of the SPI2-encoded T3SS is crucial for SCV formation and maintenance (Jennings *et al.*, 2017). The expression of these genes is regulated by the PhoPQ- and SsrAB-two-component systems (TCS) which are primarily activated by acidification and phosphate limitation (Deiwick *et al.*, 1999; Lober *et al.*, 2006). Main characteristics of the SCV are a low pH, limitation of nutrients and the presence of late endosomal and lysosomal markers decorating the SCV membrane (Liss *et al.*, 2017; Malik-Kale *et al.*, 2012). A schematic illustration of the SCV maturation is depicted in Figure III.2.

During infection, the SCV interacts with early endosomes and acquires the markers Rab4, Rab5 and EEA1 (Smith *et al.*, 2005; Smith *et al.*, 2007; Steele-Mortimer *et al.*, 1999). Within 15-60 min post infection (p.i.) the SCV maturation continues by loss of early endosomal proteins and accumulation of late endosomal and lysosomal markers like the lysosomal-associated membrane protein 1 (LAMP1), LAMP2, Rab7, Rab10, Rab11 and syntaxin11 (Malik-Kale *et al.*, 2012; Smith *et al.*, 2005; Smith *et al.*, 2007). In the maturation process, the SCV migrates along the microtubule network towards the Golgi apparatus to a perinuclear position (Ramsden *et al.*, 2007). By active manipulation of host cell membranes, a tubular membrane network of *Salmonella*-induced tubules (SIT) that emanates from the SCV and extends to the cell periphery is established (Schroeder *et al.*, 2011). A well-established SIT-network is utilized by *Salmonella* for efficient intravacuolar nutrition and dilution of antimicrobial and proteolytic components acquired by recruited vesicles (Liss *et al.*, 2017; Noster *et al.*, 2019). *Salmonella*-induced filaments (SIF) are the best studied class among SIT. SIF are microtubule-associated membranes and characterized by the presence of LAMP1. *Salmonella* is also capable of replication inside the SCV before host cell exit by inflammatory responses and spreading throughout the gastrointestinal tract occurs (Bakowski *et al.*, 2008; Knodler *et al.*, 2010; Sellin *et al.*, 2014).

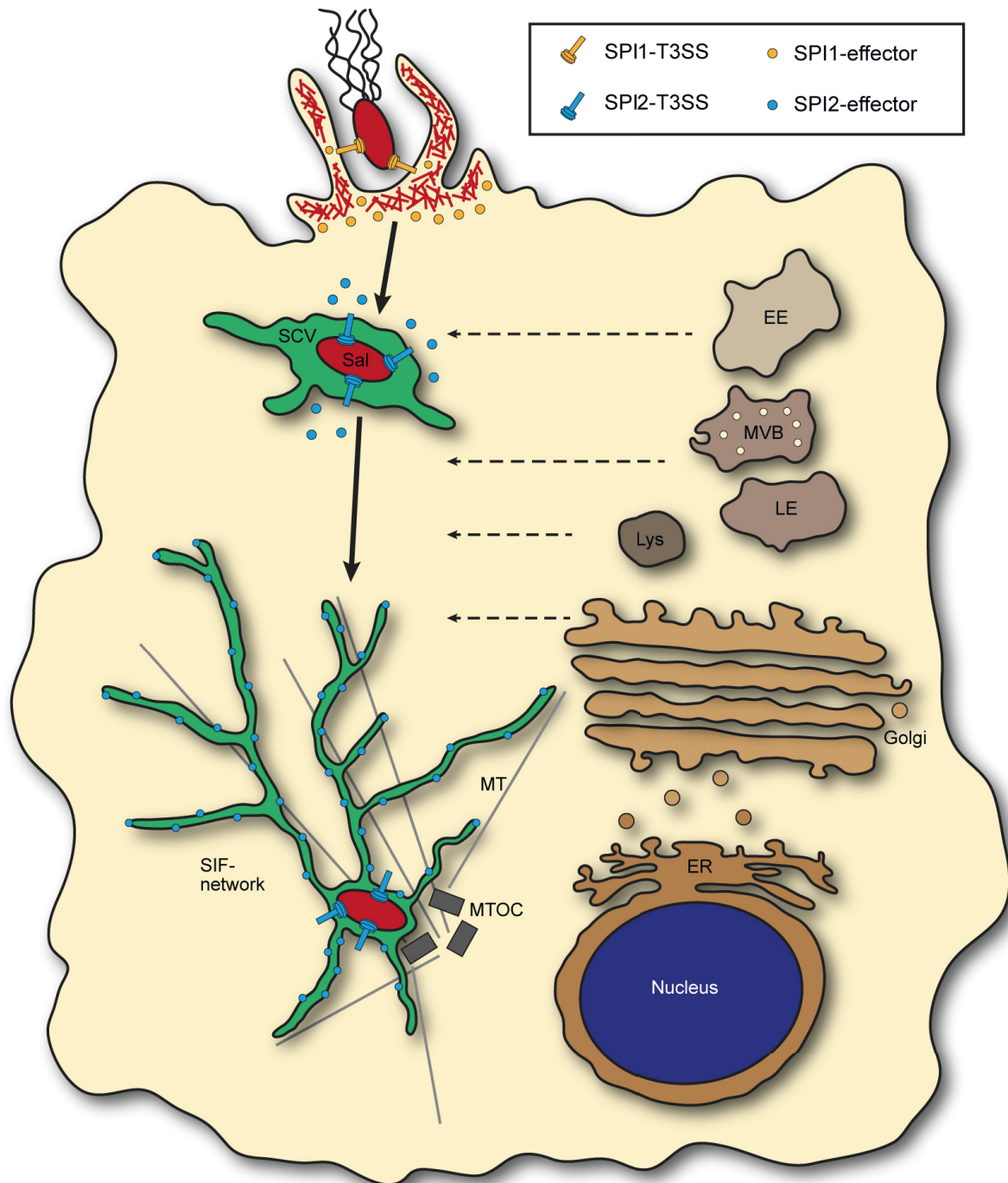


**Figure III.2. Intracellular lifestyle of *Salmonella*.** Subsequent to invasion due to rearrangement of actin filaments, *Salmonella* (Sal) is present in a spacious *Salmonella*-containing vacuole (SCV). The formation of early tubular structures is induced. In this phase, there are mainly early endosomal (EE) markers associated at the SCV membrane. In the process of SCV maturation, they get replaced by late endosomal (LE), lysosomal (Lys) and multivesicular body (MVB) markers. In late stages of infection, *Salmonella* is located near the microtubule-organizing center (MTOC) and the Golgi apparatus. Additionally, the formation of *Salmonella*-induced filaments (SIF) is induced. ER: endoplasmatic reticulum.

The SPI2-T3SS consists of multiple proteins which together form the translocation apparatus in a similar manner as described for the SPI1-T3SS (Galan *et al.*, 2014). The SPI2-T3SS is required for translocation of at least 28 effector proteins, some of which are crucial for virulence in different hosts and are therefore considered as “core” effectors (SseF, SseG, PipB, SteA, SifA, SteD, PipB2, SopD2, SseJ) (Jennings *et*

*al.*, 2017). These effectors are responsible for manipulation of various host cell functions, such as actin arrangement, vesicular transport, ubiquitination, microtubule organization, apoptosis and cytokine regulation, and thus are responsible for intracellular survival and replication of *Salmonella* inside host cells (Figueira and Holden, 2012; Jennings *et al.*, 2017).

Mutant strains lacking components of the SPI2-T3SS (e.g.  $\Delta$ *ssaV*) or one of the TCS (e.g.  $\Delta$ *ssaR*) show severe defects regarding intracellular lifestyle including no SIF-formation (Cirillo *et al.*, 1998; Hensel *et al.*, 1998; Ochman *et al.*, 1996; Rajashekar *et al.*, 2014; Salcedo *et al.*, 2001; Shea *et al.*, 1996). The effector SifA interacts with different host proteins like SKIP/PLEKHM2 and is thereby able to activate and interact with autoinhibited kinesin leading to budding and anterograde tubulation of SCV membrane along microtubules and therefore SIF-formation (Boucrot *et al.*, 2005; Dumont *et al.*, 2010; Schroeder *et al.*, 2011). Autoinhibited kinesin-1, indispensable for this process, is recruited to the SCV membrane by the effector protein PipB2 (Henry *et al.*, 2006). Mutant strains lacking SifA show loss of SCV membrane and do not form SIF (Beuzon *et al.*, 2000; Stein *et al.*, 1996). STM mutants which are residing in the cytosol after SCV rupture (e.g.  $\Delta$ *sifA*) show a hyper-replication phenotype in cultured epithelial cells (Brumell *et al.*, 2002). SseJ and SopD2 are important regulators of SCV-stability and SIF-biogenesis (Ruiz-Albert *et al.*, 2002; Schroeder *et al.*, 2011). It has been reported, that a *sseJ* mutation leads to increased tubulation of endosomal membranes (Ruiz-Albert *et al.*, 2002). SopD2 manipulates functions of host cell proteins including RILP and FYCO1 by the inhibition of the small GTPase Rab7 and thereby affects microtubule motor activity and the vesicular transport within the host cell (D'Costa *et al.*, 2015; Schroeder *et al.*, 2010). SIF-morphology itself is shaped by effector proteins SseF, SseG and PipB2. Wild-type SIF are very dynamic and show a typical double membrane structure (Liss and Hensel, 2015). SseF and SseG are tethering the SCV to the Golgi binding the Golgi network-associated proteins ACBD3 (Yu *et al.*, 2016). Close proximity of the SCV to the Golgi enables efficient acquisition of endomembranes and a lack of SseF or SseG results in thinner, instable, single membrane SIF (Krieger *et al.*, 2014; Rajashekar *et al.*, 2014). In contrast, *pipB2* mutants show formation of bulky, non-dynamic SIF (Rajashekar *et al.*, 2014). The underlying mechanism of this process is not yet fully understood, it is possible that binding of PipB2 to kinesin-1 plays a role (Alberdi *et al.*, 2020; Henry *et al.*, 2006).

Besides developing and maintaining the SCV as intracellular niche in host cells, SPI2-T3SS effector proteins also enable nutrient acquisition of SCV-inhabiting *Salmonella* (Liss *et al.*, 2017), contribute to bacterial replication inside host cells (Deiwick *et al.*, 2006; Figueira *et al.*, 2013) and manipulate innate and adaptive host cell immune responses (Jennings *et al.*, 2017). A direct suppression of proinflammatory immune response was shown for GtgA, GogA and PipA by disrupting transcriptional activation of the NF- $\kappa$ B pathway (Sun *et al.*, 2016). SseK1, SseK2 and SseK3 do not only inhibit NF- $\kappa$ B but also TNF $\alpha$  signaling (Gunster *et al.*, 2017; Yang *et al.*, 2015). Transcription of proinflammatory cytokines is prevented by phosphothreonine lyase activity of SpvC on host mitogen-activated protein kinases (Mazurkiewicz *et al.*, 2008). For many effectors, the molecular functions are still elusive. However,

effects like inhibition of dendritic cell migration are described for multiple effectors like SseF, SifA, SspH2, SlrP, PipB2 and SseI (McLaughlin *et al.*, 2014). As research continues, molecular details such as the hijacking of AP1-mediated vesicular trafficking by SteD are uncovered (Godlee *et al.*, 2022). In this way, SteD specifically targets major histocompatibility complex (MHC) class II molecules to suppress adaptive immune response (Bayer-Santos *et al.*, 2016; Godlee *et al.*, 2022).

### **III.2. Typhoidal *Salmonella***

Human specialized, typhoid fever causing *Salmonella* serovars infect approximately 20 million people every year and 200,000 people succumb to the disease annually, particularly in regions with poor economic development and limited public health infrastructure (Crump *et al.*, 2004; WHO, 2018b). Traditionally, STM has been served as surrogate to investigate systemic *Salmonella* infections because it can easily be genetically manipulated, there are well-established *in vitro* and *in vivo* infection models available using cell culture and susceptible mouse strains and research can be carried out under low biosafety level (Gerlach and Hensel, 2007; Schulte and Hensel, 2016). However, the infection process of non-typhoidal *Salmonella* (NTS) and typhoidal *Salmonella* (TS) is similar but differs in specific details. Both infections begin with an oral uptake of *Salmonella*. The infectious dose of NTS with over  $10^6$  bacteria is high and the incubation time with 1-3 days is short. NTS are capable of excessive luminal replication and trigger an inflammatory response but the local infection is self-limiting. In contrast, the infectious dose of TS is low ( $10^2$ - $10^3$  bacteria), but the incubation time with 1-3 weeks is long and the systemic infection has to be counteracted with antibiotics (Dougan and Baker, 2014; Khan *et al.*, 2012). The lack of mucosal rapid inflammation response is a unique key feature of TS. The TS infection involves replication in macrophages and a subsequent systemic dissemination by passing unnoticed through immunological checkpoints like lymph nodes to e.g. spleen, gallbladder, lymph nodes, blood and bone marrow (Hiyoshi *et al.*, 2018a). Due to resistance to high concentrations of bile, STY can form biofilms in gallbladder and on gallstones (Di Domenico *et al.*, 2017; Prouty *et al.*, 2002). The ability to avoid a massive inflammatory response and the higher frequency of persister formation, that are able to survive host immune responses and harsh antibiotic treatment, is considered as part of a ‘stealth strategy’ of TS (Dougan and Baker, 2014). A schematic illustration of substantial differences between TS and NTS infection is depicted in Figure III.3.

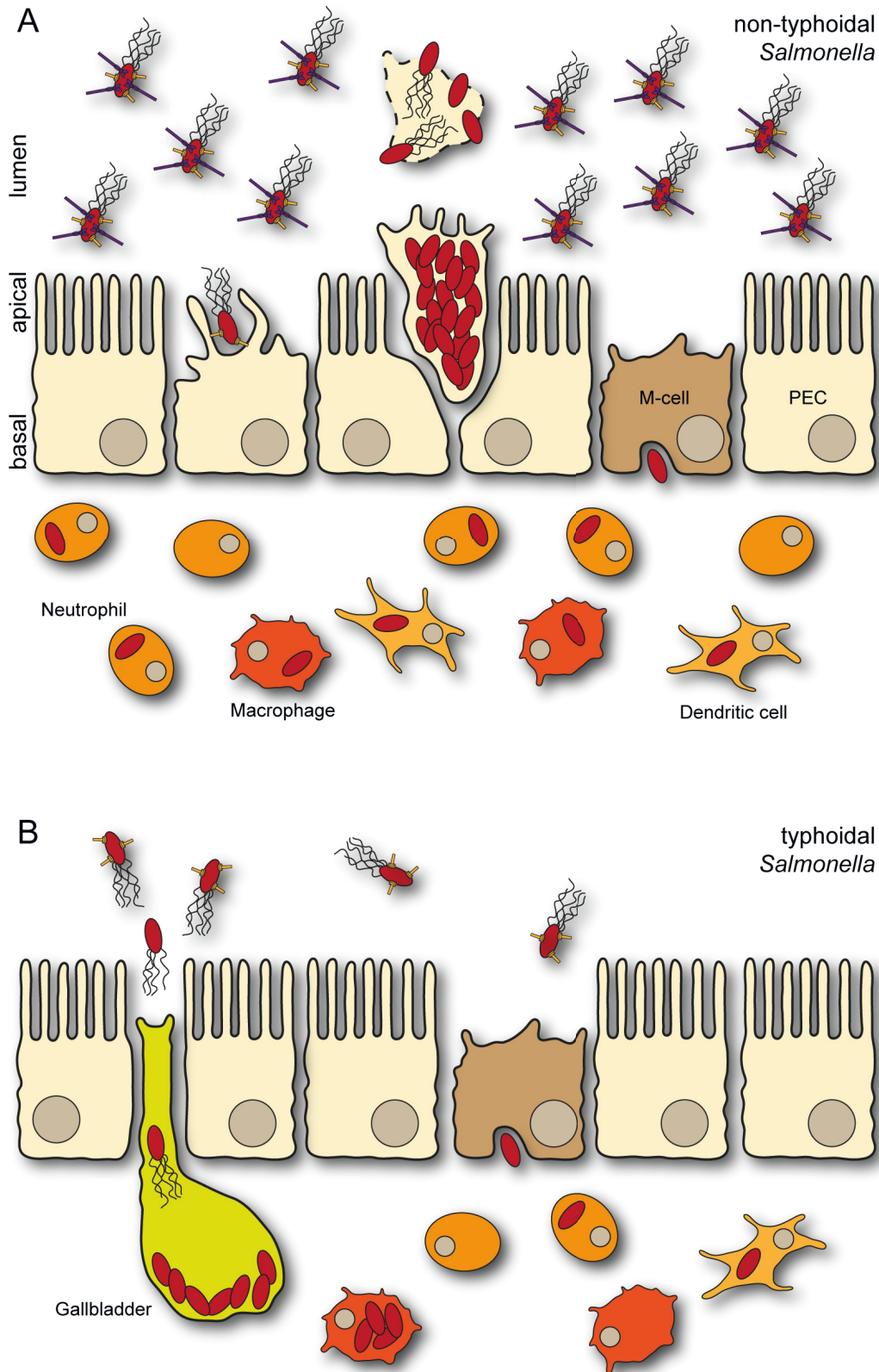


**Figure III.3. Typhoidal and non-typhoidal infections.** Schematic comparison of the infection process with non-typhoidal (NTS, A) and typhoidal (TS, B) *Salmonella*. Both NTS and TS invade the intestinal mucosa through microfold (M-) cells. NTS are also capable of invasion of polarized epithelial cells (PEC) and massive replication in epithelial cells which leads to extrusion of enterocytes. NTS trigger a massive inflammatory response by luminal replication and macrophages which leads to further attraction of immune cells. TS like SPA and STY show only limited luminal replication and do not trigger a rapid inflammatory response. The infection involves replication in macrophages and subsequent systemic dissemination to gallbladder, lymph nodes and bone marrow.



### III.2.1. Adapted armory: Genetic equipment of typhoidal *Salmonella*

Despite genomes of *Salmonella* serovars sharing often beyond 90% of genetic similarity, a hallmark of TS is the presence of a large number of pseudogenes, a characteristic which is often associated with the evolution of host restriction (Chan *et al.*, 2003; Didelot *et al.*, 2007; Holt *et al.*, 2009; McClelland *et al.*, 2004). Expression of pseudogenes is impaired due to inactivation by insertion, deletion or nucleotide substitution. Coding sequences of STY and SPA harbor over 4% pseudogenes (Holt *et al.*, 2009). Other host-specific serovars like the avian-restricted *S. Gallinarum* harbor similar amounts of pseudogenes (>6%) (Feng *et al.*, 2013; Foley *et al.*, 2013; Thomson *et al.*, 2008). In contrast, the genome of the host generalist STM harbors less than 0.9% pseudogenes and the related host generalist enterobacterium *Escherichia coli* possesses about 0.7% pseudogenes (Holt *et al.*, 2009).

Pseudogenes in TS are spread across the genome and affect SPI1-T3SS effector proteins (SopE2, SopA) or SPI2-T3SS effector proteins (SopD2, SseJ) (Holt *et al.*, 2009; Johnson *et al.*, 2018; McClelland *et al.*, 2004). Others lead to expression of proteins with altered functionality (SiiE, SptP) (Barlag and Hensel, 2015; Johnson *et al.*, 2017). Some pseudogenes may restrict the metabolic flexibility like auxotrophies of SPA and STY for cysteine and tryptophan (Sabbagh *et al.*, 2010), or affect amino acid synthesis (*asnB*), nutrient transport (*araH*, *rbsC*, *gltJ*, *yaaJ*, *cbiM*), carbon metabolism (*rhaD*, *rhaS*, *gatZ*, *uhpT*), tetrathionate reduction (*ttrS*, *ttrB*, *phsA*), vitamin biosynthesis (*cbiA*, *cbiC*, *cbiJ*, *cbiK*) or iron uptake (*fepE*, *fhuA*, *fhuE*) (Holt *et al.*, 2009; Langridge, 2010).

Additionally, TS differ in their gene expression and regulating patterns, for instance of SPI1 regulating genes *hilA* and *hilD* in SPA (Elhadad *et al.*, 2016), or *barA* and *sirA* in STY (Johnson *et al.*, 2018). In some cases, loss of genes in TS may be directly linked to host adaptation, e.g. in the case of SPI2-T3SS effector GtgE which proteolytically targets Rab29, Rab32 and Rab38 and thereby promotes replication inside murine macrophages during STM infection (Ho *et al.*, 2002; Spano and Galan, 2012; Spano *et al.*, 2011). A recently published study also stated, that SPI2 may not be required at all for intracellular survival of TS in human macrophages (Forest *et al.*, 2010).

Furthermore, additional virulence genes were also gained in the evolutionary process such as SPI7 and SPI11. SPI7 genes encode the Vi capsule, a unique feature of STY, *S. Paratyphi C* and *S. Dublin* (Pickard *et al.*, 2003). The capsule expression depends on osmolarity (Arricau *et al.*, 1998; Pickard *et al.*, 1994). In low to medium osmotic environments (<0.3 M NaCl; aqueous environment e.g. bloodstream) it is upregulated, whereas under high osmotic conditions (>0.3 M NaCl; e.g. intestinal lumen) and during the intracellular lifestyle Vi capsule expression is inhibited (Janis *et al.*, 2011). The adherence and invasiveness of STY reaches its maximum under high osmotic conditions without Vi capsule (Tartera and Metcalf, 1993), though the expression increases virulence and reduces antibody binding and the activation of the complement system (Hart *et al.*, 2016; Hornick *et al.*, 1970a, b). However, the Vi capsule is not essential for infection and TS such as SPA cause enteric disease in absence of SPI7 (Hirose *et al.*,

1997). Another notable feature of TS is the expression of typhoid toxin. It is a unique type of AB toxin and plays a key role in host-pathogen interaction and the human host due to its cytolethal capacity (Chong *et al.*, 2017; Haghjoo and Galan, 2004; Song *et al.*, 2013). Typhoid toxin binding is highly restricted to human cells through binding to *N*-acetylneuraminic acid (Neu5Ac) which is exclusively present on human cells (Song *et al.*, 2013). Expression of typhoid toxin is upregulated in intracellular TS and promotes pathogenicity (Spano *et al.*, 2008) although a recent large clinical study with human volunteers showed no clear effect in systemic infection (Gibani *et al.*, 2019). Altogether, pseudogenes, differential gene expression patterns and newly acquired genetic features may lead to differences in host interaction and intracellular lifestyle of TS. An overview of important virulence associated genes present in SPA and STY in comparison to STM is listed in Table III.1.

**Table III.1: SPI1 and SPI2 effector proteins of STM, SPA and STY.** Subset of effector proteins with differences regarding presence in *Salmonella* serovars STM, SPA or STY. Functional effectors are highlighted with check mark, pseudogenes are highlighted with “X” in red, proteins with altered function in blue and effectors only present in certain strains in orange (adapted from (Johnson *et al.*, 2018)).

T3SS	Effector	STM	SPA	STY
SPI1	SopA	✓	X	X
	SopE	X	✓	✓
	SopE2	✓	✓	X
	SopF	✓	✓	✓
	SptP	✓	X	X
SPI2	CigR	✓	✓	X
	GogB	✓		
	GtgA	✓		
	SifB	✓	X	✓
	SopD2	✓	X	X
	SpvB	✓		
	SpvC	✓		
	SseI	✓		
	SseJ	✓		X
	SseK1	✓		
	SseK2	✓		
	SseK3	X		
	SspH2	✓		✓
	SteC	✓	X	✓
SteD	✓	✓	✓	
SPI1/SPI2	AvrA	✓		
	GtgE	✓		
	SlrP	✓	X	X
	SpvB	✓		
	SteB	✓		
unknown	SteE	✓		
	GogA	✓		
	PipA	✓	✓	✓
	StoD			✓

### **III.2.2. Host specificity & limitations of model systems**

The strict host specificity of TS has limited studies of virulence mechanisms in the past. NTS like STM have been used as surrogate to provide an insight into the molecular mechanisms of the general pathogenesis of *Salmonella* but failed to enlighten the specific characteristics of typhoid disease in humans. Studies with TS were difficult or impossible to perform due to their human-restricted host tropism, although some studies with susceptible mice, primates or human volunteers have been carried out (Edsall *et al.*, 1960; Gibani *et al.*, 2019; Glynn *et al.*, 1995; Hindle *et al.*, 2002). Next generation sequencing together with modern bioinformatic approaches made it possible to analyze large amounts of clinical TS isolates and supported to uncover the evolution as well as the genetic features of TS. However, the distinct host-tropism and clinical manifestation in humans is still not well understood and needs other (infection) model systems to investigate the molecular mechanisms behind these processes. Although working with cell culture models, like HeLa, Caco-2, U937 and THP-1 cells, allow defined and easy reproducible experiment design with high throughput they do not reconstitute *in vivo* conditions. Primary immune cells isolated from blood that allow differentiation into macrophages and dendritic cells serve as option to mimic natural conditions if working with single cell is required. As alternative, humanized mouse models based on transplantation of human immune cells and genetic engineering have been developed (Karlinsky *et al.*, 2019; Mathur *et al.*, 2012). Organoids also serve as method to establish complex *in vivo* like conditions in 3D structure with a heterogeneous cell population. The organoid system, a recent methodological development probably becoming a game changer across various disciplines in life sciences is introduced in a following chapter.

### **III.3. Organoids, a game changer in life sciences?**

Organoid systems represent one of the major recent advances for biological research across biological fields including drug treatment, cancer therapy, developmental biology and also infection biology. In contrast to cell culture with only a single cell population, organoids are *in vitro* model systems of miniaturized organs suitable to recapitulate the architecture and physiology of organs in remarkable detail. Organoids can be derived from organ-specific adult stem cells (AdSC) or induced pluripotent stem cells (iPSC) and are able to reconstitute complex tissues with different cell types and physiological functions (Hofer and Lutolf, 2021). Therefore, stem cells are embedded in an artificial extracellular matrix and supplemented with a complex medium, containing growth factors that allow differentiation into various types of organs (Kim *et al.*, 2020).

#### **III.3.1. Organoids in infection biology research**

Analyses of host-pathogen interactions are a key requirement for the understanding of bacterial virulence mechanisms. Rising infection rates and frequently emerging antibiotic resistance in pathogenic bacteria as well as newly emerging zoonotic diseases like SARS-CoV-2 illustrate the importance to better understand pathogenesis for development of new strategies to counteract infections and vaccine development. Cell culture models are frequently used to study cellular interactions with a high temporal

and spatial resolution. However, these models lack the complex tissue architecture of whole tissues. For many diseases including typhoid fever, the broader biological context is necessary to elucidate infection routes, disease progression and pathogenesis of the causative agent. Most recently, organoids have become a promising tool to study host-pathogen interactions in a more *in vivo* relevant setting (Bartfeld, 2016; Dutta and Clevers, 2017; Rios and Clevers, 2018). Despite being only a recently developed method, numerous bacterial, viral and parasitic pathogens have been analyzed in organoid systems such as *Cryptosporidium*, enterohemorrhagic *Escherichia coli*, *Campylobacter jejuni*, *Clostridium difficile*, *Helicobacter pylori*, *Listeria monocytogenes*, *Shigella flexneri*, *Vibrio cholerae*, *Salmonella enterica*, Zika virus, rotavirus and SARS-CoV-2 (Bartfeld and Clevers, 2015; Finkbeiner *et al.*, 2012; Forbester *et al.*, 2015; Garcez *et al.*, 2016; He *et al.*, 2019; Heo *et al.*, 2018; Lamers *et al.*, 2021; Leslie *et al.*, 2015; Ranganathan *et al.*, 2019; Roodsant *et al.*, 2020; Tse *et al.*, 2018; Zomer-van Ommen *et al.*, 2016). Even formerly unculturable pathogens like norovirus show the high potential of organoids to become a promising model system for pathogens (Ettayebi *et al.*, 2016). Especially the research with human-restricted pathogens like TS is dependent on human cell culture with a close relation to *in vivo* conditions.

Many bacterial pathogens are using the intestinal tract as route of entry to deeper tissues and systemic spread in the host (Ribet and Cossart, 2015). The intestinal epithelium, composed of a single layer of cells, is assembled by a majority of four differentiated cell types: enterocytes, enteroendocrine cells, goblet cells and Paneth cells. Together with a small population of multipotent Lgr5<sup>+</sup> stem cells, tuft and M-cells they constitute the distinct areas of the villus and crypt domains of the intestine (Allaire *et al.*, 2018; Haegebarth and Clevers, 2009; Sato *et al.*, 2009). Enterocytes are the most abundant cell type in the intestinal epithelium and with a dense brush border they act as physical barrier and are responsible for nutrient and water absorption (Snoeck *et al.*, 2005). Goblet cells are distributed in the intestinal mucosa and secrete mucins providing a protective barrier atop the intestinal epithelium (Johansson and Hansson, 2016). M-cells are constantly sampling luminal content for presentation of particular antigens and microorganisms to immune cells at the basolateral side, thereby acting as an antigen sampling system (Kucharzik *et al.*, 2000). Enteroendocrine and tuft cells secrete hormones and cytokines in response to luminal content, such as nutrients and pathogens, and constantly regulate digestion, intestinal motility and inflammatory response (Moran *et al.*, 2008; von Moltke *et al.*, 2016). Intestinal stem cells reside at the base of the crypts and give rise to proliferative cells that differentiate as they travel up to the tip of the villus (Crosnier *et al.*, 2006). Paneth cells support stem cell function and release antimicrobial factors for efficient protection of the crypt domain (Rodriguez-Colman *et al.*, 2017). Crypt-derived intestinal organoids mimic tissue characteristics of distinct sections of the gastrointestinal tract. Therefore, stem cells of human or murine origin can be differentiated to 3D or 2D tissues with crypt formation, distinct cell populations, polarization and mucus secretion (Taelman *et al.*, 2022).

Intestinal organoids with their ability to recapitulate infection relevant characteristics such as crypt and microvilli domains, mucus production, defensive and antimicrobial peptide secretion can serve as

adequate model system for enteric pathogens (Bartfeld and Clevers, 2015; Dutta and Clevers, 2017). Further systems with gallbladder and liver organoids can help to study specific infection foci in systemic diseases in case of typhoid fever (Caiazza *et al.*, 2021; Sepe *et al.*, 2020). Co-culture models with immune cells in medium could serve as model for microenvironments like the lamina propria (Schreurs *et al.*, 2021). Altogether, a decent set of methods with organoid systems is available by now and only future will tell what a giant leap organoids represent for research in infection biology.

### **III.4. From vacuole to cytosol: Lifestyles of intracellular pathogens**

The human host is constantly patrolled by immune cells and contains lots of antibodies and other molecules, like the complement system, that can target extracellular bacteria and lead to clearance. The environment inside host cells can therefore provide a safe space to subvert the immune system. Intracellular bacteria either inhabit a specialized compartment, a pathogen-containing vacuole (PCV), or they escape into the cytosol (Creasey and Isberg, 2014). Both PCV and cytosol can be antibacterial environments if intracellular pathogens are incapable of successful manipulation of cellular immune mechanisms to establish a niche for persistence and proliferation (Asrat *et al.*, 2014; Kellermann *et al.*, 2021). Cellular immune mechanisms lead to the development of various bacterial counter mechanisms to withstand or circumvent inhibition and degradation.

#### **III.4.1. How pathogenic bacteria manipulate their host**

Several bacterial pathogens have evolved an intracellular lifestyle, such as the Gram-negative *Salmonella*, *Yersinia*, *Legionella* and *Shigella* as well as Gram-positive *Listeria*. While *Salmonella*, *Yersinia* and *Legionella* inhabit a PCV as replication niche, *Shigella* and *Listeria* actively escape out of their PCV to the host cell cytosol (Figure III.4). Maintaining the integrity of the PCV is of crucial importance to avoid degradation within the lysosomal or autophagosomal pathway. Autophagy is an adaptive process that occurs in response to different forms of stress, including nutrient deprivation, growth factor depletion and hypoxia, thereby providing nutrients for vital cell functions (Dikic and Elazar, 2018). It is also involved in elimination of unwanted, potentially harmful cytosolic material, such as damaged mitochondria or protein aggregates and also degradation of intracellular pathogens. Notably, many pathogens have evolved strategies to escape the autophagic machinery by interference with autophagosome maturation, blocking fusion of the autophagosome with the lysosome and competing with host autophagy receptors such as LC3 (Dikic and Elazar, 2018).

In the case of *Salmonella*, SPI2-T3SS effector proteins play a major role in the process of autophagic escape (Figure III.4 A). The effector protein SseL, for instance, deubiquitinates the SCV membrane and thus prevents recognition by autophagic receptors of the host cell (Mesquita *et al.*, 2012). In later stages of infection, *Salmonella* is able to recruit the negative regulator of autophagy, mTOR, to the SCV membrane, thereby preventing autophagic recognition (Tattoli *et al.*, 2012). Invasion by trigger mechanism can already lead to SCV rupture in early stages of infection (Roder and Hensel, 2020). Cellular processes

like ESCRT-dependent endolysosomal repair mechanisms and sphingomyelin scrambling play a major role in maintenance of SCV integrity (Ellison *et al.*, 2020; Goser *et al.*, 2020). Upon SCV rupture, *Salmonella* is exposed to the host cell cytosol and lipopolysaccharide (LPS) is ubiquitylated by the E3 ubiquitin ligase ring finger protein 213 (RNF213) (Otten *et al.*, 2021). However, massive hyper-replication in host cell cytosol obscures defects in vacuolar replication and fuels intestinal expansion and chronic fecal shedding (Chong *et al.*, 2021; Malik-Kale *et al.*, 2012).

In contrast, invasion of *Yersinia* by zipper mechanism involves less severe membrane ruffling at the entry site (Roder and Hensel, 2020). The signaling cascades allowing invasion into epithelial cells by invasion/ $\beta$ 1-integrins interaction have already been well studied (Isberg and Falkow, 1985; Isberg and Leong, 1990; Isberg *et al.*, 1987). In the subsequent intracellular lifestyle, *Yersinia* interferes with membrane trafficking and favors bacterial replication by activating autophagy (Figure III.4 B) (Lemarignier and Pizarro-Cerda, 2020). *Yersinia*-containing vacuoles (YCV) enlarge progressively over time by fusing with LAMP1- and LC3-positive membranes establishing a double or multimembranous compartment (Moreau *et al.*, 2010). However, degradation by fusion with lysosomes is somehow inhibited and *Yersinia* is able to replicate in a non-acidic autophagosome (Connor *et al.*, 2018; Straley and Harmon, 1984).

Following uptake by phagocytic cells, *Legionella* avoids lysosome-mediated degradation and forms a replication-permissive compartment, the *Legionella*-containing vacuole (LCV; Figure III.4 C). The LCV has a defined membrane signature due to recruitment of vesicles rich in lipids and proteins (Oliva *et al.*, 2018). Upon nutrient starvation in later stages of infection, drastic morphological changes are induced by activation of stringent response. A short, highly motile form with a thickened cell wall develops which is 10-100 times more infectious. These highly infectious bacteria are able to lyse the LCV membrane and induce host cell lysis (Hoffman, 1997; Oliva *et al.*, 2018). Recent studies demonstrated an autophagic escape mechanism by modulating host sphingolipid metabolism or autophagosome formation, e.g. by T4SS effector protein RavZ (Choy *et al.*, 2012; Rolando *et al.*, 2016).

In contrast to the bacterial pathogens above, *Shigella* and *Listeria* are not residing in a PCV. Both pathogens are able to actively move within the host cell cytosol through Arp2/3-mediated actin polymerization following escape from the PCV (Haglund and Welch, 2011; Welch and Way, 2013). Subsequently to invasion into epithelial cells, *Shigella* actively escapes from the PCV and the surface protein IcsA polymerizes host actin at the bacterial surface (Figure III.4 D) (Kocks *et al.*, 1995). *Shigella* prevents recognition of IcsA by the autophagy related protein ATG5 via the translocated effector IcsB which binds to IcsA and blocks recognition by ATG5 (Ogawa *et al.*, 2005). Additionally, the secreted effector VirA targets and inactivates RAB1 which is involved in ER-Golgi vesicular transport and is crucial in the formation of autophagosomes (Zoppino *et al.*, 2010). Subsequent to zipper invasion mediated by Internalin A (InlA) and InlB, *Listeria* actively escapes the PCV with the pore-forming protein

listeriolysin O (LLO) and recruits the host actin polymerization machinery by the surface protein ActA (Kocks *et al.*, 1995). Additionally, another surface protein InlK recruits the hosts major vault protein (MVP) which inhibits p62 recruitment and prevents recognition of the autophagosomal machinery (Dortet *et al.*, 2011). For both *Shigella* and *Listeria*, the intracellular motility is a major mechanism, enabling cell-to-cell spread and avoidance of recognition by autophagy. Mutants lacking the ability of vacuolar escape and subsequent intracellular movement are highly impaired in their pathogenicity (Ogawa *et al.*, 2011; Yoshikawa *et al.*, 2009).

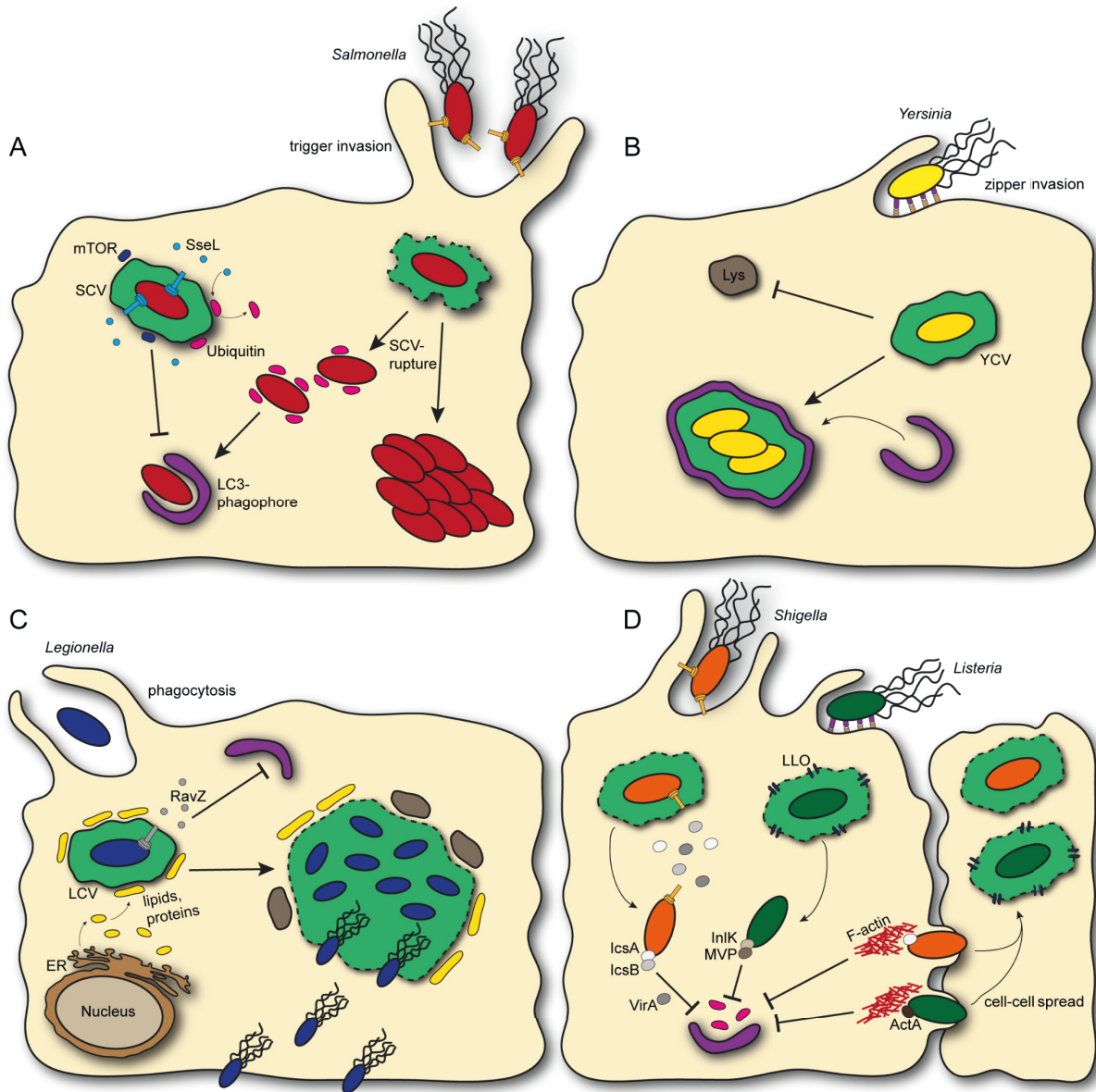


**Figure III.4. Schematic representation of bacterial inhibition and evasion of autophagy, intracellular movement and cell-to-cell spread.** (A) Recruitment of active mTOR and deubiquitinating activity of SseL inhibit autophagic recognition of *Salmonella*-containing vacuole (SCV). Upon SCV rupture, LPS of cytosolic *Salmonella* is ubiquitylated and LC3-mediated xenophagy is induced. Extensive hyper-replication can occur in host cell cytosol. (B) *Yersinia* inhibits fusion of Lysosomes (Lys) with the *Yersinia*-containing vacuole (YCV) and by this prevents degradation. By recruitment of LC3-positive membranes, the YCV matures to a double or multimembranous compartment in which *Yersinia* replicates. (C) *Legionella* recruits endoplasmic reticulum (ER)-derived vacuoles rich in lipids and proteins to establish the *Legionella*-containing vacuole (LCV). The T4SS effector RavZ inhibits autophagosome formation. In late stages of infection, *Listeria* develops into a short, highly motile and infectious form and induces LCV and host cell lysis. (D) Both *Shigella* and *Listeria* actively escape their pathogen-containing vacuole, in the case of *Listeria* by pore-forming listeriolysin O (LLO). The *Shigella* T3SS effector IcsB blocks autophagic recognition of IcsA. Additionally, the T3SS effector VirA blocks formation of LC3-phagophores. InlK and subsequent recruitment of MVP prevent ubiquitination of *Listeria*. IcsA and ActA mediate actin-based motility and xenophagic escape of *Shigella* and *Listeria*, respectively. Collision with the plasma membrane leads to protrusions and cell-to-cell spread.



## IV. Aims of this work

The strict adaptation to primate hosts limits studies of virulence mechanisms of TS. Studies investigating *Salmonella* systemic pathogenesis typically rely on NTS, and since STM causes a typhoid-like systemic infection in susceptible mice, it is often the model of choice. However, pathogenesis of human-restricted TS has several features distinct from systemic infections of STM in the mouse model. Until today, understanding of the molecular mechanisms of pathogenesis of STY and SPA is still elusive, and further research is urgently required. Multiple topics regarding the intracellular lifestyle of typhoidal *Salmonella* will be investigated in this thesis:

- i) Various studies with STM suggest a functional SPI2-T3SS as crucial factor for intracellular survival, replication and pathogenesis of *Salmonella* in general. This work will investigate the contribution of SPI2 to intracellular lifestyle of STY and SPA in comparison to STM. Is the SPI2-T3SS functional in STY and SPA? Do STY and SPA remodel the endosomal system of infected host cells to a same degree as STM? Are there differences regarding the biosynthetic capability during the intracellular lifestyle?
- ii) SPA represents an understudied *Salmonella* serovar, although a commercial vaccine is not available and antibiotic resistant strains are increasingly reported. While STM and SPA share many virulence factors, the underlying mechanisms for these differences are not fully understood. What are possible reasons for differences in host-pathogen interactions of SPA compared to STM? Does SPA exhibit similar intracellular phenotypes and gene expression patterns during epithelial cell infection?
- iii) Single cell analyses of intracellular pathogens rely on efficient bacterial and cellular reporter systems. Already established bacterial reporter systems for STM will be adapted for use in TS. Furthermore, cellular reporters will be optimized to analyze host cell responses during infection. For this purpose, stable lentiviral-transfected cell lines will be generated.
- iv) Subsequent to establishment of suitable reporter systems for single cell analyses of intracellular TS, these systems will be used to analyze the route of SPA infection and the intracellular lifestyle with regard to bacterial and host cell response. How does SPA escape from the SCV to host cell cytosol? What are possible host cell responses during the cytosolic lifestyle of SPA?
- v) Since research with cell lines lacks complex tissue architecture, another topic of this work is the establishment of a human intestinal organoid systems for further use with human-specialized TS. Imaging approaches and quantitative analyses will be adapted to analyze *Salmonella* infection processes with a focus on adhesion and invasion.

With these research projects, this work aims to develop new methods for analyses of TS infection and contribute to a better understanding of the virulence traits of TS.

## V. Results and Publications

### V.1. Single cell analyses reveal distinct adaptation of typhoidal and non-typhoidal *Salmonella enterica* serovars to intracellular lifestyle

Tatjana Reuter<sup>\*,1</sup>, Felix Scharte<sup>\*,1</sup>, Rico Franzkoch<sup>1,2</sup>, Viktoria Liss<sup>1,2</sup>, Michael Hensel<sup>1,3</sup>

\*Authors contributed equally to this work

<sup>1</sup>Abteilung Mikrobiologie, Universität Osnabrück, Osnabrück, Germany

<sup>2</sup>iBiOs - integrated Bioimaging Facility Osnabrück, Universität Osnabrück, Osnabrück, Germany

<sup>3</sup>CellNanOs - Center of Cellular Nanoanalytics Osnabrück, Universität Osnabrück, Osnabrück, Germany

The publication accessible under the following DOI corresponds to pages 21-48 in the print version of this thesis.

DOI: <https://doi.org/10.1371/journal.ppat.1009319>

Supplementary information is provided on DVD

## V.2. Intracellular *Salmonella Paratyphi A* is motile and differs in the expression of flagella-chemotaxis, SPI-1 and carbon utilization pathways in comparison to intracellular *S. Typhimurium*

Helit Cohen\*<sup>1</sup>, Claire Hoede\*<sup>2</sup>, Felix Scharte\*<sup>3</sup>, Charles Coluzzi<sup>4</sup>, Emiliano Cohen<sup>1</sup>, Inna Shomer<sup>1</sup>, Ludovic Mallet<sup>2</sup>, Sébastien Holbert<sup>5</sup>, Remy Felix Serre<sup>6</sup>, Thomas Schiex<sup>7</sup>, Isabelle Virlogeux-Payant<sup>5</sup>, Guntram A. Grassl<sup>8</sup>, Michael Hensel<sup>3,9</sup>, Hélène Chiapello<sup>2,4</sup>, Ohad Gal-Mor<sup>1,10</sup>

\*Authors contributed equally to this work

<sup>1</sup>The Infectious Disease Research Laboratory, Sheba Medical Center, Tel-Hashomer, Israel

<sup>2</sup>Université Fédérale de Toulouse, INRAE, BioinfOmics, UR MIAT, GenoToul Bioinformatics facility, 31326, Castanet-Tolosan, France

<sup>3</sup>Abteilung Mikrobiologie, Universität Osnabrück, Osnabrück, Germany

<sup>4</sup>INRAE, Université Paris-Saclay, MaIAGE, Jouy-en-Josas, France

<sup>5</sup>INRAE, Université de Tours, UMR ISP, Nouzilly, France

<sup>6</sup>INRAE, GeT-PlaGe, Genotoul, Castanet-Tolosan, France

<sup>7</sup>Université Fédérale de Toulouse, ANITI, INRAE, Toulouse, France

<sup>8</sup>Institute of Medical Microbiology and Hospital Epidemiology, Hannover Medical School and German Center for Infection Research (DZIF), Hannover, Germany

<sup>9</sup>CellNanOs - Center of Cellular Nanoanalytics Osnabrück, Universität Osnabrück, Germany

<sup>10</sup>Department of Clinical Microbiology and Immunology, Faculty of Medicine, Tel-Aviv University, Tel-Aviv, Israel

The publication accessible under the following DOI corresponds to pages 50-84 in the print version of this thesis.

DOI: <https://doi.org/10.1371/journal.ppat.1010425>

Supplementary information is provided on DVD



### **V.3. Ca<sup>2+</sup>-activated sphingomyelin scrambling and turnover mediate ESCRT-independent lysosomal repair**

Patrick Niekamp<sup>1</sup>, Felix Scharte<sup>2</sup>, Tolulope Sokoya<sup>1</sup>, Laura Vittadello<sup>3</sup>, Yeongho Kim<sup>4</sup>, Yongqiang Deng<sup>4</sup>, Elisabeth Südhoff<sup>1</sup>, Angelika Hilderink<sup>1</sup>, Mirco Imlau<sup>3</sup>, Christopher J. Clarke<sup>5</sup>, Michael Hensel<sup>2</sup>, Christopher G. Burd<sup>4</sup>, Joost C. M. Holthuis<sup>1</sup>

<sup>1</sup>Molecular Cell Biology Division, Department of Biology and Center of Cellular Nanoanalytics, University of Osnabrück, 49076 Osnabrück, Germany

<sup>2</sup>Microbiology Division, Department of Biology and Center of Cellular Nanoanalytics, University of Osnabrück, 49076 Osnabrück, Germany

<sup>3</sup>Experimental Physics Division, Department of Biology and Center of Cellular Nanoanalytics, University of Osnabrück, 49076 Osnabrück, Germany

<sup>4</sup>Department of Cell Biology, Yale School of Medicine, New Haven, CT, 06520, USA

<sup>5</sup>Department of Medicine and Cancer Center, Stony Brook University, Stony Brook, NY, 11794, USA

The publication accessible under the following DOI corresponds to pages 86-101 in the print version of this thesis.

DOI: <https://doi.org/10.1038/s41467-022-29481-4>

Supplementary information is provided on DVD

**V.4. From vacuole to cytosol – Disruptive invasion triggers cytosolic release of *Salmonella Paratyphi A* and subsequent cytosolic motility favors evasion of xenophagy**

Felix Scharte<sup>1</sup>, Rico Franzkoch<sup>1, 2</sup>, Michael Hensel<sup>1, 3</sup>

<sup>1</sup>Abteilung Mikrobiologie, Universität Osnabrück, Osnabrück, Germany

<sup>2</sup>iBiOs - Integrated Bioimaging Facility Osnabrück

<sup>3</sup>CellNanOs - Center of Cellular Nanoanalytics Osnabrück

Supplementary information is provided on DVD

#### V.4.1. Abstract

*Salmonella enterica* is a common foodborne, facultative intracellular enteropathogen. Typhoidal *S. enterica* serovars like Paratyphi A (SPA) are human restricted and cause a severe systemic disease, while many *S. enterica* serovars like Typhimurium (STM) have a broad host range and in human hosts usually lead to a self-limiting gastroenteritis. There are key differences between typhoidal and non-typhoidal *Salmonella* in pathogenesis, but underlying mechanisms remain largely unknown. Several genes encoding *Salmonella* pathogenicity island (SPI) effector proteins are absent or pseudogenes in SPA. Expression of virulence and metabolism genes show differential expression compared to STM. The intracellular transcriptomic architecture and phenotypes during presence in epithelial cells were recently described. Surprisingly, induction of motility, flagella and chemotaxis genes showed distinct expression patterns in intracellular SPA vs. STM and led to cytosolic motility of SPA. This study applies single cell microscopic analyses approaches to investigate the triggers and cellular consequences of cytosolic motility. Live cell imaging revealed that SPA invades host cells in a highly cooperative manner. Extensive membrane ruffling at the invasion site leads to increased membrane damage in the nascent SCV with subsequent cytosolic release. After release into the cytosol, motile bacteria showed same velocity as under culture conditions used for infection. Reduced decoration by autophagosomal protein LC3B was observed during LCI and electron microscopy. Our results indicate cytosolic motility as possible xenophagy evasion mechanism that could drive disease progression and contribute to dissemination of invasion-primed SPA in systemic infection.

## V.4.2. Introduction

Life inside mammalian host cells is a common virulence strategy of microbial pathogens and various forms of adaptation to life within host cell cytosol or pathogen-containing vacuoles (PCV), as well as exit strategies from host cells occur.

*Salmonella enterica* is a ubiquitous, invasive and facultative intracellular pathogen. Oral uptake of *S. enterica* by contaminated food or water causes infectious diseases ranging from self-limiting gastroenteritis to systemic infections with often fatal outcome (Dougan and Baker, 2014). While non-typhoidal *Salmonella* (NTS) serovars, such as *S. enterica* serovar Typhimurium (STM) often have broad host range, typhoidal *Salmonella* (TS) serovars such as *S. Typhi* (STY) or *S. Paratyphi A* (SPA) are characterized by adaptation to primate hosts in which typhoid or paratyphoid fever are important systemic diseases. The strict host adaptation limits studies of virulence mechanism of TS, and frequently infection models of STM in susceptible mouse strains are used as surrogate to investigate systemic *Salmonella* infections. However, SPA, STY and other TS are distinct from NTS by presence of increased accumulation of pseudogenes (Holt *et al.*, 2009; McClelland *et al.*, 2004), additional virulence factors as Vi capsule (STY) or typhoid toxin (STY, SPA), and distinct regulation of expression of virulence functions (Cohen *et al.*, 2022; Reuter *et al.*, 2021).

Both NTS and TS invade non-phagocytic mammalian cells, such as epithelial cells, by trigger invasion mediated by translocation of effector proteins by the *Salmonella* pathogenicity island 1 (SPI1)-encoded type III secretion system (T3SS). Host cell invasion is considered to initiate the intracellular lifestyle of *Salmonella*, and allows to breach epithelial barriers. Translocation of SPI1-T3SS effector proteins also evokes strong proinflammatory responses of epithelial cells, leading to intestinal inflammation, a hallmark of gastroenteritis by NTS. While SPI1-T3SS also mediates invasion by SPA and STY, intestinal inflammation usually is absent and other routes of entry appear to be used to breach epithelial barriers of the intestines in order to reach systemic sites.

Compiling data on the intracellular lifestyle in mammalian host cells reveal that STM is well-adapted to life in specific PCV, referred to as *Salmonella*-containing vacuole, or SCV. The SCV possesses canonical markers of late endosomal compartments, yet allows STM survival and proliferation. The manipulation of the host cell endosomal system mainly mediated by effector proteins of the SPI2-encoded T3SS is central to SCV formation and maintenance (Jennings *et al.*, 2017).

In addition to survival and proliferation in the SCV, further intracellular fates of STM are observed. If the integrity of the SCV is not maintained, STM is exposed to host cell cytosol. This may evoke xenophagic clearance, induce pyroptotic cell death, or may lead to cytosolic hyper-replication resulting in release of highly infected enterocytes as observed for STM (Brumell *et al.*, 2002; Knodler *et al.*, 2010).

In an approach to understand specific virulence mechanisms of TS, a comprehensive comparative transcriptional analysis of intracellular STM and SPA was performed (Cohen *et al.*, 2022). The data revealed



various differences in expression of metabolic functions and distinct patterns of expression of flagella genes. We followed potential phenotypic consequences of the distinct expression patterns and observed that a subpopulation of intracellular SPA expresses flagella and is motile in host cell cytosol. Such flagella-mediated cytosolic motility was not observed for STM present in host cell cytosol, and clearly is distinct from intracellular motility evolved by other pathogens, where host cell actin polymerization is hijacked by various surface proteins.

Here we set out to analyze why SPA is released into cytosol, and how host cells respond to intracellular motile SPA. In contrast to intracellular motility mediated by actin polymerization, intracellular motility of SPA did not allow intercellular spread. However, flagella-mediated motility enables SPA to avoid xenophagic clearance, as prerequisite of host cell exit of invasion-primed motile SPA.

### V.4.3. Results

#### Early escape to host cell cytosol depends on invasion mechanism of SPA

Although STM and SPA belong to the same species, the disease they cause in humans is very different ranging from a self-limiting gastroenteritis in case of STM infection, to severe systemic disease with potentially lethal outcome caused by SPA. We recently compared the intracellular gene expression profiles of STM and SPA during infection and identified differences in the expression of flagella/chemotaxis, SPI1, and carbon utilization pathways, and demonstrated flagella-mediated movement of SPA in cytosol of host cell (Cohen *et al.*, 2022). Flagella-mediated motility was not observed for intracellular STM, despite a small proportion of STM also enters host cell cytosol.

To further investigate phenotypic heterogeneity of intracellular SPA, we performed live cell imaging (LCI) of infected LAMP1-GFP expressing HeLa cells, and compared SPA WT to isogenic mutant strains deficient in flagella synthesis ( $\Delta fliC$ ), chemotaxis regulation ( $\Delta motAB$ ), or certain effector proteins of SPI1-T3SS ( $\Delta sopE$ ,  $\Delta sopE2$ ) or SPI2-T3SS ( $\Delta sifA$ ) crucial for early and late SCV integrity. Furthermore, a SPA strain with a synthetic zipper invasion mechanism was investigated, i.e. SPA  $\Delta invA$  [ $P_{invF}::Y.p. inv$ ] with defective SPI1-T3SS and *Yersinia pseudotuberculosis* (*Y.p.*) Invasin protein Inv synthesized under control of SPI1 promoter  $P_{invF}$ .

We quantified the intracellular phenotypes in categories of ‘cytosolic motile’ and ‘cytosolic non-motile’, while ‘other’ includes SPA residing in an SCV or showing cytosolic hyper-replication (Fig. V.4.1). In line with previous findings (Cohen *et al.*, 2022), about 38% of SPA WT-infected host cells harbored cytosolic SPA exhibiting intracellular motility, while in 5% of infected cells cytosolic SPA WT were non-motile (Fig. V.4.1AB). SPA mutant strains with defects in maintaining SCV integrity ( $\Delta sifA$ ), or lacking SPI1-T3SS effectors ( $\Delta sopE$ ,  $\Delta sopE2$ ) showed similar results of phenotypes with cytosolic motile SPA  $\Delta sopE$ ,  $\Delta sopE2$  and  $\Delta sifA$  in 30%, 39% and 40 % of infected cells, respectively. This population was absent in cells infected with non-motile mutant strains lacking flagella filament *FliC* (Fig. V.4.1A and Fig. V.4.1C) or with a defective energizing of flagella rotation ( $\Delta motAB$ ) similar to cells exposed to the antibiotics cefotaxime and ciprofloxacin affecting bacterial cell wall synthesis and DNA-replication during infection. As the  $\Delta motAB$  and  $\Delta fliC$  mutant strains are constitutive non-motile, we also tested if motility during invasion has an effect on the intracellular phenotype with inducible *motAB* expression under control of promoter  $P_{tetA}$  which can be induced by non-antibiotic derivatives of tetracycline such as anhydrotetracycline (AHT) (Schulte *et al.*, 2019). We induced expression of *motAB* with AHT in bacterial culture and omitted AHT during infection and the following incubation time to avert motility in infected HeLa cells. SPA  $\Delta motAB$  [ $P_{tetA}::motAB$ ] showed increased invasion compared to  $\Delta motAB$  (Fig. S 4) but also completely lacked cytosolic motile subpopulation. Further, we set out to evaluate the contribution of the mode of invasion to cytosolic release and subsequent intracellular motility with a mutant strain incapable of secretion of trigger invasion-mediating SPI1 effectors ( $\Delta invA$ ).

We introduced a plasmid with *Y.p. inv* under control of SPI1 promoter  $P_{invF}$ , allowing expression under similar conditions as the SPI1-T3SS and therefore enabling SPA invasion by zipper mechanism. Interestingly, this strain showed also no subpopulation of cytosolic motile bacteria in 1% of the infected cells, in fact, the cytosolic subpopulation was almost absent (5%) with SPA predominantly residing in an SCV (Fig. V.4.1A and Fig. V.4.1D). These data confirm previously published data stating trigger invasion as a promoting factor for cytosolic release (Roder and Hensel, 2020).

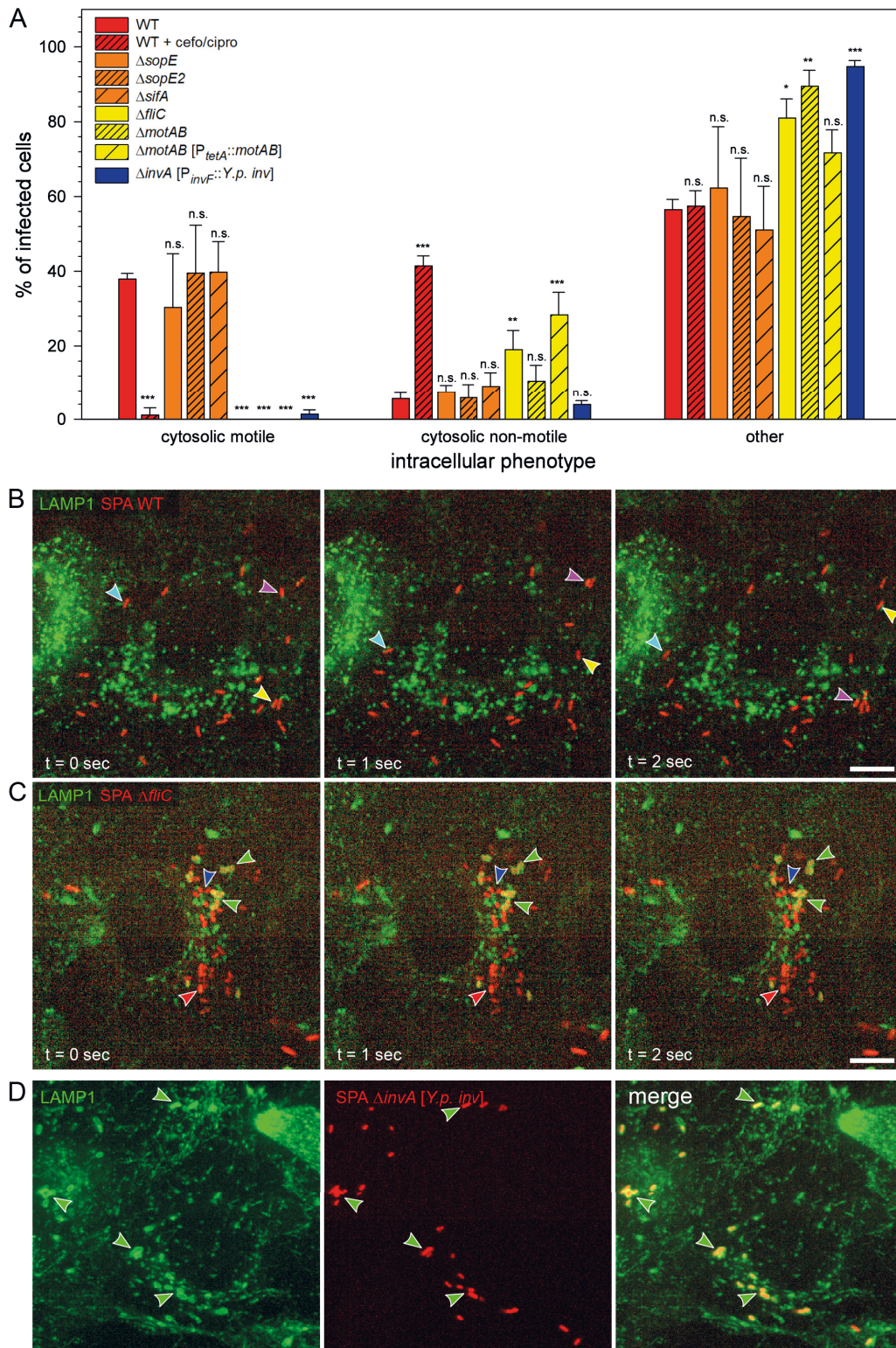


**Fig. V.4.1. Quantification of intracellular SPA phenotypes.** A-E. HeLa cells stably expressing LAMP1-GFP (green) were infected with *Salmonella* Paratyphi A (SPA) WT or isogenic mutant strains expressing mCherry (red) at MOI 30, 60, or 90 for WT,  $\Delta invA$  [ $P_{invF}::Y.p. inv$ ], or  $\Delta fliC$ ,  $\Delta motAB$ , respectively. A. Quantification of intracellular phenotypes was performed during live cell imaging. From 4-6 h p.i., at least 100 infected cells per strain were examined for intracellular phenotypes. Data are means  $\pm$  SD from three independent experiments. Statistical analysis was performed with one-way ANOVA and is indicated as n.s., not significant; \*,  $p < 0.05$ ; \*\*,  $p < 0.01$ ; \*\*\*,  $p < 0.001$ . B, C. Time-lapse images of infected HeLa-LAMP1-GFP cells showing movement of three cytosolic SPA WT (B, turquoise, magenta and yellow arrowhead), no movement of cytosolic SPA  $\Delta fliC$  (C, red and blue arrowhead) and SPA  $\Delta fliC$  residing in SCV (C, green arrowheads). D. Maximum intensity projection of HeLa-LAMP1-GFP cells infected with SPA  $\Delta invA$  [ $P_{invF}::Y.p. inv$ ] residing in SCV (green arrowheads). Scale bars: 10  $\mu$ m.

#### Cooperative trigger invasion of SPA leads to increased membrane damage of the SCV

It was previously described, that the mode of trigger invasion and also the set of involved SPI1 effectors secreted by the T3SS contribute to cytosolic release following host cell entry and that trigger invasion is often a cooperative event (Lorkowski *et al.*, 2014; Roder and Hensel, 2020). We set out to investigate membrane ruffling during invasion by live cell imaging of different STM serovars and SPA WT as well as SPA invading through zipper mechanism (Fig. V.4.2, Fig. S 1, Movie 1, Movie 2, Movie 3, Movie 4). We observed rather small membrane ruffling for STM NCTC 12023 (Fig. V.4.2A, Fig. S 1, Movie 1) and more extensive membrane ruffling for STM SL1344 (Fig. V.4.2B, Fig. S 1, Movie 2). Prolonged and extensive membrane ruffling of a larger cell area was observed for SPA WT (Fig. V.4.2C, Fig. S 1, Movie 3). SPA  $\Delta invA$  [ $P_{invF} Y.p. inv$ ] showed lowest actin rearrangement at the invasion site (Fig. V.4.2D, Fig. S 1, Movie 4). Image analysis of invasion sites indicated that STM NCTC 12023 invasion is characterized by mostly single bacteria at invasion sites (mean = 1.6) whereas during the invasion of STM SL1344 multiple bacteria are involved in the process (mean = 3.2). SPA WT showed highest accumulation of bacteria at sites of membrane rearrangement (mean = 7.3) which is reduced when SPA is invading through zipper mechanism (mean = 2.1).

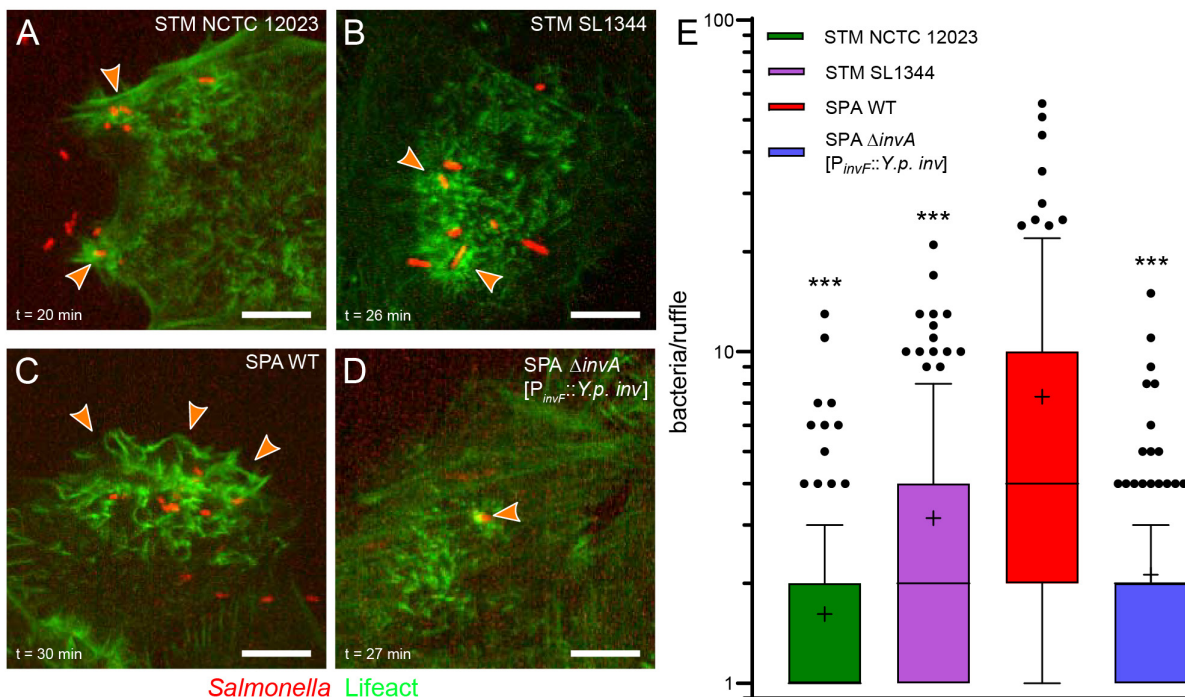


**Fig. V.4.2. SPA induces massive membrane ruffles during trigger invasion, and invades in highly cooperative manner.** A-D. HeLa cells stably expressing Lifeact-eGFP (green) were infected with STM NCTC 12023 (A), STM SL1344 (B), SPA WT (C), or SPA  $\Delta invA$  [ $P_{invF}::Y.p. inv$ ] (D) expressing mCherry (red) at MOI 75. Cells in chambered coverslips were infected on microscope stage and imaged for 1 h by spinning disc confocal microscopy with intervals of 3-5 min between images. Still images from time-lapse are shown. Arrowheads indicate sites of ongoing invasion. Scale bars: 10  $\mu$ m. E. Image series were assessed for invading bacteria per ruffle. Shown are Tukey's box plots of invading bacteria per ruffle during infection with error bars including data of 1.5 x interquartile range (IQR). Outliers beyond the 1.5 x IQR are shown as dots. Middle lines and "+" denote median and mean value, respectively. Compiled from three independent experiments, 200, 169, 170, and 130 individual invasion events were analyzed for STM NCTC 12023, STM SL1344, SPA WT, and SPA  $\Delta invA$  [ $P_{invF}::Y.p. inv$ ], respectively. Statistical analysis compared to SPA WT was performed with unpaired two-tailed t test and is indicated as \*\*\* for  $p < 0.001$ .

#### Trigger invasion enhances membrane damage at nascent SCVs

Previous work revealed that the SCV is prone to ruptures, which are targeted by membrane damage markers like galectins, sphingomyelin or the ESCRT machinery (Ellison *et al.*, 2020; Goser *et al.*, 2020; Paz *et al.*, 2010; Thurston *et al.*, 2012). We used an engineered version of equinatoxin II (EqtSM) as rapid membrane damage reporter that is binding cytosol-exposed sphingomyelin (Deng *et al.*, 2016; Niekamp *et al.*, 2022) and infected HeLa cells expressing Halo-tagged EqtSM with SPA WT or SPA  $\Delta invA$  [ $P_{invF}::Y.p. inv$ ] to assess contribution of invasion mechanism to membrane damage of the nascent SCV (Fig. V.4.3). LCI revealed that trigger invasion of SPA WT enhances SCV disruption in 45% of counted SCVs, in contrast to 14% when SPA is invading through zipper mechanism (Fig. V.4.3D). The results reinforce the notion that the invasion mechanism plays a major role in SCV integrity in subsequent intracellular lifestyle.

#### Motility of cytosolic SPA delays xenophagic clearance

A subset of intracellular pathogens such as *Listeria monocytogenes* (*L.m.*) or *Shigella flexneri* actively escape the early PCV. As the host cell cytosol is a hostile environment for cytosolic bacteria, e.g. due to recognition and clearance by cell-autonomous defense mechanisms such as the autophagosomal machinery, these pathogens evolved sophisticated defense mechanisms to avoid decoration and degradation by expression of proteins interfering and inhibiting xenophagy. Such mechanisms have not been reported for cytosolic *Salmonella*. An intermediate step in autophagic clearance of cytosol-invading bacteria is the ubiquitylation of bacterial structures such as LPS (Otten *et al.*, 2021). While we could also observe ubiquitylation of cytosol-invading SPA (Fig. S 2), we analyzed cytosolic motility of SPA as possible xenophagy counter-mechanism, interfering with decoration of late-autophagic proteins like LC3B, by infecting HeLa cells stably expressing LC3B-GFP and assessed decoration of intracellular SPA with LC3B (Fig. V.4.4, Movie 5, Movie 6). We compared SPA WT with SPA  $\Delta motAB$  [ $P_{tetA}::motAB$ ] (motile during infection but no intracellular motility) and SPA WT treated with cefotaxime and ciprofloxacin (non-motile and non-replicative) regarding LC3B-decoration. SPA infected cells show heterogenous population as representative images in Fig. V.4.4D-F illustrate. The number of bacteria and also the degree of LC3B decoration varies from cell to cell (Fig. V.4.4D-F, Movie 5, Movie 6).

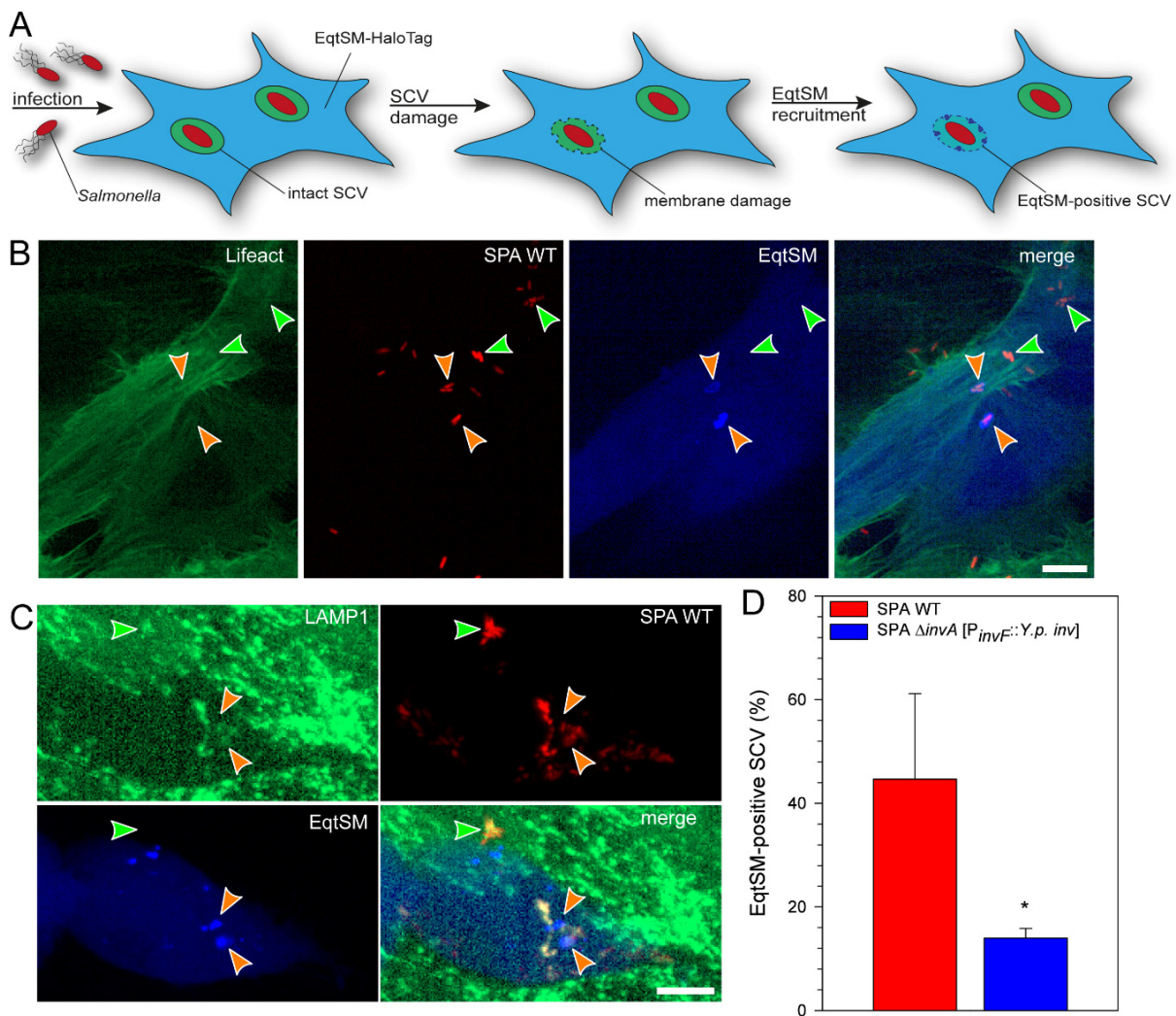


**Fig. V.4.3. Trigger invasion by SPA destabilizes nascent SCVs.** A. To localize sites of SPA-induced membrane damage and to quantify the frequency of SCV damage, HeLa cells stably expressing Lifeact-eGFP (B) or LAMP1-GFP (C) (green) were transfected for expression of EqtSM-HaloTag and labeled with HaloTag-ligand (blue). Subsequently, cells were infected with SPA WT or SPA  $\Delta invA$  [ $P_{invF}::Y.p. inv$ ] expressing mCherry (red). Infected cells were imaged 1-2 h p.i. and representative infected cells are shown as maximum intensity projection. Arrowheads indicate intact SCVs (green), or SCVs targeted by EqtSM (orange). Scale bars: 10  $\mu$ m. D. SCVs were scored for association with EqtSM-HaloTag. Data are means + SD from three independent experiments. Statistical analysis was performed with unpaired two-tailed t test and is indicated as \* for  $p < 0.05$ .

Image analysis of more than 170 infected cells with over 1,200 bacteria per condition (Fig. V.4.4A, Fig. V.4.4B) revealed that residing in an SCV efficiently avoids LC3B decoration for all strains (4.5% LC3B-positive SPA WT, 5.7% LC3B-positive SPA  $\Delta motAB$  [ $P_{tetA}::motAB$ ]) with the highest rate of LC3B decoration observed in cefo/cipro-treated SPA WT (9% LC3B-positive, Fig. V.4.4C), possibly due to failure of maintaining SCV integrity due to antibiotics treatment. However, the cytosolic populations of the respective strains showed significant differences regarding LC3B decoration. The whole cytosolic population of SPA WT showed about 41.5% LC3B-positive bacteria, whereas cytosolic populations of SPA  $\Delta motAB$  [ $P_{tetA}::motAB$ ] and SPA WT + cefo/cipro both showed a high grade of LC3B decoration (70.6%, 79.7%, respectively, Fig. V.4.4C). We further split the cytosolic population into groups of non-motile and motile to analyze the contribution of motility to xenophagic escape.

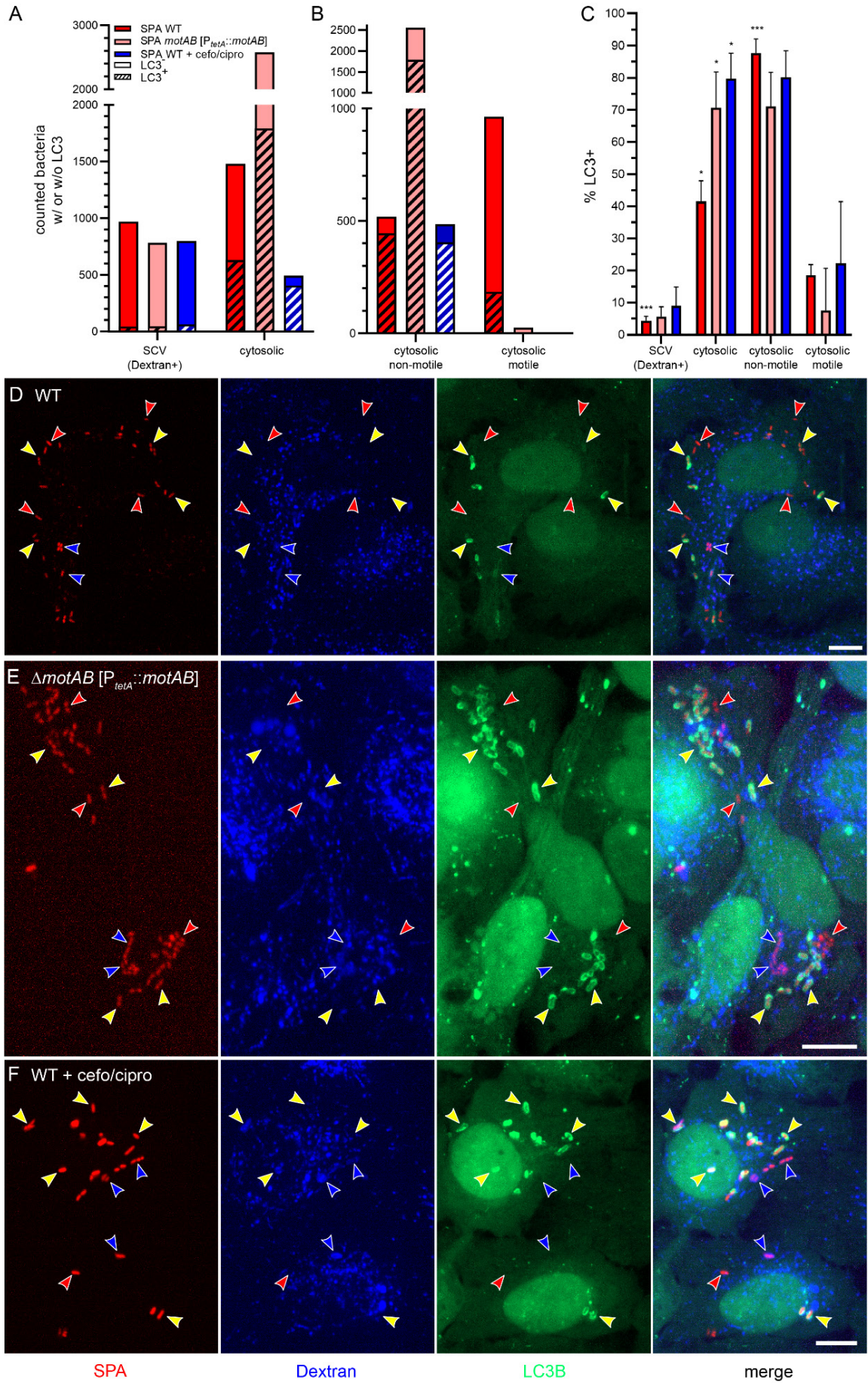


**Fig. V.4.4. Cytosolic non-motile SPA are targeted by autophagosomal membranes.** A-C. HeLa cells stably expressing LC3B-GFP (green) were pulse-chased with Dextran-Alexa647 (blue) and infected with SPA WT or SPA  $\Delta motAB$  [ $P_{tetA}::motAB$ ] expressing mCherry (red) at MOI 30. 100  $\mu\text{g} \times \text{ml}^{-1}$  cefotaxime and ciprofloxacin were added to infected cells at 2 h p.i. if indicated. At 3-4 h p.i. randomly selected cells were imaged and later assessed for SPA associated with LC3B-positive membranes. A, B. Total counts of SPA with (dashed bars) or without (bars) LC3B decoration, compiled from three independent experiments. B. Cytosolic SPA quantified in A were further scored as motile or non-motile, and assessed for LC3B decoration. C. Percentage of SPA targeted by LC3B-containing membranes calculated from data shown in A and B. Data are means  $\pm$  SD of 195 infected cells with 2,450 bacteria for WT, 171 infected cells with 3,360 bacteria for  $\Delta motAB$  [ $P_{tetA}::motAB$ ], and 215 infected cells with 1,291 bacteria for WT + cefto/cipro from three independent experiments. Statistical analysis was performed with one-way ANOVA and is indicated as n.s., not significant; \*,  $p < 0.05$ ; \*\*,  $p < 0.01$ ; \*\*\*,  $p < 0.001$ . D-F. Representative images showing subpopulations in SPA-infected cells. Arrowheads indicate SPA residing in SCV (blue), cytosolic SPA (red), LC3B-decorated SPA (yellow). Images are shown as single Z-plane from stack (D) or as maximum intensity projection (E, F). Scale bars: 10  $\mu\text{m}$ .

Surprisingly, SPA WT showed a high grade of LC3B decoration in the non-motile population (87.7%) and a moderate value of the motile fraction (18.6%). In contrast, the motile fraction is almost absent for SPA  $\Delta motAB$  [ $P_{tetA}::motAB$ ] and SPA WT + cefto/cipro strains with only 31 and 8 counted bacteria, respectively (Fig. V.4.4B). Thus, the grade of LC3B decoration of the cytosolic population of the two strains reflects that of the non-motile fraction with 71.1% and 80.2%, respectively. In summary, our data proposes cytosolic motility as major factor for xenophagic escape.

We also performed correlative light and electron microscopy (CLEM) analyses in order to reveal differences in ultrastructure of the heterogeneous populations (Fig. V.4.5). Light microscopy allowed identification of cytosolic motile and non-motile, as well as SCV-inhabiting SPA for subsequent transmission electron microscopy (TEM) analyses. Whereas cytosolic motile SPA showed no contact to membranous structures, we observed SCV harboring SPA with distinct membrane morphology in close contact to the bacterial envelope (Fig. V.4.5D, E). Cytosolic non-motile SPA showed enclosing LC3B-positive membranes (Fig. V.4.5F).



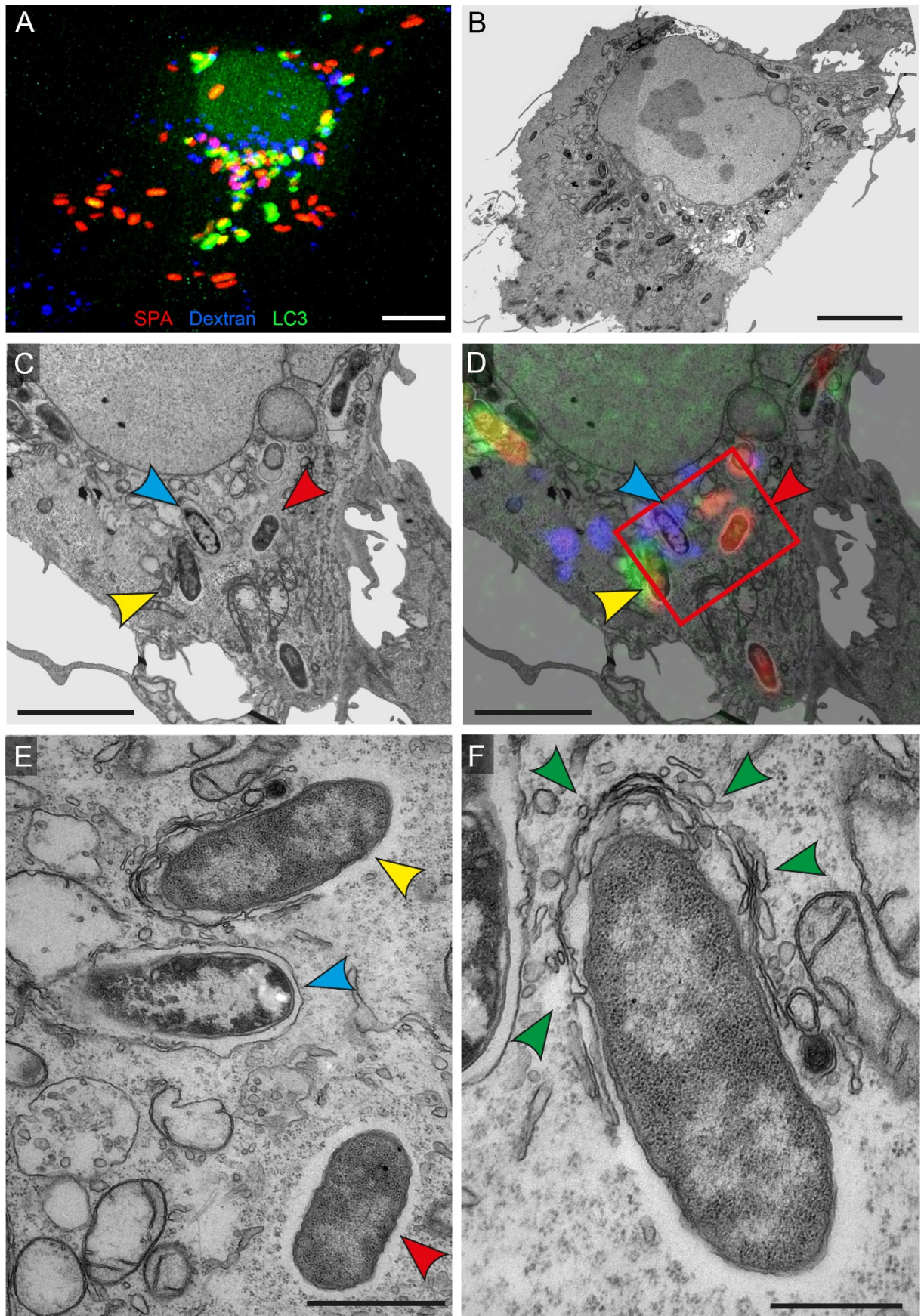


**Fig. V.4.5. Various degrees of xenophagic capture of distinct subpopulations of intracellular SPA.** HeLa cells expressing LC3B-GFP (green) were pulse-chased with Dextran-Alexa647 (blue) and infected with SPA WT expressing mCherry (red) at MOI 30. Cells were fixed 4 h p.i. during LCI (A) and afterwards processed for

transmission electron microscopy (TEM) of ultrathin sections. LCI and TEM images were superimposed for correlation (D) and details are shown at higher magnification (E, F). Arrowheads indicate SPA residing in SCV (blue), cytosolic SPA (red) and SPA targeted by LC3B-positive autophagosomal membrane (yellow). Partial enclosure by autophagosomal membranes is indicated by green arrowheads. Scale bars: 10  $\mu\text{m}$  (A, B), 5  $\mu\text{m}$  (C, D), 1  $\mu\text{m}$  (E), 500 nm (F).

#### Increasing LC3B decoration hinders motility of cytosolic SPA

For many bacteria of different shapes, flagellar movement acts as an important mode of locomotion in their habitat. The rotation of one or multiple flagellar filaments is thereby mediating the forward motion, interrupted by stops to measure chemical gradients and determine the direction. We set out to investigate the maximum velocity of flagella-mediated movement of cytosolic SPA. As previously demonstrated for multiple other bacteria, swimming speed is dependent on type of flagellation and rotation speed of the flagellum (reviewed in Wadhwa and Berg, 2022). First, we compared maximum velocity during different growth conditions in LB medium (Fig. V.4.6A). SPA cultures grown under aerobic conditions showed a median maximum velocity of 11  $\mu\text{m s}^{-1}$  when grown overnight and 42  $\mu\text{m s}^{-1}$  when grown for 3.5 h while SPI1-inducing microaerophilic conditions lead to a median maximum velocity of 26  $\mu\text{m s}^{-1}$ . Other intracellular pathogens such as *L.m.* utilize actin polymerization as a mode of locomotion in host cell cytosol. We observed a median maximum velocity of cytosolic *L.m.* of 0.5  $\mu\text{m s}^{-1}$  (Fig. V.4.6B) which is within the range of previously published data (Lacayo and Theriot, 2004). In contrast, cytosolic SPA were able to move almost as fast as SPA grown under microaerophilic conditions (25  $\mu\text{m s}^{-1}$ ; Fig. V.4.6C).

As described above, a subpopulation of LC3B-decorated SPA is still able to move (Fig. V.4.4, Movie 5, Movie 6). We set out to correlate the maximum velocity of cytosolic SPA with the degree of LC3B-decoration by tracking of individual SPA and parallel measurement of LC3B-GFP fluorescence intensity over time (Fig. V.4.6D, Fig. S 3). Our data indicate a decrease of velocity during increasing decoration by LC3B. Linear regression with principal component analysis shows a negative slope ( $y = -19.5x + 21.9$ ) with maximum velocity dropping down to  $<5 \mu\text{m s}^{-1}$  at a relative LC3B-GFP fluorescence of 0.86 which reflects an almost complete enclosure of SPA.

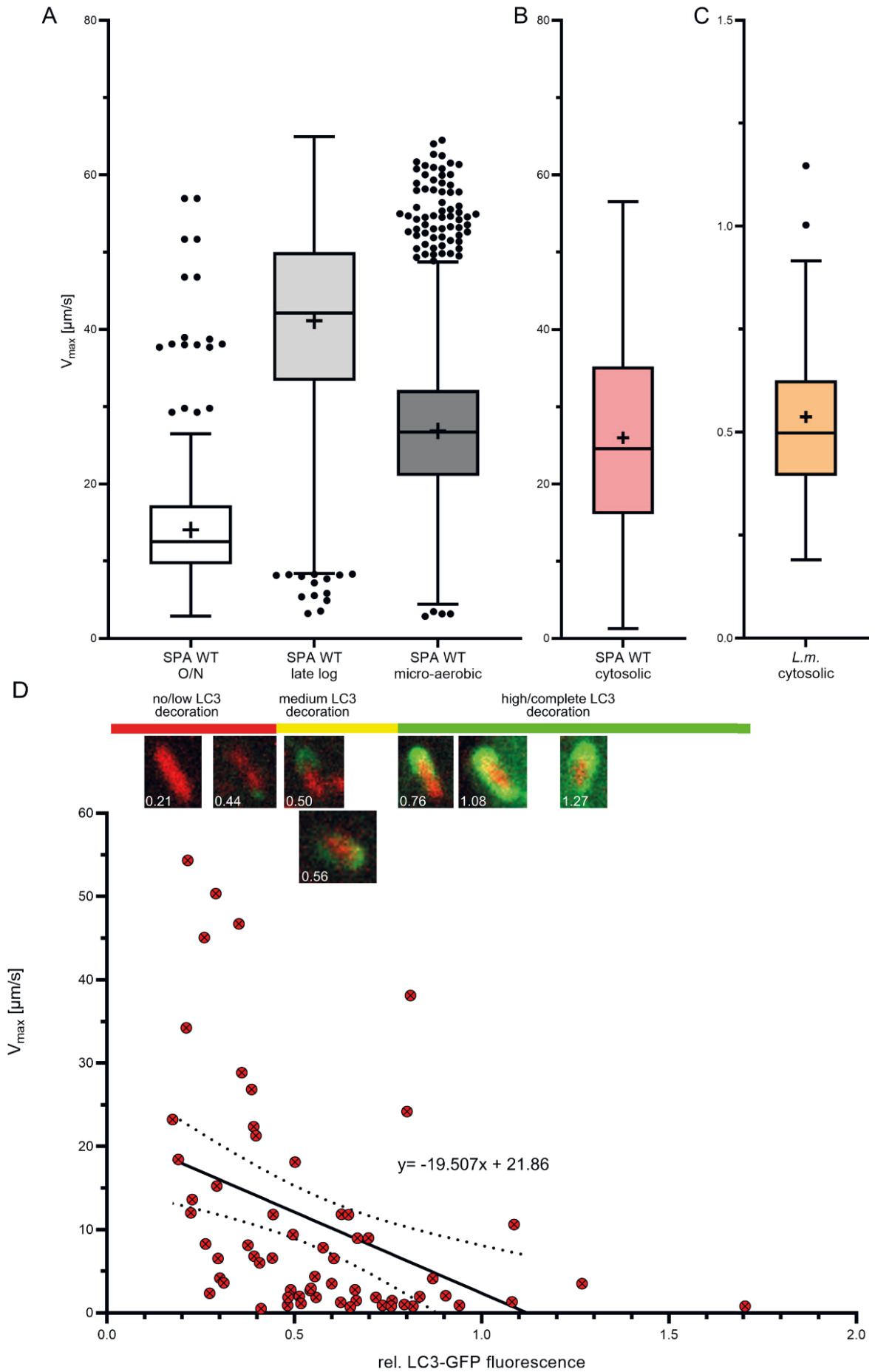


**Fig. V.4.6. Xenophagic capture reduces velocity of intracellular motile SPA.** Single bacterial cells after culture in broth media (A), or within infected host cells (B, C) were registered by LCI. Subsequently, bacterial motility was analyzed by automated (A, C) or manual (B) tracking analyses. A-C. Maximum velocity of single bacterial cells from tracking SPA grown in culture (A), or intracellular SPA (B) or *L.m.* (C). For single cell analyses, tracks of 476 SPA WT from O/N culture, 7,058 SPA WT from late log culture, 2,998 SPA WT from micro-aerobic culture were collected from one experiment. For intracellular bacteria, tracks of 16,248 cytosolic SPA WT were collected from three independent experiments, and 42 tracks for *L.m.* from one experiment. Data are shown as Tukey's box plots with error bars including data of 1.5 x IQR. Outliers beyond the 1.5 x IQR are shown as dots. Middle line denotes median and "+" mean value. D. Plotting of SPA-associated relative LC3B-GFP intensity against maximum velocity of individual cytosolic SPA. Representative images from measurement of fluorescence intensity are shown as single Z-plane from image stacks. Linear regression and 95% confidence bands were calculated for analyses of 63 cytosolic SPA from two independent experiments.

#### V.4.4. Discussion

Our study investigated the causes and contributions of the recently described cytosolic motility of SPA to intracellular lifestyle. We demonstrated that the mode of invasion and the set of SPI1-T3SS effector proteins is substantial for membrane damage at the nascent SCV membrane and cytosolic release in early stage of infection. Furthermore, we could show non-motile SPA are targeted by autophagosomal membranes. However, the population of cytosolic motile SPA is able to delay or escape xenophagic clearance as infection progresses. The main observations of this study are summarized in Fig. V.4.7.

Based on our observations, we propose that release of SPA into cytosol occurs early after invasion, and is likely due to the inability to form a stable nascent SCV. We frequently observed clusters of invading SPA that induce high levels of local actin recruitment, and extensive membrane ruffles. Such events likely lead to incomplete formation of an SCV and may allow clusters of bacteria to directly enter cytosol. This early exit from a labile nascent SCV is so rapid that the transcriptional profile cannot be adjusted to the SCV-specific repression of SPI1 and flagella regulons. We propose that a large proportion of intracellular SPA maintains the transcriptional profile of invading bacteria. This hypothesis may be tested by labelling of flagella, infection, and live cell imaging to follow the fate of flagella on SPA single cells after invasion.

SPA possesses both SopE and SopE2. We previously demonstrated that STM harboring SopE2 and SopE induce more severe membrane ruffles compared to the majority of STM strains only harboring SopE2 (Roder and Hensel, 2020). The more overt trigger invasion by SopE-positive STM was associated with increased cytosolic release, also occurring early after invasion. This may be similar to the nascent SCV damage induced by SPA. However, we did not observe flagella-mediated intracellular motility of SopE/SopE2-positive STM SL1344 (Cohen *et al.*, 2022), indicating further differences between STM and SPA. SPA possesses functional *sopE* and *sopE2*, while STY strains possess functional *sopE* and pseudogenic *sopE2* (Valenzuela *et al.*, 2015), thus damage of nascent SCVs after invasion of STY may be less pronounced compared to SPA.

A factor possible contributing to decreased stability of the nascent SCV is the altered function of SptP, a SPI1-T3SS effector protein with activity antagonistic to SopE. Prior work showed that host cells fails to restore normal actin cytoskeleton organization when SptP is defective and SopE activity overrules (Kubori and Galan, 2003). Recent work by Johnson *et al.* (Johnson *et al.*, 2017) demonstrated that SptP in STY and SPA have several amino acid exchanges that affect the binding of chaperone SicP, and by this the efficiency of translocation.

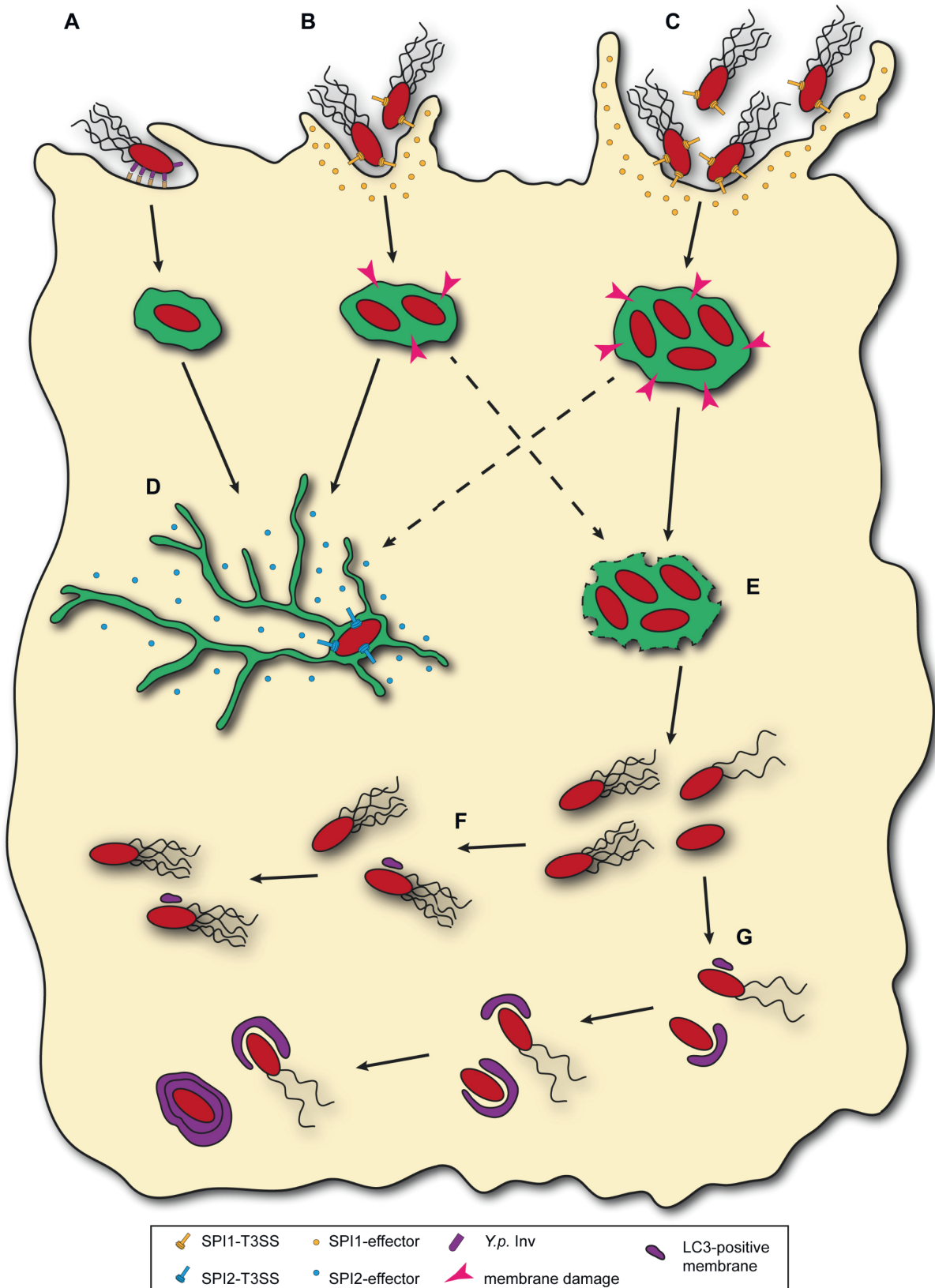


**Fig. V.4.7. Model for SPA entry into host cell cytosol and autophagic decoration.** Zipper and trigger invasion with little membrane ruffling (A, B) primarily lead to an intracellular lifestyle with SCV maturation (D). Trigger invasion with extensive membrane ruffling and increased cooperative invasion (C) lead to membrane damage and

rupture of the nascent SCV (E) and a cytosolic lifestyle of SPA. Flagellated and motile cytosolic SPA delay or escape xenophagic capture (F). Non-motile cytosolic SPA are captured by LC3B-positive membranes (G).

Actin-based intracellular motility enables cell-to-cell spread, and thus enables infection of new host cells without demanding exit and exposure to antimicrobial mechanisms acting on extracellular bacteria. We did not observe intercellular spread of SPA. This may be explained by lower force generated by flagella rotation compared to actin polymerization, and/or the switch between swimming and tumbling that may limit the generation of membrane protrusions that are productive in infection of neighboring cells. Yet, we have to consider that the applied model of confluent cultured non-polarized epithelial cells may not reflect host cell types relevant during infection of human hosts as main host cells of SPA are phagocytic cells, leading to dissemination through the lymphatic system and further colonization of internal organs such as the liver, spleen, bone marrow and gall bladder. Motility of SPA inside phagocytic cell line U937 has only been observed in spacious vacuoles rather than in the cytosol of host cells (Cohen *et al.*, 2022) probably because presence of bacteria in cytosol of phagocytic cells most likely results in inflammatory cell death, so-called pyroptosis (Castanea and Garcia-Del Portillo, 2017). Similar observations were made for STM in gallbladder epithelium (Knodler *et al.*, 2010). In contrast to STM, SPA shows a lower replication rate in host cells (Reuter *et al.*, 2021) and does not induce massive inflammatory response in systemic infections due to bacteria-induced extrusion of infected cells which is considered to contribute to stealth strategy of TS (reviewed in Dougan and Baker, 2014; Hiyoshi *et al.*, 2018a). Certain features of immune evasion, such as avoidance of neutrophil oxidative burst have convergently evolved, i.e. by expression of Vi capsule (STY) or the very long O-antigen of LPS (SPA) (Hiyoshi *et al.*, 2018b). Flagella-mediated intracellular motility has not been reported for STY, and we did not observe increased numbers of cytosolic STY, nor detected flagella expressed by intracellular STY. Functional flagella are expressed by intracellular *Legionella pneumophila* during transition from the replicative to non-replicative, transmissive forms, and a recent study showed that flagellated subpopulations emerge in the *Legionella*-containing vacuole (Schell *et al.*, 2016; Striednig *et al.*, 2021). This transition occurs at the end of the intracellular replication cycle, and stimulates host cell pyroptotic death, and release of *L. pneumophila* for new rounds of host cell infection (Schell *et al.*, 2016). We did not observe induction of host cell death by cytosolic motile SPA, but this host cell response is highly cell type dependent. Further understanding of physiological consequences of intracellular motility of SPA demand analyses in improved infection models such as organoids of human origin that are capable to simulate tissues closely related to *in vivo* conditions (Sepe *et al.*, 2020).

Deficits in metabolic utilization of nutrient sources in host cell cytosol such as glucose-6-phosphate and amino acids and low SPI2-mediated replication inside SCV may contribute to reduced replication numbers of intracellular SPA (Cohen *et al.*, 2022; Forest *et al.*, 2010; Holt *et al.*, 2009). Further analyses with fluorescence reporters regarding intracellular activities would be of interest in the future (Fig. S 5). We showed that the cytosolic population is escaping xenophagic clearance by flagella-based motility and cytosolic replication is reduced. Motile bacteria showed same maximum velocity in host cell cytosol

as under conditions used for infection, interfering with decoration by autophagosomal membranes, although cytosolic bacteria are already ubiquitylated. If decoration by LC3B-positive membranes is only delayed to late time points of infection and if this also leads to lysosomal degradation of engulfed bacteria deserves further investigation. For several *Yersinia* strains it was reported that degradation by fusion with lysosomes is inhibited and *Yersinia* is able to replicate in a non-acidic autophagosome (Connor *et al.*, 2018; Lemarignier and Pizarro-Cerda, 2020; Moreau *et al.*, 2010; Straley and Harmon, 1984). Further investigations assessing acidification of LC3B-positive compartments and interfering with autophagosome formation using Lysotracker, siRNA approaches and autophagy inhibitors such as 3-methyladenine (3-MA) in combination with replication assays could help to understand the host-pathogen interactions in SPA in more detail.

#### **V.4.5. Acknowledgements**

We thank Hans-Peter Schmitz from the division of genetics for help with FACS of HeLa-LC3B-GFP cells. *Listeria monocytogenes* expressing RFP was kindly provided by Martin Loessner, ETH Zürich. This work was supported by the DFG through grant HE1964/23-1 as part of priority program SPP 2225 ‘Exit strategies’, and SFB 944 project Z.



## V.4.6. Materials and Methods

### Bacterial strains and growth conditions

In this study, *Salmonella enterica* serovar Typhimurium (STM) NCTC 12023, STM SL1344 and *S. enterica* serovar Paratyphi A (SPA) 45157 were used as wild-type (WT) strains. All mutant strains are isogenic to the respective WT and **Table V.4.1** shows the characteristics. STM and SPA strains were routinely cultured at 37 °C on Luria-Bertani (LB) agar or in LB broth using a roller drum at 60 rpm. *Listeria monocytogenes* was grown on brain heart infusion (BHI) agar or in BHI broth using a roller drum at 60 rpm. Antibiotics for maintenance of plasmids listed in **Table V.4.2** were added to LB in concentrations of 50 µg x ml<sup>-1</sup> carbenicillin, 50 µg x ml<sup>-1</sup> kanamycin, or 12 µg x ml<sup>-1</sup> chloramphenicol.

### Generation of bacterial strains

Isogenic mutant strains were generated by λ Red recombineering for insertion of kanamycin resistance (*aph*) cassettes amplified from template plasmids pKD4 or pKD13 as described before (Chakravortty *et al.*, 2002; Datsenko and Wanner, 2000) using oligonucleotides listed in **Table V.4.3**. Insertion of *aph* cassettes was confirmed by colony PCR. If required, the *aph* cassette was removed by introduction of pE-FLP for FLP-mediated recombination.

### Construction of plasmids

Plasmids were generated by Gibson assembly as described before (Roder *et al.*, 2021; Roder and Hensel, 2020; Schulte *et al.*, 2019) using oligonucleotides listed in **Table V.4.3**. Plasmids used in this study are listed in **Table V.4.2** and were introduced into the respective strains by electroporation.

### Host cell culture and infection

Host cells were cultured and infected as described previously (Cohen *et al.*, 2021). In short, HeLa cells (ATCC no. CCL-2) were seeded in surface-treated 8-well chambered coverslips (ibidi) 24 or 48 h prior to infection to reach ~80% confluency (~80,000 cells) and were then used for infection. Cells were continuously maintained in high-glucose (4.5 g x l<sup>-1</sup>) DMEM (Merck) supplemented with 10% inactivated fetal calf serum (iFCS, Sigma) at 37 °C in a humidified atmosphere with 5% CO<sub>2</sub>. If indicated, cells were pulse-chased with 100 µg x ml<sup>-1</sup> fluid phase marker Dextran AlexaFluor 647 (Thermo Fisher Scientific) 16 h prior infection. STM strains for infection experiments were subcultured from an overnight culture (1:31) in fresh LB medium and grown for 3.5 h at 37 °C under aerobic conditions using a roller drum at 60 rpm. SPA strains for infection were grown for 8 h under aerobic conditions as described above and subcultured (1:100) in fresh LB medium and stationary-phase subcultures were grown for 16 h under microaerophilic conditions as described in (Elhadad *et al.*, 2015a). For infection with *Listeria monocytogenes*, overnight cultures grown under aerobic conditions were used. Bacteria were adjusted to an optical density of 0.2 at 600 nm in PBS and used for infection with the respective MOI (between 5 and 90, dependent on strain and experiment). Bacteria were centrifuged onto the cells for 5 min at 500

x g to synchronize infection and incubated for 25 min. After washing thrice with PBS, cells were incubated in medium containing 100  $\mu\text{g} \times \text{ml}^{-1}$  of gentamicin to kill extracellular bacteria. Afterwards, cells were maintained in medium containing 10  $\mu\text{g} \times \text{ml}^{-1}$  gentamicin until fixation or LCI. To image invasion of *Salmonella* into HeLa cells, cells were infected directly on microscope stage and imaged for ~1 h.

#### Generation of HeLa cells stably expressing LC3B::GFP

HeLa cells stably expressing LC3B-GFP were generated using 3<sup>rd</sup> generation lentiviral vectors and subsequent fluorescence-activated cell sorting (FACS) (TRC, 2015). Supernatant containing lentivirus was generated by seeding 3.8 x 10<sup>5</sup> cells x ml<sup>-1</sup> HEK 293FT cells (Invitrogen R700-07) in 10 cm tissue culture plates (10 ml per plate, TPP) in antibiotic-free growth media (high-glucose DMEM + 10% iFCS). After 24 h, cells should be 70-80% confluent and were then transfected with lentiviral packaging plasmid (9  $\mu\text{g}$  psPAX2), envelope plasmid (0.9  $\mu\text{g}$  pMD2.G) and pLX304 carrying eGFP-LC3B (9  $\mu\text{g}$ ) using Opti-MEM (Fisher Scientific) and FuGENE HD transfection reagent (Promega). Transfection mix was incubated for 30 min at room temperature before added to cells dropwise. Cells were incubated for at least 18 h and medium was changed to 15 ml growth medium containing 30% iFCS. Medium containing lentivirus was harvested after 24 h and 48 h and centrifuged at 350 x g for 5 min to pellet any residual packaging cells. Supernatant was stored in sterile polypropylene storage tubes and stored at -80 °C. Half of the harvested supernatant was filtered using fast flow & low binding filters (Merck Millipore).

HeLa cells were seeded in 24-well plates (1 x 10<sup>5</sup> cells x ml<sup>-1</sup>) and incubated for 24 h before 8  $\mu\text{g} \times \text{ml}^{-1}$  Polybrene (Sigma) was added to the cells. Filtered supernatant containing lentivirus was added to cells 48 h after seeding. 48 h after lentivirus was added to cells, medium was exchanged to DMEM containing 10  $\mu\text{g} \times \text{ml}^{-1}$  Blasticidin (Invitrogen) and incubated for 72 h. Medium was changed to DMEM without antibiotics to allow growth for 24 h before cells were detached to culture them in tissue culture flasks (TPP) to get a sufficient number of cells for FACS.

For FACS of lentivirus transfected HeLa cells, cells were detached from tissue culture flask and resuspended in appropriate amount of medium to reach concentration of 1 x 10<sup>7</sup> cells x ml<sup>-1</sup>. A 100  $\mu\text{m}$  cell strainer (BD Falcon) was used to prevent aggregation of cells prior to FACS. Cells were sorted for GFP fluorescence with BD FACS Aria. A mixed population of cells with different GFP expression levels was obtained. GFP-positive cells were cultured again in tissue culture flasks before a second round of FACS with Sony SH800S was conducted. Single cells were sorted into 96-well plates to obtain single clones of LC3B-GFP expressing cells. Cell clones were analyzed regarding GFP intensity, cell division and intracellular *Salmonella* phenotypes prior to be used in further experiments.

### Live cell imaging (LCI)

Prior to LCI, medium of infected HeLa cells was changed to high glucose DMEM without phenol red supplemented with 30 mM HEPES. LCI was performed at 37 °C and an atmosphere of 5% CO<sub>2</sub> with Cell Observer microscope (Zeiss) equipped with Yokogawa Spinning Disc Unit CSU X1a5000, an incubation chamber, 63x objective ( $\alpha$ -Plan-Apochromat, NA 1.46) and 40x objective (Plan-Apochromat, NA 1.4), two ORCA Flash 4.0 V3 cameras (Hamamatsu) and appropriate filters for the respective fluorescence proteins or dyes.

### Correlative light and electron microscopy (CLEM)

CLEM of HeLa LC3B-GFP infected by SPA was performed as previously described (Krieger *et al.*, 2014). Briefly, HeLa LC3B-GFP cells were grown on MatTek dishes with gridded coverslips. Cells were fixed with 4% paraformaldehyde (Electron Microscopy Sciences) and 0.1% glutaraldehyde (Electron Microscopy Sciences) in 200 mM HEPES directly on microscope stage during imaging of cytosolic motile SPA. Cells were incubated for 30 min and were then rinsed thrice with 200 mM HEPES buffer. Cells were subsequently fixed with 2.5% glutaraldehyde in 200 mM HEPES for 1 h, washed thrice with buffer and post-fixed with 2% osmium-tetroxide (Electron Microscopy Sciences), 0.1% ruthenium red (Applichem) and 1.5% potassium ferrocyanide (Sigma) in 200 mM HEPES on ice. After several washing steps, the cells were dehydrated in a cold graded series of ethanol and finally one rinse in anhydrous ethanol and two rinses in anhydrous acetone at room temperature. Infiltration was performed with increasing concentrations of EPON812 (Sigma) in anhydrous acetone. Utilizing the coordinate system, the ROI from light microscopy was relocated on the EPON block, trimmed and 70 nm serial sections were cut with an ultramicrotome (Leica EM UC7, Leica, Wetzlar, Germany) and collected on formvar coated copper slot grids (Plano). Grids were post-stained for 30 min with 2% uranyl acetate (Roth) and 20 min with 3% lead citrate (Leica). TEM images were acquired using a Zeiss Leo 912 Omega (Zeiss, Oberkochen, Germany) equipped with a CCD camera (TRS, Moorenwies, Germany). Overlays of the light and electron microscopic images were generated using LAS AF (Leica) and Photoshop CS6 (Adobe).

### Tracking analyses

For microscopic tracking analyses, bacterial cultures were imaged with Cell Observer microscope (Zeiss) equipped with 100x objective ( $\alpha$ -Plan-Apochromat, NA 1.46) and CoolSNAP camera at ~8 frames per second (fps) over 1 min. For tracking of intracellular SPA, infected cells were imaged with Cell Observer microscope (Zeiss) equipped with Yokogawa Spinning Disc Unit CSU X1a5000, an incubation chamber, 63x objective ( $\alpha$ -Plan-Apochromat, NA 1.46), two ORCA Flash 4.0 V3 cameras (Hamamatsu) and appropriate filters for the respective fluorescence proteins at ~18 fps over 1 min. Tracking analyses were performed in Fiji with TrackMate v5.0.2 plugin (Tinevez *et al.*, 2017) with minimal displacement threshold of 1  $\mu$ m. For tracking of intracellular *L.m.*, infected cells were imaged

with setup as described for intracellular SPA at ~0.1 fps over 10-30 min. Tracking analyses were performed in FIJI with manual tracking plugin.

#### Analyses of LC3B-decoration

For analyses of LC3B-decoration of intracellular SPA, randomly selected infected cells were imaged 3-4 h p.i. as described above and were analyzed manually regarding LC3B-GFP signal at SPA cell bodies. 100 µg x ml<sup>-1</sup> cefotaxime and ciprofloxacin were added 2 h p.i. if indicated.

For correlation of maximum velocity and LC3B decoration of cytosolic SPA, individual bacteria were analyzed regarding LC3B-GFP fluorescence intensity using ZEISS Efficient Navigation (ZEN) software. Manual tracking with the same bacteria was performed as described above.

#### Transfection of HeLa cells with Halo-tagged EqtSM

HeLa cells were maintained and infected as described above. In short, cells were seeded in 8-wells 2 d prior infection. Cells were transfected with Halo-tagged EqtSM expression construct 1 d prior infection using FuGENE HD in 1:2 ratio. Infected cells were labeled with 100 nM Janelia Fluor 646 HaloTag (Promega, GA1120) for 30 min, washed five times with PBS and subsequently imaged using the Zeiss Cell Observer SD microscope set-up.

#### Immuno-staining and fluorescence microscopy

For immuno-staining of HeLa LAMP1-GFP cells infected by SPA, cells were seeded in 24-well plates (TPP) on coverslips 24 h or 48 h prior infection to reach ~80% confluency (~180,000 cells). Cultivation of bacteria and infection of HeLa cells was carried out as described above. Infected cells were fixed with 3% PFA at the desired time point. After washing thrice with PBS, cells were incubated in blocking solution (2% goat serum, 2% BSA, 0.1% saponin in PBS) for 30 min. Next, cells were incubated for 1 h at RT with mouse monoclonal antibodies against Ubiquitin (Biomol PW 8810). After washing cells thrice with PBS, cells were incubated with primary antibodies against *Salmonella* O-Antigen of SPA (BD Difco 229471) for 1 h. After washing thrice with PBS, cells were stained with the appropriate secondary antibodies for 1 h (Invitrogen A11031, Dianova 111-607-003). After three washing steps with PBS, coverslips were mounted with Fluoroshield (Sigma) and sealed with Entellan (Merck). Microscopy of fixed samples was performed with Leica SP5 confocal laser-scanning microscope using 100x objective (HCX PL APO CS, NA 1.4-0.7) and polychroic mirror TD 488/543/633.

#### Flow cytometry

The assay was performed as described previously (Reuter *et al.*, 2021). Briefly, HeLa cells were seeded in 12-well plates (TPP) 48 h prior infection to reach confluency (~4 x 10<sup>5</sup> cells per well) on the day of infection. Cells were infected with STM and SPA cultures at MOI 30 as described above. The bacterial strains harbored fluorescence reporter plasmids. At 1 h and 3 h p.i., cells were washed thrice with PBS,

detached from culture plates, fixed with 3% PFA and analyzed by flow cytometry using Attune NxT cytometer. At least 3,000 infected cells were measured and analyzed regarding expression of fluorescence reporter.

#### Gentamicin protection assays

The assay was performed as described before (Kuhle and Hensel, 2002). Briefly, HeLa cells were seeded in 24-well plates (TPP) 48 h prior infection to reach confluency ( $\sim 2 \times 10^5$  cells per well) on the day of infection. Cells were infected with STM and SPA cultures at MOI 5 as described above. Cells were washed thrice with PBS and lysed using 0.1% Triton X-100 at 1 h and 16 h p.i. Colony forming units were determined by plating serial dilutions of lysates and inoculum on Mueller-Hinton II agar and incubated overnight at 37 °C. The percentage of internalized bacteria of the inoculum (from subcultures) and the replication rate of intracellular bacteria was calculated.

## V.4.7. Tables

Table V.4.1. Bacterial strains used in this study

Designation	Relevant characteristics	Reference
<i>S. Typhimurium</i> NCTC 12023 (ATCC 14028) (MvP)	wild type, <i>sopE2</i>	Lab collection
MvP503	$\Delta$ <i>sifA</i> ::FRT	(Kuhle and Hensel, 2002)
MvP1890	$\Delta$ <i>ssaV</i> ::FRT	(Noster <i>et al.</i> , 2019)
MvP2769	$\Delta$ <i>uhpT</i> ::aph	This study
MvP2801	$\Delta$ <i>uhpT</i> ::FRT	This study
MvP818	$\Delta$ <i>invC</i> ::FRT	(Gerlach <i>et al.</i> , 2008)
<i>S. Typhimurium</i> SL1344	wild type, <i>sopE</i> , <i>sopE2</i>	Lab collection
<i>S. Paratyphi</i> A 45157 (SPA)	wild type, clinical isolate, Nepal outbreak in 2009	(Gal-Mor <i>et al.</i> , 2012)
SPA146	$\Delta$ <i>sopE</i> ::aph	This study
SPA147	$\Delta$ <i>sopE2</i> ::aph	This study
SPA110	$\Delta$ <i>sifA</i> ::aph	(Reuter <i>et al.</i> , 2021)
SPA144	$\Delta$ <i>fliC</i> ::FRT	(Cohen <i>et al.</i> , 2022)
SPA145	$\Delta$ <i>motAB</i> ::aph	This study
SPA <i>invA</i>	$\Delta$ <i>invA</i> ::FRT	(Elhadad <i>et al.</i> , 2015b)
SPA <i>ssaR</i>	$\Delta$ <i>ssaR</i> ::FRT	(Reuter <i>et al.</i> , 2021)
<i>Listeria monocytogenes</i> EGD	EGDe::pPL2P <sub><i>xyl</i>long</sub> -Lm RFP	(Studer <i>et al.</i> , 2016)

Table V.4.2. Plasmids used in this study

Designation	Relevant characteristics	Reference
p3589	P <sub>ppsM</sub> ::mCherry, Cm <sup>r</sup>	(Lorkowski <i>et al.</i> , 2014)
pFPV-mCherry	P <sub>ppsM</sub> ::mCherry, Carb <sup>r</sup>	(Drecktrah <i>et al.</i> , 2008)
pKD4	template <i>aph</i> cassette	Datsenko and Wanner, 2000
pKD13	template <i>aph</i> cassette	Datsenko and Wanner, 2000
pWRG730	Red recombinase expression	(Hoffmann <i>et al.</i> , 2017)
pMD2.G	2 <sup>nd</sup> generation lentiviral packaging vector, Carb <sup>r</sup>	Addgene #12259
psPAX2	VSV-G envelope expressing vector, Carb <sup>r</sup>	Addgene #12260
p3776	P <sub>EM7</sub> ::RFP P <sub>ssaG</sub> ::sfGFP, Carb <sup>r</sup>	(Roder and Hensel, 2020)
p5400	pLX304 eGFP::LC3B, 3 <sup>rd</sup> generation lentivirus vector, Carb <sup>r</sup>	This study, based on Addgene #25890
p4114	P <sub>invF</sub> :: <i>Y.p. inv</i> , Carb <sup>r</sup>	(Roder and Hensel, 2020)
p4889	P <sub>EM7</sub> ::RFP P <sub>uhpT</sub> ::sfGFP, Carb <sup>r</sup>	(Roder and Hensel, 2020)
p5212	STM <i>uhpABCT</i> , Kan <sup>r</sup>	This study
p5387	P <sub>EM7</sub> ::mScarlet-I P <sub>sopE</sub> ::sfGFP, Carb <sup>r</sup>	This study
p5776	EqtSMcyto::HaloTag in pLX304, Carb <sup>r</sup>	This study, based on (Niekamp <i>et al.</i> , 2022)
p5825	P <sub>sopE</sub> ::sfGFP::LVA, Carb <sup>r</sup>	This study
p5833	P <sub>invF</sub> :: <i>Y.p. inv</i> P <sub>EM7</sub> ::tagRFP-T, Carb <sup>r</sup>	This study
p6159	tetR P <sub>tetA</sub> ::motAB, Carb <sup>r</sup>	This study

Table V.4.3. Oligonucleotides used in this study

Designation	Sequence 5' - 3'
<b>Red mutagenesis</b>	
sopE-Del-For	GGGCCGGCAGTGTGGACAAATAAAGTCGTTAAAGATTTTGTGTAGGCTGGAGCTGCTTC
sopE-Del-Rev	AGGAAGAGGCTCCGCATATTTTTGGTTTTTCAGTGTTCACATATGAATATCCTCCTTAG
sopE2-Red-Del-For	AAAGTGTAGCTATGCATAGTTATCTAAAAGGAGAACTACCGTGTAGGCTGGAGCTGCTTC
sopE2-Red-Del-Rev	TTAATTCATATGTTAATAGCAGTATTTACTACCACATATGAATATCCTCCTTAG
MotA-Del13-For	CAACAGCGGAAGGATGATGTCGTCTTATCTTATTAGTTATTCGGGGGATCCGTCGACC
MotB-Del13-Rev	TTCCGCTTTGGCGATGTGGTACGCTTGCCGGGGGCTGTAGGCTGGAGCTGCTTCG
uhpT Del13 For	CCATTCGCAGGTATAAAAATTAGCTCAGGAGTAATCCATGATTCGGGGGATCCGTCGACC
uhpT Del13 Rev	CGTTACCAAAATGCACACATTTAAGCGATATTGACTTGTGCTGTAGGCTGGAGCTGCTTCG
<b>Check PCR</b>	
K2-red-del	CGGTGCCCTGAATGAACTGC
SopE-Delcheck-Rev	TTAGCACTGGTAAATGACGGTTTA
sopE2-ckeek-rev4	GCGTCGCCATAAAAAACGAATA
MotB-Check-Rev	CCTGCAGAAATAGTGAAGCCG
Q5SDM-ins-sfGFP-Rev	GCACCACACCCGGTAAACA
Seq-For	CGCCAGGGTTTTCCCAAGTCACGAC
MotA-Check-Rev	ATCATCGCCGTCATAAAATC
uhpT DelCheck For	GCTGTTGCCATTTCTGAACG
uhpT DelCheck Rev	ACAGGATGCCCA TCATAACG
<b>Gibson assembly</b>	
Vf-p3776 5	GATCCTACGTACCCGGGAAAGAGGAGAAAAGTATGC
Vr-p4589 3	AGAAAA TAATAAAAAAGCCGGATTAATAATCTG
1f-SPA-PsopE	GATTATTAATCCGGCTTTTTATTAATTTTCGGCCAGTGTACGTTCAA
1r-SPA-PsopE	TCCCGGTACGTAGGATCGGTAATGATCCTTTTATATGTACATAAC
Vf-PtetA	TCCGGGATGATTCACCCGAC
Vr-PtetA	TTACATTTTCCTACTACTGATAGGGAGTGGTA
1f-ptetA-SPAmotAB	CCCTATCAGTGATAGAGAAAAGTGAAAGTGTCTTATCTTATTAGGTTACCTGGT
1r-SPAmotAB-ptetA	GGTGAATCAATCGCCGGATCACCCICGGTTCGGCTTTTG



#### V.4.8. Movies

**Movie 1: Live-cell imaging of STM NCTC 12023 trigger invasion.** HeLa cells stably expressing Lifeact-GFP (green) were infected with STM NCTC 12023 WT expressing mCherry (red) and imaged over 1 h. Movie shows 2 individual clips successively. Time stamp in upper corner indicates hrs:min:sec. Scale bar: 10  $\mu$ m.

**Movie 2: Live-cell imaging of STM SL1344 trigger invasion.** HeLa cells stably expressing Lifeact-GFP (green) were infected with STM SL1344 WT expressing mCherry (red) and imaged over 1 h. Movie shows 3 individual clips successively. Time stamp in upper corner indicates hrs:min:sec. Scale bar: 10  $\mu$ m.

**Movie 3: Live-cell imaging of SPA WT trigger invasion.** HeLa cells stably expressing Lifeact-GFP (green) were infected with SPA WT expressing mCherry (red) and imaged over 1 h. Movie shows 2 individual clips successively. Time stamp in upper corner indicates hrs:min:sec. Scale bar: 10  $\mu$ m.

**Movie 4: Live-cell imaging of SPA zipper invasion.** HeLa cells stably expressing Lifeact-GFP (green) were infected with SPA *invA* [*Y.p. inv*] expressing mCherry (red) and imaged over 1 h. Movie shows 3 individual clips successively. Time stamp in upper corner indicates hrs:min:sec. Scale bar: 10  $\mu$ m.

**Movie 5: Live-cell imaging of intracellular SPA WT targeted by LC3B.** HeLa cells stably expressing LC3B-GFP (green) were infected with SPA WT expressing mCherry (red) and imaged every two minutes over two hours. Movie shows 3 individual clips with various degrees of xenophagic capture successively. Time stamp in upper corner indicates minutes. Scale bar: 10  $\mu$ m.

**Movie 6: Real-time imaging of intracellular SPA WT.** HeLa cells stably expressing LC3B-GFP (green) were infected with SPA WT expressing mCherry (red) and pulse-chased with Dextran AlexaFluor 647 (blue) if indicated and imaged at a frame rate of 2-3 frames per second. Movie shows 3 individual clips with various degrees of xenophagic capture successively. Time stamp in upper corner indicates sec:ms. Scale bar: 10  $\mu$ m.

V.4.9. Supplementary Figures

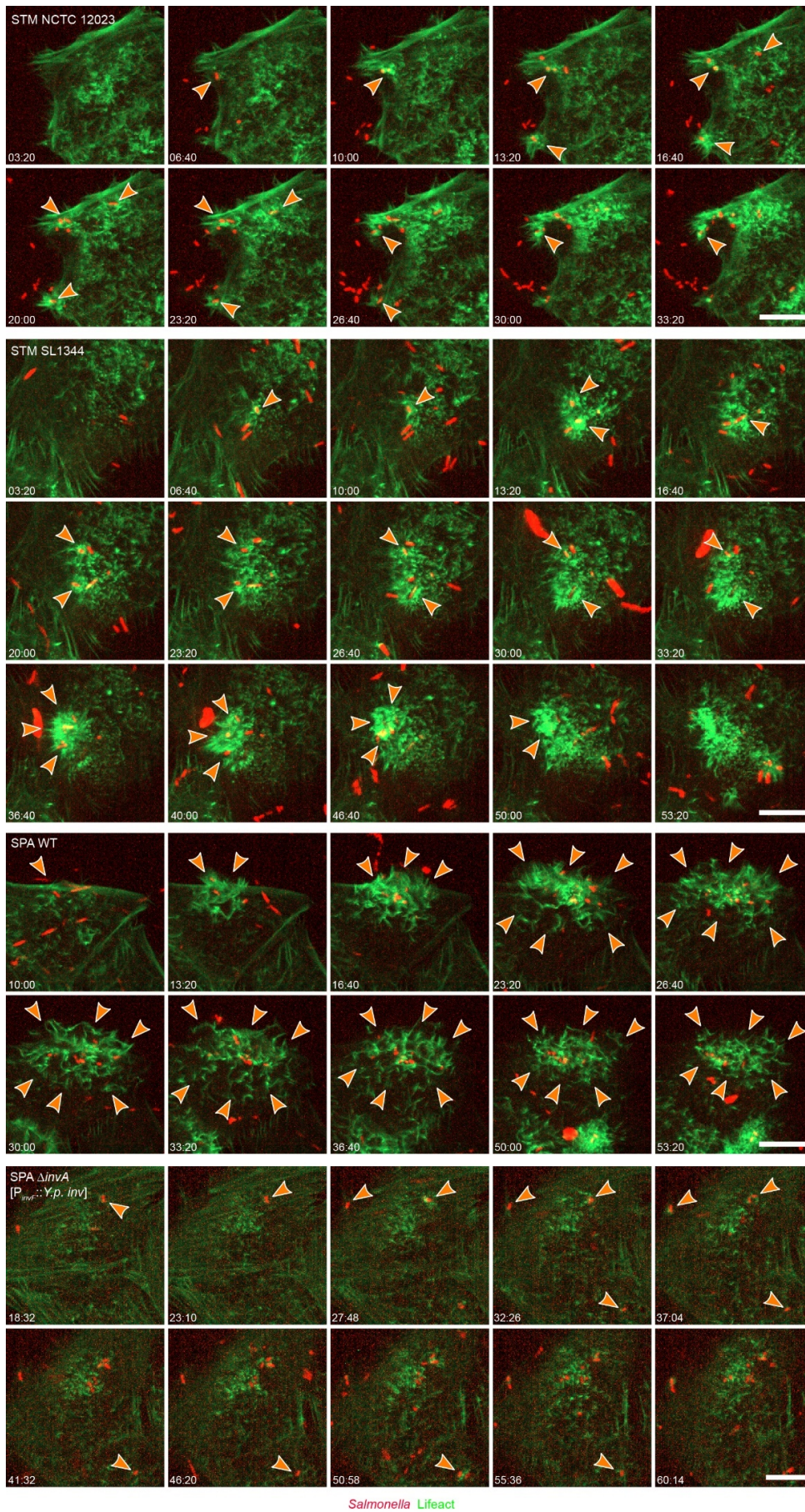


**Fig. S 1. SPA trigger invasion induces massive membrane ruffles and mediates highly cooperative invasion.** HeLa cells stably expressing Lifeact-eGFP (green) were infected as indicated with STM NCTC 12023, STM SL1344, SPA WT, or SPA  $\Delta invA$  [ $P_{invA}::Y.p. inv$ ] expressing mCherry (red) at MOI 75. Cells were infected on microscope stage and imaged for 1 h by spinning disc confocal microscopy. Still images from representative time-lapse series are shown, corresponding with the quantitative analyses shown in Fig. V.4.2. Time stamp indicating min:sec. Sites of ongoing invasion used for quantification of number of bacteria are indicated by arrowheads. Scale bars: 10  $\mu$ m.

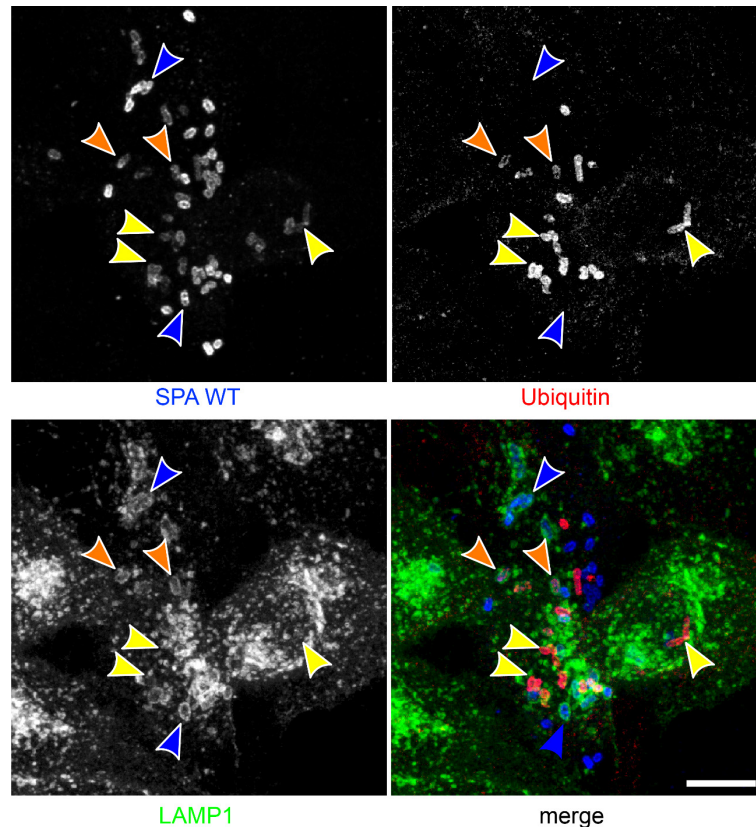


**Fig. S 2. Ubiquitylation of cytosolic SPA.** HeLa cells expressing LAMP1-GFP (green) were infected with SPA WT at MOI 30. Cells were fixed at 7 h p.i. and immunolabeled for SPA LPS (blue) and ubiquitin (red) prior to confocal microscopy. A representative maximum intensity projection of an infected host cell is shown. Arrowheads indicate SPA in SCV without ubiquitin signal (white), cytosolic SPA with ubiquitin signal (yellow), and SPA within partially intact SCV and ubiquitin signal (orange), Scale bar: 10  $\mu$ m.

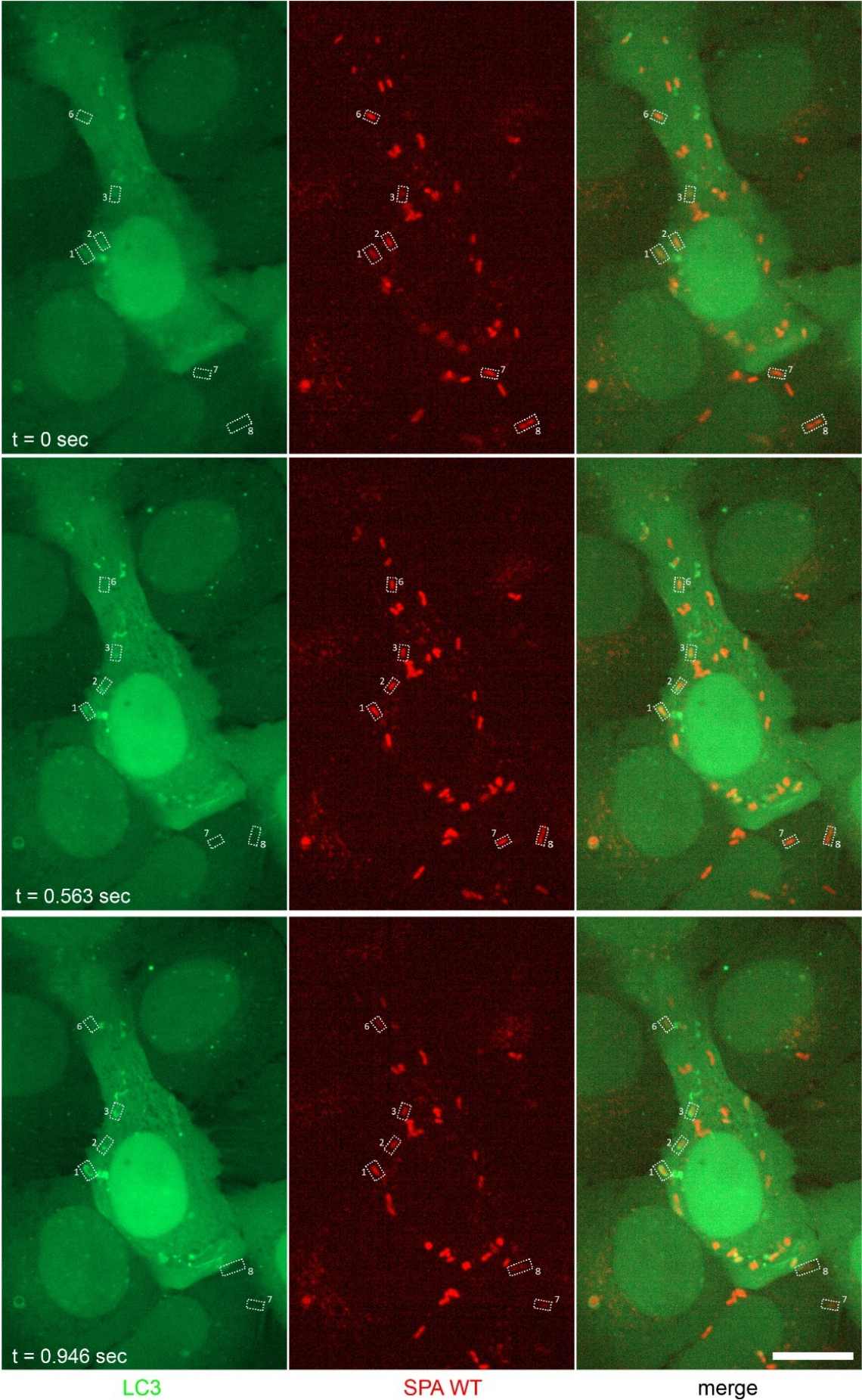


**Fig. S 3. Single cell quantification of LC3B-GFP fluorescence intensity and velocity of cytosolic SPA.** HeLa LC3B-GFP cells were infected with SPA WT expressing mCherry at MOI 30. At 3-4 h p.i. cells were imaged and cytosolic SPA were identified (boxes). For single SPA cells LC3B-GFP fluorescence signal intensity was recorded, and velocity was determined by single cell tracking. Three time points of a representative time lapse series are shown, and quantitative data are displayed in Fig. V.4.6. Images shown are single Z-planes from a stack. Scale bar: 10  $\mu$ m.

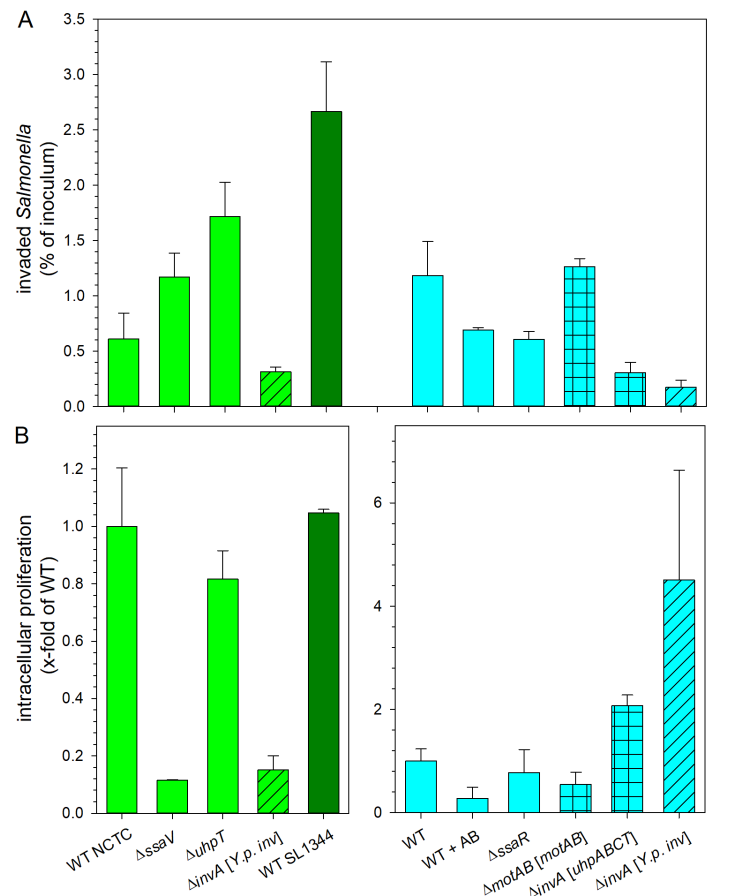


**Fig. S 4. Host cell invasion and intracellular replication of various STM and SPA strains.** HeLa cells were infected with STM (green) or SPA (cyan) WT or isogenic mutant strains at MOI 5. Presence of plasmids for expression of *Y.p. inv*,  $P_{tetA}::motAB$  or STM *uhpABCT* is indicated by hatched bars. AB indicates addition of antibiotics cefotaxime and ciprofloxacin. Invasion (A) and intracellular replication (B) were determined by gentamicin protection assays comparing CFU counts of inoculum with lysates 1 h and 16 h p.i. Depicted are means  $\pm$  SD of one biological replicate performed as triplicate.

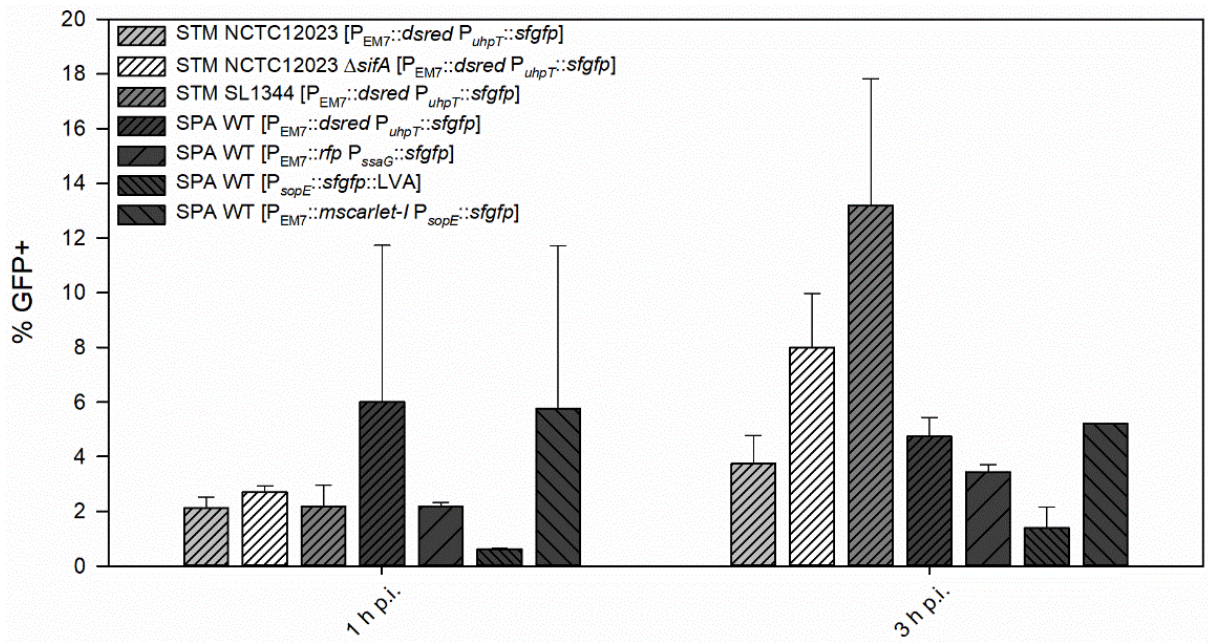


**Fig. S 5. Intracellular fate of STM and SPA.** HeLa cells infected with *Salmonella* were fixed at 1 h and 3 h p.i. and at least 3,000 bacteria per condition were analyzed by flow cytometry to determine induction of dual fluorescence reporter plasmids. Depicted are means +/- SD of one biological replicate performed as duplicate.

#### V.4.10. References

- Brumell, J.H., Tang, P., Zaharik, M.L., and Finlay, B.B. (2002). Disruption of the *Salmonella*-containing vacuole leads to increased replication of *Salmonella enterica* serovar typhimurium in the cytosol of epithelial cells. *Infect Immun* 70, 3264-3270.
- Castanheira, S., and Garcia-Del Portillo, F. (2017). *Salmonella* Populations inside Host Cells. *Front Cell Infect Microbiol* 7, 432.
- Chakravorty, D., Hansen-Wester, I., and Hensel, M. (2002). *Salmonella* pathogenicity island 2 mediates protection of intracellular *Salmonella* from reactive nitrogen intermediates. *J Exp Med* 195, 1155-1166.
- Cohen, E., Azriel, S., Auster, O., Gal, A., Zitronblat, C., Mikhlin, S., Scharte, F., Hensel, M., Rahav, G., and Gal-Mor, O. (2021). Pathoadaptation of the passerine-associated *Salmonella enterica* serovar Typhimurium lineage to the avian host. *PLoS Pathog* 17, e1009451.
- Cohen, H., Hoede, C., Scharte, F., Coluzzi, C., Cohen, E., Shomer, I., Mallet, L., Holbert, S., Serre, R.F., Schiex, T., *et al.* (2022). Intracellular *Salmonella* Paratyphi A is motile and differs in the expression of flagella-chemotaxis, SPI-1 and carbon utilization pathways in comparison to intracellular *S. Typhimurium*. *PLoS Pathog* 18, e1010425.
- Connor, M.G., Pulsifer, A.R., Chung, D., Rouchka, E.C., Ceresa, B.K., and Lawrenz, M.B. (2018). *Yersinia pestis* Targets the Host Endosome Recycling Pathway during the Biogenesis of the *Yersinia*-Containing Vacuole To Avoid Killing by Macrophages. *mBio* 9.
- Datsenko, K.A., and Wanner, B.L. (2000). One-step inactivation of chromosomal genes in *Escherichia coli* K-12 using PCR products. *Proc Natl Acad Sci U S A* 97, 6640-6645.
- Deng, Y., Rivera-Molina, F.E., Toomre, D.K., and Burd, C.G. (2016). Sphingomyelin is sorted at the trans Golgi network into a distinct class of secretory vesicle. *Proc Natl Acad Sci U S A* 113, 6677-6682.
- Dougan, G., and Baker, S. (2014). *Salmonella enterica* serovar Typhi and the pathogenesis of typhoid fever. *Annu Rev Microbiol* 68, 317-336.
- Drecktrah, D., Levine-Wilkinson, S., Dam, T., Winfree, S., Knodler, L.A., Schroer, T.A., and Steele-Mortimer, O. (2008). Dynamic behavior of *Salmonella*-induced membrane tubules in epithelial cells. *Traffic* 9, 2117-2129.
- Elhadad, D., Desai, P., Rahav, G., McClelland, M., and Gal-Mor, O. (2015a). Flagellin Is Required for Host Cell Invasion and Normal *Salmonella* Pathogenicity Island 1 Expression by *Salmonella enterica* Serovar Paratyphi A. *Infect Immun* 83, 3355-3368.
- Elhadad, D., McClelland, M., Rahav, G., and Gal-Mor, O. (2015b). Feverlike Temperature is a Virulence Regulatory Cue Controlling the Motility and Host Cell Entry of Typhoidal *Salmonella*. *J Infect Dis* 212, 147-156.
- Ellison, C.J., Kukulski, W., Boyle, K.B., Munro, S., and Randow, F. (2020). Transbilayer Movement of Sphingomyelin Precedes Catastrophic Breakage of Enterobacteria-Containing Vacuoles. *Curr Biol* 30, 2974-2983 e2976.
- Forest, C.G., Ferraro, E., Sabbagh, S.C., and Daigle, F. (2010). Intracellular survival of *Salmonella enterica* serovar Typhi in human macrophages is independent of *Salmonella* pathogenicity island (SPI)-2. *Microbiology* 156, 3689-3698.
- Gal-Mor, O., Suez, J., Elhadad, D., Porwollik, S., Leshem, E., Valinsky, L., McClelland, M., Schwartz, E., and Rahav, G. (2012). Molecular and cellular characterization of a *Salmonella enterica* serovar Paratyphi a outbreak strain and the human immune response to infection. *Clin Vaccine Immunol* 19, 146-156.
- Gerlach, R.G., Claudio, N., Rohde, M., Jackel, D., Wagner, C., and Hensel, M. (2008). Cooperation of *Salmonella* pathogenicity islands 1 and 4 is required to breach epithelial barriers. *Cell Microbiol* 10, 2364-2376.
- Goser, V., Kehl, A., Roder, J., and Hensel, M. (2020). Role of the ESCRT-III complex in controlling integrity of the *Salmonella*-containing vacuole. *Cell Microbiol* 22, e13176.
- Hiyoshi, H., Tiffany, C.R., Bronner, D.N., and Baumler, A.J. (2018a). Typhoidal *Salmonella* serovars: ecological opportunity and the evolution of a new pathovar. *FEMS Microbiol Rev* 42, 527-541.

- Hiyoshi, H., Wangdi, T., Lock, G., Saechao, C., Raffatellu, M., Cobb, B.A., and Baumler, A.J. (2018b). Mechanisms to Evade the Phagocyte Respiratory Burst Arose by Convergent Evolution in Typhoidal *Salmonella* Serovars. *Cell reports* 22, 1787-1797.
- Hoffmann, S., Schmidt, C., Walter, S., Bender, J.K., and Gerlach, R.G. (2017). Scarless deletion of up to seven methyl-accepting chemotaxis genes with an optimized method highlights key function of CheM in *Salmonella* Typhimurium. *PLoS One* 12, e0172630.
- Holt, K.E., Thomson, N.R., Wain, J., Langridge, G.C., Hasan, R., Bhutta, Z.A., Quail, M.A., Norbertczak, H., Walker, D., Simmonds, M., *et al.* (2009). Pseudogene accumulation in the evolutionary histories of *Salmonella enterica* serovars Paratyphi A and Typhi. *BMC Genomics* 10, 36.
- Institute, T.R.C.T.B. (2015). Lentivirus production of ShRNA, CRISPR, or ORF-pLX clones in 10 cm dishes or 6-well plates.
- Jennings, E., Thurston, T.L.M., and Holden, D.W. (2017). *Salmonella* SPI-2 Type III Secretion System Effectors: Molecular Mechanisms And Physiological Consequences. *Cell Host Microbe* 22, 217-231.
- Johnson, R., Byrne, A., Berger, C.N., Klemm, E., Crepin, V.F., Dougan, G., and Frankel, G. (2017). The Type III Secretion System Effector SptP of *Salmonella enterica* Serovar Typhi. *J Bacteriol* 199.
- Knodler, L.A., Vallance, B.A., Celli, J., Winfree, S., Hansen, B., Montero, M., and Steele-Mortimer, O. (2010). Dissemination of invasive *Salmonella* via bacterial-induced extrusion of mucosal epithelia. *Proc Natl Acad Sci U S A* 107, 17733-17738.
- Krieger, V., Liebl, D., Zhang, Y., Rajashekar, R., Chlanda, P., Giesker, K., Chikkaballi, D., and Hensel, M. (2014). Reorganization of the endosomal system in *Salmonella*-infected cells: the ultrastructure of *Salmonella*-induced tubular compartments. *PLoS Pathog* 10, e1004374.
- Kubori, T., and Galan, J.E. (2003). Temporal regulation of *Salmonella* virulence effector function by proteasome-dependent protein degradation. *Cell* 115, 333-342.
- Kuhle, V., and Hensel, M. (2002). SseF and SseG are translocated effectors of the type III secretion system of *Salmonella* pathogenicity island 2 that modulate aggregation of endosomal compartments. *Cell Microbiol* 4, 813-824.
- Lacayo, C.I., and Theriot, J.A. (2004). *Listeria monocytogenes* actin-based motility varies depending on subcellular location: a kinematic probe for cytoarchitecture. *Mol Biol Cell* 15, 2164-2175.
- Lemarignier, M., and Pizarro-Cerda, J. (2020). Autophagy and Intracellular Membrane Trafficking Subversion by Pathogenic *Yersinia* Species. *Biomolecules* 10.
- Lorkowski, M., Felipe-Lopez, A., Danzer, C.A., Hansmeier, N., and Hensel, M. (2014). *Salmonella enterica* invasion of polarized epithelial cells is a highly cooperative effort. *Infect Immun* 82, 2657-2667.
- McClelland, M., Sanderson, K.E., Clifton, S.W., Latreille, P., Porwollik, S., Sabo, A., Meyer, R., Bieri, T., Ozersky, P., McLellan, M., *et al.* (2004). Comparison of genome degradation in Paratyphi A and Typhi, human-restricted serovars of *Salmonella enterica* that cause typhoid. *Nat Genet* 36, 1268-1274.
- Moreau, K., Lacas-Gervais, S., Fujita, N., Sebbane, F., Yoshimori, T., Simonet, M., and Lafont, F. (2010). Autophagosomes can support *Yersinia pseudotuberculosis* replication in macrophages. *Cell Microbiol* 12, 1108-1123.
- Niekamp, P., Scharfe, F., Sokoya, T., Vittadello, L., Kim, Y., Deng, Y., Sudhoff, E., Hilderink, A., Imlau, M., Clarke, C.J., *et al.* (2022). Ca(2+)-activated sphingomyelin scrambling and turnover mediate ESCRT-independent lysosomal repair. *Nat Commun* 13, 1875.
- Noster, J., Chao, T.C., Sander, N., Schulte, M., Reuter, T., Hansmeier, N., and Hensel, M. (2019). Proteomics of intracellular *Salmonella enterica* reveals roles of *Salmonella* pathogenicity island 2 in metabolism and antioxidant defense. *PLoS Pathog* 15, e1007741.
- Otten, E.G., Werner, E., Crespillo-Casado, A., Boyle, K.B., Dharamdasani, V., Pathe, C., Santhanam, B., and Randow, F. (2021). Ubiquitylation of lipopolysaccharide by RNF213 during bacterial infection. *Nature* 594, 111-116.
- Paz, I., Sachse, M., Dupont, N., Mounier, J., Cederfur, C., Enninga, J., Leffler, H., Poirier, F., Prevost, M.C., Lafont, F., *et al.* (2010). Galectin-3, a marker for vacuole lysis by invasive pathogens. *Cell Microbiol* 12, 530-544.



- Reuter, T., Scharte, F., Franzkoch, R., Liss, V., and Hensel, M. (2021). Single cell analyses reveal distinct adaptation of typhoidal and non-typhoidal *Salmonella enterica* serovars to intracellular lifestyle. *PLoS Pathog* 17, e1009319.
- Roder, J., Felgner, P., and Hensel, M. (2021). Comprehensive Single Cell Analyses of the Nutritional Environment of Intracellular *Salmonella enterica*. *Front Cell Infect Microbiol* 11, 624650.
- Roder, J., and Hensel, M. (2020). Presence of SopE and mode of infection result in increased *Salmonella*-containing vacuole damage and cytosolic release during host cell infection by *Salmonella enterica*. *Cell Microbiol* 22, e13155.
- Schell, U., Simon, S., and Hilbi, H. (2016). Inflammasome Recognition and Regulation of the *Legionella* Flagellum. *Curr Top Microbiol Immunol* 397, 161-181.
- Schulte, M., Sterzenbach, T., Miskiewicz, K., Elpers, L., Hensel, M., and Hansmeier, N. (2019). A versatile remote control system for functional expression of bacterial virulence genes based on the *tetA* promoter. *Int J Med Microbiol* 309, 54-65.
- Sepe, L.P., Hartl, K., Iftekhar, A., Berger, H., Kumar, N., Goosmann, C., Chopra, S., Schmidt, S.C., Gurumurthy, R.K., Meyer, T.F., *et al.* (2020). Genotoxic Effect of *Salmonella* Paratyphi A Infection on Human Primary Gallbladder Cells. *mBio* 11.
- Straley, S.C., and Harmon, P.A. (1984). *Yersinia pestis* grows within phagolysosomes in mouse peritoneal macrophages. *Infect Immun* 45, 655-659.
- Striednig, B., Lanner, U., Niggli, S., Katic, A., Vormittag, S., Brulisauer, S., Hochstrasser, R., Kaech, A., Welin, A., Fliieger, A., *et al.* (2021). Quorum sensing governs a transmissive *Legionella* subpopulation at the pathogen vacuole periphery. *EMBO Rep* 22, e52972.
- Studer, P., Staubli, T., Wieser, N., Wolf, P., Schuppler, M., and Loessner, M.J. (2016). Proliferation of *Listeria monocytogenes* L-form cells by formation of internal and external vesicles. *Nat Commun* 7, 13631.
- Thurston, T.L., Wandel, M.P., von Muhlinen, N., Foeglein, A., and Randow, F. (2012). Galectin 8 targets damaged vesicles for autophagy to defend cells against bacterial invasion. *Nature* 482, 414-418.
- Tinevez, J.Y., Perry, N., Schindelin, J., Hoopes, G.M., Reynolds, G.D., Laplantine, E., Bednarek, S.Y., Shorte, S.L., and Eliceiri, K.W. (2017). TrackMate: An open and extensible platform for single-particle tracking. *Methods* 115, 80-90.
- TRC (2015). Lentivirus production of shRNA, CRISPR, or ORF-pLX clones in 10 cm dishes or 6-well plates (The RNAi Consortium (TRC), Broad Institute).
- Valenzuela, L.M., Hidalgo, A.A., Rodriguez, L., Urrutia, I.M., Ortega, A.P., Villagra, N.A., Paredes-Sabja, D., Calderon, I.L., Gil, F., Saavedra, C.P., *et al.* (2015). Pseudogenization of *sopA* and *sopE2* is functionally linked and contributes to virulence of *Salmonella enterica* serovar Typhi. *Infect Genet Evol* 33, 131-142.
- Wadhwa, N., and Berg, H.C. (2022). Bacterial motility: machinery and mechanisms. *Nat Rev Microbiol* 20, 161-173.

## **V.5. Establishment of a novel infection model for *Salmonella* adhesion and invasion - human intestinal organoids**

Nathalie Sander<sup>\*,1</sup>, Felix Scharte<sup>\*,1</sup>, Rico Franzkoch<sup>1,2</sup>, Michael Kim<sup>1</sup>, Olympia E. Psathaki<sup>2,3</sup>, Guntram A. Grassl<sup>4</sup> and Michael Hensel<sup>1,3</sup>

\*Authors contributed equally to this work

<sup>1</sup>Abteilung Mikrobiologie, Universität Osnabrück, Osnabrück, Germany

<sup>2</sup>iBiOs - integrated Bioimaging Facility Osnabrück, Universität Osnabrück, Osnabrück, Germany

<sup>3</sup>CellNanOs - Center of Cellular Nanoanalytics Osnabrück, Universität Osnabrück, Osnabrück, Germany

<sup>4</sup>Institute of Medical Microbiology and Hospital Epidemiology, Hannover Medical School and German Center for Infection Research (DZIF), Hannover, Germany

### V.5.1. Abstract

*Salmonella* spp. are classified into typhoidal and non-typhoidal serovars and can cause a range of food-borne illnesses from self-limiting gastroenteritis to life threatening systemic disease. Analyses of host-pathogen interactions is a key requirement for the understanding of bacterial virulence mechanisms. In former studies, cell culture models as HeLa, MDCK and CaCo cell-lines were frequently used to investigate interactions with *Salmonella* in high temporal and spatial resolution. However, these models lack the complex tissue architecture of whole tissues, therefore interpretation of the results and transition to the human host is limited. Thus, the need for a cell culture system, displaying all different cell types of organs, is essential to gain more insights in physiological processes. Most recently, organoids have become a promising tool to study host-pathogen interactions in a setting resembling the *in vivo* situation. Especially the research with human-restricted pathogens like typhoidal *Salmonella* is dependent on human cell culture with a close relation to *in vivo* conditions. In contrast to cell culture with only a single cell population, crypt-derived intestinal organoids mimic tissue characteristics of distinct sections of the gastrointestinal tract. Stem cells of human or murine origin can be differentiated to 3D or 2D tissues with crypt formation, distinct cell populations, polarization and mucus secretion.

Here, we demonstrate the use of murine and human intestinal organoids in 3D and 2D to study virulence mechanisms of both typhoidal and non-typhoidal *Salmonella* regarding adhesion, invasion, and extra- and intracellular lifestyles. We performed infections with *Salmonella enterica* Typhimurium (STM) and Paratyphi A (SPA), quantified invaded bacteria, and imaged infection. For this, we adapted our imaging approaches to analyze *Salmonella* infection with confocal spinning disc microscopy (SDCM), scanning electron microscopy (SEM) and transmission electron microscopy (TEM). Using different labeling techniques, we aimed to identify cell types important in *Salmonella* infection.

Previous investigations in cell culture models led to definition of hallmark virulence functions such as invasion with induction of massive membrane ruffles, formation of *Salmonella*-containing vacuoles (SCV), and remodeling of the endosomal system of host cells, resulting in *Salmonella*-induced filament (SIF) formation. An established organoid model will help to critically analyze if these phenotypes also occur in more tissue-like organoid infection models and also offers options to investigate the cellular mechanisms of pathogen exit from infected host cells.

## V.5.2. Introduction

### V.5.2.1. Characteristics and cultivation of patient-derived organoids

The development of a cell culture model, representing all different cell types of an organ or tissue, was shown to be scientifically transformative with various applications in epithelial and cell biology, including tissue polarity, adhesion, growth control and differentiation, pathology and clinical applications (Fujii *et al.*, 2016; Urbischek *et al.*, 2019; van de Wetering *et al.*, 2015). The critical aspect of organoid cultivation is the culture medium, containing defined ingredients, controlling growth, proliferation and differentiation, as R-spondins, potentiating Wnt pathway, and Noggin, inhibiting differentiation signals from the bone morphogenetic protein (BMP) pathway (Urbischek *et al.*, 2019).

Besides tissue development and regeneration, metabolic diseases and other biological processes, intestinal organoids can be used to study host-pathogen interactions as in the *Salmonella* infection process. The intestinal epithelium displays an effective barrier against the invasion of microorganisms (Turner, 2009). Simpler cell culture models like Madin-Darby canine kidney (MDCK) cells or Henrietta Lacks (HeLa) cells only consist of a single cell type and are derived from tumors, thus they have error-filled genomes and investigations of host-pathogen interactions are more difficult to interpret (Beskow, 2016; Gaush *et al.*, 1966; Ponce de Leon-Rodriguez *et al.*, 2019). The possibility of intestinal organoids that can be isolated from stem cells of the crypts, let scientists now gain insights in infection processes much closer to reality (Figure V.5.1).

The intestine is surrounded by a monolayer of epithelial cells, typically forming villi and crypts to enlarge the surface of the intestine (Figure V.5.1 A). The epithelium consists of four major differentiated cell types (enterocytes, enteroendocrine cells (EEC), goblet cells and Paneth cells), multipotent stem cells, namely Lgr5<sup>+</sup> crypt based columnar (CBC) cells and +4 cells, and a small population of epithelial cells that include tuft and microfold (M)-cells (Beumer and Clevers, 2016; Gerbe and Jay, 2016; Iismaa *et al.*, 2018; Takashima *et al.*, 2013). These different cell types are part of distinct areas of the villus and crypt, respectively. EEC, enterocytes, goblet cells and M cells migrate to the tip of the villus, whereas Paneth cells are located at the bottom of the crypt, involved in stem cell maintenance (Gassler, 2017; Gomez and Boudreau, 2021). Enterocytes are the most abundant cell type here (Egi Kardia, 2020). Goblet cells function in production and secretion of mucus and EEC synthesize hormones and neuropeptides. Absorptive cells are not only involved in metabolic and digestive functions, but also express specific reporters on their surface important for innate immune response (Pott and Hornef, 2012; van der Flier and Clevers, 2009). By the recognition of luminal antigens and microorganisms, M cells are associated with the immunological vigilance and maturation (Peterson and Artis, 2014). The different cell types of the mammalian intestine are constantly being renewed after reaching the villus tip 4-5 days after their generation (Iismaa *et al.*, 2018). As the intestine has a cellular and molecular complexity, investigating the mechanisms of the regulation of the epithelial homeostasis is difficult and the usage of conventional

cell lines was more beneficial (Ponce de Leon-Rodriguez *et al.*, 2019). However, progress in the organoid cultivation now allows the successful growth of intestinal organoids in 3D (Figure V.5.1) and 2D (Figure V.5.15).

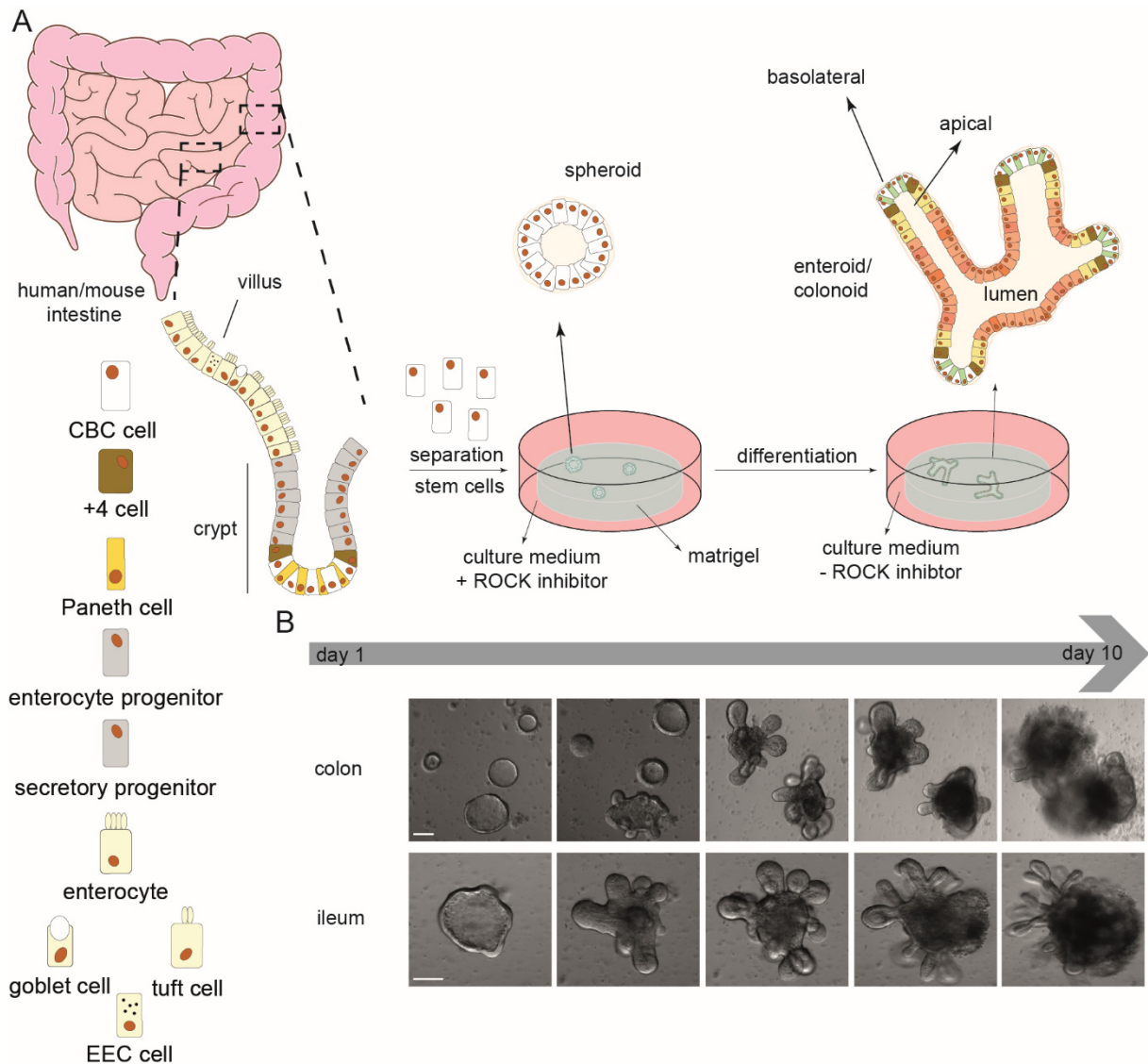


**Figure V.5.1. Cultivation of 3D intestinal organoids from biopsy samples.** A) Schematic overview of cultivation of 3D intestinal organoids. The epithelial layer of the intestine consists of villi and crypts. The villi are built up from differentiated epithelial cells, including enterocytes, enteroendocrine cells (EEC), tuft cells and goblet cells. The crypts consist of paneth cells, +4 cells and crypt base columnar cells (CBC). Paneth cells represent mature cells that remain in the crypts and influence the stem cell environment. By continuous proliferation of the CBC, new cells are provided during differentiation of the villus. Stem cells are isolated from the crypts of intestinal biopsy samples and seeded in a Matrigel-culture medium mix, allowing growth of 3D cultured cells reproducing the physiology and structure of the intestine. Initially, the culture medium is supplemented with growth factors and 10  $\mu$ M Y27623 for inhibition of the Rho-associated, coiled-coil containing protein kinase (ROCK) pathway, improving the survival of stem cells in the initiation of differentiation protocols (Ishizaki *et al.*, 2000; Reznia *et al.*, 2014). Y27623 inhibits stem cell differentiation, so spheroids are formed. For differentiation, the medium is exchanged after 3 days with supplemented medium without Y27623, allowing differentiation. The intestinal organoids form villi and crypts and after 10 days, organoids can be dissociated and seeded again. B) Micrographs of intestinal organoid growth over time. Exemplary shown are murine colonoids and enteroids. Scale bar: 100  $\mu$ m.

After first cultivation attempts with murine small intestine segments, the approach extended to other parts of the intestine, resulting in growth of colonoids, if colon was used, and enteroids, if the small

intestine was used (Sato *et al.*, 2009; Stelzner *et al.*, 2012). One of the most essential cell types during enteroid formation are the Lgr5<sup>+</sup> CBC cells, which differentiate to enterocytes, goblet cells, EEC and Paneth cells (Sato *et al.*, 2009) (Figure V.5.1 A). These cells initially form spheroids under cultivation conditions with Rho-associated, coiled-coil containing protein kinase (ROCK) pathway inhibitor (Y27623), improving the survival of stem cells in the initiation of differentiation protocols (Ishizaki *et al.*, 2000; Rezaia *et al.*, 2014). Following spheroid stadium, protrusions are formed, mimicking crypts and the intestinal architecture (Sato and Clevers, 2013). It was also shown that Paneth cells are crucial for organoids and the maintenance of intestinal stem cells (Sato *et al.*, 2011). Organoids can grow under *in vitro* conditions, but the medium has to be supplemented with factors and molecules normally composing their natural niche (Gomez and Boudreau, 2021). To provide this essential environment, organoids are cultured in semi-viscous medium, enriched with an extracellular matrix (Matrigel) to allow differentiation and interactions of the cells. Additionally, a cocktail of biological enhancers is added to the medium, containing the bone morphogenetic protein inhibitor R-spondin, Wnt3a, Noggin and epidermal growth factors (Ootani *et al.*, 2009; Sato *et al.*, 2011; Sato *et al.*, 2009). Following spheroid assembly, the ROCK inhibitor is removed from the medium and the spheroids break the symmetry, leading to crypt formation. Intestinal organoids form a lumen with an apical side, in which apoptotic cells and metabolites are ejected (Gomez and Boudreau, 2021). In contrast to the gut epithelium, the external milieu is not in touch with the apical side of the organoid, but with the basolateral side (Sato *et al.*, 2009). This organization makes infection models and analyses of host-pathogen interactions more difficult. However, new strategies were devised that allow to reverse this polarity, leading to new infection protocols and analyses of infection processes.

#### IV.5.2.2. Organoids as model for infection biology

Infectious diseases are one of the most common causes of death and represent a major health problem around the world (WHO, 2008). In times of rising infection rates and frequently emerging antibiotic-resistance in pathogenic bacteria as well as newly emerging zoonotic diseases as SARS-CoV-2, it is of crucial importance to better understand their pathogenesis for development of new strategies to counteract infections or for vaccine development (WHO, 2014).

Organoid systems are one of the major recent advances for biological research across biological research fields including drug treatment, cancer therapy, developmental biology and also infection biology. Organoids can be derived from induced and adult stem cells and are able to reconstitute complex tissues with different cell types and physiological functions. For many diseases, the broader biological context is necessary to elucidate infection routes, disease progression and pathogenesis of the causative agent. With their ability to mimic the *in vivo* context, organoids can therefore serve as model in infection biology (Bartfeld, 2016; Dutta and Clevers, 2017; Rios and Clevers, 2018). Despite being only a recently developed method, numerous bacterial, viral and parasitic pathogens have been analyzed in organoid systems such as *Cryptosporidium*, enterohemorrhagic *Escherichia coli*, *Campylobacter jejuni*,

*Clostridium difficile*, *Helicobacter pylori*, *Listeria monocytogenes*, *Shigella flexneri*, *Vibrio cholerae*, *Salmonella enterica*, Zika virus, rotavirus and SARS-CoV-2 (Bartfeld and Clevers, 2015; Finkbeiner *et al.*, 2012; Forbester *et al.*, 2015; Garcez *et al.*, 2016; He *et al.*, 2019; Heo *et al.*, 2018; Lamers *et al.*, 2021; Leslie *et al.*, 2015; Ranganathan *et al.*, 2019; Roodsant *et al.*, 2020; Tse *et al.*, 2018; Zomer-van Ommen *et al.*, 2016). Even formerly, unculturable pathogens like norovirus show the high potential of organoids to become a promising model system for pathogens, especially if they are adapted to the human host (Ettayebi *et al.*, 2016).

Many bacterial pathogens using the intestinal tract as route of entry to deeper tissues and systemic spread in the host (Ribet and Cossart, 2015). Intestinal organoids with their ability to recapitulate infection relevant characteristics such as crypt and microvilli domains, mucus production, defensive and antimicrobial peptide secretion can serve as adequate model system for enteric pathogens (Bartfeld and Clevers, 2015; Dutta and Clevers, 2017). Further systems with gallbladder and liver organoids can help to study specific infection foci in systemic diseases (Caiazza *et al.*, 2021; Sepe *et al.*, 2020). Co-culture models with immune cells in medium could serve as model for microenvironments like the lamina propria (Schreurs *et al.*, 2021). A decent set of methods for infection biology research with organoid systems is available by now which is schematically presented in Figure V.5.2.

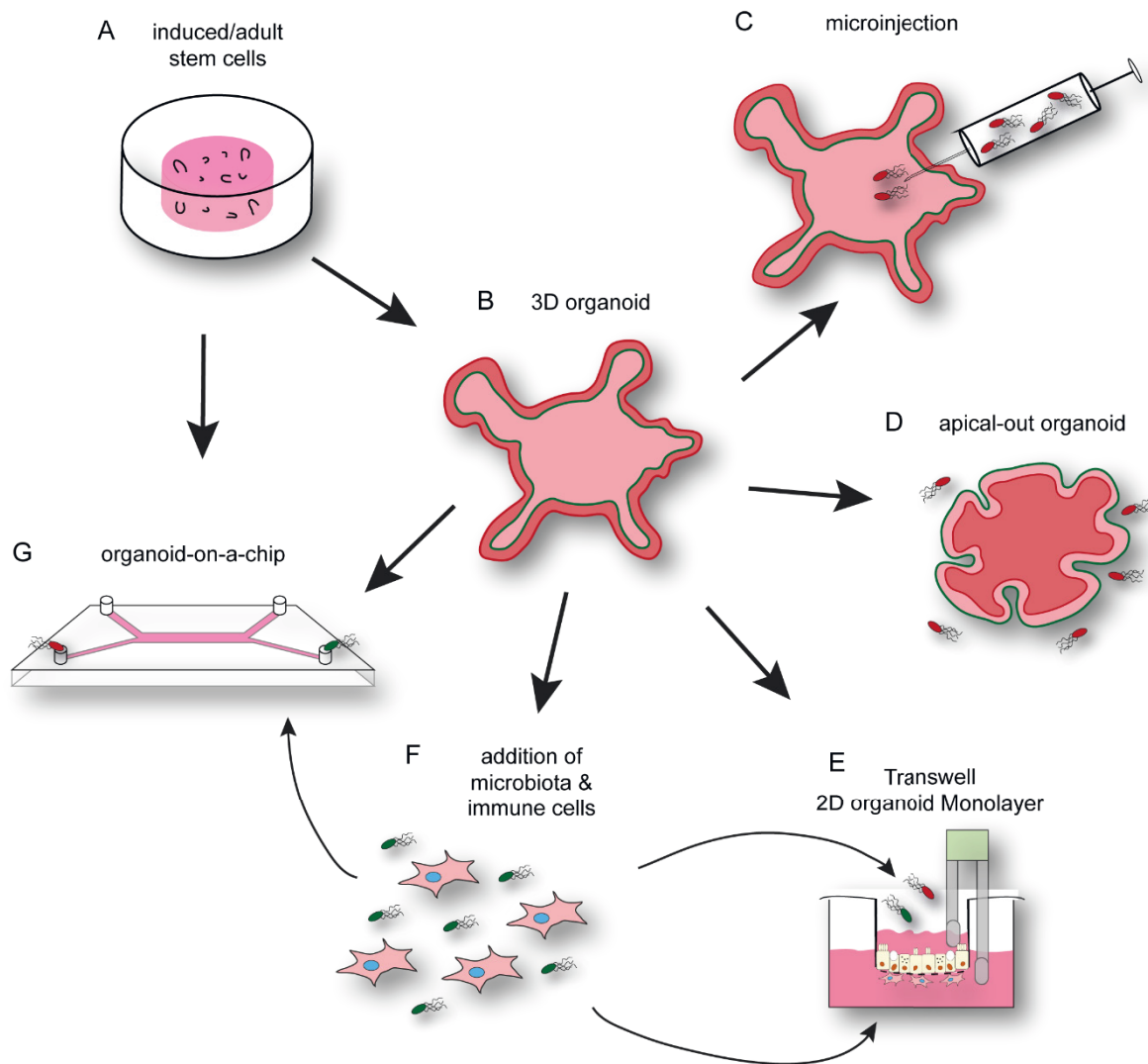


**Figure V.5.2. Methods of infection studies with 3D and 2D organoids.** A) stem cells are cultured in Matrigel as described in figure V.5.1 until they develop 3D organoids (B). C) To allow pathogens access to the apical side of 3D organoids, microinjection can be performed. D) Generation of apical-out organoids allows infection with pathogens added directly to the culture medium. E) Organoid-derived monolayers allow infection from the apical side in a more defined manner described in figure III.4.15. F) Microbiota and immune cells can be added to organoids grown on transwells (E) and in microfluidic chambers (G).

### *Salmonella enterica*

One of the most prevalent enteropathogens belongs to the family *Salmonella enterica* that can cause diseases ranging from self-limiting gastroenteritis to life-threatening systemic infections (typhoid fever) (Johnson *et al.*, 2018). The pathogenic, Gram-negative bacteria are rod-shaped and live facultative anaerobic. There are over 2,500 serovars within the genus of *Salmonella* which can be highly human-specific like *Salmonella enterica* serovar Typhi (STY) or *S. enterica* serovar Paratyphi A (SPA), or with a broad host range like *S. enterica* serovar Typhimurium (STM) (Pui, 2011). The ability of invasion and subsequent intracellular lifestyle in epithelial and immune cells is a major characteristic of *Salmonella*. The pathogenesis is thereby mediated by virulence genes which are mainly encoded on *Salmonella* pathogenicity islands (SPI), large chromosomal regions harboring several virulence-associated genes (Gerlach and Hensel, 2007; Hensel, 2004). *Salmonella* is able to actively invade polarized epithelial



cells by the so-called trigger mechanism (Gerlach *et al.*, 2008). Prior invasion, the giant non-fimbrial adhesin SiiE mediates first close contact to the apical side of the target cell. SiiE is secreted by the SPI4-encoded type 1 secretion system (SPI4-T1SS). In the further process of the infection, effector proteins are translocated via a SPI1-encoded type 3 secretion system (SPI1-T3SS) into the target cell and thereby induce manipulation of the actin cytoskeleton in enterocytes (Ly and Casanova, 2007). This process leads to membrane protrusions (membrane ruffles) and subsequently the non-phagocytic cells internalize the *Salmonella* in a phagocytic-like manner (Galan and Curtiss, 1989; Gerlach *et al.*, 2008). After invasion, *Salmonella* is present in the *Salmonella*-containing vacuole (SCV), similar to a phagosome. The following intracellular lifestyle with maturation of the SCV and as well as replication is depending on effector proteins which are translocated via a SPI2-encoded T3SS (SPI2-T3SS). Human-specific typhoidal *Salmonella* serovars replicate in immune cells like macrophages and are able to systemic disseminate to gallbladder, lymph nodes, bone marrow and liver as the infection progresses (Dougan and Baker, 2014).

### V.5.3. Results

#### 3D imaging of intestinal organoids

Organoids possess complex structures and are embedded in hydrogel that reconstitute an extracellular matrix and allows growth in 3D. These circumstances make microscopy approaches of whole-mount organoids challenging and imaging is highly dependent on specimen preparation, microscope and objective properties. Staining of organoids with fluorescent probes can be performed directly in suitable cell culture chambers or with detached organoids, released from Matrigel. Imaging is then performed in the respective chambered coverslip or after embedding of the detached organoids on conventional microscope slides (Figure V.5.3). Imaging quality is further dependent on working distance, parfocal length and numerical aperture of the used objective and the wavelength of light used to illuminate the specimen.

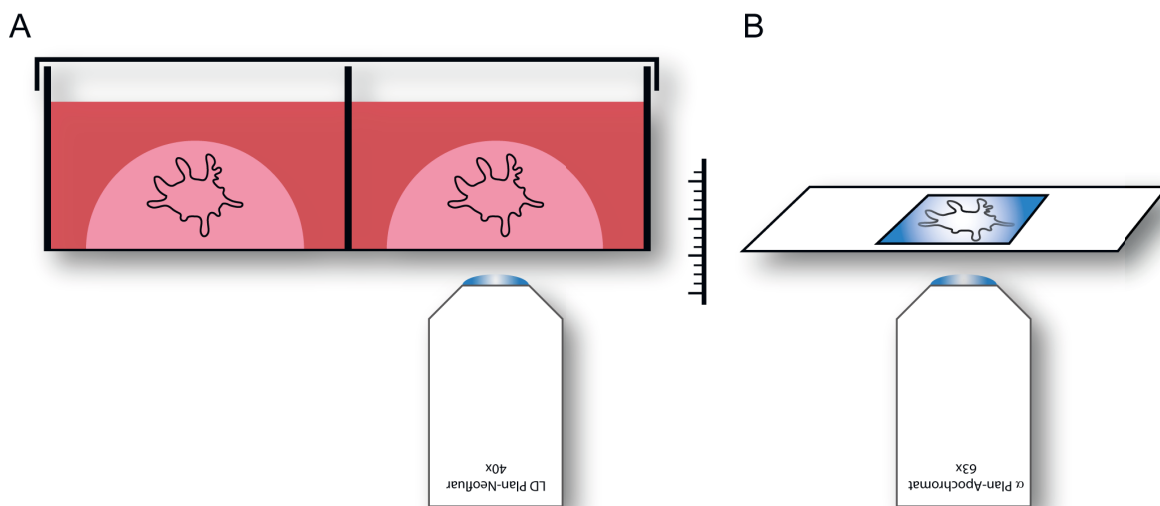


**Figure V.5.3. Light microscopy of whole-mount intestinal organoids.** A) Distance from specimen to microscope objective is higher in setups with organoids cultured in Matrigel in a  $\mu$ -slide chambered coverslip (ibidi) than with fixed organoids that were mounted on microscope slides (B).

Scanning electron microscopy (SEM) gives an impression of the dimensions of 3D organoids (Figure V.5.4 A). A side view of 3D enteroids cultured in chambered coverslips reveals how challenging fluorescence microscopy with such large specimen can be (Figure V.5.4 B). With up to 500  $\mu\text{m}$  in diameter, not nearly half of the organoid can be imaged properly in Z dimension with loss of focus and decreasing fluorescence signal with increasing imaging height. Especially the illumination with shorter wavelengths for DAPI or Alexa488 fluorescence samples is problematic as penetration depth in confocal microscopy is typically limited to less than 100  $\mu\text{m}$  (Graf and Boppart, 2010). However, the organoid side near the coverslip bottom and also some crypt domains were imaged in adequate resolution (Figure V.5.4 B, C, C'). Staining with DAPI, phalloidin and CellMask can give an insight into the general organization of a fully differentiated enteroid. CellMask allowed a uniform staining of the plasma membrane without cell-type differences exhibited by lectins and shows the dimensions of the enteroid. Nuclei

staining with DAPI and F-actin staining with phalloidin showed the distribution and orientation of cells in the organoid. High F-actin accumulation was visible at the apical side of the epithelial cells, which showed a high order of polarization with a high number of microvilli that were densely packed on the apical surface. The apical side faced the lumen of the enteroid. DAPI stained nuclei were located at the basolateral side.

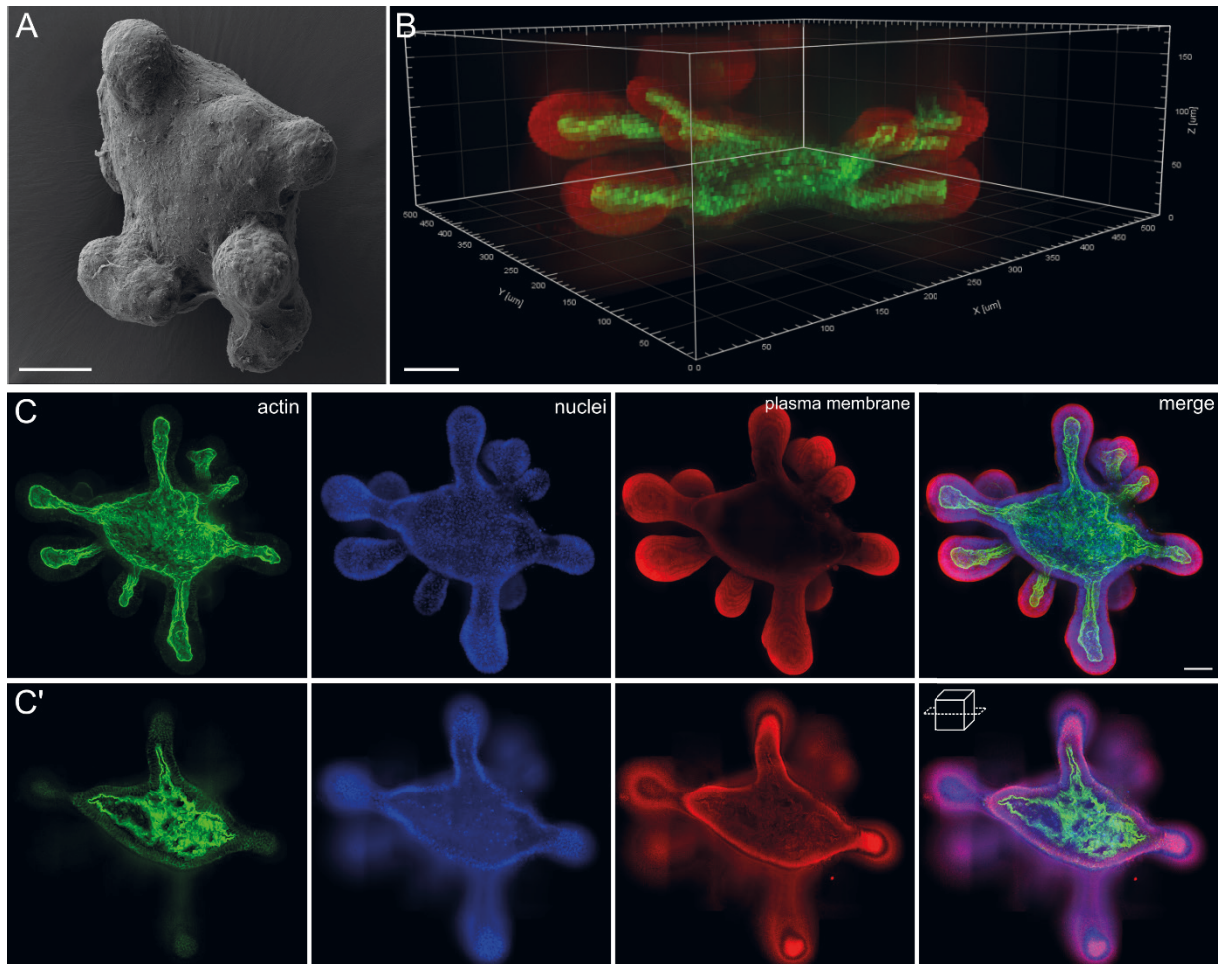


**Figure V.5.4. Imaging and fluorescence labeling of 3D enteroids.** A) SEM image of mouse intestinal organoid. 3D side view (B), maximum intensity projection (C) and cross-section (C') of whole-mount enteroid. Murine ileum organoids were cultured, fixed and stained with phalloidin-iFluor647 (green), DAPI (blue) and CellMask Deep Red (red) in  $\mu$ -slide chambered coverslip before imaging. Imaging with 40x objective. Multiple images with overlaps were acquired and stitched. Scale bars: 50  $\mu$ m.

Imaging of enteroids released from Matrigel and embedded on microscope slides is easier in terms of microscope prerequisites. Due to flattening of the organoids between microscope slide and coverslip and the resulting lower distance between objective and specimen, imaging of whole organoids in full Z was possible (Figure V.5.5). This allowed imaging with higher magnifying objectives and detailed characterization of cells e.g. at the apical side of enterocytes (Figure V.5.5 C'). Additionally, the brush border with microvilli structures was visible in detail.

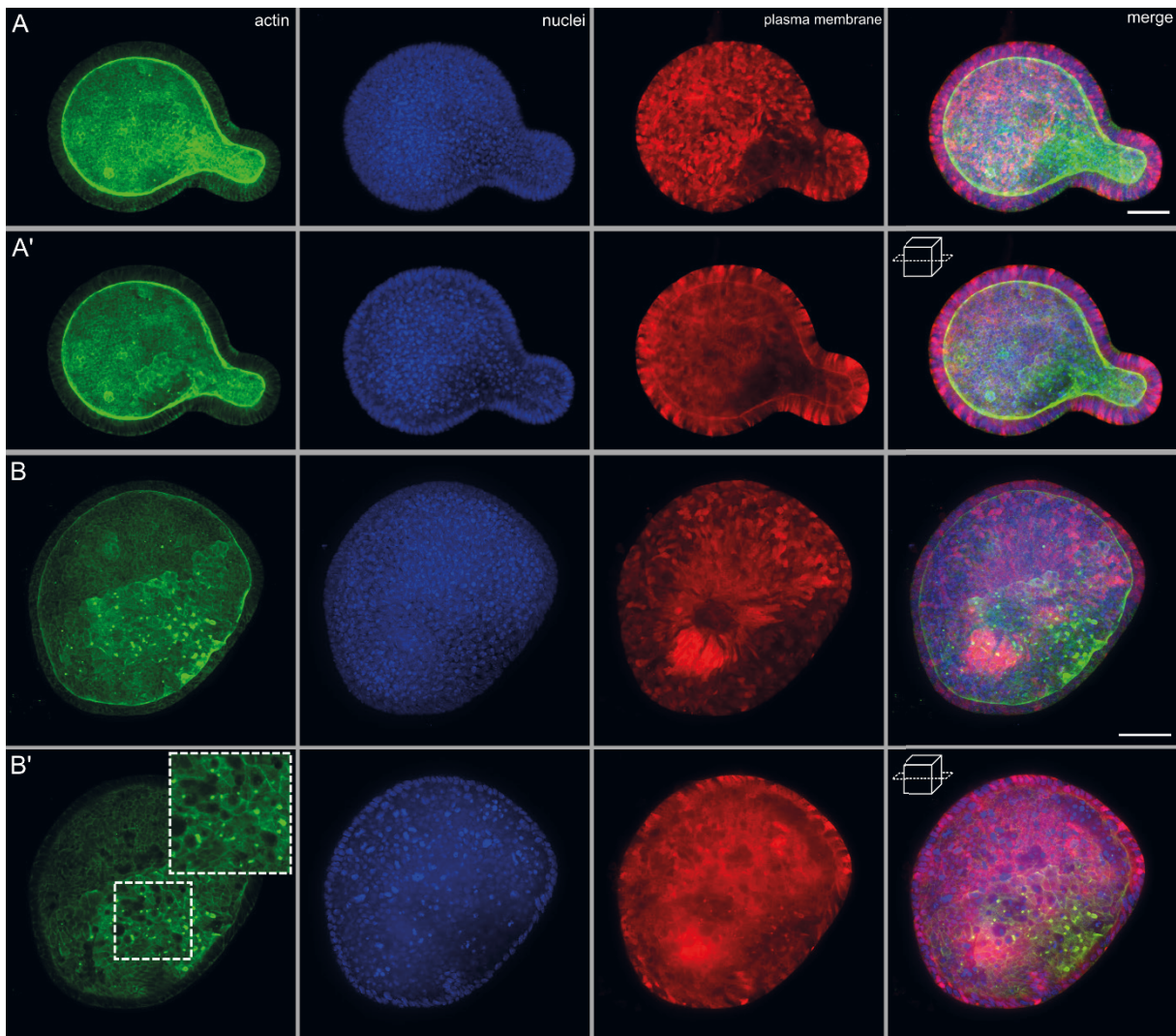


**Figure V.5.5. Imaging and fluorescence labeling of 3D enteroids.** A and B) Maximum intensity projection and cross-section (A', B') of whole-mount murine ileum organoids that were cultured and fixed in a 24-well, detached and stained with phalloidin-iFluor647 (green), DAPI (blue) and CellMask Deep Red (red) before mounted on microscope slide for imaging. Imaging with 63x objective. Multiple images with overlaps were acquired and stitched. Scale bars: 50  $\mu\text{m}$ .

Transmission electron microscopy (TEM) of ultrathin sections of a 3D-cultured enteroid revealed differences regarding the ultrastructure of various cell types (Figure V.5.6). The apical side of epithelial cells that are facing the lumen of the enteroid showed highly ordered microvilli structure, which therefore were defined as brush border (Figure V.5.6 A). Goblet cells were easily distinguishable by TEM because of their unique cellular architecture. A large volume of the goblet cell was densely packed with mucus containing secretory vesicles with large glycoproteins called mucins (Figure V.5.6 B). Due to harsh fixation methods necessary for TEM, the structure of carbohydrate-rich polymeric mucins may be disrupted, yet secretion of it was also visible in Figure V.5.6 B.

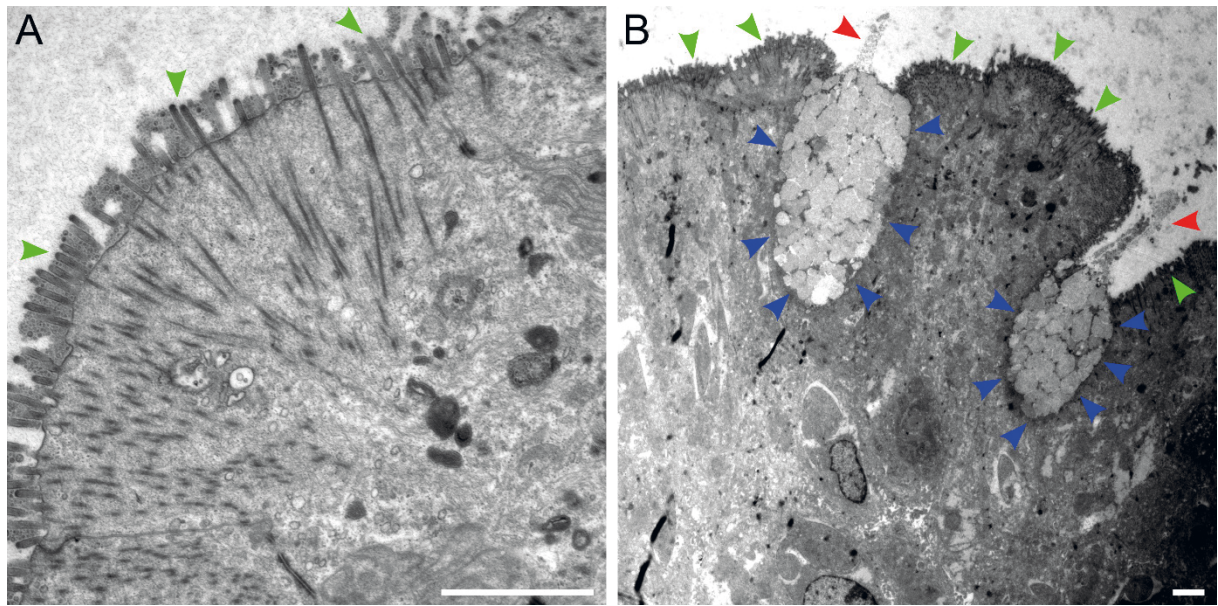


**Figure V.5.6. 3D organoids develop multiple cell types with brush border and mucus secretion.** TEM image of mouse intestinal organoid. A+B) Green arrowheads indicate microvilli in a brush border. B) Goblet cells with secretory vesicles (blue arrowheads) inside of the cell and secreted mucus (red arrowheads) are shown. Scale bars: 2  $\mu\text{m}$ .

Lectins like wheat germ agglutinin (WGA) with a high affinity for sialic acid and N-acetylglucosamine can be used to distinguish between certain cell types within organoids e.g. goblet and Paneth cells. WGA-stained murine and human enteroids showed expected high WGA signal predominantly in crypt domains (Figure V.5.7 A, B), the area where goblet and Paneth cells are mainly present (Figure V.5.1) (Birchenough *et al.*, 2015). Imaging in higher magnification also revealed single cells with secreted mucus at the apical side of the cell, these cells also showed less F-actin signal (Figure V.5.7 C, C', C\*). Note that WGA also stains the nuclear envelope, which was therefore also visible.

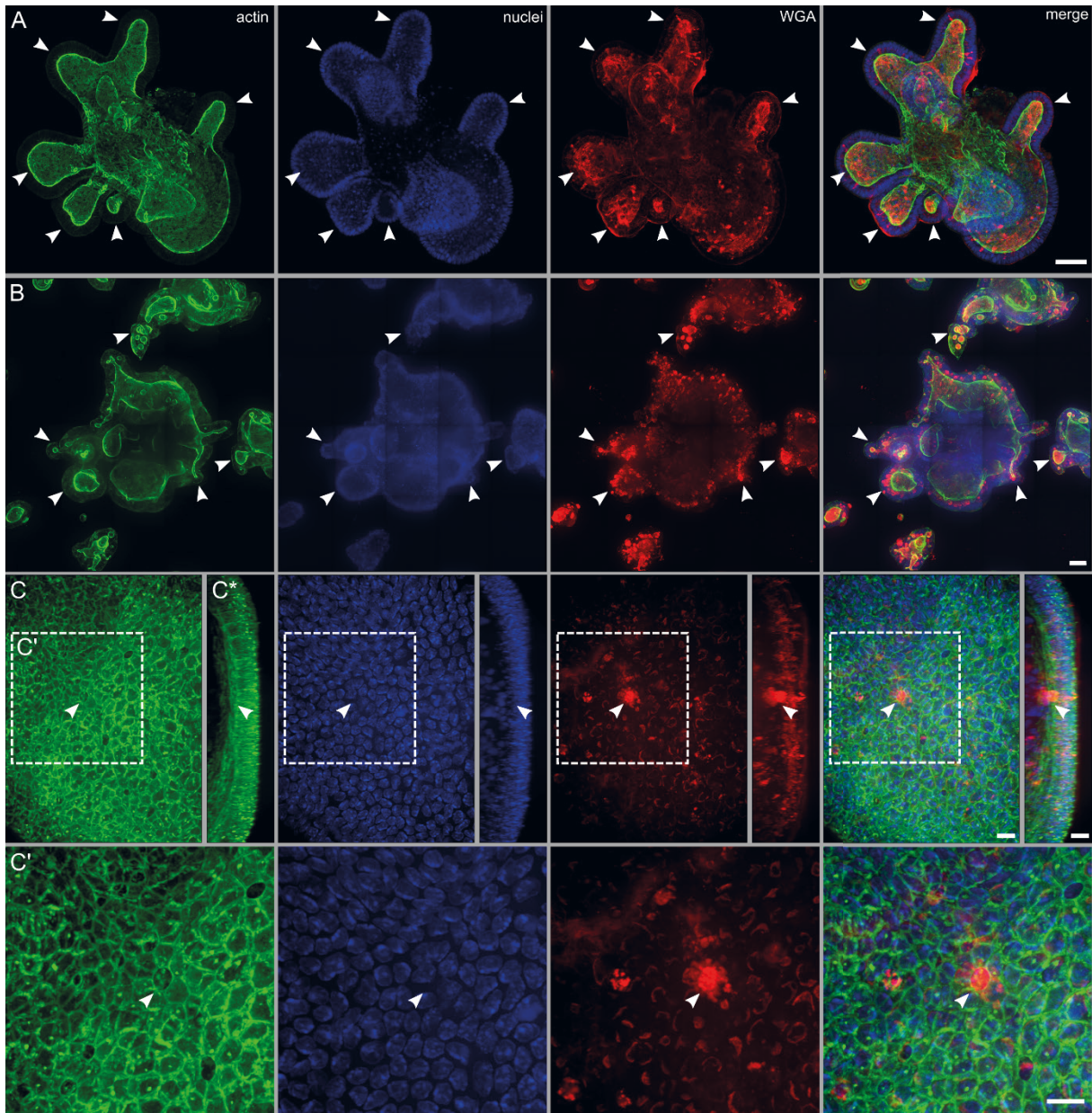


**Figure V.5.7. Fluorescence analysis of 3D enteroids with wheat germ agglutinin.** Murine (A) and human (B, C, C', C\*) enteroids were cultured, fixed and stained with AlexaFluor488-phalloidin (green), DAPI (blue) and CF@640R WGA (red) in  $\mu$ -slide chambered coverslip before imaging. (C') and (C\*) show magnification and side view of a region of interest. Arrowheads indicate accumulation of WGA signal. Images are shown as maximum intensity projection. Imaging with 40x objective (A, B) and 63x objective (C, C', C\*). Multiple images with overlaps were acquired and stitched. Scale bars: 50  $\mu$ m (A, B), 10  $\mu$ m (C, C', C\*).

### Lentiviral transfection

To further analyze host-pathogen interactions without additional staining, we aimed to stably transfect the organoids with LifeAct-GFP by lentiviral transduction as a highly efficient method of gene transfer into mammalian cells (Figure V.5.8) (Miyoshi and Stappenbeck, 2013). The organoids were grown for 2-4 days in 3D organoid medium, supplemented with ROCK inhibitor, to generate as many stem cells as possible. As the lentiviruses interfere with the Matrigel, the organoids were seeded on a thin Matrigel layer. Following this step, we incubated the organoids for 3 days to allow differentiation. After 7 days, we started selection by Blasticidin treatment for 24 h. Blasticidin is a selection antibiotic, acting on eukaryotic and prokaryotic cells. The cell death induced by Blasticidin occurs rapidly and allows selection of transfected cell lines carrying a Blasticidin resistance gene within one week (Miyoshi and Stappenbeck, 2013). Additionally, organoids were selected without Blasticidin treatment (Figure V.5.8) and non-transduced organoids were treated with Blasticidin (not shown).

After selection with Blasticidin, we obtained successfully transfected human colon and ileum organoids with a rate of approximately 50% (Figure V.5.8). We found a varying distribution of the GFP signal among the survived organoids ranging from only one to a few cells, up to nearly all cells of a single organoid. Interestingly, we found partly damaged organoids after Blasticidin treatment (Figure V.5.8). Thus, as the untreated organoids showed less to no damage, the Blasticidin concentration has to be decreased. However, we passaged the successfully transduced organoids and tried to further select for organoids with many positive cells to increase the amount in the population. The stable transfection was tested over several months and could be confirmed for most of the selected organoids. In future attempts, sorting of the stem cells by FACS or by visual inspection during passaging could lead to a monoclonal population of stably transfected organoids (Miyoshi and Stappenbeck, 2013). In a next step, these stably transfected organoids can then be used for 2D analyses or apical-out approaches to gain more insights into STM, SPA or STY infection process under nearly physiological parameters.

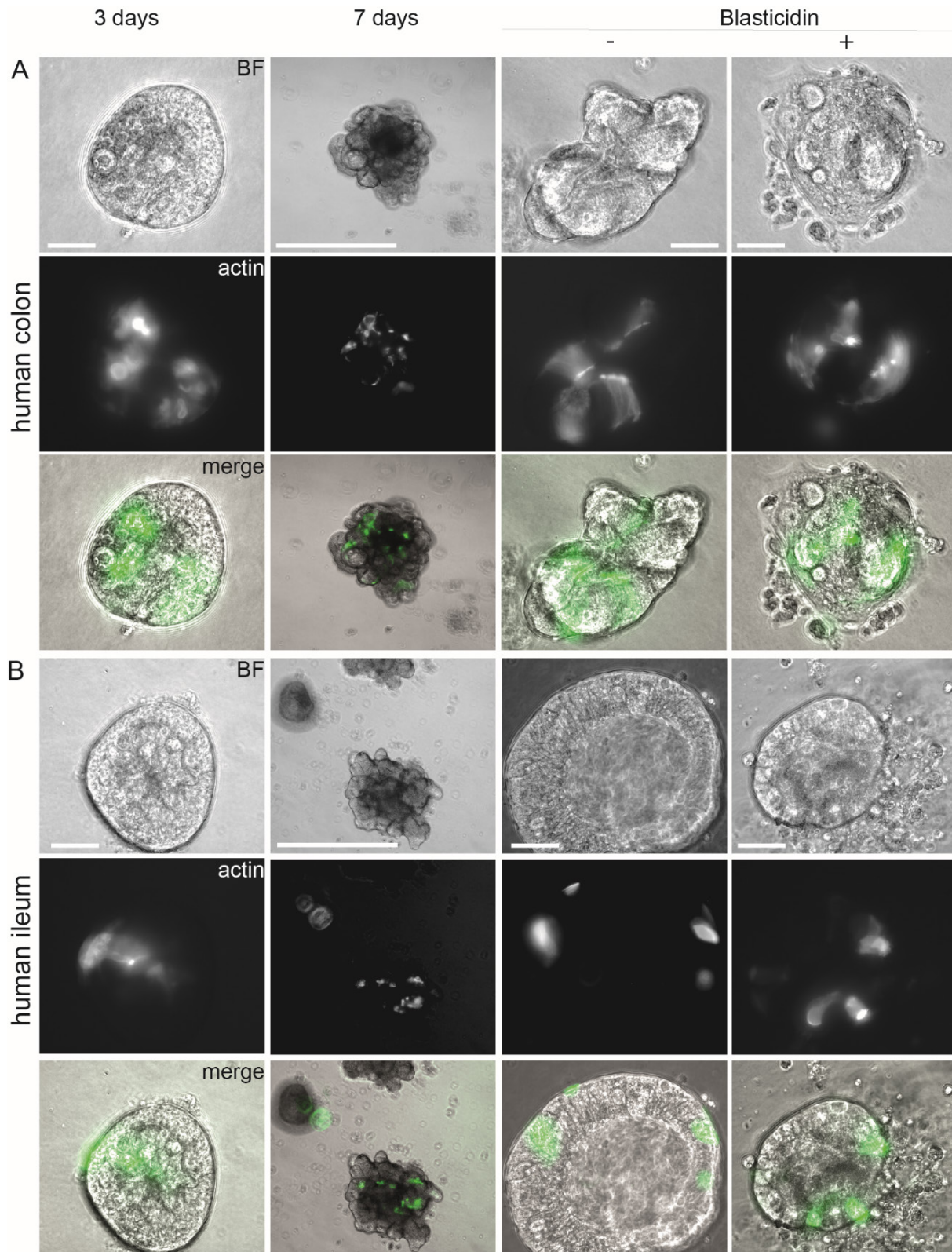


**Figure V.5.8. Lentiviral transfection of human organoids with LifeAct-GFP.** Microscopic analyses of the lentiviral transduction and following selection. Human organoids were lentiviral transfected for 24 h. After 24 h transduction, medium was exchanged, organoids covered with additional Matrigel and covered with medium. Selection occurred with Blasticidin. Microscopy was performed with the Zeiss Axio Vert.A1. Scale bar: 100  $\mu$ m. A) Human colon spheroids (left) and colonoids (center and right). B) Human ileum spheroids (left) and enteroids (center and right).



In addition to human organoids, we successfully transfected murine enteroids (Figure V.5.9). These cell line survived the Blasticidin treatment and showed no damaged organoids.

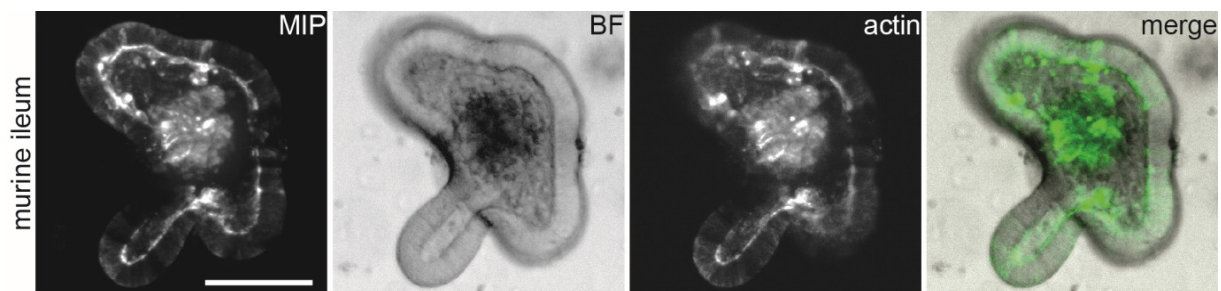


**Figure V.5.9. Murine enteroids stably transfected with lentivirus.** Microscopic analyses of the lentiviral transduction of murine enteroids. Organoids were transfected with LifeAct-GFP lentiviruses. Procedure as described in Figure V.5.8. Images show maximum intensity projection (MIP), brightfield (BF) and fluorescence microscopy images with LifeAct-GFP (green, actin) of stably transfected enteroids after blasticidin treatment. Scale bar: 100  $\mu\text{m}$ .

Analysis of intestinal organoids microinjected with *Salmonella**Fluorescence microscopy of human organoids microinjected with *Salmonella**

One challenge in using organoids to study pathogen-host interactions is the difficulty in accessing the apical, or luminal, surface of the epithelium, which is enclosed by the organoid cell layer. Infection of 3D cultured organoids with *Salmonella* by microinjection is a method to allow apical invasion of the pathogenic bacteria to mimic *in vivo* conditions. Microinjection with a glass micropipette is used to enable *Salmonella* to invade the apical side. Often, not fully differentiated organoids with crypts are used, but mostly round shaped spheroids in early cultivation because microinjection is much easier with these.

Figure V.5.10 shows an exemplary image of a 3D human colonoid microinjected with STM WT carrying a plasmid for constitutive expression of GFP. For microinjection, a fluorescence microscope was used to control injection of STM (Figure V.5.10 B). STM were visible inside the glass micropipette and the round shaped organoid but also leaking out of the injection side. Microinjected human colonoids were fixed for fluorescence imaging, detached, stained with DAPI, phalloidin and CellMask and mounted on microscope slides. Multiple small round shaped organoids were visible as well as a large organoid with approximately 350  $\mu\text{m}$  in diameter (Figure V.5.10 A). Some STM were visible outside of the organoid and at the basolateral side. A large number of poorly visible individual STM were dispersed in the organoid lumen. At the injection site, tissue damage could be detected as well as a huge accumulation of STM. Invasion sites could not be analyzed in detail because of the tissue damage that occurred during microinjection and the staining and embedding steps. Also, the flattening of the organoid due to mounting on microscope slides hamper the determination of individual infection sites at the bacterial-cell contact site.

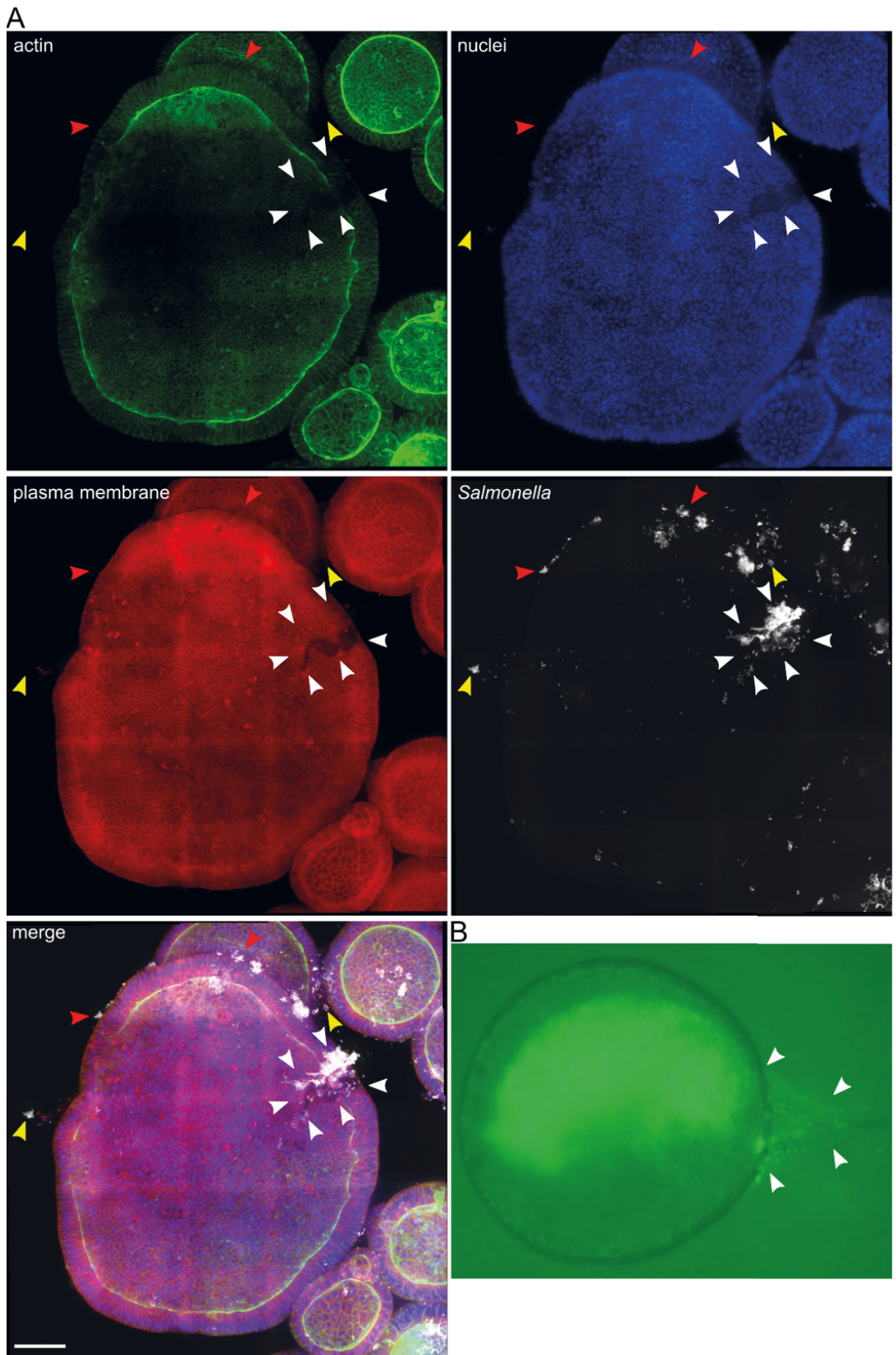


**Figure V.5.10. Fluorescence imaging of 3D human colonoid microinjected with *Salmonella* Typhimurium.** A) Human colonoids were microinjected with STM WT expressing GFP (white), fixed at 1-1.5 h p.i. and stained with phalloidin-iFluor647 (green), DAPI (blue) and CellMask Deep Red (red) before imaging. Arrowheads indicate STM at injection site inside and outside of the organoid (white) and with and without direct contact to basolateral side of the enteroid (red, yellow, respectively). Images are shown as maximum intensity projection. Imaging with 40x objective. Multiple images with overlaps were acquired and stitched. Scale bar: 50  $\mu\text{m}$ . B) Exemplary image of microinjection process with STM WT expressing GFP (green). Arrowheads indicate injection site with STM leaking off the lumen.

*TEM analysis of murine and human organoids microinjected with Salmonella*

Murine organoids were fixed 60 to 90 min p.i. with STM WT. The organoid shown in Figure V.5.11 possessed a diameter of approximately 330  $\mu\text{m}$ . It had a round shape and consists of a mixture of monolayers and multilayers, some with different cell types (Figure V.5.11 B), surrounding a large, central lumen (Figure V.5.11 A, B). Both, in the lumen and outside of the organoid, a multitude of *Salmonella* were visible (Figure V.5.11 A, B, C). While there were no microvilli on the basolateral side of the cells, a large amount can be detected on the apical side (Figure V.5.11 E), where also some invading *Salmonella* could be observed (Figure V.5.11 C - F). Two bacteria were already completely enclosed by the plasma membrane of the host cell, and were located in a SCV in the distal area of the cell (Figure V.5.11 C - D). At another site of the organoid, the *Salmonella* were only half-enclosed by the host membrane (Figure V.5.11 E, F). In both cases, however, much of the microvilli around the invasion site were effaced and the cell showed an extensive membrane ruffle around the bacteria (Figure V.5.11 D - F), similar to previously described membrane ruffles in polarized cell culture models (Gerlach *et al.*, 2008).

In another murine organoid, *Salmonella* had already fully invaded both from basolateral and apical side and were located in an area near the nucleus, and possess a SCV (Figure V.5.12). Possibly, due to the embedding protocol, the SCV were no longer completely preserved. It seems that in this organoid sample mainly basolateral invasion happened. A high number of *Salmonella* and also most of the invasion events were detected at the basolateral side, which could indicate that invasion happened primarily at this side (Figure V.5.12 A).

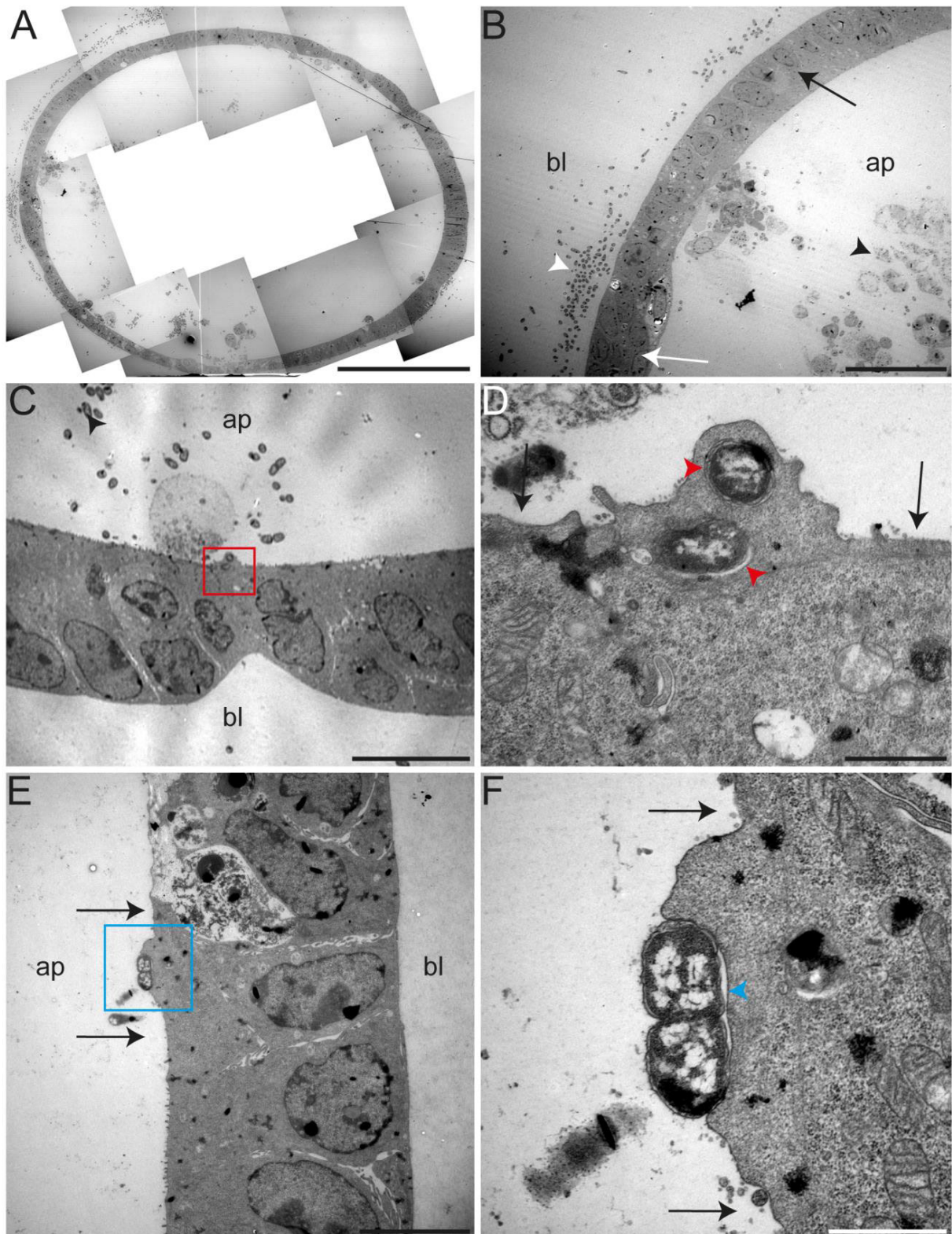


**Figure V.5.11. TEM images of a murine colonoid microinjected with *Salmonella Typhimurium*.** Murine colonoids were microinjected with STM WT and fixed for TEM 1-1.5 h p.i. A) Overview image of the murine colonoid. B) Magnified area from (A) showing presence of STM on the basolateral side (bl) outside of the organoid (white arrowhead), the monolayer (black arrow) and multilayer (white arrow) surrounding the lumen (ap), and the cellular debris located in the lumen (black arrowhead). C) Section of the cell layer surrounding the lumen. Some STM are located on the apical side (ap) (black arrowhead); bl (basolateral). D) Detailed view of two invading STM with SCVs partially present (red arrowheads) and microvilli effacement (black arrows). E) Section of cell layer of an intestinal organoid showing apical (ap) and basolateral (bl) sides and absence of microvilli (black arrows). F)

A detailed view shows dividing invading STM that trigger membrane protrusion but that have not yet formed an SCV (blue arrowhead). No microvilli are present in the vicinity of the invasion site (black arrows). Scale bars: 100  $\mu\text{m}$  (A), 25  $\mu\text{m}$  (B), 10  $\mu\text{m}$  (C), 1  $\mu\text{m}$  (D, F), 5  $\mu\text{m}$  (E).

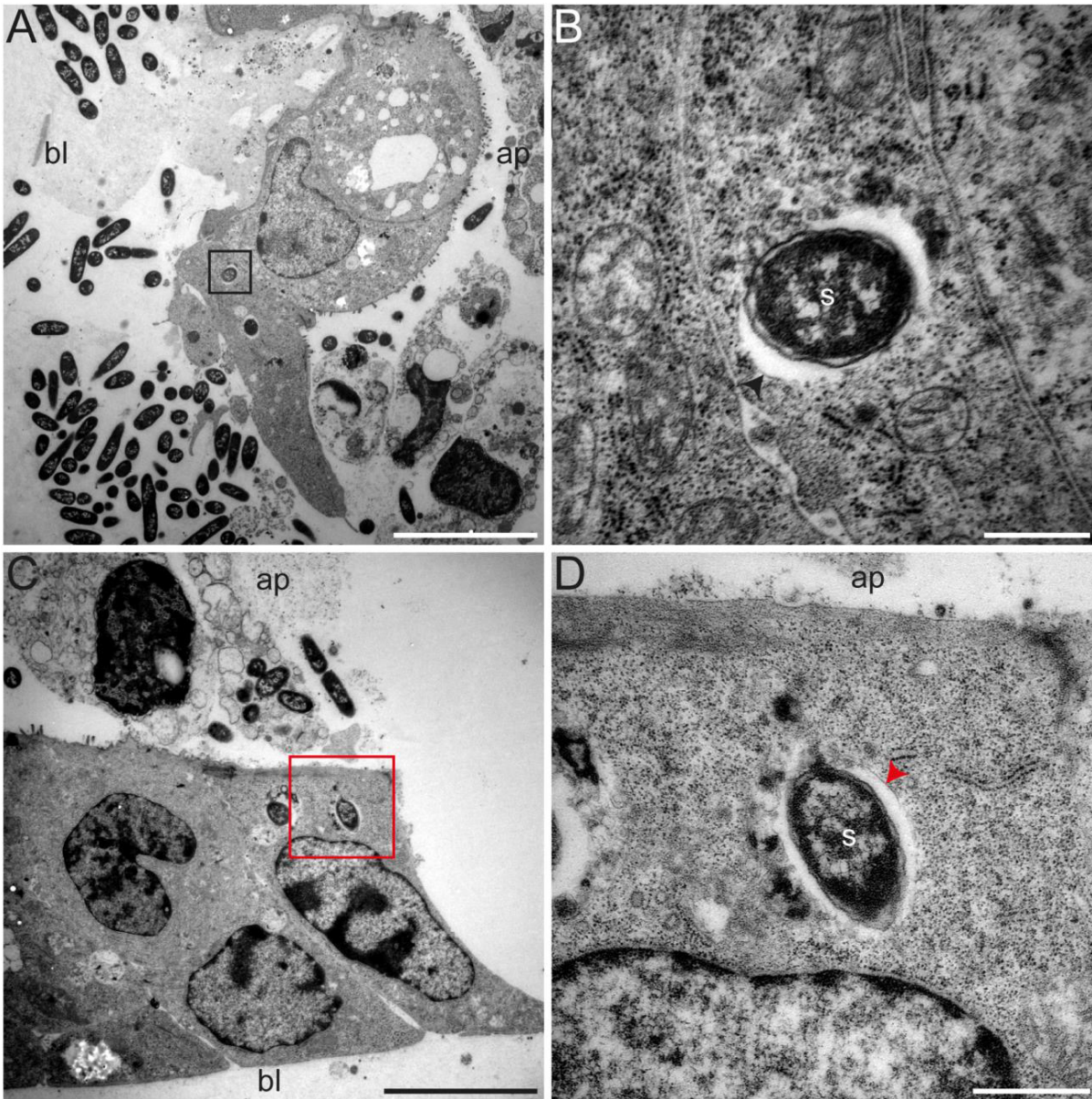


**Figure V.5.12. TEM images of a murine colonoids microinjected with *Salmonella Typhimurium*.** Murine colonoids were microinjected with STM WT and fixed for TEM 1-1.5 h p.i. A) Overview image of the murine colon organoid showing apical (ap), basolateral (bl) side and several intracellular STM, one is located near the nucleus (black box). B) Detailed view from A shows STM (s) is located within an SCV with a single membrane (black arrowhead). C) Overview image from another area of the organoid showing apical (ap) and basolateral (bl) sides, as well as intracellular STM on the basolateral side near the nucleus. D) Detailed view from C showing intracellular STM (s) enclosed by an SCV with a single membrane (red arrowhead). Scale bars: 7  $\mu\text{m}$  (A), 500 nm (B), 5  $\mu\text{m}$  (C), 750 nm (D).

The human intestinal organoids were microinjected as mentioned above, but they were fixed for TEM already 30 min after injection. The organoid shown in Figure V.5.13 A had a diameter of approximately 540  $\mu\text{m}$  at its widest point, and again *Salmonella* were present both outside (Figure V.5.13 A) and inside of the organoid (Figure V.5.13 E). With an alternation between monolayer and multilayer, with partly different cell types, a similar organization as in the murine variant was observed (Figure V.5.13 B). Several invading *Salmonella* could be recognized, which just contact the host cell membrane, so that a membrane ruffle was formed (Figure V.5.13 G, I). In the posterior part of this protrusion, fine elongated structures could be observed, which have morphological similarity to cytoskeletal components (Figure V.5.13 G). In close vicinity to the invading *Salmonella*, small round structures were visible and the microvilli of the apical side of the cells were still present (Figure V.5.13 I). Furthermore, *Salmonella* were observed to be located, together with other materials, in an electron-light compartment enclosed by a membrane (Figure V.5.13 F).

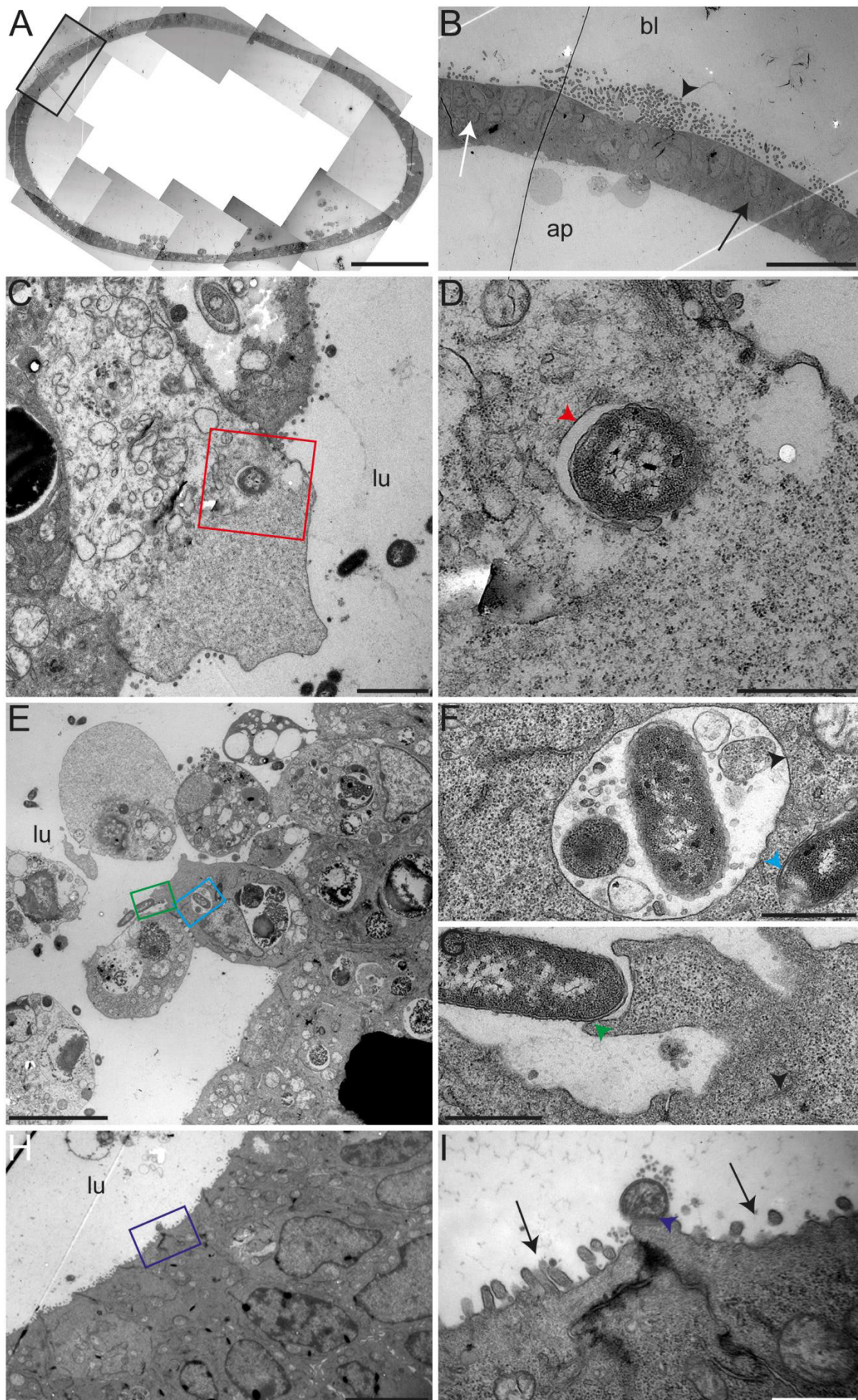




**Figure V.5.13. TEM images of a human colon organoid microinjected with *Salmonella Typhimurium*.** Human colonoids were microinjected with STM WT and fixed for TEM 30 min p.i. A) Overview image of the human colon organoid. B) Magnified area from (A) shows presence of STM (black arrowhead) on the basolateral (bl) side, the apical (ap) side, and the monolayer (black arrow) and multilayer (white arrow) surrounding the lumen. C) Overview of a possibly apoptotic cell with intracellular STM near the lumen (lu). D) Detailed view of STM from C shows enclosure within an SCV with a single membrane (red arrowhead). E) Detail of another area of the organoid showing cells in the luminal region (lu). F, G) Detail from E. F) Detail of two STM located along with other unknown structures within a single membrane compartment (black arrowhead) and STM in an SCV (blue arrowhead). G) A close-up shows STM in contact with a membrane protrusion (green arrow), but not invaded. H) Overview of a part of the cell layer of the organoid. I) Detailed view of invading STM with contact to a membrane protrusion (purple arrow) and surrounding microvilli (black arrows). Scale bars: 100  $\mu\text{m}$  (A), 25  $\mu\text{m}$  (B), 3  $\mu\text{m}$  (C), 750 nm (D, F, G, I), 7  $\mu\text{m}$  (E), 5  $\mu\text{m}$  (H).

#### Generation of apical-out intestinal organoids

Another method to infect 3D organoids without physical injury is the generation of apical-out organoids (Co *et al.*, 2019). The reversal of the polarity of 3D organoids enables analyses of pathogen-host interactions at the apical side without microinjection. For the generation of apical-out organoids, murine enteroids were cultured as regular for 7-10 days in Matrigel. These normal 3D basal out enteroids were dislodged and solubilized to remove the Matrigel. The solubilized enteroids were re-seeded in medium without Matrigel in low-attachment plates or with a minimal amount of Matrigel to immobilize the organoids at the bottom of the chambered coverslips. In first attempts, mostly enteroids with mixed polarity could be observed (Figure V.5.14 A, B). Mixed-polarity enteroids were fixed and stained with DAPI, phalloidin and CellMask whereas high F-actin signal indicates the apical side. In cross-sections of mixed polarity enteroids both apical-out and basal out areas were visible (Figure V.5.14 A'). The formation of apical-out organoids is highly heterogenic; however, it allows to infect multiple 3D organoids directly within the medium without microinjection.

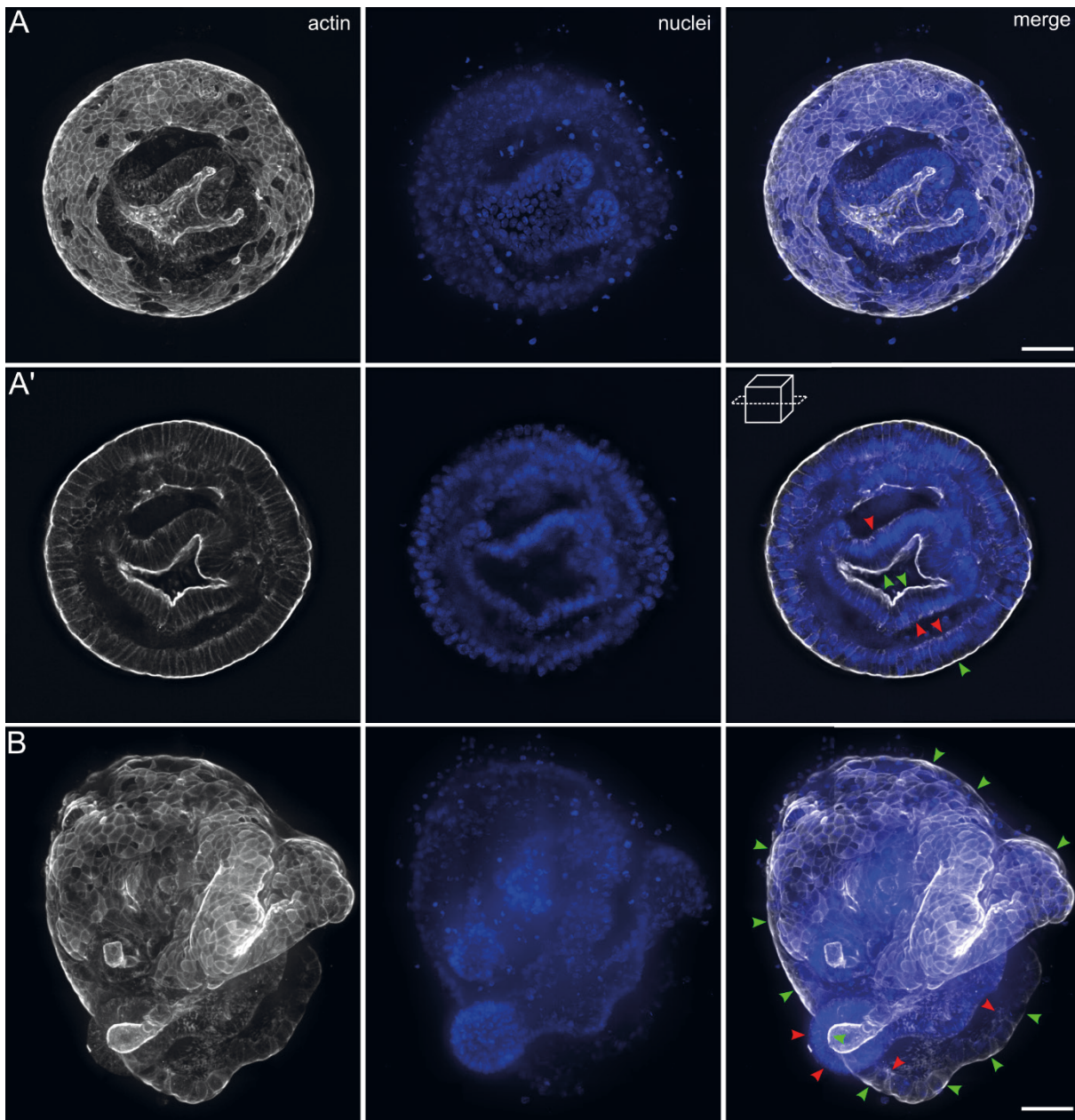


**Figure V.5.14. Fluorescence imaging of 3D apical-out enteroids.** Maximum intensity projection (A, B) and cross-section (A') of induced mixed polarity murine ileum organoids. Murine ileum organoids were cultured with minimal amount of Matrigel. Arrowheads indicate apical (green) and basal (red) regions. Cultivation, fixation and staining with phalloidin-iFluor647 (white) and DAPI (blue) in  $\mu$ -slide chambered coverslip before imaging. Imaging with 40x objective. Multiple images with overlaps were acquired and stitched. Scale bars: 50  $\mu$ m.

## 2D cultivation, characterization and infection

### *Organoid cultivation on transwells – from 3D to 2D*

In addition to 3D cultivated organoids, enzymatic dissected organoids can be seeded on a flat plastic surface or transwells (Figure V.5.15). The attachment of the organoid fragments or single cells requires coating with complex matrices, e.g. Matrigel, or gelatin, collagen or fibronectin (Aguilar *et al.*, 2021). The complex matrix on the one hand provides a suitable coating surface, but on the other hand has several disadvantages like the presence of growth factors and other components like gentamicin with batch-to-batch variability (Aguilar *et al.*, 2021). To obtain a confluent cell layer, parameters as seeded cell number and medium composition has to be considered. With the medium composition, cell differentiation can be inhibited or induced for example. The advantages of organoid-derived monolayers are the access to the apical side without the need of special equipment. Pathogens can easily be added or removed, as well as cell debris and waste products. Additionally, due to the usually flat monolayer, microscopic analysis should be also more straightforward. Single cells can easily be analyzed by high-throughput screenings. However, cell characteristics like differentiation and intercellular connections can differ between organoids and organoid-derived monolayers (Aguilar *et al.*, 2021).

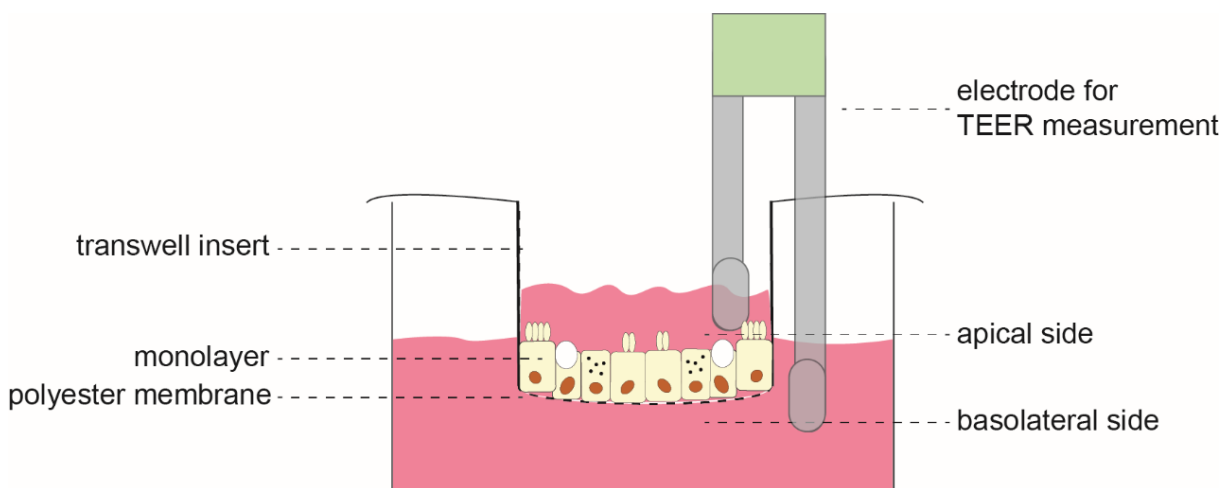


**Figure V.5.15. Cultivation of organoid-derived monolayers on transwells.** The organoids are enzymatically dissected and single cells are seeded on a matrix-coated membrane (here polyester). Growth is dependent on the cell number seeded, medium composition as well as the coating matrix. The cells of the monolayer have access to nutrients from both cellular surfaces, enabling a more physiological growth. To assess monolayer confluence, transepithelial electrical resistance (TEER) is measured.

Transwells or other permeable inserts can be used to get access to both sides of the epithelium, increasing the possibilities of investigations. Thus, the cells are able to take up molecules from both cellular surfaces, leading to a more physiological metabolic activity. The confluence of transwell monolayers is assessed by measuring the transepithelial electrical resistance (TEER). The confluent layer then can be used for specific staining, e.g. PAS staining or immunostaining, and infections.

*PAS staining of murine tissue and 2D cultured intestinal organoids*

The periodic acid-Schiff (PAS) reaction is one of the most frequently used chemical methods in histology. As unstained structures are low in contrast under the light microscope, staining with peroxide solution and Schiff's reagent increases contrast and can help to distinguish forms and structures. This method was already used for other biopsy samples and scientific approaches (Adams and Dilly, 1989; Lauren and Sorvari, 1969; Nikiforou *et al.*, 2016; Osho *et al.*, 2017; Spicer, 1960). During the PAS reaction, the samples are treated with periodic acid, resulting in the oxidation of the 1,2-glycols into aldehyde groups. Following oxidation, fuchsin-sulfuric acid (Schiff's reagent) is added to the samples, causing a reaction of the aldehydes to form a red color. Thus, this reaction yields a specific color reaction with unsubstituted polysaccharides, neutral mucopolysaccharides, muco- and glycoproteins, and glyco- and phospholipids and can be used as evidence for mucus production. We wanted to investigate potential mucus production of our human 2D monolayers (Figure V.5.16 A and B) before infection to get a better insight and result interpretation. Additionally, for comparison, we stained freshly prepared and embedded murine gut samples (Figure V.5.16 D). As a control, we performed a toluidine staining (Richart, 1963; Sridharan and Shankar, 2012) (Figure V.5.16 C). Besides nucleic acids, toluidine blue also stains mucins, amyloids and granules from mast cells and endocrine cells and is described for epoxy resin embedded thin sections (Sridharan and Shankar, 2012).

We stained the human organoid monolayers after 3 days and 11 days, directly before infection (Figure V.5.16 A and B). We were able to find smaller areas high in contrast, as exemplarily indicated. After 3 days, the amount of these spots was less than after 11 days, indicating a differentiation of the cells also in our 2D monolayers. Thus, we concluded that infections can be performed under mucus producing conditions with these cells. Additionally, we found an increased mucus production and potential goblet cells in colon monolayers in comparison to ileum monolayers. Furthermore, epoxy resin embedded thin sections of murine gut samples showed an increased signal in toluidine stain (Figure V.5.16 C) and also PAS reaction (Figure V.5.16 D). Hence, we performed infections for 30 min and 60 min and demonstrated that usage of organoid cell culture can lead to a more complex result in comparison to conventional and simpler cell culture models (Figure V.5.18).

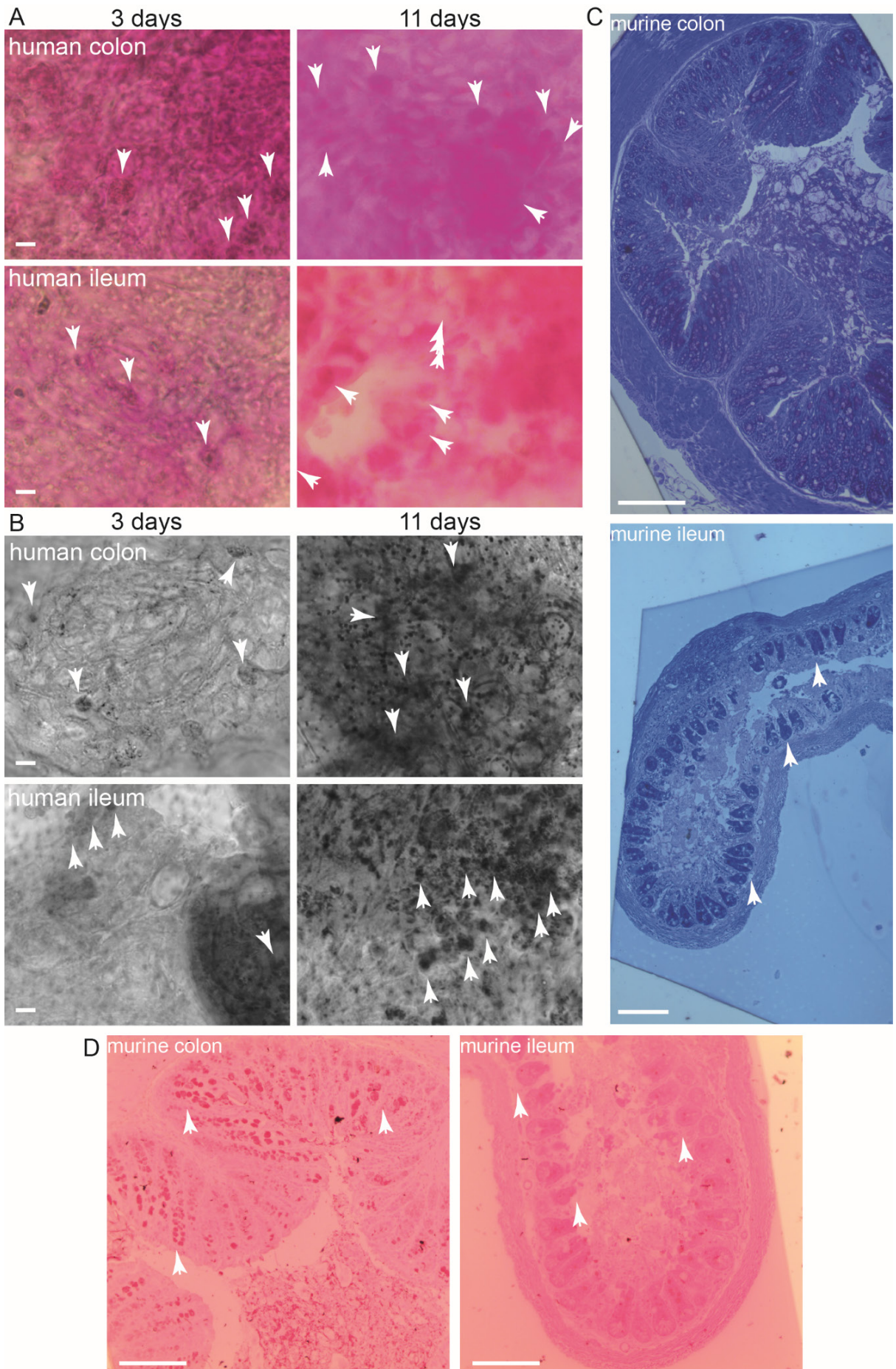


**Figure V.5.16. PAS analysis of human organoid monolayer and murine biopsy samples.** PAS staining of human colonoids and enteroids (A and B), as well as toluidine stained murine biopsy samples (C) and PAS stained murine biopsy samples (D). Arrows indicate stained structures. A and B) Monolayers were fixed with 3% PFA in PBS and incubated with periodic acid solution (10%). After washing, samples were incubated with Schiff's reagent. Following these preparations, the samples were fixed on microscope slides. For microscopy, 10x and 20x magnification were used, respectively. Scale bars: A) and B) 10  $\mu\text{m}$ , C) 50  $\mu\text{m}$ , D) 100  $\mu\text{m}$ .

### 2D infections – TEER measurements

Various cells can be cultured on porous filters. However, due to optical properties of the filter material and cell shape, the quality of the cell monolayer is difficult to evaluate (Chen *et al.*, 2015). However, the TEER measurement can be used as an indicator of the polarization level quality for the cultivation. It is described that completely differentiated cell cultures possess a stable TEER between 500 and 1,100  $\Omega/\text{cm}^2$  (Chen *et al.*, 2015).

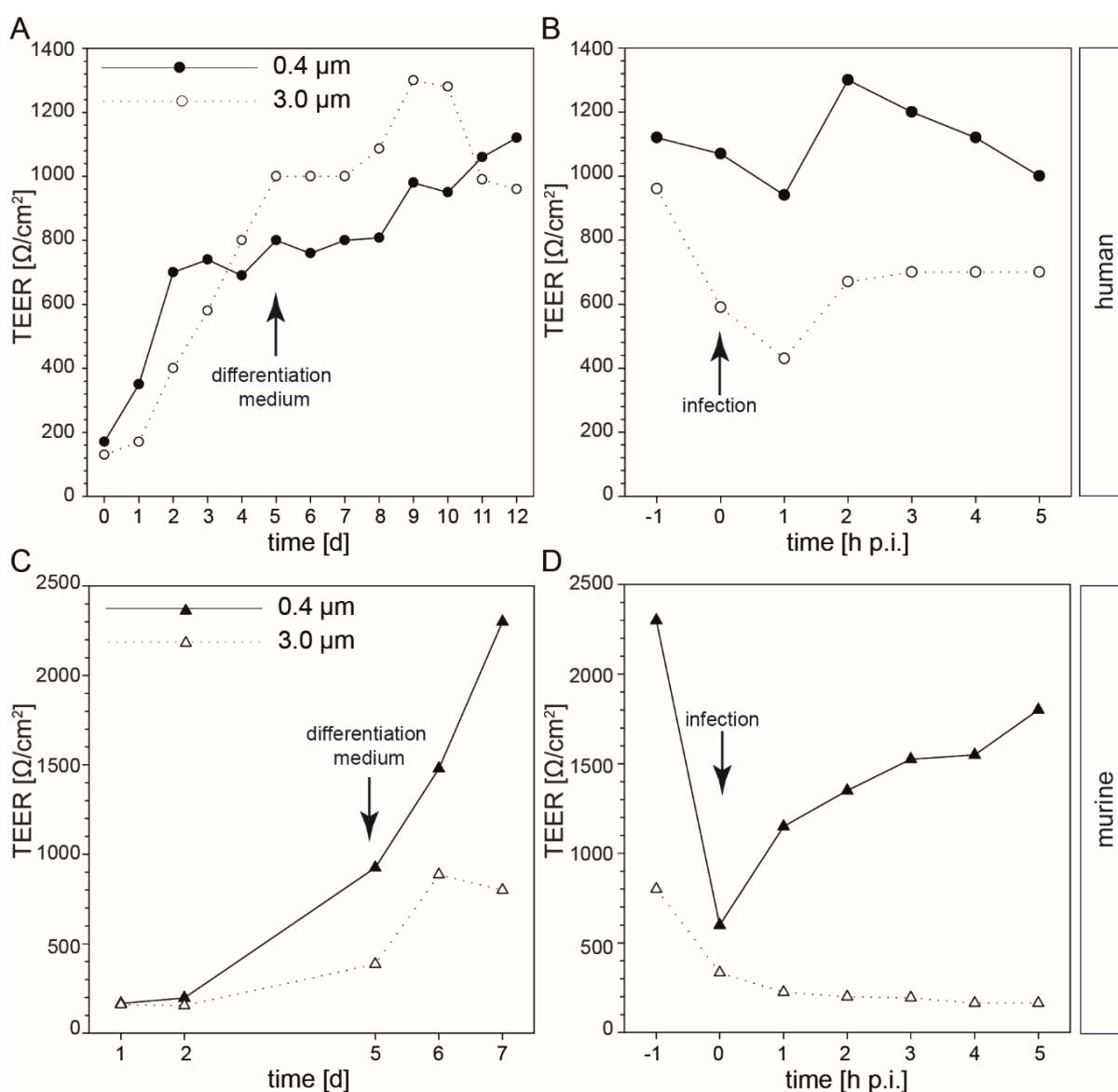


**Figure V.5.17. TEER measurement during infection process of intestinal organoid monolayers.** Shown are TEER measurements during growth (A, C) and infection of human- and mouse-derived monolayers (B, D). The transepithelial electrical resistance (TEER) was measured every day after seeding the cells (A) or every hour post infection (p.i.) (B). A)  $1 \times 10^5$  cells/well were seeded in 2D monolayer medium at day 0. At day 5, medium was

changed to differentiation medium as indicated. Monolayers were grown for 12 days before infection. B) For infection, 2.5 h subcultures of infective STM were grown and organoid monolayers were infected at MOI of 50 for 60 min. The cells were treated with 100  $\mu\text{g}/\text{ml}$  gentamicin per well for 1 h, washed three times with prewarmed PBS and incubated with 10  $\mu\text{g}/\text{ml}$  gentamicin per well for additional 4 h. C) Growth of murine-derived monolayer. Set-up as described for human-derived monolayer, with exception of  $1.5 \times 10^5$  cells/well were seeded. TEER measurement as indicated. D) Infection of mouse-derived monolayer as described for human-derived monolayer.

During cultivation of our 2D monolayers of murine and human organoids, we measured the TEER daily, (Figure V.5.17 A, C) whereas during infection, it was determined every hour (Figure V.5.17 B, D), respectively. We used transwells with polyester membranes with a pore size 0.4  $\mu\text{m}$  (= 0.4  $\mu\text{m}$  transwell) and 3.0  $\mu\text{m}$  (= 3.0  $\mu\text{m}$  transwell), respectively, to investigate growth (Figure V.5.17 A) and also behavior of the cell layer during infection (Figure V.5.17 B). 3.0  $\mu\text{m}$  transwells were tested, because potential exit strategies were aimed to be analyzed, allowing the bacteria to cross the filter more easily after passaging the 2D monolayer. In the first growth phase with 2D monolayer medium, TEER of human-derived monolayers increased almost exponentially from day 0 (170  $\Omega/\text{cm}^2$ ) to day 3 (740  $\Omega/\text{cm}^2$ ) on 0.4  $\mu\text{m}$  transwells and from day 0 (130  $\Omega/\text{cm}^2$ ) to day 5 (1,000  $\Omega/\text{cm}^2$ ) on 3.0  $\mu\text{m}$  transwells. For the mouse-derived monolayer we measured a TEER of  $\Omega/\text{cm}^2$  on 0.4  $\mu\text{m}$  transwells and 387  $\Omega/\text{cm}^2$  on 3.0  $\mu\text{m}$  transwells after 5 days (Figure V.5.17 B). The growth curve of the human-derived monolayers on 0.4  $\mu\text{m}$  filter flattened earlier than on 3.0  $\mu\text{m}$  transwells, indicating an earlier saturation regarding cell-cell contacts and differentiation. At day 5 we changed the medium to differentiation medium and observed a saturation of the human-derived monolayers up to day 7 (1,000  $\Omega/\text{cm}^2$ ) on the 3.0  $\mu\text{m}$  transwells, whereas TEER of the monolayer continuously increased on 0.4  $\mu\text{m}$  transwells to 1,120  $\Omega/\text{cm}^2$ . Between day 7 and 10, TEER increased up to 1,300  $\Omega/\text{cm}^2$  on the 3.0  $\mu\text{m}$  transwells and decreased back to 960  $\Omega/\text{cm}^2$ . Thus, on both transwells we were able to reach an optimal TEER for the human-derived monolayers, indicating a confluent and differentiated monolayer. In contrast to this, mouse-derived monolayers at day 7 with a TEER of 800  $\Omega/\text{cm}^2$  (3.0  $\mu\text{m}$ ) and 2,967  $\Omega/\text{cm}^2$  (0.4  $\mu\text{m}$ ) were infected (Figure V.5.17 D).

In a next step, we infected the monolayers with STM WT and measured the TEER during infection over 5 h (Figure V.5.17 B, D). Directly at the point of infection, the TEER of the monolayer on the 3.0  $\mu\text{m}$  transwells decreased to 590  $\Omega/\text{cm}^2$  (human) and 335  $\Omega/\text{cm}^2$  (murine), whereas TEER of the monolayer on the 0.4  $\mu\text{m}$  transwells remained stable at 1,070  $\Omega/\text{cm}^2$  (human). Contrary, the TEER of the mouse-derived monolayer decreased to 820  $\Omega/\text{cm}^2$  on 0.4  $\mu\text{m}$  transwells. After 1 h, a minimum for human-derived monolayers was measured on both filters (3.0  $\mu\text{m}$ : 430  $\Omega/\text{cm}^2$ ; 0.4  $\mu\text{m}$ : 940  $\Omega/\text{cm}^2$ ) (Figure V.5.17 B). Whereas the TEER of the mouse-derived monolayer on 0.4  $\mu\text{m}$  transwells was slightly increasing (1,300  $\Omega/\text{cm}^2$ ), TEER on 3.0  $\mu\text{m}$  transwells was still decreasing until the end of the measurement (Figure V.5.17 D). At 2 h p.i. the TEER of the human-derived monolayer on the 3.0  $\mu\text{m}$  transwells reached 700  $\Omega/\text{cm}^2$ , not fully recovering to its initial value of 960  $\Omega/\text{cm}^2$ , indicating a loss of barrier integrity. In contrast to this, the TEER of the monolayer on the 0.4  $\mu\text{m}$  transwells reached a maximum of 1,300  $\Omega/\text{cm}^2$  2 h p.i., slowly decreasing to 1,000  $\Omega/\text{cm}^2$  after 5 h p.i., similar to the starting TEER.

Thus, we concluded a full recovery of the monolayer on 0.4  $\mu\text{m}$  transwells. Comparably, the TEER of the mouse-derived monolayer also increased on 0.4  $\mu\text{m}$  transwells to 2,200  $\Omega/\text{cm}^2$ , not reaching fully recovered start TEER 5 h p.i. (Figure V.5.17 D). This loss of barrier integrity and recovery during invasion of STM is already described and we concluded that the selected parameters are compatible with the chosen system and can be used for further investigations on infection of mutant strains (Figure V.5.18) and also of STY/SPA. Additionally, in combination with lentiviral transfected organoids, a microscopic analysis of the infection process and actin remodeling can be possible in a next step.

### *2D infections – quantification of invasion*

As there are known described phenotypes regarding the SPI1 and SPI4 in cell lines as HeLa, MDCK and CaCo2 (Gerlach and Hensel, 2007; Gerlach *et al.*, 2007), in a next step we aimed to investigate the invasion of cells in human organoid monolayers. It was already shown that distinct SPI are important for different stages of infection (Gerlach and Hensel, 2007). Whereas the SPI4 and its giant substrate SiiE are essential for adhesion and invasion of polarized cells by supporting translocation of the SPI1-T3SS effector proteins, SPI4 function is not required for invasion of non-polarized cells (Gerlach *et al.*, 2008; Wagner *et al.*, 2011). In contrast to this, the SPI1-encoded T3SS is essential for a successful invasion of polarized and non-polarized cells. Thus, we decided to analyze these known phenotypes in monolayers of human enteroid- and colonoid-derived cells. As we demonstrated mucus production of the cells (Figure V.5.16), these monolayers differ from simple tumor-based cell culture lines like polarized MDCK and non-polarized HeLa cells. We infected the human monolayers for 30 and 60 min, lysed the cells, plated lysates onto agar plates and determined colony forming units to quantify invasion (Figure V.5.18) of STM WT,  $\Delta spi4$  and  $\Delta invC$  strains. Because of co-regulation of the SPI with other systems, important during invasion, it was shown that *invC* deletion specifically inhibits SPI1-T3SS assembly (Gerlach *et al.*, 2008; Gerlach *et al.*, 2007).

Interestingly, for STM WT we found a 9-fold higher invasion of colon cells 30 min p.i. in comparison to ileum (Figure V.5.18 A), whereas invasion of colon cells was slightly lower 60 min p.i. (76.5%) (Figure V.5.18 C). At both time points and for both types of organoids, the  $\Delta invC$  strain showed the most decrease in invasion compared to WT and  $\Delta spi4$  (Figure V.5.18 B, D). An exception to this is the invasion of colon cells after 30 min, indicating the essential role of the SPI1-T3SS for invasion as already described. With an invasion of 2.2% of WT (Figure V.5.18 B),  $\Delta spi4$  showed an even more decreased invasion of colon cells after 30 min in comparison to  $\Delta invC$  (10% of WT). Invasion of ileum cells was less influenced by a *spi4* deletion 30 min p.i. (65% of WT) than 60 min p.i. (27.4% of WT). Thus, we concluded a higher invasion of ileum cells by the WT over time, which is not possible if *spi4* is deleted, as invasion of ileum cells by the WT was increased 13-fold of 60 min p.i. in comparison to 30 min p.i. In contrast to this,  $\Delta spi4$  invasion of colon cells 60 min p.i. was increased in comparison to 30 min infection (43.7%). Hence, we assumed that invasion of colon cells is partly possible after 1 h, even if only the SPI1-T3SS is expressed. If the SPI4-T1SS is not expressed for mediating adhesion to the apical



side, SPI1-T3SS is possibly affected in the efficient translocation of the effector proteins into the host cell. Thus, we gained first insights in the SPI1- and SPI4-dependent invasion of human-derived cells 30 min p.i. and 60 min p.i., showing distinct differences and making further investigations favorable.

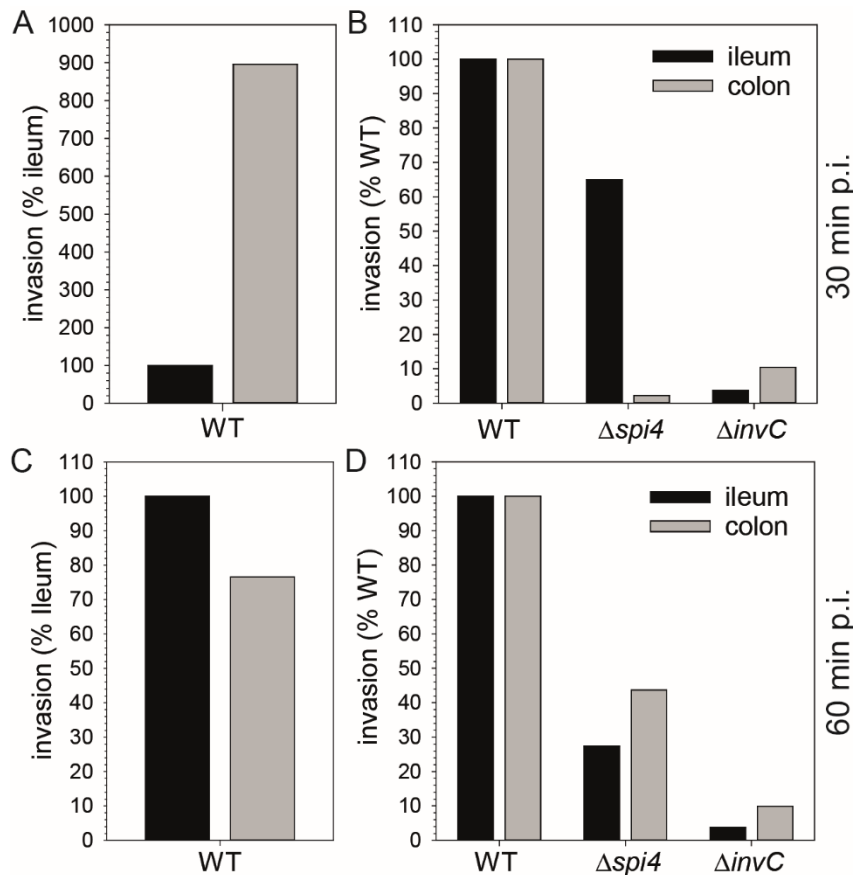


**Figure V.5.18. Infection of intestinal organoid monolayers with STM.** Shown are representative infections of exemplary chosen human enteroid and colonoid monolayers on 0.4  $\mu\text{m}$  transwells as indicated with STM WT,  $\Delta spi4$  and  $\Delta invC$ . Infection occurred as described above for 30 min or 60 min at MOI 50. To determine invasion, cells were treated with 100  $\mu\text{g/ml}$  gentamicin per well for 1 h, washed thrice with prewarmed PBS and lysed with 0.5% deoxycholate in PBS (freshly prepared) for 10 min. The samples of inoculum and lysates were diluted and plated to determine CFU. The percentages of invaded bacteria were calculated. A) Comparison of the invasion of ileum and colon monolayers by STM WT 30 min p.i. B) Invasion of ileum and colon monolayers by  $\Delta spi4$  and  $\Delta invC$  in comparison to STM WT 30 min p.i. C) Comparison of the invasion of ileum and colon monolayers by STM WT 60 min p.i. B) Invasion of ileum and colon monolayers by  $\Delta spi4$  and  $\Delta invC$  in comparison to STM WT 60 min p.i.

In conclusion, we were able to establish a way to quantify the invasion of 2D cultured intestinal organoids by STM. As the typhoidal serovars STY and SPA are pathogens that are highly adapted to the human host, analysis of these will be of great interest.

#### *2D cultivation and infection – microscopy*

Imaging of cells grown on transwells is challenging due to the high position of the cells in the well and the transwell membrane interfering with illumination. For microscopic analysis, the cell culture inserts have to be taken out of the culture well and transwell membranes have to be punched out. This makes

live cell imaging nearly impossible. However, microscopy of fixed membranes, embedded on microscope slides or taped on SEM stubs is possible and analysis is described below.

After fixation and preparation of 2D cultured intestinal organoids for SEM, monolayers could be analyzed in highest magnification (Figure V.5.19). Ultrastructural analysis of monolayers of human colon, human ileum and murine ileum organoids show adjacent growing cells with a densely packed apical brush border that is also intact at the cell borders (Figure V.5.19A, B, C, D). A detailed view of the brush border shows microvilli in a high order with almost identical length (Figure V.5.19 D). Some areas of the monolayer show higher heterogeneity regarding the morphology of cells (Figure V.5.19 E, E'). This may indicate the successful cultivation of distinct cell types, e.g. goblet cells that possess less microvilli on their apical side and a large secretion pore on their apical side in the center of the cell (Figure V.5.19 E') similarly shown in the side-view TEM image above (Figure V.5.6 B).

Monolayers infected with STM and SPA WT were also analyzed (Figure V.5.20). The *Salmonella*-induced rearrangement of the actin cytoskeleton into membrane ruffles during the invasion process has been studied in detail in our lab (Gerlach *et al.*, 2008; Kommnick and Hensel, 2021; Kommnick *et al.*, 2019; Lorkowski *et al.*, 2014). We identified *Salmonella*-induced membrane ruffles at adhesion and invasion sites on 2D cultured murine enteroid-derived monolayers (Figure V.5.20). STM WT induced the formation of small membrane pedestals at adhesion sites (Figure V.5.20 A) and small bulky membrane ruffles at invasion sites with multiple bacteria inside (Figure V.5.20 B, B', B''). First infection experiments with human-adapted typhoidal SPA showed less invasiveness and almost no invasion sites at cells with dense brush border. Membrane ruffles were only observed at cell borders and cells largely lacking microvilli (Figure V.5.20 C, C').

Fluorescence microscopy of STM-infected monolayers was performed (Figure V.5.21). The murine enteroid monolayers show adjacent growing cells with high F-actin accumulation at the apical site, indicating a densely packed brush border. Multiple invasion sites with microvilli effacement are visible at low and high magnification (Figure V.5.21 A, B, C).

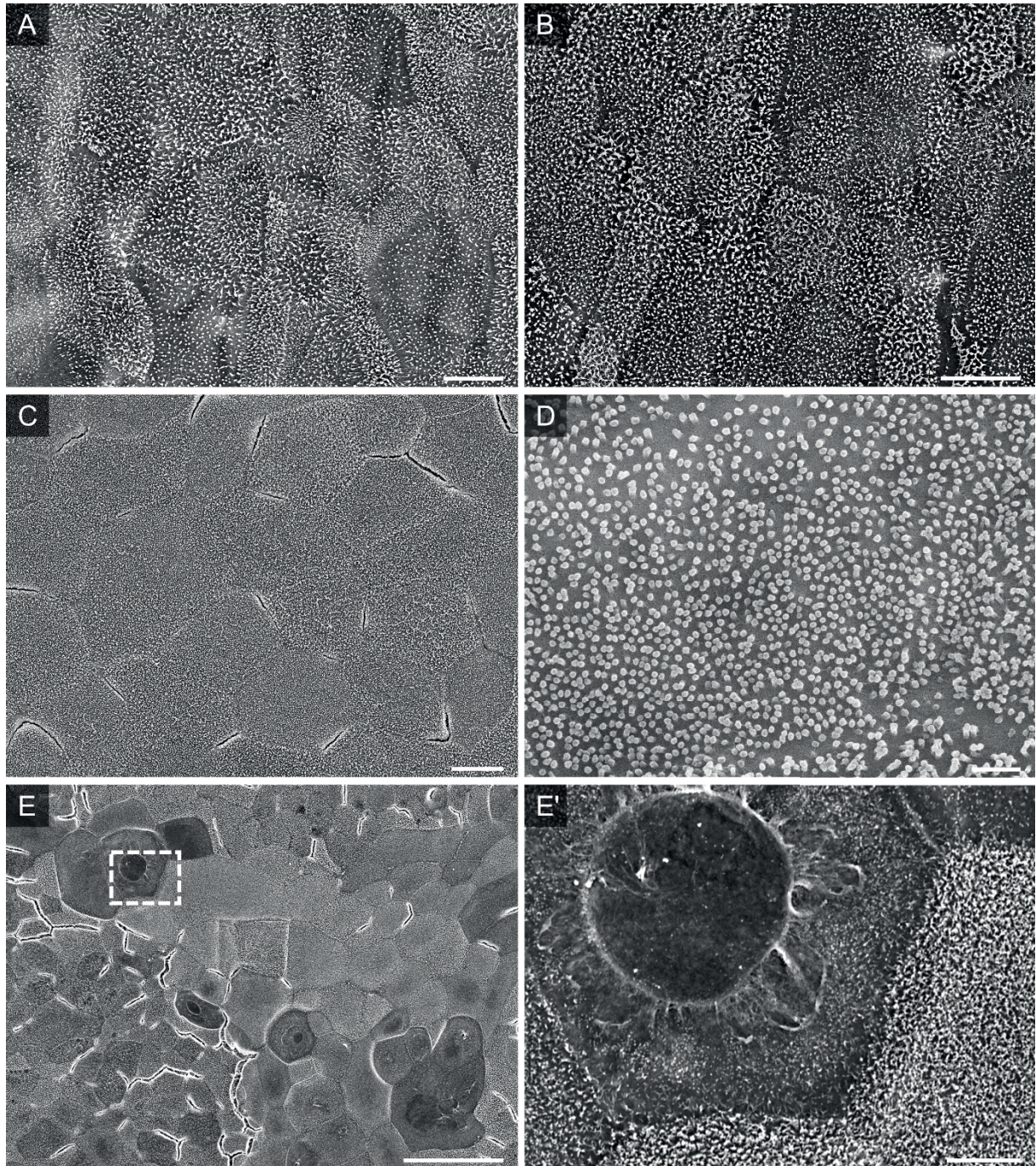


**Figure V.5.19. SEM imaging of 2D cultured organoids.** Organoids were cultured on transwell cell culture inserts and fixed for SEM. Overview of 2D cultured human colon (A), human ileum (B) and murine (C, D, E, E') enteroids. Inset (E') shows a possible goblet cell. Scale bars: 10 μm (A, B, C), 50 μm (E), 1 μm (E').

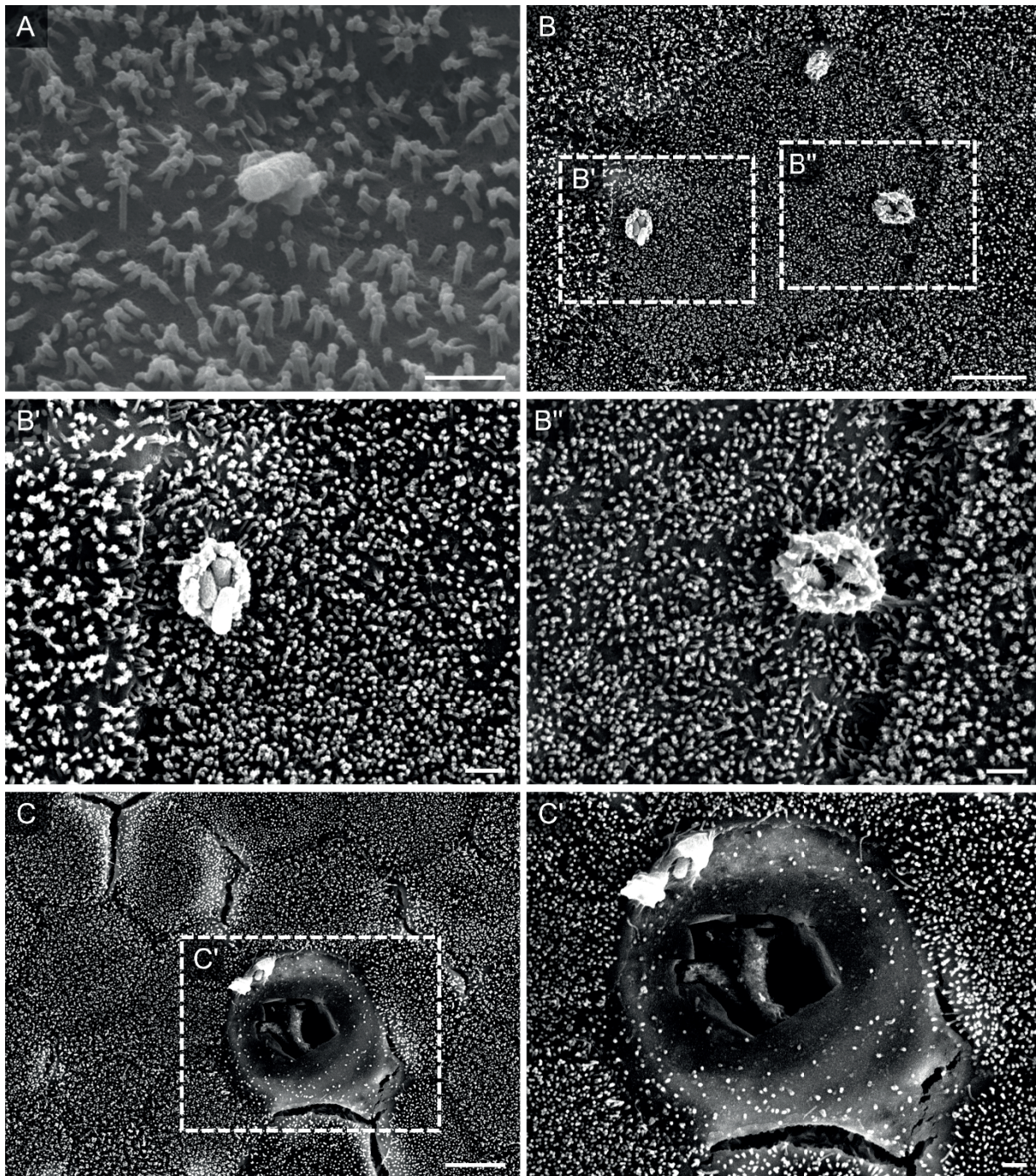


**Figure V.5.20. SEM imaging of 2D cultured STM and SPA infected organoids.** Murine ileum enteroids were cultured on transwell cell culture inserts and fixed 30-60 p.i. for SEM. Adhesion (A) and invasion sites (B, B', B'') of STM WT on apical side of enterocytes. Invasion site of SPA WT at a cell with less prominent brush border (C, C') Scale bars: 1  $\mu\text{m}$  (A, B', B'', C'), 5  $\mu\text{m}$  (B, C).

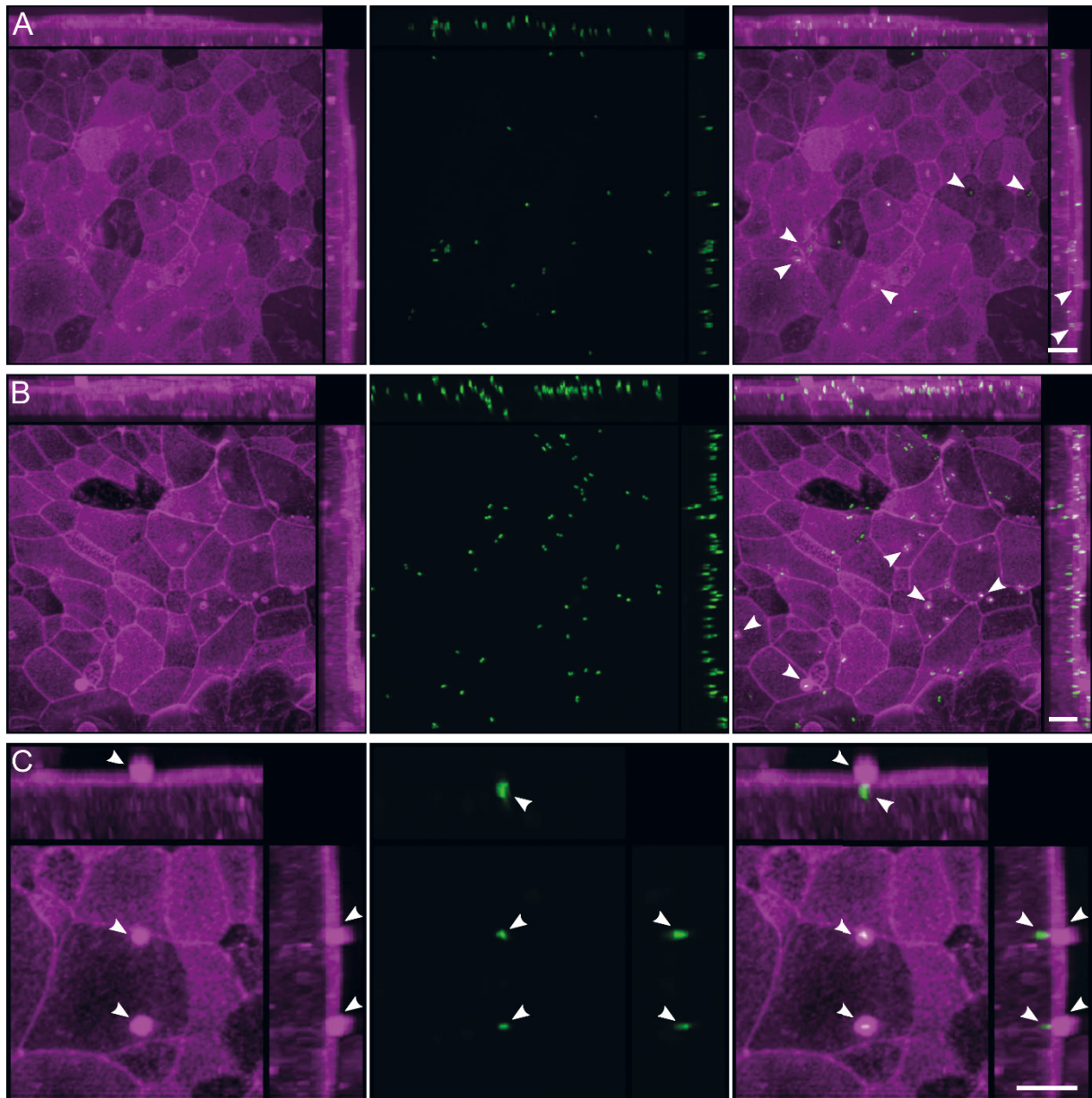


**Figure V.5.21. Fluorescence imaging of 2D cultured STM infected organoids.** Murine ileum enteroids were cultured on transwell cell culture inserts and fixed 30-60 min p.i. for fluorescence microscopy and stained with phalloidin-iFluor647 for actin visualization (magenta). Adhesion and invasion sites of STM WT expressing GFP (green) on apical side of enterocytes with membrane ruffles are indicated with arrowheads. Images are shown as maximum intensity projection of X-Y, X-Z and Y-Z plane. Scale bars: 10  $\mu$ m.

All in all, we established intestinal organoids in 2D and 3D as infection models for *S. enterica*. Here, we demonstrated a wide range of methods, possible to use for investigation of STM and SPA infection.

#### V.5.4. Discussion

Frequently used cell culture models were over several years the tool to unravel virulence mechanisms in host-pathogen interactions. However, the experimental design was restricted to one cell type for most of the cell culture-based assays. While it was possible to investigate cellular interactions of pathogens with high temporal and spatial resolution, these experiments lacked complex tissue architecture and were not suitable to reflect *in vivo* relevant settings. Most recently, organoid systems have been established in a wide field of biological research, including infection biology. Stem-cell derived organoids are capable to reconstitute a certain degree of multicellular complexity with a close relation to *in vivo* conditions in a 3D environment. But still, organoid culture remains complex, expensive and time consuming with some issues in reproducibility between labs because of the highly heterogenic nature.

The results presented here show uninfected and infected 3D and 2D grown organoids of human and murine origin that were labeled and imaged across scales as well as analyzed regarding their behavior during infection. Organoids are difficult to image because of their dimensions in X, Y and Z. Imaging in Z is limited, which is dependent on working distance, parfocal length and numerical aperture of the used objectives and the wavelength of light used to illuminate the specimen (Figure V.5.3). SDCM of 3D organoids revealed the overall architecture with enterocytes facing inward with their apical side but imaging of higher Z planes resulted in blurry images with loss of focus and high background (Figure V.5.4). The penetration depth of confocal microscopy is roughly limited to less than 100  $\mu\text{m}$  (Graf and Boppart, 2010). Multiphoton microscopy can improve penetration depth at least 2-fold (Centonze and White, 1998), but lateral resolution is worse and it may lead to photo toxic and bleaching effects due to higher light intensities (Hopt and Neher, 2001). Recently developed methods like light sheet-based microscopy offer live cell imaging well suited for large specimens with more photons and less photo damage (Reynaud *et al.*, 2008). Dipping objectives could be used to reduce distance to specimens (Rakotoson *et al.*, 2019). Matrigel may interfere with fluorescence excitation and emission and may result in higher background.

Better resolution and less background can be achieved by releasing organoids from Matrigel and mounting them on microscope slides (Figure V.5.5). This method may simplify imaging approaches but could create artefacts because of the treatment of the organoids. Detachment and preparation with multiple staining and washing steps in solution could damage the specimens. Large, complex organoids may disrupt during this procedure and in result, only round shaped spheroids are being analyzed. Flattening of the organoids between coverslip and microscope slide can also falsify the interpretation of infection sites. However, imaging of organoids mounted on microscope slides allows analyses of cell structures in more detail.

Immunostaining and other labeling techniques are commonly used to identify structures of interest. Also, in the context of organoids as infection model, these methods can help to shed light on the cell

types important in infection processes. Frequently used antibodies and fluorescent probes are e.g. villin (polarized epithelium), mucin 2 (goblet cells), MMP7 (Paneth cells), chromogranin A (enteroendocrine cells), Ki67 (dividing cells), lysozyme (Paneth cells), ZO1 (tight-junctions), wheat germ agglutinin (goblet cells, Paneth cells, mucus), ulex europaeus agglutinin I (goblet cells, Paneth cells, mucus, M cells), phalloidin (F-actin) and also histological staining like PAS are used to determine certain cell types and structures (Broguiere *et al.*, 2018; Farin *et al.*, 2016; Fatehullah *et al.*, 2013; Noel *et al.*, 2017a, b). Through WGA staining we also could identify regions of interest with secretory granules inside cells and mucus in crypt domains in enteroids and colonoids as well as the general structure with a combination of phalloidin, DAPI and CellMask staining (Figure V.5.7). However, it was difficult to analyze staining with first and secondary antibodies due to high background. The used methods have to be improved for further experimental procedures. Flow cytometry, especially if combined with reporters that provide information about the physiological state of *Salmonella* (SPI1-T3SS & SPI2-T3SS activity, induced stress, and metabolic pathways), could also represent a powerful tool to investigate cell types targeted by *Salmonella* in single cell-based studies (Reuter *et al.*, 2021; Röder *et al.*, 2021a, b; Schulte *et al.*, 2021a, b).

To investigate infection processes in organoids, it is crucial to allow pathogens access to the apical side of organoids. One of the techniques to facilitate that is the microinjection of pathogens into the lumen of the organoids. This method has been used successfully with *Helicobacter pylori*, *Clostridium difficile*, *Escherichia coli*, *Salmonella enterica* and even SARS-CoV-2 (Aguilar *et al.*, 2021; Bartfeld and Clevers, 2015; Hentschel *et al.*, 2021; Lamers *et al.*, 2021; Ramirez-Flores and Knoll, 2021; Tindle *et al.*, 2021). Technical limitations such as the highly heterogenic nature of organoids and the labor- and cost-intensive infection are drawbacks of this method. Further, the penetration with an injection needle can damage cell layers and spillage of pathogens into the medium could favor unwanted infections at the basal site of the organoid. Our microinjection experiments showed exactly these injuries at the injection site (Figure V.5.10) and *Salmonella* infection sites at the basolateral side of intestinal organoids (Figure V.5.10, Figure V.5.11, Figure V.5.12, Figure V.5.13). We could observe *Salmonella*-containing compartments in microinjected intestinal organoids (Figure V.5.11, Figure V.5.12, Figure V.5.13) with a localization near the nucleus as described before (Abrahams and Hensel, 2006; Salcedo and Holden, 2003) and in an electron-light compartment which probably represents a phago-lysosome with subsequent degradation of the pathogen (Buchmeier and Heffron, 1991; Carrol *et al.*, 1979). Due to the early fixation time points, no *Salmonella*-induced tubular structures such as SIF could be observed (Krieger *et al.*, 2014; Yin and Zhou, 2018a, b). Krieger *et al.* (2014) described these tubular structures in detail with a CLEM approach in epithelial cell culture. However, no CLEM compatible methods have been yet developed for such large specimens as organoids.

Another method to circumvent physical injury of the organoids is the addition of the pathogens directly to the culture medium. To prevent infection processes from happening at the basolateral side it is

possible to control the epithelial polarity to generate apical-out organoids (Co *et al.*, 2019; Co *et al.*, 2021) (Figure V.5.22). We were indeed able to reproduce this recently published method to generate organoids with mixed polarity (Figure V.5.14). As in all the other 3D-based methods, the generated apical-out organoids are highly heterogenic which could hamper experimental design and reproducibility. However, apical-out organoids could represent a possibility of a 3D infection model without the drawbacks of microinjection.

All the 3D-based methods described above are difficult to combine with live cell imaging techniques. Lentiviral transfected organoids may help to develop live cell imaging approaches in the future (Maru *et al.*, 2016). Interpretation of fixed samples is often hard to analyze e.g. time and location of invasion sites (apical or basal side) and also fixation with aldehydes may interfere with surface structures such as mucus. It was also reported that invasion of *Salmonella* is higher in secretory cells, but for some methods as microinjection, not fully differentiated spheroids are utilized which possess only a low number of these cell types (Gagnon *et al.*, 2013; Yin and Zhou, 2018a, b). TEM analyzes are also challenging due to the sheer size of the specimen with several hundred micrometers in contrast to the ultrathin sections with a thickness of about 70 nm used for TEM. Also, interactions with cell debris that accumulates inside of 3D organoids is problematic. Newly developed organoid-on-a-chip models could represent a future technique to address this issue, even in combination with a defined microbiota applied to the organoid tissue (May *et al.*, 2017; Wang *et al.*, 2021).



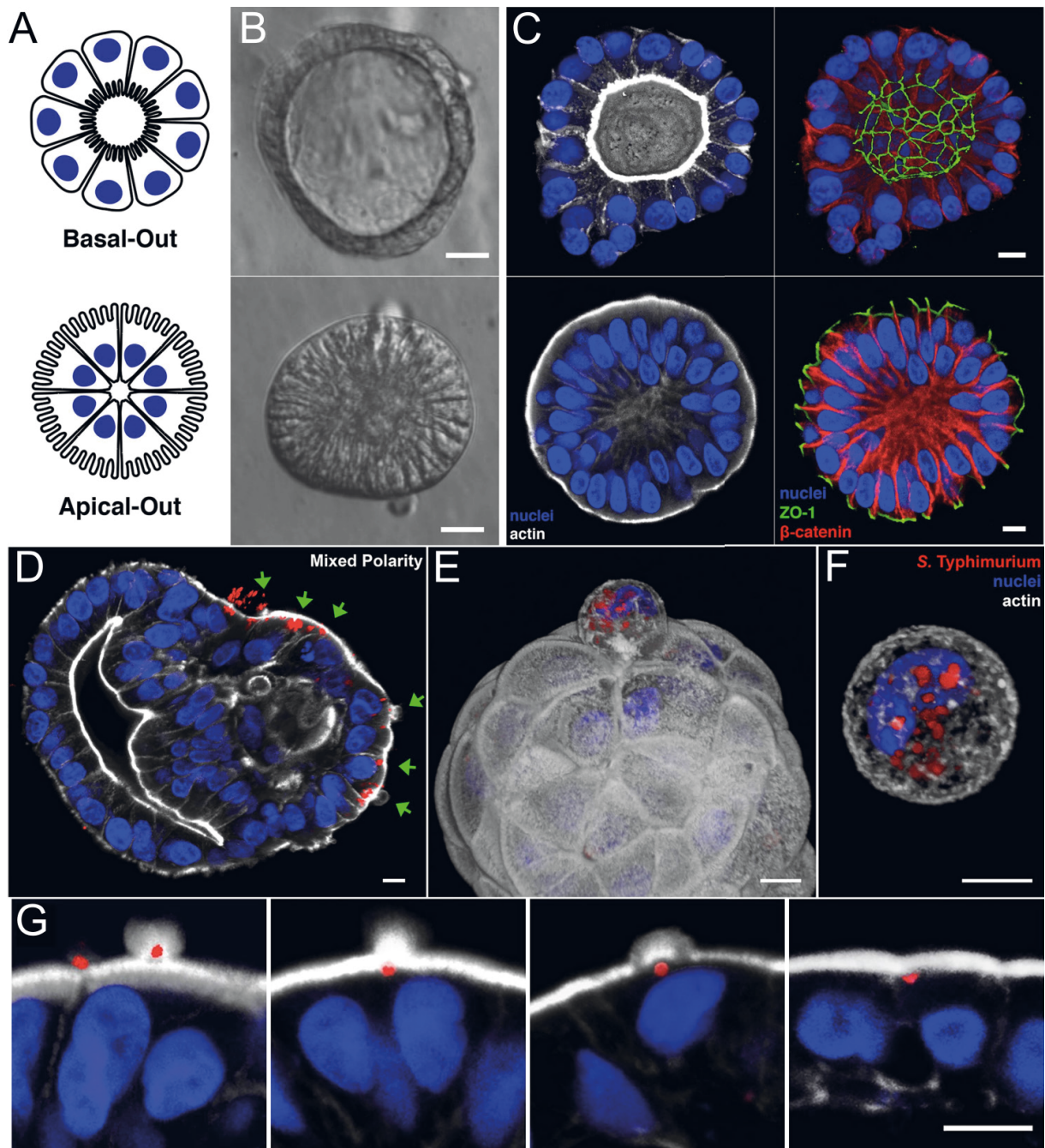


**Figure V.5.22. Generation and infection of apical-out enteroids.** A-E) Basal-out enteroids and apical-out enteroids are depicted schematically (A), imaged using modulation contrast microscopy (B) and imaged using confocal microscopy (C). D) STM selectively invades the exposed apical surface (green arrows) of a mixed polarity enteroid. E-F) 3D confocal reconstruction of STM within an epithelial cell in the process of extruding from the apical enteroid surface (E) or within a fully extruded cell after 6 h of infection (F). G) STM at different stages of invasion of apical-out enteroid. Nuclei in blue, actin in white, ZO-1 in green,  $\beta$ -catenin/STM in red. Scale bars 10  $\mu$ m (B, C). Figure adapted from Co *et al.* (2019) under CC BY license.

To investigate host-pathogen interactions, organoid-derived monolayers can have many advantages in comparison to 3D organoids as they provide access to the apical side of the cells (Aguilar *et al.*, 2021). Thus, pathogens, debris and solutes can be added or removed and a microscopic analysis is even better possible and single cells can be analyzed by high-throughput screening. 2D monolayers were already successfully used for analysis of infections, including *Helicobacter pylori* (Bartfeld and Clevers, 2015;

Boccellato *et al.*, 2019; Schlaermann *et al.*, 2016), *Escherichia coli* (VanDussen *et al.*, 2015), norovirus (Ettayebi *et al.*, 2016; Hosmillo *et al.*, 2020) and Epstein Barr virus (EBV) (Wallaschek *et al.*, 2021) infections. Here, we demonstrated the possibility of 2D cultivation of human- and murine-derived organoids (Figure V.5.16-Figure V.5.21). By high-resolution SEM, we were able to image the intestinal brush border on the apical side and conclude a high number of enterocytes in intestinal 2D monolayers (Figure V.5.19, Figure V.5.20). Together with TEER measurements, we can assess cell integrity and differentiation of the cells. In contrast to 3D approaches, no further equipment, e.g. for microinjections, is necessary and growth and infection parameters can be controlled more easily as already described (Aguilar *et al.*, 2021). Additionally, TEER measurement allows assessment of the cell integrity during infection (Figure V.5.17). With the calculated number of cells or staining, we are now able to calculate the MOI and are consequently able to quantify the adhesion, invasion and intracellular replication, not possible in 3D organoids. For comparison and also further applications, mucine-producing cell line HT29 can be used, which is an adherent epithelial cell line, derived from human colon cancer tumor. This cell line was already used to determine viral titers of the human parechovirus (Abed and Boivin, 2006) and to analyze *Bifidobacterium* and *Lactobacillus* strains counteraction to the toxic effect of *Clostridium difficile* (Boonma *et al.*, 2014; He *et al.*, 2002; Wang *et al.*, 2014). In future investigations, we are now able to combine infections with specific staining and/or transfected organoid-derived cells, to analyze if different *Salmonella* serovars preferentially invade distinct cell types. Experimental setups can easily be adjusted, like disadvantageous growth of 2D monolayers on transwells on complex matrices like Matrigel, which can be bypassed by using alternatives as collagen (Aguilar *et al.*, 2021). Growth on collagen was already shown to be a good alternative for stomach and intestinal organoids (Hosmillo *et al.*, 2020; Kayisoglu *et al.*, 2021; Lulla *et al.*, 2019; Schlaermann *et al.*, 2016). Furthermore, it is possible to grow cells in an air-liquid interface, where the cells are in contact with the culture medium only from the basolateral side, whereas the apical side is exposed to air (Aguilar *et al.*, 2021). This model showed a higher cell differentiation induced by the air exposure (Boccellato *et al.*, 2019; Li *et al.*, 2014a; Li *et al.*, 2014b; Sachs *et al.*, 2019; Sepe *et al.*, 2020).

Besides the microscopic analysis, we were also able to quantify STM infection in human-derived organoid monolayers (Figure V.5.18). Interestingly, STM WT showed reduced invasion of organoid-derived monolayers than in other published cell lines (Gerlach *et al.*, 2008; Gerlach *et al.*, 2007; Kommnick and Hensel, 2021). Invasion increased 60 min p.i. Thus, we concluded that the mucus layer, we stained by PAS stain, slowed down the invasion of the cells. Whereas invasion of colon 30 min p.i. was 9-fold higher in comparison to ileum, invasion was comparable 60 min p.i., indicating that invasion of STM of colon cells is faster than ileum cells.  $\Delta spi1$  could not invade, as published before, indicating mucus and different cell types do not alter invasion depletion. Interestingly,  $\Delta spi4$  showed different phenotypes in ileum and colon monolayers, as well as 30 min p.i. and 60 min p.i. No invasion of colon cells was observed 30 min p.i., but approximately 70% invasion of WT of ileum cells, indicating a more important

role of the SPI4 for invasion of colon-derived monolayers. 60 min p.i. invasion of  $\Delta spi4$  was comparable to slightly increased invasion of colon-derived monolayers. We concluded that invasion of colon cells without SPI4-T1SS is more difficult. Thus, we were able to gain new insights in STM infection by using human organoid-derived monolayers.

### V.5.5. Outlook

Organoids have advanced infection research, leading to better understanding of host-pathogen interactions and diseases. During cellular and molecular pathways triggered by pathogen interactions, the organoids maintain tissue architecture. By combining infections with stained and transfected organoids, we can gain further insights into host-pathogen interactions and preferred cell types for invasion and proliferation. Thus, this knowledge will allow us to treat *Salmonella* infections more targetedly or prevent them, especially those of typhoidal serovars. As the typhoidal serovars are highly adapted to the human host, the analysis of their infection process is of great interest. As STY during infection influences and reprograms host functions and protection mechanisms as immune response to evade immune defense in intestinal human organoids (Nickerson *et al.*, 2018), further details about *Salmonella* infection can provide new input into future vaccine development. Furthermore, M cell differentiation by addition of Receptor activator of NF- $\kappa$ B ligand (RANKL) could be of great importance as M cells represent a common portal for pathogen invasion (Jepson and Clark, 1998) and controlled testing of these cells will lead to a better understanding of *Salmonella* infection.

Infection process can be analyzed in intestinal organoids, but to analyze the systemic infection of typhoidal *Salmonella* also other organoids, e.g. derived from gall bladder or liver, can shed new light on *Salmonella* infection. In general, first insights of the typhoidal serovars were already gained in intestinal and gallbladder organoids in 3D and 2D (Nickerson *et al.*, 2018; Scanu *et al.*, 2015). Scanu *et al.* found indications that STY can be a causative agent of gallbladder cancer by transforming genetically predisposed cells (Scanu *et al.*, 2015). STM was also already shown to be able to induce tumor growth in those predisposed cells in primary mouse fibroblast model (Scanu *et al.*, 2015). Sepe *et al.* observed host cell DNA damages in invaded epithelial cells, where double-strand breaks are induced by the CdtB subunit of the typhoid toxin also in neighboring non-infected cells (Sepe *et al.*, 2020). However, the typhoid toxin was found to be not involved in initial cell cycle arrest during air-liquid infection of polarized monolayers. Thus, with help of the constantly growing field of different organoids, we gain more and more insights in *Salmonella* and other infections and by optimizing growth and infection conditions get closer to processes induced in the human body.

### V.5.6. Acknowledgements

We thank the division of Neurobiology for providing murine tissue for PAS staining and Christian Meyer from the division of Zoology for help with embedding of murine tissue.

### V.5.7. Materials and Methods

#### Bacterial strains and growth conditions

Bacterial strains used in this study are listed in Table V.5.1. Bacteria were grown aerobically in LB or on LB agar plates, if necessary supplemented with carbenicillin (cb, 50 µg/ml). Subcultures were grown for 2.5 h (1:31).

**Table V.5.1. Bacterial strains used in this study.**

Designation	Relevant characteristics	Reference
<b>S. Typhimurium ATCC14028s</b>	wild type	<i>Salmonella</i> genetic stock center, University of Calgary
<b>MvP589</b>	$\Delta spi4::FRT$	(Gerlach and Hensel, 2007)
<b>MvP818</b>	$\Delta invC::FRT$	(Gerlach and Hensel, 2007)
<b>S. Paratyphi A 45157</b>	wild type, clinical isolate, Nepal outbreak 2009	(Gal-Mor <i>et al.</i> , 2012)

#### Plasmids used in this study

Plasmids used in this study are listed in Table V.5.2.

**Table V.5.2. Plasmids used in this study.**

Plasmid	Relevant characteristics, resistance	Reference
<b>pFPVmCherry</b>	const. mCherry	(Drecktrah <i>et al.</i> , 2008)
<b>pFPV25.1</b>	const. GFP	(Valdivia and Falkow, 1996)
<b>p4878</b>	pLX304 LifeAct::GFP, 3 <sup>rd</sup> generation lentivirus vector	based on Addgene #25890
<b>pMD2.G</b>	2 <sup>nd</sup> generation lentiviral packaging plasmid	Addgene #12259
<b>psPAX2</b>	VSV-G envelope expressing plasmid	Addgene #12260

#### Cell culture

Murine and human organoids and protocols were kindly provided by Guntram Grassl. The organoids were cultured in defined medium, mentioned in Table V.5.3. The organoids were incubated at 37 °C with 5% CO<sub>2</sub>. Every 7 to 10 days after seeding, the enteroids were passaged. For passaging, the medium was removed and 1 ml ice-cold DPBS was added to each well. The Matrigel was broken up by pipetting back and forth (20x with P-1000 tip + 15x with P-1000 + P-200 µL tip on top). All wells were collected in one 15 ml conical tube on ice, filled up with ice-cold PBS and centrifuged for 5 min at 4 °C at 250 x g. The supernatant was discarded and the dissociated organoids were resuspended in an organoid medium-

Matrigel mix (50:50). 50  $\mu$ l were spotted in each well and overlaid with 500  $\mu$ l organoid medium (3D). Every other day, medium was replaced. The first two days, the medium additionally was conditioned with 10  $\mu$ M Y27623.

**Table V.5.3. Ingredients for organoid medium.**

	<b>2D monolayer medium</b>	<b>2D differentiation medium</b>	<b>3D medium</b>
<b>L-WRN conditioned supernatant</b>	50%	5%	50%
<b>DMEM F-12/Glutamax</b>			
<b>Y27623</b>	10 $\mu$ M		10 $\mu$ M (only early culture)
<b>Pen/Strep</b>	100 $\mu$ g/ml		100 $\mu$ g/ml
<b>FCS</b>	20%	20%	
<b>rm-EGF</b>	50 ng/ml	50 ng/ml	50 ng/ml
<b>DAPT</b>		5 $\mu$ M	
<b>Gastrin I</b>			10 nM
<b>HEPES</b>			10 mM
<b>A83-01</b>			500 nM
<b>SB202190</b>			10 $\mu$ M
<b>ACC</b>			1 mM
<b>B27</b>			1x

For infections, we also used monolayers of intestinal murine and human organoids. Matrigel was mixed with cold DPBS and 200  $\mu$ l were filled into the transwells and incubated for at least 1.5 h at 37  $^{\circ}$ C, 5% CO<sub>2</sub>. The medium was removed from all wells with 3D crypt organoids and 2 wells were resuspended with 1 ml cold DPBS. As described above, organoids were resuspended and collected in 15 ml tubes, pre-filled with cold DPBS. The tubes were centrifuged at 500 x g. Following centrifugation, supernatant was discarded and the pellet was resuspended in 1 ml warm 0.05% Trypsin/EDTA and incubated for 5 min at 37  $^{\circ}$ C in a water bath. Cells were then resuspended 20x with P-1000 tip + 15x with P-1000 + P-200  $\mu$ L tip on top. We added 10 ml cold DMEM with 10% FCS and centrifuged an additional time for 5 min at 4  $^{\circ}$ C at 500 x g. Supernatant was discarded and the pellet was resuspended in monolayer medium (Table V.5.3). For human organoids 1\*10<sup>5</sup> cells/well and for murine organoids 1.5\*10<sup>5</sup> cells/well were seeded. Every other day medium was replaced and transepithelial electrical resistance (TEER) was measured every day. At approximately day 5 (TEER 500-1000), medium was changed to differentiation medium (Table V.5.3).

### Lentiviral transfection

For microscopic analysis, we transfected organoids with third generation lentivirus system (Table V.5.2) (Miyoshi and Stappenbeck, 2013). The organoids were cultured in 24-well plates in 3D for 10 days. The organoids were resuspended as described above and centrifuged for 5 min at 4 °C at 400 x g and then trypsinized for 5-10 min in 1 ml PBS. Trypsin digestion was stopped by addition of 5 ml cold DPBS and cells were centrifuged again for 5 min at 4 °C at 400 x g. Cells were resuspended in 3D organoid medium, supplemented with 10 µM Y27623. Organoid solution was spotted on Matrigel, prepared before. After 16 h, the medium was discarded and organoids were coated with additional Matrigel (incubation for 20 min) and 3D organoid medium, supplemented with 10 µM Y27623. The organoids were incubated 2-4 days to generate many stem cells. In the following, the organoids were extracted with medium and Matrigel and transferred into 15 ml tubes. The organoids were centrifuged for 5 min at 400 x g and supernatant was carefully removed and were resuspended in 1 ml warm 0.05% Trypsin/EDTA and incubated for 5 min at 37 °C in a water bath. We added 5 ml cold DPBS and centrifuged an additional time. Cells were resuspended in 3D organoid medium, supplemented with 10 µM Y27623. Organoids were adhered to a thin layer of Matrigel for 15 min at 37 °C, prepared before, because of the interference of the lentiviruses with the Matrigel. Lentiviral particles were prepared by C. Kommnick and V. Göser. We added lentivirus and 8 µg/mL polybrene to the cells on hardened Matrigel in a 12-well plate. We incubated the organoids 24 h with the lentivirus-polybrene mix, discarded the supernatant and coated the cells with additional Matrigel and added 3D organoid medium, supplemented with 10 µM Y27623. We incubated the organoids for 3 days, changed the medium to 3D organoid medium without ROCK inhibitor and started selection with 10 µg/ml Blastocidin (pLX304 p4878\_5) after 7 days for 24 h.

### Fluorescence labeling of murine and human organoids

For microscopic analysis of uninfected and infected 3D and 2D cultured organoids, we washed the cells thrice with DPBS and fixed them with 3% PFA in PBS for 25 min at RT. Organoids grown on transwells were stamped out with the membrane before staining. Fixed cells were washed thrice with DPBS and incubated in blocking solution (2% goat serum, 2% bovine serum albumin) with 0.5% Triton-X100 for 30 min. For staining, the samples were incubated within the respective reagents, diluted in blocking solution with 0.2% Triton-X100 and incubated for 1 h at RT. Following this step, the samples were washed thrice with DPBS and were mounted on microscope slides, using Fluoroshield (Sigma) and Entellan (Merck).

**Table V.5.4 Reagents used for fluorescence microscopy**

fluorescence excitation	reagent	concentration	reference
488	AlexaFluor488-phalloidin	1:100	Molecular Probes
405	DAPI	1:1000	Sigma
588	CellMask Deep Red	2 µg/ml	ThermoFisher Scientific
642	CF®640R WGA	5 µg/ml	Biotium
647	phalloidin-iFluor647	1:100	AAT Bioquest

#### PAS staining of intestinal organoid monolayers and mouse tissue

As the PAS (periodic acid-Schiff) reaction is one of the most frequently used chemical methods for histology, we used this method to investigate the mucus layer of our intestinal organoid monolayers. First, the fixed monolayers (3% PFA in PBS) were washed with MQ for 1 min. In a next step, periodic acid solution (10%) was added and incubated for 5 min. The samples were washed for 3 min with MQ. Schiff's reagent was added and samples were incubated for 15 min. The washing step was repeated for 3 min. Following this step, the samples were fixed on microscope slides, using Entellan. Mouse ileum and colon tissue was acquired from C57BL/6 mouse kindly provided by the division Neurobiology (Osnabrueck University). The dissected tissue was cut in 0.5 cm pieces and fixed for 24 h in 10% formaldehyde. Dehydration was done with ethanol series at RT with 10% for 15 min, 30% for 30 min, 50% for 1 h, 70% for 2 h, 70% for 72 h, 80% for 4 h, 80% for 16 h, 90% for 24 h and two steps with 100% ethanol for 24 h each. Samples were embedded with Technovit 8100 according to manufacturer instructions (1:1 ethanol:Technovit step for at least 2 h at 4 °C, Technovit and hardener 1 for 72 h at 4 °C, Technovit and hardener 1+2 for 48 h at 4 °C under anerobic conditions). Trimming and semithin sectioning (5 µm) was done with conventional microtome. Toluidine staining was performed with one drop of filtered toluidine blue stain solution and let dry. Excess stain was rinsed gently with water and dried before microscopy. PAS staining with mouse tissue was performed as described in manufacturer protocol from Roth. Briefly, semithin sections were rinsed with distilled water, incubated in 1% periodic acid solution for 10 min and rinsed with tap water afterwards for 10 min. After two 2 min washing steps with distilled water, sections were stained with Schiff's reagent for 10-20 min and rinsed with warm tap water afterwards for 5 min. For microscopy, Zeiss Axio Observer.Z1 was used. with LD Plan-Neofluar 20x/0.6 objective. Imaging with CoolSNAP camera with a camera adapter 1.0x, total magnification 20x, zoom 1.0x. Additionally, a Zeiss Axio lab A1 with 10x and 20x objectives and Bresser MicroCam SP 3.1 was used. Images were further processed with MicroCamLab II, version x64, 3.7.8752.

### Invasion assay of human organoid monolayers

For infection, 2.5 h subcultures of infecting STM were grown, intestinal organoids on 0.4  $\mu\text{m}$  porous filters were infected at multiplicity of infection (MOI) of 50, and incubated for 30 min or 60 min at 37 °C in an atmosphere of 5% CO<sub>2</sub>. The cells were washed three times with prewarmed PBS. To determine invasion, cells were treated with 200  $\mu\text{l}$  medium containing 100  $\mu\text{g/ml}$  gentamicin per well for 1 h, washed three times with prewarmed PBS and lysed with 0.5% deoxycholate in PBS (freshly prepared). Lysis was performed for 10 min at 37 °C on a shaking platform. Lysates were collected in single tubes and serial dilutions of inoculum and lysates were plated logarithmic on MH plates to determine CFU. Plates were incubated o/N at 37 °C and CFU were counted the next day with Acolyte software. The percentages of invaded bacteria were calculated. Additionally, single wells were fixed with PFA and stained for microscopy as described above. For microscopy, Zeiss Axio Observer.Z1 was used. The used objective was the LD Plan-Neofluar 40x/0.6 Korr. Imaging with CoolSNAP camera with a camera adapter 1.0x, total magnification 40x, zoom 1.0x. Bacteria were imaged for 60 s with 150 ms exposure time and 2x2 binning.

### Infection of organoid monolayers for microscopy

For imaging of infections, Organoids were cultured in 2D as described above. STM infection was carried out as described above. SPA WT strain was grown for 8 h under aerobic conditions, subcultured (1:100) in fresh LB medium to stationary phase for 16 h under microaerophilic conditions as described in (Elhadad *et al.*, 2015). Bacteria were adjusted to an optical density of 0.2 at 600 nm in PBS, used for infection with MOI 50 and incubated for 30-60 min at 37 °C. After washing thrice with PBS or HEPES, cells were fixed for fluorescence or scanning electron microscopy, respectively.

### 3D Organoid cultivation for imaging

Ileum and colon organoids of murine and human origin were seeded on surface-treated  $\mu$ -slide 8-well chamber slides. 8-wells were cooled during seeding to prevent solidification of Matrigel and allow organoids to settle near the polymer coverslip bottom of the chamber. Imaging was performed with Cell Observer microscope (Zeiss) equipped with Yokogawa Spinning Disc Unit CSU-X1a5000, an incubation chamber, two ORCA Flash 4.0 V3 cameras (Hamamatsu) and appropriate filters for the respective fluorescence dyes. The following objectives were used: 40x (LD-Plan-Neofluar, NA 0.6), 40x (Plan-Apochromat, NA 1.4) and 63x ( $\alpha$ -Plan-Apochromat, NA 1.4). For imaging of large areas of 3D organoids, multiple images with overlaps were acquired and stitched.

### Microinjection of 3D cultured organoids

For microinjection, STM WT was cultured under microaerobic conditions as described above. Organoids were microinjected with Zeiss Axio Observer A1 with Eppendorf FemtoJet combined with



InjectMan N12. Organoids were fixed at desired time points either 30 min (human colon) or between 60-90 min p.i. (murine colon).

#### Generation of immobilized apical-out enteroids for microscopy

Immobilized apical-out enteroids for microscopy were prepared as described in Co *et al.* (2019). In brief, enteroids were grown as described above for 7-10 days, dislodged with sterile spatula and solubilized in 5 mM EDTA in PBS for 1 h at 4°C on a rotating platform. 10 µl Matrigel was spread in a cooled µ-slide as described above to form a thin layer and polymerized for 10 min at 37 °C. Enteroids were centrifuged at 200 x g for 3 min at 4 °C and supernatant was removed. Enteroids were resuspended in 30 µl organoid medium, spotted on solidified Matrigel and incubated for 15 min at 37 °C before organoid medium was added to well for cultivation. Fixation, staining and imaging was performed 1-3 days after seeding as described above.

#### Sample preparation for electron microscopy

##### *Sample preparation for SEM*

After the desired incubation time, cells were washed thrice with 0.2 M HEPES and fixed with 2.5% glutaraldehyde (Sciences Services, Germany) in 0.2 M HEPES for 20 min at 37 °C. Dehydration was done with ethanol series at RT with 10%, 30% and 50% ethanol once for 10 min each step and 70%, 90% and 100% ethanol twice for 10 min each step. For chemical drying, hexamethyldisilazane (HMDS), diluted with pure ethanol in ratios of 1:3, 1:1, 1:3 was used for 15 min for each step and 100% HMDS for 20 min at RT. After the final step, samples were air dried until HMDS has completely evaporated. Transwell membrane was stamped out with biopsy punch and taped on aluminum SEM pin stubs with leit-taps before they were coated with 6 nm gold with sputter coater Leica EM ACE600. For imaging, Jeol SEM JSM-IT200 was used.

3D organoids were fixed for 2 h at room temperature (RT) in 2.5% glutaraldehyde in 0.1 M cacodylate buffer pH 7.4 (Sciences Services, Germany) subsequently washed twice in 0.1 M cacodylate buffer pH 7.4 and dehydrated stepwise in a graded ethanol series. Samples were critical point dried in 100% ethanol with a critical point drying machine (CPD300, Leica) and mounted on aluminum stubs as described above. Samples were sputter-coated with a 10 nm thin gold layer and imaged with Zeiss SEM Auriga at 4 kV

##### *Sample preparation for TEM*

For TEM, organoids were fixed for 2 h at room temperature (RT) in 2.5% glutaraldehyde in 0.1 M cacodylate buffer pH 7.4, subsequently washed in 0.1 M cacodylate buffer pH, 7.4, post-fixed for 2 h at RT in 1% osmium tetroxide in 0.1 M cacodylate buffer pH 7.4, dehydrated stepwise in a graded ethanol series and embedded in Epon 812 (Fluka, Buchs, Switzerland). Ultrathin sections (70 nm, ultramicrotome EM UC7, Leica, Wetzlar, Germany) were afterwards stained for 30 min with 1% uranyl acetate

(Leica, Germany) and 20 min in 3% lead citrate (Leica, Germany). Sections were analyzed in a transmission electron microscope with a Zeiss TEM 902 (Oberkochen, Germany) at 80 kV.

For TEM analysis of microinjected organoids, specimens were fixed with 2.5% glutaraldehyde in 0.2 M HEPES buffer for 1 h at RT. Samples were washed thrice with buffer and incubated in 2% osmium tetroxide (Electron Microscopy Sciences) in 0.2 M HEPES buffer with 0.1% ruthenium red and 1.5% potassium ferrocyanide for 1 h at 4 °C in the dark. After five rinses with buffer, organoids were gradually dehydrated with 30%, 50%, 70%, 80%, 90%, 100% ethanol at 4 °C with one incubation in 100% anhydrous ethanol and two rinses in anhydrous acetone at RT for 10 min each step. For infiltration, samples were incubated in mixtures of EPON 812 (Sigma-Aldrich) and acetone. Namely 25% and 75% EPON for 1 h each, 100% EPON overnight and 100% EPON for 8 h. Polymerization of the resin was conducted for 72 h at 60 °C. Ultrathin sectioning (70 nm) was performed with a Leica EM UC7 (Leica, Wetzlar, Germany) and sections were collected on formvar-coated copper slot grids. Sections were contrasted with 2% uranyl acetate and 3% lead citrate using a Leica EM AC20 (Leica, Wetzlar, Germany) and analyzed with a Zeiss TEM 902 A, operated at 80 kV and equipped with a 2K wide-angle slow-scan CCD camera (TRS, Moorenweis, Germany). Images were collected using the software ImageSP (TRS image SysProg, Moorenweis, Germany).

### V.5.8. References

- Abed, Y., and Boivin, G. (2006). Human parechovirus types 1, 2 and 3 infections in Canada. *Emerg Infect Dis* 12, 969-975.
- Abrahams, G.L., and Hensel, M. (2006). Manipulating cellular transport and immune responses: dynamic interactions between intracellular *Salmonella enterica* and its host cells. *Cell Microbiol* 8, 728-737.
- Adams, G.G., and Dilly, P.N. (1989). Differential staining of ocular goblet cells. *Eye (Lond)* 3 ( Pt 6), 840-844.
- Aguilar, C., Alves da Silva, M., Saraiva, M., Neyazi, M., Olsson, I.A.S., and Bartfeld, S. (2021). Organoids as host models for infection biology - a review of methods. *Exp Mol Med* 53, 1471-1482.
- Bartfeld, S. (2016). Modeling infectious diseases and host-microbe interactions in gastrointestinal organoids. *Dev Biol* 420, 262-270.
- Bartfeld, S., and Clevers, H. (2015). Organoids as Model for Infectious Diseases: Culture of Human and Murine Stomach Organoids and Microinjection of *Helicobacter pylori*. *J Vis Exp*.
- Beskow, L.M. (2016). Lessons from HeLa Cells: The Ethics and Policy of Biospecimens. *Annu Rev Genomics Hum Genet* 17, 395-417.
- Beumer, J., and Clevers, H. (2016). Regulation and plasticity of intestinal stem cells during homeostasis and regeneration. *Development* 143, 3639-3649.
- Birchenough, G.M., Johansson, M.E., Gustafsson, J.K., Bergstrom, J.H., and Hansson, G.C. (2015). New developments in goblet cell mucus secretion and function. *Mucosal Immunol* 8, 712-719.
- Boccellato, F., Woelffling, S., Imai-Matsushima, A., Sanchez, G., Goosmann, C., Schmid, M., Berger, H., Morey, P., Denecke, C., Ordemann, J., *et al.* (2019). Polarised epithelial monolayers of the gastric mucosa reveal insights into mucosal homeostasis and defence against infection. *Gut* 68, 400-413.
- Boonma, P., Spinler, J.K., Venable, S.F., Versalovic, J., and Tumwasorn, S. (2014). *Lactobacillus rhamnosus* L34 and *Lactobacillus casei* L39 suppress *Clostridium difficile*-induced IL-8 production by colonic epithelial cells. *BMC Microbiol* 14, 177.
- Brogiere, N., Isenmann, L., Hirt, C., Ringel, T., Placzek, S., Cavalli, E., Ringnalda, F., Villiger, L., Zullig, R., Lehmann, R., *et al.* (2018). Growth of Epithelial Organoids in a Defined Hydrogel. *Adv Mater* 30, e1801621.
- Buchmeier, N.A., and Heffron, F. (1991). Inhibition of macrophage phagosome-lysosome fusion by *Salmonella typhimurium*. *Infect Immun* 59, 2232-2238.
- Caiazza, C., Parisi, S., and Caiazza, M. (2021). Liver Organoids: Updates on Disease Modeling and Biomedical Applications. *Biology (Basel)* 10.
- Carrol, M.E., Jackett, P.S., Aber, V.R., and Lowrie, D.B. (1979). Phagolysosome formation, cyclic adenosine 3':5'-monophosphate and the fate of *Salmonella typhimurium* within mouse peritoneal macrophages. *J Gen Microbiol* 110, 421-429.
- Centonze, V.E., and White, J.G. (1998). Multiphoton excitation provides optical sections from deeper within scattering specimens than confocal imaging. *Biophys J* 75, 2015-2024.
- Chen, S., Einspanier, R., and Schoen, J. (2015). Transepithelial electrical resistance (TEER): a functional parameter to monitor the quality of oviduct epithelial cells cultured on filter supports. *Histochem Cell Biol* 144, 509-515.
- Co, J.Y., Margalef-Catala, M., Li, X., Mah, A.T., Kuo, C.J., Monack, D.M., and Amieva, M.R. (2019). Controlling Epithelial Polarity: A Human Enteroid Model for Host-Pathogen Interactions. *Cell Rep* 26, 2509-2520 e2504.
- Co, J.Y., Margalef-Catala, M., Monack, D.M., and Amieva, M.R. (2021). Controlling the polarity of human gastrointestinal organoids to investigate epithelial biology and infectious diseases. *Nat Protoc* 16, 5171-5192.
- Dougan, G., and Baker, S. (2014). *Salmonella enterica* serovar Typhi and the pathogenesis of typhoid fever. *Annu Rev Microbiol* 68, 317-336.
- Drecktrah, D., Levine-Wilkinson, S., Dam, T., Winfree, S., Knodler, L.A., Schroer, T.A., and Steele-Mortimer, O. (2008). Dynamic behavior of *Salmonella*-induced membrane tubules in epithelial cells. *Traffic* 9, 2117-2129.

- Dutta, D., and Clevers, H. (2017). Organoid culture systems to study host-pathogen interactions. *Curr Opin Immunol* 48, 15-22.
- Egi Kardia, M.F., Tanja Strive, Xi-Lei Zeng, Mary Estes, Robyn N. Hall (2020). Isolation, culture and maintenance of rabbit intestinal organoids, and organoid-derived cell monolayers.
- Elhadad, D., Desai, P., Rahav, G., McClelland, M., and Gal-Mor, O. (2015). Flagellin Is Required for Host Cell Invasion and Normal *Salmonella* Pathogenicity Island 1 Expression by *Salmonella enterica* Serovar Paratyphi A. *Infect Immun* 83, 3355-3368.
- Ettayebi, K., Crawford, S.E., Murakami, K., Broughman, J.R., Karandikar, U., Tenge, V.R., Neill, F.H., Blutt, S.E., Zeng, X.L., Qu, L., *et al.* (2016). Replication of human noroviruses in stem cell-derived human enteroids. *Science* 353, 1387-1393.
- Farin, H.F., Jordens, I., Mosa, M.H., Basak, O., Korving, J., Tauriello, D.V., de Punder, K., Angers, S., Peters, P.J., Maurice, M.M., *et al.* (2016). Visualization of a short-range Wnt gradient in the intestinal stem-cell niche. *Nature* 530, 340-343.
- Fatehullah, A., Appleton, P.L., and Nathke, I.S. (2013). Cell and tissue polarity in the intestinal tract during tumorigenesis: cells still know the right way up, but tissue organization is lost. *Philos Trans R Soc Lond B Biol Sci* 368, 20130014.
- Finkbeiner, S.R., Zeng, X.L., Utama, B., Atmar, R.L., Shroyer, N.F., and Estes, M.K. (2012). Stem cell-derived human intestinal organoids as an infection model for rotaviruses. *mBio* 3, e00159-00112.
- Forbester, J.L., Goulding, D., Vallier, L., Hannan, N., Hale, C., Pickard, D., Mukhopadhyay, S., and Dougan, G. (2015). Interaction of *Salmonella enterica* Serovar Typhimurium with Intestinal Organoids Derived from Human Induced Pluripotent Stem Cells. *Infect Immun* 83, 2926-2934.
- Fujii, M., Shimokawa, M., Date, S., Takano, A., Matano, M., Nanki, K., Ohta, Y., Toshimitsu, K., Nakazato, Y., Kawasaki, K., *et al.* (2016). A Colorectal Tumor Organoid Library Demonstrates Progressive Loss of Niche Factor Requirements during Tumorigenesis. *Cell Stem Cell* 18, 827-838.
- Gagnon, M., Zihler Berner, A., Chervet, N., Chassard, C., and Lacroix, C. (2013). Comparison of the Caco-2, HT-29 and the mucus-secreting HT29-MTX intestinal cell models to investigate *Salmonella* adhesion and invasion. *J Microbiol Methods* 94, 274-279.
- Gal-Mor, O., Suez, J., Elhadad, D., Porwollik, S., Leshem, E., Valinsky, L., McClelland, M., Schwartz, E., and Rahav, G. (2012). Molecular and cellular characterization of a *Salmonella enterica* serovar Paratyphi A outbreak strain and the human immune response to infection. *Clin Vaccine Immunol* 19, 146-156.
- Galan, J.E., and Curtiss, R., 3rd (1989). Cloning and molecular characterization of genes whose products allow *Salmonella* Typhimurium to penetrate tissue culture cells. *Proc Natl Acad Sci U S A* 86, 6383-6387.
- Garcez, P.P., Loiola, E.C., Madeiro da Costa, R., Higa, L.M., Trindade, P., Delvecchio, R., Nascimento, J.M., Brindeiro, R., Tanuri, A., and Rehen, S.K. (2016). Zika virus impairs growth in human neurospheres and brain organoids. *Science* 352, 816-818.
- Gassler, N. (2017). Paneth cells in intestinal physiology and pathophysiology. *World J Gastrointest Pathophysiol* 8, 150-160.
- Gaush, C.R., Hard, W.L., and Smith, T.F. (1966). Characterization of an established line of canine kidney cells (MDCK). *Proc Soc Exp Biol Med* 122, 931-935.
- Gerbe, F., and Jay, P. (2016). Intestinal tuft cells: epithelial sentinels linking luminal cues to the immune system. *Mucosal Immunol* 9, 1353-1359.
- Gerlach, R.G., Claudio, N., Rohde, M., Jackel, D., Wagner, C., and Hensel, M. (2008). Cooperation of *Salmonella* pathogenicity islands 1 and 4 is required to breach epithelial barriers. *Cell Microbiol* 10, 2364-2376.
- Gerlach, R.G., and Hensel, M. (2007). *Salmonella* pathogenicity islands in host specificity, host pathogen-interactions and antibiotics resistance of *Salmonella enterica*. *Berl Munch Tierarztl Wochenschr* 120, 317-327.
- Gerlach, R.G., Jackel, D., Geymeier, N., and Hensel, M. (2007). *Salmonella* pathogenicity island 4-mediated adhesion is coregulated with invasion genes in *Salmonella enterica*. *Infect Immun* 75, 4697-4709.

- Gomez, D.P., and Boudreau, F. (2021). Organoids and Their Use in Modeling Gut Epithelial Cell Lineage Differentiation and Barrier Properties During Intestinal Diseases. *Front Cell Dev Biol* 9, 732137.
- Graf, B.W., and Boppart, S.A. (2010). Imaging and analysis of three-dimensional cell culture models. *Methods Mol Biol* 591, 211-227.
- He, D., Sougioultzis, S., Hagen, S., Liu, J., Keates, S., Keates, A.C., Pothoulakis, C., and Lamont, J.T. (2002). *Clostridium difficile* toxin A triggers human colonocyte IL-8 release via mitochondrial oxygen radical generation. *Gastroenterology* 122, 1048-1057.
- He, Z., Gharaibeh, R.Z., Newsome, R.C., Pope, J.L., Dougherty, M.W., Tomkovich, S., Pons, B., Mirey, G., Vignard, J., Hendrixson, D.R., *et al.* (2019). *Campylobacter jejuni* promotes colorectal tumorigenesis through the action of cytolethal distending toxin. *Gut* 68, 289-300.
- Hensel, M. (2004). Evolution of pathogenicity islands of *Salmonella enterica*. *Int J Med Microbiol* 294, 95-102.
- Hentschel, V., Arnold, F., Seufferlein, T., Azoitei, N., Kleger, A., and Muller, M. (2021). Enteropathogenic Infections: Organoids Go Bacterial. *Stem Cells Int* 2021, 8847804.
- Heo, I., Dutta, D., Schaefer, D.A., Iakobachvili, N., Artegiani, B., Sachs, N., Boonekamp, K.E., Bowden, G., Hendrickx, A.P.A., Willems, R.J.L., *et al.* (2018). Modelling *Cryptosporidium* infection in human small intestinal and lung organoids. *Nat Microbiol* 3, 814-823.
- Hopt, A., and Neher, E. (2001). Highly nonlinear photodamage in two-photon fluorescence microscopy. *Biophys J* 80, 2029-2036.
- Hosmillo, M., Chaudhry, Y., Nayak, K., Sorgeloos, F., Koo, B.K., Merenda, A., Lillestol, R., Drumright, L., Zilbauer, M., and Goodfellow, I. (2020). Norovirus Replication in Human Intestinal Epithelial Cells Is Restricted by the Interferon-Induced JAK/STAT Signaling Pathway and RNA Polymerase II-Mediated Transcriptional Responses. *mBio* 11.
- Iismaa, S.E., Kaidonis, X., Nicks, A.M., Bogush, N., Kikuchi, K., Naqvi, N., Harvey, R.P., Husain, A., and Graham, R.M. (2018). Comparative regenerative mechanisms across different mammalian tissues. *NPJ Regen Med* 3, 6.
- Ishizaki, T., Uehata, M., Tamechika, I., Keel, J., Nonomura, K., Maekawa, M., and Narumiya, S. (2000). Pharmacological properties of Y-27632, a specific inhibitor of rho-associated kinases. *Mol Pharmacol* 57, 976-983.
- Jepson, M.A., and Clark, M.A. (1998). Studying M cells and their role in infection. *Trends Microbiol* 6, 359-365.
- Johnson, R., Mylona, E., and Frankel, G. (2018). Typhoidal *Salmonella*: Distinctive virulence factors and pathogenesis. *Cell Microbiol* 20, e12939.
- Kayisoglu, O., Weiss, F., Niklas, C., Pierotti, I., Pompaiah, M., Wallaschek, N., Germer, C.T., Wiegering, A., and Bartfeld, S. (2021). Location-specific cell identity rather than exposure to GI microbiota defines many innate immune signalling cascades in the gut epithelium. *Gut* 70, 687-697.
- Kommnick, C., and Hensel, M. (2021). Correlative Light and Scanning Electron Microscopy to Study Interactions of *Salmonella enterica* with Polarized Epithelial Cell Monolayers. *Methods Mol Biol* 2182, 103-115.
- Kommnick, C., Lepper, A., and Hensel, M. (2019). Correlative light and scanning electron microscopy (CLSEM) for analysis of bacterial infection of polarized epithelial cells. *Sci Rep* 9, 17079.
- Krieger, V., Liebl, D., Zhang, Y., Rajashekar, R., Chlanda, P., Giesker, K., Chikkaballi, D., and Hensel, M. (2014). Reorganization of the endosomal system in *Salmonella*-infected cells: the ultrastructure of *Salmonella*-induced tubular compartments. *PLoS Pathog* 10, e1004374.
- Lamers, M.M., van der Vaart, J., Knoop, K., Riesebosch, S., Breugem, T.I., Mykityn, A.Z., Beumer, J., Schipper, D., Bezstarosti, K., Koopman, C.D., *et al.* (2021). An organoid-derived bronchioalveolar model for SARS-CoV-2 infection of human alveolar type II-like cells. *EMBO J* 40, e105912.
- Lauren, P.A., and Sorvari, T.E. (1969). The histochemical specificity of mucicarmine staining in the identification of epithelial mucosubstances. *Acta Histochem* 34, 263-272.
- Leslie, J.L., Huang, S., Opp, J.S., Nagy, M.S., Kobayashi, M., Young, V.B., and Spence, J.R. (2015). Persistence and toxin production by *Clostridium difficile* within human intestinal organoids result in disruption of epithelial paracellular barrier function. *Infect Immun* 83, 138-145.

- Li, X., Nadauld, L., Ootani, A., Corney, D.C., Pai, R.K., Gevaert, O., Cantrell, M.A., Rack, P.G., Neal, J.T., Chan, C.W., *et al.* (2014a). Oncogenic transformation of diverse gastrointestinal tissues in primary organoid culture. *Nat Med* 20, 769-777.
- Li, Y., Xu, C., and Ma, T. (2014b). In vitro organogenesis from pluripotent stem cells. *Organogenesis* 10, 159-163.
- Lorkowski, M., Felipe-Lopez, A., Danzer, C.A., Hansmeier, N., and Hensel, M. (2014). *Salmonella enterica* invasion of polarized epithelial cells is a highly cooperative effort. *Infect Immun* 82, 2657-2667.
- Lulla, V., Dinan, A.M., Hosmillo, M., Chaudhry, Y., Sherry, L., Irigoyen, N., Nayak, K.M., Stonehouse, N.J., Zilbauer, M., Goodfellow, I., *et al.* (2019). An upstream protein-coding region in enteroviruses modulates virus infection in gut epithelial cells. *Nat Microbiol* 4, 280-292.
- Ly, K.T., and Casanova, J.E. (2007). Mechanisms of *Salmonella* entry into host cells. *Cell Microbiol* 9, 2103-2111.
- Maru, Y., Orihashi, K., and Hippo, Y. (2016). Lentivirus-Based Stable Gene Delivery into Intestinal Organoids. *Methods Mol Biol* 1422, 13-21.
- May, S., Evans, S., and Parry, L. (2017). Organoids, organs-on-chips and other systems, and microbiota. *Emerg Top Life Sci* 1, 385-400.
- Miyoshi, H., and Stappenbeck, T.S. (2013). In vitro expansion and genetic modification of gastrointestinal stem cells in spheroid culture. *Nat Protoc* 8, 2471-2482.
- Nickerson, K.P., Senger, S., Zhang, Y., Lima, R., Patel, S., Ingano, L., Flavahan, W.A., Kumar, D.K.V., Fraser, C.M., Faherty, C.S., *et al.* (2018). *Salmonella* Typhi Colonization Provokes Extensive Transcriptional Changes Aimed at Evading Host Mucosal Immune Defense During Early Infection of Human Intestinal Tissue. *EBioMedicine* 31, 92-109.
- Nikiforou, M., Jacobs, E.M., Kemp, M.W., Hornef, M.W., Payne, M.S., Saito, M., Newnham, J.P., Janssen, L.E., Jobe, A.H., Kallapur, S.G., *et al.* (2016). Intra-amniotic *Candida albicans* infection induces mucosal injury and inflammation in the ovine fetal intestine. *Sci Rep* 6, 29806.
- Noel, G., Baetz, N.W., Staab, J.F., Donowitz, M., Kovbasnjuk, O., Pasetti, M.F., and Zachos, N.C. (2017a). Erratum: A primary human macrophage-enteroid co-culture model to investigate mucosal gut physiology and host-pathogen interactions. *Sci Rep* 7, 46790.
- Noel, G., Baetz, N.W., Staab, J.F., Donowitz, M., Kovbasnjuk, O., Pasetti, M.F., and Zachos, N.C. (2017b). A primary human macrophage-enteroid co-culture model to investigate mucosal gut physiology and host-pathogen interactions. *Sci Rep* 7, 45270.
- Ootani, A., Li, X., Sangiorgi, E., Ho, Q.T., Ueno, H., Toda, S., Sugihara, H., Fujimoto, K., Weissman, I.L., Capecchi, M.R., *et al.* (2009). Sustained in vitro intestinal epithelial culture within a Wnt-dependent stem cell niche. *Nat Med* 15, 701-706.
- Osho, S.O., Wang, T., Horn, N.L., and Adeola, O. (2017). Comparison of goblet cell staining methods in jejunal mucosa of turkey poults. *Poult Sci* 96, 556-559.
- Peterson, L.W., and Artis, D. (2014). Intestinal epithelial cells: regulators of barrier function and immune homeostasis. *Nat Rev Immunol* 14, 141-153.
- Ponce de Leon-Rodriguez, M.D.C., Guyot, J.P., and Laurent-Babot, C. (2019). Intestinal in vitro cell culture models and their potential to study the effect of food components on intestinal inflammation. *Crit Rev Food Sci Nutr* 59, 3648-3666.
- Pott, J., and Hornef, M. (2012). Innate immune signalling at the intestinal epithelium in homeostasis and disease. *EMBO Rep* 13, 684-698.
- Pui, C.F., Wong, W. C., Chai, L. C., Tunung, R., Jeyaletchumi, P., Noor Hidayah, M. S., Ubong, A., Farinazleen, M. G., Cheah, Y. K. and Son, R (2011). *Salmonella*: A foodborne pathogen. *International Food Research Journal* 18, 465-473.
- Rakotoson, I., Delhomme, B., Djian, P., Deeg, A., Brunstein, M., Seebacher, C., Uhl, R., Ricard, C., and Oheim, M. (2019). Fast 3-D Imaging of Brain Organoids With a New Single-Objective Planar-Illumination Two-Photon Microscope. *Front Neuroanat* 13, 77.
- Ramirez-Flores, C.J., and Knoll, L.J. (2021). Breakthroughs in microbiology made possible with organoids. *PLoS Pathog* 17, e1010080.
- Ranganathan, S., Doucet, M., Grassel, C.L., Delaine-Elias, B., Zachos, N.C., and Barry, E.M. (2019). Evaluating *Shigella flexneri* Pathogenesis in the Human Enteroid Model. *Infect Immun* 87.

- Reuter, T., Scharte, F., Franzkoch, R., Liss, V., and Hensel, M. (2021). Single cell analyses reveal distinct adaptation of typhoidal and non-typhoidal *Salmonella enterica* serovars to intracellular lifestyle. *PLoS Pathog* 17, e1009319.
- Reynaud, E.G., Krzic, U., Greger, K., and Stelzer, E.H. (2008). Light sheet-based fluorescence microscopy: more dimensions, more photons, and less photodamage. *HFSP J* 2, 266-275.
- Rezania, A., Bruin, J.E., Arora, P., Rubin, A., Batushansky, I., Asadi, A., O'Dwyer, S., Quiskamp, N., Mojibian, M., Albrecht, T., *et al.* (2014). Reversal of diabetes with insulin-producing cells derived in vitro from human pluripotent stem cells. *Nat Biotechnol* 32, 1121-1133.
- Ribet, D., and Cossart, P. (2015). How bacterial pathogens colonize their hosts and invade deeper tissues. *Microbes Infect* 17, 173-183.
- Richart, R.M. (1963). A clinical staining test for in vivo delination of Dysplasia and Carcinoma in Situ. *Am J Obst Gynecol*, 703.
- Rios, A.C., and Clevers, H. (2018). Imaging organoids: a bright future ahead. *Nat Methods* 15, 24-26.
- Röder, J., Felgner, P., and Hensel, M. (2021a). Comprehensive Single Cell Analyses of the Nutritional Environment of Intracellular *Salmonella enterica*. *Front Cell Infect Microbiol* 11, 624650.
- Röder, J., Felgner, P., and Hensel, M. (2021b). Single-cell analyses reveal phosphate availability as critical factor for nutrition of *Salmonella enterica* within mammalian host cells. *Cell Microbiol* 23, e13374.
- Roodsant, T., Navis, M., Aknouch, I., Renes, I.B., van Elburg, R.M., Pajkrt, D., Wolthers, K.C., Schultsz, C., van der Ark, K.C.H., Sridhar, A., *et al.* (2020). A Human 2D Primary Organoid-Derived Epithelial Monolayer Model to Study Host-Pathogen Interaction in the Small Intestine. *Front Cell Infect Microbiol* 10, 272.
- Sachs, N., Papaspyropoulos, A., Zomer-van Ommen, D.D., Heo, I., Bottinger, L., Klay, D., Weeber, F., Huelsz-Prince, G., Iakobachvili, N., Amatngalim, G.D., *et al.* (2019). Long-term expanding human airway organoids for disease modeling. *EMBO J* 38.
- Salcedo, S.P., and Holden, D.W. (2003). SseG, a virulence protein that targets *Salmonella* to the Golgi network. *EMBO J* 22, 5003-5014.
- Sato, T., and Clevers, H. (2013). Growing self-organizing mini-guts from a single intestinal stem cell: mechanism and applications. *Science* 340, 1190-1194.
- Sato, T., Stange, D.E., Ferrante, M., Vries, R.G., Van Es, J.H., Van den Brink, S., Van Houdt, W.J., Pronk, A., Van Gorp, J., Siersema, P.D., *et al.* (2011). Long-term expansion of epithelial organoids from human colon, adenoma, adenocarcinoma, and Barrett's epithelium. *Gastroenterology* 141, 1762-1772.
- Sato, T., Vries, R.G., Snippert, H.J., van de Wetering, M., Barker, N., Stange, D.E., van Es, J.H., Abo, A., Kujala, P., Peters, P.J., *et al.* (2009). Single Lgr5 stem cells build crypt-villus structures in vitro without a mesenchymal niche. *Nature* 459, 262-265.
- Scanu, T., Spaapen, R.M., Bakker, J.M., Pratap, C.B., Wu, L.E., Hofland, I., Broeks, A., Shukla, V.K., Kumar, M., Janssen, H., *et al.* (2015). *Salmonella* Manipulation of Host Signaling Pathways Provokes Cellular Transformation Associated with Gallbladder Carcinoma. *Cell Host Microbe* 17, 763-774.
- Schlaermann, P., Toelle, B., Berger, H., Schmidt, S.C., Glanemann, M., Ordemann, J., Bartfeld, S., Mollenkopf, H.J., and Meyer, T.F. (2016). A novel human gastric primary cell culture system for modelling *Helicobacter pylori* infection in vitro. *Gut* 65, 202-213.
- Schreurs, R., Baumdick, M.E., Drewniak, A., and Bunders, M.J. (2021). In vitro co-culture of human intestinal organoids and lamina propria-derived CD4(+) T cells. *STAR Protoc* 2, 100519.
- Schulte, M., Olschewski, K., and Hensel, M. (2021a). Fluorescent protein-based reporters reveal stress response of intracellular *Salmonella enterica* at level of single bacterial cells. *Cell Microbiol* 23, e13293.
- Schulte, M., Olschewski, K., and Hensel, M. (2021b). The protected physiological state of intracellular *Salmonella enterica* persists reduces host cell-imposed stress. *Commun Biol* 4, 520.
- Sepe, L.P., Hartl, K., Iftexhar, A., Berger, H., Kumar, N., Goosmann, C., Chopra, S., Schmidt, S.C., Gurumurthy, R.K., Meyer, T.F., *et al.* (2020). Genotoxic Effect of *Salmonella* Paratyphi A Infection on Human Primary Gallbladder Cells. *mBio* 11.
- Spicer, S.S. (1960). A correlative study of the histochemical properties of rodent acid mucopolysaccharides. *J Histochem Cytochem* 8, 18-35.

- Sridharan, G., and Shankar, A.A. (2012). Toluidine blue: A review of its chemistry and clinical utility. *J Oral Maxillofac Pathol* 16, 251-255.
- Stelzner, M., Helmrath, M., Dunn, J.C., Henning, S.J., Houchen, C.W., Kuo, C., Lynch, J., Li, L., Magness, S.T., Martin, M.G., *et al.* (2012). A nomenclature for intestinal in vitro cultures. *Am J Physiol Gastrointest Liver Physiol* 302, G1359-1363.
- Takashima, S., Gold, D., and Hartenstein, V. (2013). Stem cells and lineages of the intestine: a developmental and evolutionary perspective. *Dev Genes Evol* 223, 85-102.
- Tindle, C., Fuller, M., Fonseca, A., Taheri, S., Ibeawuchi, S.R., Beutler, N., Katkar, G.D., Claire, A., Castillo, V., Hernandez, M., *et al.* (2021). Adult stem cell-derived complete lung organoid models emulate lung disease in COVID-19. *Elife* 10.
- Tse, C.M., In, J.G., Yin, J., Donowitz, M., Doucet, M., Foulke-Abel, J., Ruiz-Perez, F., Nataro, J.P., Zachos, N.C., Kaper, J.B., *et al.* (2018). Enterohemorrhagic *E. coli* (EHEC)-Secreted Serine Protease EspP Stimulates Electrogenic Ion Transport in Human Colonoid Monolayers. *Toxins (Basel)* 10.
- Turner, J.R. (2009). Intestinal mucosal barrier function in health and disease. *Nat Rev Immunol* 9, 799-809.
- Urbiscek, M., Rannikmae, H., Foets, T., Ravn, K., Hyvonen, M., and de la Roche, M. (2019). Organoid culture media formulated with growth factors of defined cellular activity. *Sci Rep* 9, 6193.
- Valdivia, R.H., and Falkow, S. (1996). Bacterial genetics by flow cytometry: rapid isolation of *Salmonella* Typhimurium acid-inducible promoters by differential fluorescence induction. *Mol Microbiol* 22, 367-378.
- van de Wetering, M., Francies, H.E., Francis, J.M., Bounova, G., Iorio, F., Pronk, A., van Houdt, W., van Gorp, J., Taylor-Weiner, A., Kester, L., *et al.* (2015). Prospective derivation of a living organoid biobank of colorectal cancer patients. *Cell* 161, 933-945.
- van der Flier, L.G., and Clevers, H. (2009). Stem cells, self-renewal, and differentiation in the intestinal epithelium. *Annu Rev Physiol* 71, 241-260.
- VanDussen, K.L., Marinshaw, J.M., Shaikh, N., Miyoshi, H., Moon, C., Tarr, P.I., Ciorba, M.A., and Stappenbeck, T.S. (2015). Development of an enhanced human gastrointestinal epithelial culture system to facilitate patient-based assays. *Gut* 64, 911-920.
- Wagner, C., Polke, M., Gerlach, R.G., Linke, D., Stierhof, Y.D., Schwarz, H., and Hensel, M. (2011). Functional dissection of SiiE, a giant non-fimbrial adhesin of *Salmonella enterica*. *Cell Microbiol* 13, 1286-1301.
- Wallaschek, N., Reuter, S., Silkenat, S., Wolf, K., Niklas, C., Kayisoglu, O., Aguilar, C., Wiegering, A., Germer, C.T., Kircher, S., *et al.* (2021). Ephrin receptor A2, the epithelial receptor for Epstein-Barr virus entry, is not available for efficient infection in human gastric organoids. *PLoS Pathog* 17, e1009210.
- Wang, S.M., Zhang, L.W., Fan, R.B., Han, X., Yi, H.X., Zhang, L.L., Xue, C.H., Li, H.B., Zhang, Y.H., and Shigwedha, N. (2014). Induction of HT-29 cells apoptosis by lactobacilli isolated from fermented products. *Res Microbiol* 165, 202-214.
- Wang, Y., Wang, P., and Qin, J. (2021). Microfluidic Organs-on-a-Chip for Modeling Human Infectious Diseases. *Acc Chem Res* 54, 3550-3562.
- WHO (2008). The global burden of disease: 2004 update.
- WHO (2014). Antimicrobial resistance: global report on surveillance 2014.
- Yin, Y., and Zhou, D. (2018a). Corrigendum: Organoid and Enteroid Modeling of *Salmonella* Infection. *Front Cell Infect Microbiol* 8, 257.
- Yin, Y., and Zhou, D. (2018b). Organoid and Enteroid Modeling of *Salmonella* Infection. *Front Cell Infect Microbiol* 8, 102.
- Zomer-van Ommen, D.D., Pukin, A.V., Fu, O., Quarles van Ufford, L.H., Janssens, H.M., Beekman, J.M., and Pieters, R.J. (2016). Functional Characterization of Cholera Toxin Inhibitors Using Human Intestinal Organoids. *J Med Chem* 59, 6968-6972.



## V.6. Contributions of co-authors

(\* authors contributed equally)

### **Single cell analyses reveal distinct adaptation of typhoidal and non-typhoidal *Salmonella enterica* serovars to intracellular lifestyle**

Tatjana Reuter\*, Felix Scharte\*, Rico Franzkoch, Viktoria Liss, Michael Hensel

T.R.: conceptualization, data curation, formal analysis, investigation, methodology, validation, visualization, writing – original draft; F.S.: conceptualization, data curation, formal analysis, investigation, methodology, project administration, validation, visualization, writing – original draft; R.F.: formal analysis, investigation, methodology, visualization, writing – original draft; V.L.: formal analysis, investigation, methodology, validation, visualization, writing – original draft; M.H.: conceptualization, data curation, formal analysis, funding acquisition, investigation, methodology, project administration, resources, supervision, validation, visualization, writing – original draft, writing – review & editing

### **Intracellular *Salmonella Paratyphi A* is motile and differs in the expression of flagella-chemotaxis, SPI-1 and carbon utilization pathways in comparison to intracellular *S. Typhimurium***

Helit Cohen\*, Claire Hoede\*, Felix Scharte\*, Charles Coluzzi, Emiliano Cohen, Inna Shomer, Ludovic Mallet, Sébastien Holbert, Remy Felix Serre, Thomas Schiex, Isabelle Virlogeux-Payant, Guntram A. Grassl, Michael Hensel, H  l  ne Chiapello, Ohad Gal-Mor

H.Co.: data curation, investigation, methodology, validation; C.H.: conceptualization, data curation, formal analysis, investigation, methodology; F.S.: conceptualization, data curation, formal analysis, investigation, methodology, visualization, writing – original draft, writing – review & editing; C.C.: data curation, formal analysis, investigation, methodology; E.C.: data curation, formal analysis, investigation, validation, visualization; I.S.: formal analysis, investigation, methodology; L.M.: data curation, formal analysis, investigation, software; S.H.: formal analysis, investigation, validation, writing – review & editing; R.F.S.: formal analysis, methodology, resources; T.S.: conceptualization, funding acquisition, project administration, supervision; I.V.-P.: conceptualization, funding acquisition, investigation, project administration, supervision, writing – review & editing; G.A.G.: conceptualization, funding acquisition, investigation, methodology, project administration, supervision, writing – review & editing; M.H.: conceptualization, formal analysis, funding acquisition, investigation, methodology, project administration, resources, supervision, visualization, writing – original draft, writing – review & editing; H.Ch.: data curation, formal analysis, investigation, project administration, software, supervision; O.G.-M.: conceptualization, formal analysis, funding acquisition, investigation, methodology, project administration, resources, supervision, validation, visualization, writing – original draft, writing – review & editing

**Ca<sup>2+</sup>-activated sphingomyelin scrambling and turnover mediate ESCRT-independent lysosomal repair**

Patrick Niekamp, Felix Scharte, Tolulope Sokoya, Laura Vittadello, Yeongho Kim, Yongqiang Deng, Elisabeth Südhoff, Angelika Hilderink, Mirco Imlau, Christopher J. Clarke, Michael Hensel, Christopher G. Burd, Joost C. M. Holthuis

P.N. and J.C.M.H. designed the research and wrote the manuscript; P.N. performed the bulk of experiments and analyzed the results; F.S. carried out the *Salmonella* infection experiments, with critical input from M.H.; T.S. and A.H. generated and analyzed the SMS-KO, TMEM16F-KO, nSMase-2-KO, and pInd-SMS1 cell lines; L.V. and M.I. assisted with 2-photon laser damage; Y.K., Y.D., and C.G.B. designed and characterized the equinatoxin probes; E.S. performed EqtSM and LAMP1 co-localization experiments; C.J.C. provided intellectual expertise and helped to interpret experimental results. All authors discussed results and commented on the manuscript.

**From vacuole to cytosol – Disruptive invasion triggers cytosolic release of *Salmonella* Paratyphi A and subsequent cytosolic motility favors evasion of xenophagy**

Felix Scharte, Rico Franzkoch, Michael Hensel

F.S. and M.H. designed the research and wrote the manuscript; F.S. performed all experiments and analyzed the results; R.F. carried out the TEM imaging

**Establishment of a novel infection model for *Salmonella* adhesion and invasion - human intestinal organoids**

Nathalie Sander\*, Felix Scharte\*, Rico Franzkoch, Michael Kim, Olympia E. Psathaki, Guntram A. Grassl and Michael Hensel

N.S.: conceptualization, data curation, formal analysis, investigation, methodology, validation, visualization, writing – original draft parts: abstract, introduction part 1, lentiviral transfection, 2D cultivation, PAS staining of 2D organoids, TEER measurements and plate assays, discussion part 2, outlook and associated methods; F.S.: conceptualization, data curation, formal analysis, investigation, methodology, validation, visualization, writing – original draft parts: abstract, introduction part 2, 3D imaging, results microinjection, apical out, PAS staining of murine tissue, microscopy of 2D cultured organoids, discussion part 1, outlook and associated methods; R.F.: provided data and text for part TEM of microinjected intestinal organoids and associated methods; M.K.: provided data for lentiviral transfection and TEER measurements O.E.P.: provided data for SEM and TEM of 3D organoids; G.A.G.: provided material and methods for cultivation of intestinal organoids and provided microinjected, fixed organoids for TEM and LM analyses; M.H.: conceptualization, funding acquisition, project administration, resources, supervision, writing – review & editing

## VI. Discussion

Human infection by different *S. enterica* serovars results in diverse clinical manifestations and represent a major public health concern with global prevalence. Whereas infection with NTS like STM induces a self-limiting gastroenteritis, human-restricted TS like SPA and STY elicit systemic enteric fever, with completely different clinical presentations than gastroenteritis. Research on STY and SPA is challenging due to host restriction, but since STM causes a typhoid-like disease in mice, it was widely used as model organism to mimic human TS infection. Although results gained by research on STM could provide major insights in *Salmonella* virulence in general, the specific virulence mechanisms of TS are far from being understood.

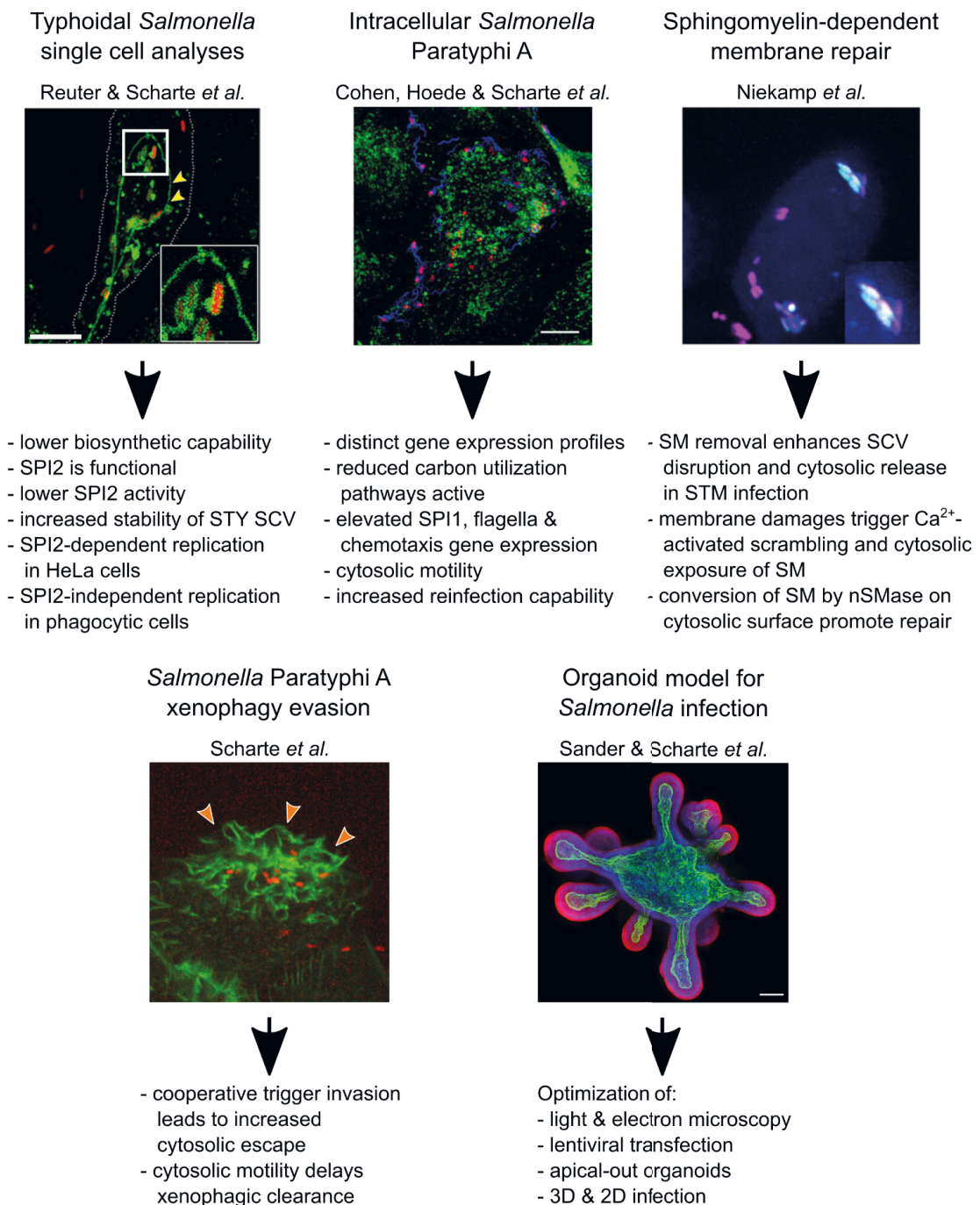


**Figure VI.1. Summary of the results and publications presented in this thesis.** The results presented in chapter V contributed to understanding of typhoidal *Salmonella* virulence functions. Extensive analyses of intracellular activities of STY and SPA in comparison to STM have been performed utilizing flow cytometry and various imaging approaches. Analyses of transcriptomic landscape of extracellular and intracellular SPA and STM have been performed and a previously unknown intracellular phenotype of SPA could be described. Using a novel membrane damage sensor, we could contribute to unraveling the role of sphingomyelin scrambling and turnover in lysosomal repair. Extensive live cell imaging approaches led to description of xenophagy evasion mechanism of SPA deploying cytosolic motility. Last, we established and optimized 3D and 2D cultivation of intestinal organoids for analyses of *Salmonella* infection.

In this work, we investigated the intracellular lifestyles of STY and SPA in more detail (Figure VI.1.). We analyzed intracellular activities of STY and SPA in different host cells on a single cell level and showed that STY and SPA deploy SPI2-T3SS to actively manipulate their host cells, but with far lower frequency than STM, and that reduced intracellular activities contribute to the stealth strategy of STY and SPA, facilitating systemic spread and persistence (Chapter V.1.; (Reuter *et al.*, 2021)). Furthermore, we compared the global gene expression patterns and intracellular phenotypes during human epithelial cell infection of SPA and STM. We identified different expression patterns in key virulence and metabolic pathways, cytosolic motility and increased reinvasion of SPA, following exit from infected cells and hypothesize, that these differences contribute to the invasive and systemic disease developed following SPA infection in humans (Chapter V.2.; (Cohen *et al.*, 2022)). Using a dual-fluorescence reporter that enables dynamic and sensitive detection of STM exposure to host cell cytosol and a host cell reporter for membrane wounding, we contributed to a model how Ca<sup>2+</sup>-activated sphingomyelin scrambling and turnover promote restoration of damaged lysosomal membranes (Chapter V.3.; (Niekamp *et al.*, 2022)). We further utilized the membrane damage reporter together with a newly established cell line to investigate the route of SPA to host cell cytosol and contribution of subsequent cytosolic motility for intracellular lifestyle. Microscopic single cell analyses identified the mode of invasion of SPA as key factor in triggering cytosolic escape and subsequent motility as contributing factor to xenophagic evasion (Chapter V.4.; Scharte *et al.*, unpublished). Last, we established a murine and human organoid system and optimized imaging approaches for further investigation of host-pathogen interactions in a more *in vivo* relevant context (Chapter V.5.; Sander *et al.*, unpublished).

## **VI.1. Differences in typhoidal and non-typhoidal *Salmonella* infection**

In this work, we focused on the intracellular phase of TS infection. Since most of the previous research was done with STM as surrogate for investigation of systemic *Salmonella* infection, we critically analyzed if results gained by research on STM can be transferred to infection scenarios caused by SPA and STY.

### **VI.1.1. Deploying the needle – Role of SPI2-T3SS in typhoidal *Salmonella***

TS and NTS differ significantly in their genetic equipment. Accumulation of pseudogenes as well as loss and gain of genes during their evolution, are likely to result in changes of host-tropism and clinical manifestation. A majority of the pseudogenes functionally classified in STY were related to metabolic processes, e.g. carbohydrate metabolism, amino acid transport and metabolism and inorganic ion

transport (Baddam *et al.*, 2014). It is therefore possible, that STY and SPA have different metabolic demands in intracellular lifestyle compared to STM. During measurements of the biosynthetic activity, STY and SPA exhibited higher heterogeneity with subpopulations of non-induced and weakly induced cells. Furthermore, we observed a continuous loss of activity over time for intracellular SPA and STY, suggesting a lower overall capacity than STM to maintain a biosynthetic active state over prolonged presence in host cells. The SCV represents a niche with limited access to nutrients and the biogenesis of an extensive tubular SIF-network is thought to contribute to efficient intravacuolar nutrition and dilution of antimicrobial factors (Liss *et al.*, 2017; Noster *et al.*, 2019). Studies with STY suggest a less pronounced function of SPI2-T3SS during infection of human macrophages (Forest *et al.*, 2010). A genome-wide screen for genes required for survival in STY in humanized mice did not reveal contributions of SPI2-T3SS or effector proteins (Karlinsky *et al.*, 2019). Since the initial screen was performed using a rather short infection period of 24 h, identification of STY factor relevant in formation of adaptive immune response were not identified. Future analyses under conditions allowing persistent infection will be of interest.

We demonstrated that the SPI2-T3SS is functional in STY and SPA and that they inhabit an SCV together with efficient remodeling of the endosomal system during infection of human epithelial cells, although the average level of translocated SPI2-T3SS effector proteins detected in STY- or SPA-infected cells were lower than for STM-infected HeLa cells. Using a dual fluorescence reporter system, we measured SPI2 gene expression on a single cell level. We analyzed expression of *ssaG* promoter as representative gene encoding a SPI2-T3SS subunit. We observed that expression of  $P_{ssaG}$  varies between STM, SPA and STY and depends on the host cell. Furthermore, the infection time had a significant impact showing a delay in  $P_{ssaG}$  expression in TS. By assessing the intracellular replication, we showed that SPI2-T3SS of STY was not essential in RAW264.7 macrophages and U937 cells but in HeLa cells. STM is prone to cytosolic release, mainly in late stages of infection (Malik-Kale *et al.*, 2012). This bimodal vacuolar and cytosolic lifestyle obscures defects in vacuolar replication and fuels intestinal expansion and chronic fecal shedding of STM (Chong *et al.*, 2021; Malik-Kale *et al.*, 2012). We assessed SCV integrity and cytosolic release of STM and STY and observed that SCV harboring STY are less prone to damage, and less events of cytosolic access of STY occur. Increased SCV stability and reduced intracellular biosynthetic capability might result in increased persisters formation (Schulte *et al.*, 2021). The overall low intracellular activity and replication rate of STY and SPA may contribute to their stealth strategy to avoid a pronounced inflammatory response and facilitate systemic spread and persistence. Loss or pseudogenization of multiple SPI2-T3SS effectors could contribute to lower SPI2-dependent replication and could also trigger cytosolic release of STY and SPA because of the detrimental role of SPI2-T3SS effectors in maintaining SCV integrity and promoting replication through recruitment of host cell vesicles. GtgE, a SPI2-T3SS effector protein absent in STY and SPA, has been described as mediator for host restriction (Spano and Galan, 2012; Spano *et al.*, 2011). Due to its proteolytic activity

targeting Rab29, Rab32 and Rab38, it blocks recruitment of these Rab GTPases to the SCV and promotes replication inside murine macrophages. Complementation of GtgE in STY also promotes replication inside murine macrophages. Another SPI2-T3SS effector, SopD2, is a pseudogene in STY and SPA. In STM it functions as GAP for Rab32 and is also responsible for interaction with Rab7 to regulate endosomal trafficking and SCV membrane dynamics (D'Costa *et al.*, 2015). Expression of *sopD2* in STY led to decreased invasion of human epithelial cells (Trombert *et al.*, 2011). The ability for SIF biogenesis is linked to a small set of SPI2-T3SS effectors (Jennings *et al.*, 2017). Besides SopD2, SseJ also belongs to this set of “core” effectors. SseJ regulates membrane dynamics alongside SifA in STM but is absent in SPA and a pseudogene in STY. Expression of *sseJ* in STY results in reduced cytotoxicity in cultured epithelial cells but also leads to increased intracellular replication (Trombert *et al.*, 2010). Loss of *gtgE*, *sopD2* and *sseJ* may prevent excessive replication of TS in human host cells and represent a host-restriction feature (Galan, 2016). Complementation of SPI2-T3SS effectors with subsequent microscopic analyses of SIF biogenesis and replication analyses by flow cytometry in different cell lines, including human epithelial cells, phagocytic cells and fibroblasts could help to further understand the role of SPI2 in TS. The development of cell culture models like organoid-on-a-chip, which allow prolonged infection times, would help to mimic *in vivo* conditions of TS infection with infection times of multiple days.

### **VI.1.2. Choosing the right equipment –Host-restriction factors in typhoidal *Salmonella***

Factors responsible for the human-restricted host tropism of TS have not been identified yet. Host specificity is often associated to multiple factors like gain or loss of gene function, altered protein function and gene regulation patterns or acquisition of new virulence traits through insertion of phage genes or plasmids. The contribution of SPI2 in this regard has already been discussed before (VI.1.1.). Another factor that could be involved in this evolutionary process is the absence of virulence plasmid pSLT in TS. It was already demonstrated that this plasmid is important for STM replication inside host cells (Guiney *et al.*, 1995; Sabbagh *et al.*, 2010). Lack of this virulence plasmid might limit the ability of SPA and STY to replicate within host cells. Noteworthy, absence of this plasmid is also described for other host-restricted *Salmonella* serovars such as *S. Gallinarum* and *S. Pullorum* which are highly adapted to the avian host and cause fowl typhoid and pullorum disease, respectively (Shivaprasad, 2000). As these serovars and evolutionary related serovars cause a typhoid-like disease in chicken and also accumulated a high number of pseudogenes (Cohen *et al.*, 2021; Thomson *et al.*, 2008), they could be used as alternative infection model for typhoid.

The formation of a polysaccharide capsule is a common bacterial virulence factor of pathogens confronted with host immune responses. It is described to mediate resistance against phagocytosis and antimicrobial peptides, molecular mimicry, and masking of surface-associated antigens (Hu *et al.*, 2017; Spinosa *et al.*, 2007). STY, *S. Paratyphi C* and *S. Dublin* also express the so-called Vi capsule. SPA has evolved a different immune evasion mechanism with expression of very long O-antigen of LPS (Hiyoshi

*et al.*, 2018b). The contribution of these factors to virulence varies from serovar to serovar and deserves further investigation. It is already known that capsule expression is only activated in a subset of the STY population (Hu *et al.*, 2017). Furthermore, immune evasion can favor prolonged infection. Characterization of the contribution of Vi capsule to populations of intracellular STY could be determined by single cell analyses with flow cytometry and microscopy in further studies, with special regard to differences in epithelial cells and phagocytic cells.

Another additional virulence factor of TS is the typhoid toxin (TT). The transport mechanism and its contribution to virulence is still unclear. The development of symptoms specific for typhoid fever is linked to neuropathies as treatment of animals with purified TT led to development of symptoms associated with the acute phase of disease like stupor, malaise and a reduced number of circulating leukocytes (Galan, 2016; Song *et al.*, 2013). Some NTS carry genes of TT but show altered structures of the subunits and fail to export a toxin resembling comparable function as in TS infection (Lee *et al.*, 2020; Miller *et al.*, 2018; Miller and Wiedmann, 2016). Especially the connections to SPI2-T3SS activity and the intracellular transport are still controversially discussed and remain to be further investigated (Chang *et al.*, 2022; Chang *et al.*, 2016; Geiger *et al.*, 2020). As TT function is thought to generate a systemic effect in both the central nervous system and in immune response, cell culture systems might not be the optimal model to investigate these phenotypes. In a humanized mouse model, TT function promoted host survival and the establishment of a persistent asymptomatic infection (Del Bel Belluz *et al.*, 2016). Furthermore, mice infected with TT-expressing STM showed less intestinal inflammation and activation of genes linked to inflammation and immunity became less active. Infection of human volunteers with STY with and without TT expression did not identify substantial differences in clinical symptoms related to TT (Gibani *et al.*, 2019). Organoid systems have already been used to study the genotoxic effect of TT in SPA infection on human primary gallbladder cells (Sepe *et al.*, 2020) and will further improve research on the contribution of specific virulence factors of TS.

### **VI.1.3. Regulation is key – Transcriptional adaptation to host environment**

Although STM and SPA share about 89% of their genes and express many common virulence factors, the disease they cause in humans is very different (McClelland *et al.*, 2004). Distinct expression of genes involved in host-pathogen interactions is expected to contribute to the different pathogenicity. It was previously described that in *Salmonella* grown to late logarithmic phase, SPI1 genes are expressed and secreted at significantly lower levels by SPA compared to STM (Elhadad *et al.*, 2016). Furthermore, differences in the regulatory setup of the flagella-chemotaxis pathway were observed between STM, SPA and STY (Elhadad *et al.*, 2015a; Elhadad *et al.*, 2015b).

Flagella are an important virulence factor mediating motility and acting as adhesive structure in host-cell infection allowing colonization of favorable niches in host organisms. Flagella expression in STM is coregulated with SPI1 and SPI4 in a *flhDC*-dependent manner. During infection, flagella expression

is activated and motility ensures reaching the infection site (Furter *et al.*, 2019; Misselwitz *et al.*, 2012; Stecher *et al.*, 2004). Following adhesion, invasion genes are activated by HilD. Since motility is not favorable to achieve invasion, *hilD* expression and subsequent activation of SPI1 leads to repression of *flhDC* (Ellermeier and Slauch, 2003). Differences regarding flagella expression in STY and SPA in comparison to STM are manifold. While STM has two antigenically distinct flagellin genes *fliC* and *fliB*, both STY and SPA share a monophasic *fliC* phenotype. Flagella and chemotaxis gene expression in STM is induced at various temperatures contributing to adhesion and invasion at environmental temperatures relevant for agriculture (20, 16, 12, 8 °C) and host infection (37 °C) (Elpers *et al.*, 2022). STY and SPA show a temperature-dependent downregulation of motility and invasion genes at fever-like temperatures (39, 42 °C) (Elhadad *et al.*, 2015b) and high oxygen concentrations (Elhadad *et al.*, 2016). Furthermore, expression of Vi capsule in STY leads to repression of *fliC* and *hilD* (Hiyoshi *et al.*, 2018a). The distinct expression patterns of motility and invasion genes by environmental cues in TS may serve as switch from initial invasive stage of infection over systemic spread to persistent phase. By limiting the number of motile and invading bacteria that are able to cross epithelial tissues to systemic sites, bacterial load in the lymphatic system and in blood is controlled avoiding sepsis and consequently death of the host is prevented. In-line with this hypothesis, TS are rarely associated with septic shock, in contrast to many other Gram-negative pathogens (Elhadad *et al.*, 2015b; Tsolis *et al.*, 2008).

In order to survive, persist and replicate in host cells, *Salmonella* has to adapt its metabolic pathways to the specific conditions and nutrients found in the intracellular environment. As STY and SPA are auxotrophic for cysteine and tryptophan (McClelland *et al.*, 2004), the demand for supply with amino acids is higher than for prototrophic STM. In this work, we set out to compare the transcriptional landscape of STM and SPA during epithelial cell infection. We identified 234 differently expressed genes that showed distinct expression patterns in intracellular SPA. We observed differences in carbon utilization pathways of SPA and STM regarding citrate, galactonate and ethanolamine. While STM is able to better utilize these carbon sources, defects in these pathways may contribute to lower replication rate in SPA. As ethanolamine is a ubiquitous molecule within the host, it can serve as carbon and nitrogen source for bacteria in the intestine and within epithelial cells (Bakovic *et al.*, 2007). Furthermore, ethanolamine is released by host tissues during inflammation (Thiennimitr *et al.*, 2011). While increased replication by utilization of galactonate, citrate and ethanolamine benefits STM infection (Arunima *et al.*, 2017; Thiennimitr *et al.*, 2011; Utley *et al.*, 1998), absence of a massive inflammatory response in SPA infection might have led to loss of ethanolamine utilization pathways. A factor possibly contributing to hyper-replication in STM infected cells is the *uhp* operon allowing direct utilization of cytosolic glucose-6-phosphate (Roder and Hensel, 2020). Due to pseudogene formation in the sensor regulator system encoded by *uhpABC* (Holt *et al.*, 2009), carbon sources are more restricted for cytosolic SPA, compared to cytosolic STM, explaining limited intracellular growth. As discussed before, an overall lower replication rate of SPA could also prevent detection by the immune system in systemic infection. The



intracellular nutritional content and the metabolic pathways required during intracellular growth are largely undefined. Further analyses with reporters for genes involved in nutrient acquisition and utilization could contribute to analyze the nutritional environment in *Salmonella* infection (Roder *et al.*, 2021a, b).

While substantial downregulation in the expression of genes associated with SPI1, flagella and chemotaxis has been observed in intracellular STM (Hautefort *et al.*, 2008; Liu *et al.*, 2015), exactly the opposite was the case for intracellular SPA. Observation of intracellular phenotypes during LCI revealed more heterogeneous phenotypes of SPA. We showed that while the majority of STM are non-motile and reside within an SCV, a significant proportion of intracellular SPA are motile and compartmentalized in the cytosol. Cytosolic motile SPA are primed for reinfection and showed increased invasiveness following exit from host cells. How intracellular heterogeneity, especially in the case of SPA, might contribute to pathogenicity of TS is discussed in the following chapter.

#### **VI.1.4. The many-faced pathogen – Intracellular heterogeneity of SPA**

Within host cells, STM is compartmentalized into a modified phagosome, known as SCV. Inside the SCV, STM manipulates the host endolysosomal pathways to build up an extensive SIF-network and achieve survival and replication (Haraga *et al.*, 2008). The contribution of SPI2-T3SS in these processes and possible differences has been discussed before (VI.1.1.). Later in infection, a small subpopulation escapes into the cytosol where conditions are more prone to bacterial growth. Cytosolic escape may lead to hyper-replication, epithelial cell lysis and bacterial release (Knodler, 2015). This process contributes to induce intestinal inflammation that helps STM to compete with the gut microbiota, reinfection of the intestinal epithelium and fecal shedding (Chong *et al.*, 2021; Haraga *et al.*, 2008).

In contrast to the well-established model of STM intracellular lifestyle with a preferred vacuolar localization (~90%) and a small fraction of cytosolic bacteria (~10%), we observed a rather small population of SIF-building STY and SPA in infected epithelial cells. It was previously demonstrated that SPI2-T3SS-mediated SIF biogenesis augments nutritional supply of SCV-inhabiting STM, and also leads to reduction of antimicrobial factors acting on bacteria in the SCV (Liss *et al.*, 2017; Noster *et al.*, 2019). Since SIF formation is less frequent in host cells infected by STY or SPA, this may indicate a restricted nutritional supply, leading to limited intracellular proliferation. Further single cell analyses can address potential correlation between SIF formation and proliferation for intracellular TS.

We observed a pronounced stability of the SCV in STY, leading to the assumption that STY population in infected host cells is more homogenous and exposure to effectors of host-cell defense mechanisms together with the reduced intracellular biosynthetic capability might result in increased persister formation (Schulte *et al.*, 2021). Analyses of intracellular phenotypes of SPA showed similar results regarding SIF-biogenesis occurring only in a small population in about 10% of infected cells. In contrast to STY, SPA showed more diverse phenotypes with bacteria present in host cell cytosolic in about 40%

of the infected cells. In contrast to STM, these bacteria showed no hyper-replication phenotype probably due to defects in nutrient utilization pathways as discussed above (VI.1.3.). We were first in demonstrating flagella-mediated motility of SPA in host cell cytosol of infected epithelial cells, although strong SPI1-T3SS and flagella gene expression has already been demonstrated in STM infected cells in late stage of hyper-replication (Knodler *et al.*, 2010). The described differences in gene expression and cellular phenotypes may result from the distinct intracellular localization of SPA versus STM (cytosolic vs. SCV), but may also contribute to the invasive nature of paratyphoid fever and the ability of SPA to disseminate beyond the intestinal lamina propria.

Eukaryotic cell membranes are vulnerable to mechanical and chemical stressors due to their single lipid bilayer membrane structure. Several membrane repair mechanisms have evolved to efficiently repair such injuries (Cooper and McNeil, 2015). Previous work revealed that PCVs are prone to sporadic ruptures, e.g. due to physical stress occurring from insertion of translocon pores of the T3SS or mechanical stress during bacterial proliferation. Pathogens can exploit host cell mechanisms like the ESCRT machinery, autophagy machinery, or sphingomyelin scrambling to facilitate membrane repair (Birmingham *et al.*, 2006; Ellison *et al.*, 2020; Goser *et al.*, 2020; Kreibich *et al.*, 2015; Lopez-Jimenez *et al.*, 2018; Niekamp *et al.*, 2022). Various reporters have been used to assess membrane damage during pathogen infection such as the sphingomyelin-binding toxins lysenin and equinatoxin (Deng *et al.*, 2016; Ellison *et al.*, 2020) or carbohydrate-binding proteins like galectins (Thurston *et al.*, 2012). Membrane damage during pathogen invasion is also partly dependent on the mode of entry. It was previously shown that trigger invasion leads to formation of early SCV more prone to damage than compartments formed after zipper-mediated entry which involves less severe membrane ruffling at the entry site (Roder and Hensel, 2020). Furthermore, presence of the additional SPI1-T3SS effector protein SopE leads to pronounced cytosolic release in *Salmonella*-infected cells. In this thesis we also observed that increased cooperative trigger invasion enhances membrane damage at nascent SCVs. SPA possesses both SopE and SopE2 which could explain the larger cytosolic population. Furthermore, SptP, a protein acting as antagonist of SopE by restoring normal cytoskeleton organization subsequent to invasion, is defective in STY (Johnson *et al.*, 2017). Failure of cytoskeleton restoration might lead to prolonged membrane ruffling at the entry site and favors cooperative invasion which in turn leads to pronounced membrane damage of the nascent SCV. As already described in STY, our used SPA strain shares the same amino acid changes within the chaperone-binding domain of SptP, leading to instability of the protein. Interestingly, another study showed lower expression profile of *sptP* in SPA and failed to detect the resulting protein in Western blotting, suggesting that instability of SptP may be a common feature in TS. In line with this, other studies demonstrated attenuated virulence of STM when *sptP* is deleted (Chaudhuri *et al.*, 2013; Kaniga *et al.*, 1996).

Other pathogens like *Listeria* and *Shigella* have evolved strategies to actively escape from the vacuole and continue their life cycle in the cytosol (Ray *et al.*, 2009). The cytosol provides a rich source of

nutrients, but bacteria inhabiting host cell cytosol have to subvert cell-autonomous defense systems such as antimicrobial peptides and xenophagy. Furthermore, cytosolic detection of pathogen-associated molecular patterns (PAMPs) such as flagella and LPS might trigger NAIP/NLRC4 inflammasomes, leading to pyroptotic cell death (Gram *et al.*, 2021; Sellin *et al.*, 2014; Wandel *et al.*, 2020). This host cell response is highly cell type dependent with different outcome in epithelial cells, fibroblasts or phagocytic cells (Castanheira and Garcia-Del Portillo, 2017). It is well established, that expression of flagella and chemotaxis genes is highly repressed by intracellular STM (Eriksson *et al.*, 2003; Liu *et al.*, 2017; Liu *et al.*, 2015; Nunez-Hernandez *et al.*, 2013), supporting a nonmotile state of intracellular STM, possibly to prevent inflammatory response by the NAIP/NLRC4 inflammasome (Fattinger *et al.*, 2021). Induction of host cell death by cytosolic motile SPA has not been investigated yet and should be subject of future research with different host cell types involved. *Listeria* and *Shigella* avoid host cell death by repression of intracellular flagella expression and actin-based motility. Actin-based intracellular motility also enables cell-to-cell spread, and thus enables infection of new host cells without demanding exit and exposure to antimicrobial mechanisms acting on extracellular bacteria. Furthermore, this motility contributes to xenophagic escape. In contrast, SPA utilizes flagella to achieve cytosolic motility in infected epithelial cells. Motility of SPA inside phagocytic cells has only been observed in spacious vacuoles rather than in the cytosol, probably because macrophages are more prone to pyroptosis (Castanheira and Garcia-Del Portillo, 2017). Elevated expression of motility-chemotaxis and SPI1 genes, in conjunction with flagella-mediated motility, prime SPA toward a new cycle of host cell infection, supporting systemic dissemination in the human body. Further studies are needed to reveal which cells or tissues of infected host organisms are affected by intracellular motility of SPA and its effect on inflammasome activation and host cell death pathways. Previous studies observed a distinct immune response to SPA infection *in vivo* with elevated secretion of interleukin-8 (IL-8), IL-6, IL-10 and tumor necrosis factor alpha (TNF- $\alpha$ ) (Gal-Mor *et al.*, 2012). In-line with these findings, an induced expression of *hilA* led to increased epithelium disruption and secretion of IL-8 (Elhadad *et al.*, 2016). While IL-8 is a potent neutrophil chemotactic factor and leads to mucosal inflammatory response, IL-6 has possible anti-inflammatory properties and may exert protective effects in different tissues (Eckmann *et al.*, 1993; Haraga *et al.*, 2008; Xing *et al.*, 1998). IL-10 is an anti-inflammatory cytokine, which inhibits antigen presentation to T cells and suppresses phagocytosis and intracellular killing (Spellberg and Edwards, 2001). Our findings suggest that elevated expression of invasion genes and cytosolic motility contribute to the invasive and systemic disease developed following SPA infection in humans. How pronounced cytosolic presence of SPA in certain cells or tissues is connected to the immune response has to be further investigated.

Cellular and biophysically aspects of flagella-mediated cytosolic motility of SPA have not been studied yet. Flagella-mediated motility is influenced by temperature, viscosity and molecular crowding of the medium, as well as by the structure and length of the flagella apparatus (Bente *et al.*, 2020; Kumar and

Philominathan, 2010; Nord *et al.*, 2022; Schneider and Doetsch, 1974; Sporing *et al.*, 2018). As the cytosol is considered to be a viscous environment and largely crowded with macromolecules, organelles and cytoskeleton, *in vitro* studies investigating flagella synthesis and function in different environments could help understanding the biophysical aspects of the newly described cytosolic motility phenotype. Furthermore, the contribution of chemotactic regulation should be considered in future experiments, because it is hard to believe that the observed back and forth motion of cytosolic motile bacteria is dependent on intracellular chemical stimuli.

### **VI.1.5. Catch me if you can – Xenophagic escape of cytosolic motile SPA**

Autophagy-associated proteins, such as LC3, p62 and NDP52 are recruited to cytosolic *Salmonella* (Birmingham *et al.*, 2006; Cemma *et al.*, 2011). Only recently, RNF213 has been identified to mediate ubiquitylation of LPS (Otten *et al.*, 2021). Other cytosolic pathogens like *Shigella* and *Listeria* prevent autophagic recognition by effector protein function at their cell surface. IcsB blocks recognition of cytosolic *Shigella* by ATG5 (Ogawa *et al.*, 2005). Additionally, VirA targets and inactivates RAB1 which is crucial in the formation of autophagosomes (Zoppino *et al.*, 2010). InlK recruits MVP to the surface of *Listeria* which inhibits p62 recruitment and prevents recognition by the autophagosomal machinery (Dortet *et al.*, 2011). Certain SPI1- and SPI2-T3SS effector proteins contribute to xenophagy evasion of STM, such as SopB, SopF, SseF, SseG and SseL (Chatterjee *et al.*, 2022; Feng *et al.*, 2018; Mesquita *et al.*, 2012; Xu *et al.*, 2019), although this function is only described for the vacuolar population and their effect on the cytosolic population is largely unknown. All of the mentioned effectors are also present in STY and SPA. If they possess similar function or also share functional differences as observed for SptP has to be further analyzed. A systematic screening targeting cytosolic motility and xenophagic escape may identify bacterial and host factors involved in these processes.

*Shigella* and *Listeria* are able to actively move within the host cell cytosol by polymerization of host actin at the bacterial surface (Kocks *et al.*, 1995). For both *Shigella* and *Listeria*, the intracellular motility is a major mechanism, enabling cell-to-cell spread and avoidance of recognition by autophagy. Mutants lacking the ability of vacuolar escape and subsequent intracellular movement are highly impaired in their pathogenicity (Ogawa *et al.*, 2011; Yoshikawa *et al.*, 2009). In contrast to intracellular motility mediated by actin polymerization, intracellular motility of SPA did not allow intercellular spread. However, we identified flagella-mediated motility of SPA in host cell cytosol as factor contributing to delay or avoidance of xenophagic capture. The contribution of the different subpopulations of SPA to the intracellular lifestyle has to be further clarified. Quantitative assessment of the cytosolic and vacuolar populations could be achieved by using chloroquine which allows selective inactivation of vacuolar *Salmonella* (Knodler *et al.*, 2014). In combination with bacterial reporters for single cell analyses like flow cytometry and microscopy, the fate of intracellular SPA could be investigated. In our study we only included early infection time points. Long-term experiments in combination with lysotracker would allow analysis if decoration by LC3-positive membranes leads to formation of functional autolysosomes

and degradation of SPA. For several *Yersinia* strains it was reported that degradation by fusion with lysosomes is inhibited and *Yersinia* is able to replicate in a non-acidic autophagosome (Connor *et al.*, 2018; Lemarignier and Pizarro-Cerda, 2020; Moreau *et al.*, 2010; Straley and Harmon, 1984). Interference with autophagy processes using siRNA approaches or chemical inhibitors such as 3-MA in combination with replication assays could further clarify the role of autophagy in SPA infection. Interference with motility using the introduced *motAB*-system or the influence of feverlike temperatures to intracellular motility and xenophagic escape deserve further investigation. Further understanding of the physiological consequences of intracellular motility of SPA demand analyses in other cell types and improved infection models such as organoids of human origin.

## VI.2. Organoids – Biology’s next top model?

Various cell culture models have been used widely across many disciplines in biology. They are relatively cheap, easy to handle and offer a certain degree of reproducibility across different labs. However, immortalized cell lines accumulated mutations in their genome and can also undergo rapid genetic diversification (Liu *et al.*, 2019). More recently, organoids have become a promising model system for analyses of host-pathogen interactions (Aguilar *et al.*, 2021). However, organoid cultivation remains complex, time-consuming and cost intensive. Moreover, due to their highly heterogenous nature, they affect reproducibility between labs. Nonetheless, due to their ability to reconstitute tissue complexity with a close relation to *in vivo* conditions, they represent a promising tool for research in infection biology, especially for human-restricted pathogens with limited model systems available.

We successfully established an intestinal organoid culture model of human and murine origin to study *Salmonella* infection. We demonstrated growth characteristics in 3D and 2D and optimized imaging approaches in the context of STM and SPA infection. A major hurdle during organoid imaging is the sheer size of 3D organoids in Matrigel that can grow up to several micrometers in diameter. Especially in ultrastructural analyses by EM, which is done with ultrathin sections of only several nm thickness. In fluorescence microscopy, imaging especially in Z direction comes with limitation due to the high working distance. Automated volumetric EM as well as multi-photon or light sheet microscopy might be used to overcome these hurdles and the mentioned fluorescence microscopy techniques are also suited for live cell imaging of large specimens. Matrigel, which is needed for 3D cell culture, is known to interfere with fluorescence imaging and may result in higher background, dependent on excitation wavelength. Isolation of single organoids from Matrigel could help getting less background fluorescence but also may result in artefacts due to the treatment. Detached organoids could also be used in approaches involving flow cytometry to assess *Salmonella* tropism for distinct cell populations, especially if combined with bacterial fluorescence reporters.

For investigation of infection processes in organoids, it is crucial to allow pathogens access to the apical side of organoids. As 3D organoids grow in a basal-out orientation, few techniques are suitable to

facilitate infection at the apical side. Microinjection is one of these methods but is limited due to the highly time-consuming process and difficulties adjusting an MOI. Furthermore, the tissue is damaged and pathogens may spill out of the injection site which could result in unwanted basolateral infection. A more promising method is the generation of apical-out organoids in which pathogens can directly be added to the medium (Co *et al.*, 2021). However, the yield during generation of apical-out organoids is relatively low and further amplifies heterogeneity (Co *et al.*, 2019).

We also used organoid-derived monolayers in 2D infection experiments. Advantages of these techniques are the relatively low heterogeneity and decent options to monitor growth such as TEER measurements. Also, infection is easier to conduct with defined parameters. However, LCI approaches with cell culture inserts like transwells are highly limited. Nonetheless, we investigated the contribution of SPI4-T1SS and its substrate SiiE in STM during colonoid- and enteroid-derived monolayer infection. During infection, loss of membrane integrity was observed with TEER measurements. Noteworthy, we found differences regarding invasion phenotype of STM WT and  $\Delta spi4$  between ileum- and colon-derived monolayers. The role of SPI4 in STY and SPA also deserves further investigation. Due to multiple frame-shifts, *siiE* is a pseudogene in STY (Parkhill *et al.*, 2001). In SPA, in frame deletions of 9 (of 53) bacterial immunoglobulin (BIg) domains result in length alteration, but SiiE surface expression still occurs (preliminary data). SPI4 and SPI1 expression are coregulated by SirA and HilA during STM infection (Gerlach *et al.*, 2007). Differential regulation patterns of HilA/HilD regulon in SPA (Elhadad *et al.*, 2016; Elhadad *et al.*, 2015b) could also affect SPI4 expression. However, both STY and SPA show a significantly lower invasion rate in PEC infection compared to STM (Elhadad *et al.*, 2016; Elhadad *et al.*, 2015a; Elhadad *et al.*, 2015b; Gal-Mor *et al.*, 2012). Absence of PEC infection in the gastrointestinal tract might contribute to a lower inflammatory response observed in TS infection (Dougan and Baker, 2014; Hiyoshi *et al.*, 2018a). In ultrastructural analyses by SEM we only observed SPA invasion at cells largely lacking microvilli. How a shortened SiiE could contribute to SPA adhesion and invasion deserves further investigation.

Intestinal M-cells are exploited by *Salmonella* and various other pathogens as route of invasion. The specialized antigen-sampling cells of the mucosal immune system possess an irregular brush border and reduced microvilli (Jepson and Clark, 1998, 2001). A population of M-cells is usually absent in organoid culture. However, M-cell differentiation can be induced by addition of RankL to organoid culture (de Lau *et al.*, 2012). Co-culture models with Raji B lymphocytes could also drive M-cell differentiation in HT-29 and CaCo-2 cells (Araujo *et al.*, 2016; Araujo and Sarmiento, 2013). A primary human macrophage-enteroid co-culture has already been used to investigate host-pathogen interactions (Noel *et al.*, 2017) and could serve as promising tool to study TS infection in a more *in vivo* relevant context, especially with regard to transmigration of the intestinal epithelium to reach systemic body sites (Fulde *et al.*, 2021). Furthermore, organoids derived from various tissues could resemble the infection pathway

of TS. Possible tissues of interest could be gallbladder, liver and spleen as these are systemic sites where TS are able to survive and replicate during infection (Gal-Mor, 2019).

TS are able to resist high concentrations of bile and can therefore reside in the gallbladder, both intracellularly and extracellularly (Gunn *et al.*, 2014). Furthermore, bile induces persister cell formation of STY and associated tolerance to antibiotics (Walawalkar *et al.*, 2016). By formation of biofilms in the gallbladder and on gallstones, TS are able to form a reservoir from which bacteria are intermittently shed into the duodenum (Crawford *et al.*, 2008; Crawford *et al.*, 2010; Gonzalez-Escobedo and Gunn, 2013; Gonzalez-Escobedo *et al.*, 2011). Constant inflammation of gallbladder tissue during persistent infection might lead to development of gallbladder cancer (Di Domenico *et al.*, 2017). However, the formation of biofilm enables STY to adapt a carrier state in the host, which occurs in 3% - 5% of patients (Gunn *et al.*, 2014; Prouty *et al.*, 2002; Walawalkar *et al.*, 2016). We measured less metabolic activity of intracellular STY and SPA, compared to STM in different host cells 16 h and 24 h p.i. which likely leads to less pronounced replication and increased transition to persister state. Future studies involving gallbladder organoids could help study the influence of bacterial persisters and possible association with gallbladder cancer (Sepe *et al.*, 2020).

### VI.3. Concluding remarks

Incidence rates of typhoid and paratyphoid fever are rising in Asia and Africa and extensively drug-resistant STY and especially SPA strains are frequently emerging in these regions. As research on TS is limited due to their host restriction, distinct virulence traits are largely unknown. Research on *Salmonella* has been predominantly done with STM as surrogate for TS infection. Some studies have been carried out with STY but even less have been conducted with SPA, therefore only little literature is available. SPA has become more relevant concerning health policy of the WHO.

Typhoid conjugate vaccine (TCV) has been used safely and effectively as part of outbreak response efforts in Pakistan to control an extensively drug-resistant typhoid outbreak that began 2016 in Zimbabwe. TCV was afterwards successfully introduced in Nepal, Bangladesh and central Africa in the last years and months and showed over 80% efficiency against typhoid. However, it only provides weak cross-reactive immune response against SPA because it is based on the Vi capsule and therefore only induces antibody production against Vi-positive strains (Pakkanen *et al.*, 2014). The oral live vaccine Ty21a contains a Ty2 mutant strain deficient in LPS and Vi synthesis together with about 25 accumulated mutations. It provides a significant protection against STY of 50% to 80% and also elicit a decent cross-protection against other *Salmonella* strains, including SPA (Levine *et al.*, 2007; Pakkanen *et al.*, 2012). Only recently, clinical trials of a new developed paratyphoid vaccine have started (University of Oxford). Until development of new effective vaccines is successful, better sanitation and clean water remain crucial to prevent TS infection.

The development of vaccines and effective disease treatment strategies relies on fundamental research in molecular sciences to identify potential targets e.g. for drug development or favorable mutations for live vaccines. Virulence factors such as the Vi capsule, typhoid toxin, adhesins, effector proteins of SPI1- and SPI2-T3SS and also cytosolic motility could represent such targets. This thesis focused on the intracellular lifestyle of TS using SPA and STY strains from outbreaks in Nepal in 2009 and south-east Asia in 2012, respectively. With our work we contributed to the understanding of distinct virulence functions of SPA and STY in epithelial cells and macrophages. Furthermore, we described and characterized a new intracellular phenotype of SPA. Alterations in the virulence repertoire and distinct gene expression patterns of TS suggest that STM is not always an appropriate model for typhoidal disease and that certain virulence functions may be required for systemic disease in mice or other hosts but not in humans. With our work in establishing a human organoid system for TS infection we laid foundation for new studies in a context closer related to *in vivo* conditions. The insights gained in this thesis and open questions are summarized in Figure VI.2. Future studies concerning various single cell, state-of-the-art microscopy techniques and improved infection models will further contribute to understanding of host-pathogen interactions of *Salmonella*.



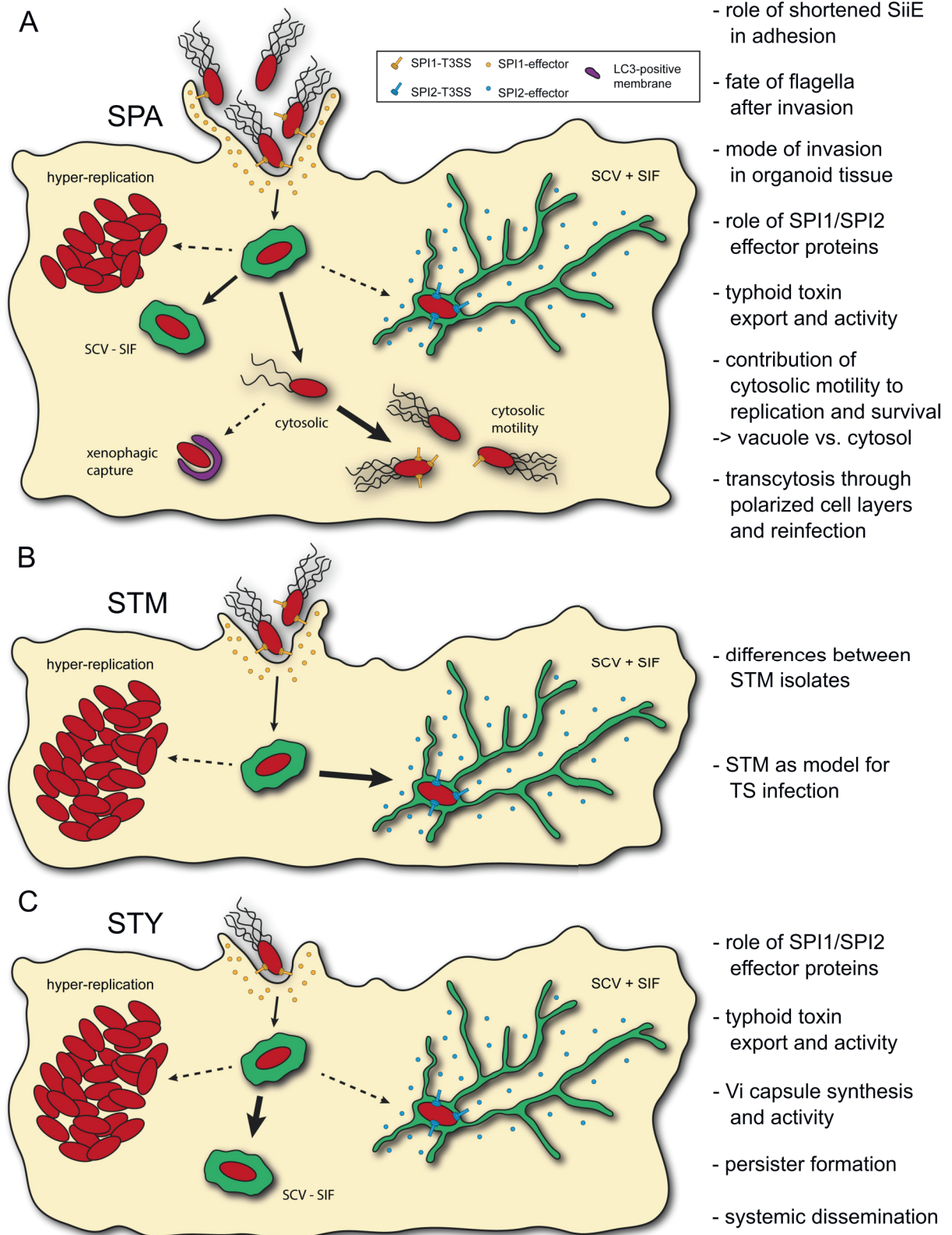


**Figure VI.2. Working model summarizing the differences between intracellular SPA, STM and STY in epithelial cells.** (A-C) After invasion, SPA, STM and STY are present in a *Salmonella*-containing vacuole (SCV). (A) SPA invades in a more cooperative manner and is subsequently less likely to be present in an SCV with extensive *Salmonella*-induced filament (SIF)-network. Intracellular SPA either stays in a SIF-less SCV or becomes cytosolic. Cytosolic SPA show moderate replication rates but express high levels of flagella-chemotaxis and SPI1 genes. Cytosolic motility favors evasion from xenophagic capture. (B) STM is almost exclusively present in SIF-associated SCV and express higher levels of SPI2 genes. (C) STY is almost exclusively present in a SIF-less SCV with high stability and shows lower biosynthetic capability.

## VII. References

- Aguilar, C., Alves da Silva, M., Saraiva, M., Neyazi, M., Olsson, I.A.S., and Bartfeld, S. (2021). Organoids as host models for infection biology - a review of methods. *Exp Mol Med* 53, 1471-1482.
- Alberdi, L., Vergnes, A., Manneville, J.B., Tembo, D.L., Fang, Z., Zhao, Y., Schroeder, N., Dumont, A., Lagier, M., Bassereau, P., *et al.* (2020). Regulation of kinesin-1 activity by the *Salmonella enterica* effectors PipB2 and SifA. *J Cell Sci* 133.
- Allaire, J.M., Crowley, S.M., Law, H.T., Chang, S.Y., Ko, H.J., and Vallance, B.A. (2018). The Intestinal Epithelium: Central Coordinator of Mucosal Immunity. *Trends Immunol* 39, 677-696.
- Altier, C., Suyemoto, M., Ruiz, A.I., Burnham, K.D., and Maurer, R. (2000). Characterization of two novel regulatory genes affecting *Salmonella* invasion gene expression. *Mol Microbiol* 35, 635-646.
- Antimicrobial Resistance, C. (2022). Global burden of bacterial antimicrobial resistance in 2019: a systematic analysis. *Lancet* 399, 629-655.
- Araujo, F., Pereira, C., Costa, J., Barrias, C., Granja, P.L., and Sarmiento, B. (2016). In vitro M-like cells genesis through a tissue-engineered triple-culture intestinal model. *J Biomed Mater Res B Appl Biomater* 104, 782-788.
- Araujo, F., and Sarmiento, B. (2013). Towards the characterization of an in vitro triple co-culture intestine cell model for permeability studies. *Int J Pharm* 458, 128-134.
- Arricau, N., Hermant, D., Waxin, H., Ecobichon, C., Duffey, P.S., and Popoff, M.Y. (1998). The RcsB-RcsC regulatory system of *Salmonella typhi* differentially modulates the expression of invasion proteins, flagellin and Vi antigen in response to osmolarity. *Mol Microbiol* 29, 835-850.
- Arunima, A., Yelamanchi, S.D., Padhi, C., Jaiswal, S., Ryan, D., Gupta, B., Sathe, G., Advani, J., Gowda, H., Prasad, T.S.K., *et al.* (2017). "Omics" of Food-Borne Gastroenteritis: Global Proteomic and Mutagenic Analysis of *Salmonella enterica* Serovar Enteritidis. *OMICS* 21, 571-583.
- Asrat, S., de Jesus, D.A., Hempstead, A.D., Ramabhadran, V., and Isberg, R.R. (2014). Bacterial pathogen manipulation of host membrane trafficking. *Annu Rev Cell Dev Biol* 30, 79-109.
- Baddam, R., Kumar, N., Shaik, S., Lankapalli, A.K., and Ahmed, N. (2014). Genome dynamics and evolution of *Salmonella Typhi* strains from the typhoid-endemic zones. *Sci Rep* 4, 7457.
- Bakovic, M., Fullerton, M.D., and Michel, V. (2007). Metabolic and molecular aspects of ethanolamine phospholipid biosynthesis: the role of CTP:phosphoethanolamine cytidyltransferase (Pcyt2). *Biochem Cell Biol* 85, 283-300.
- Bakowski, M.A., Braun, V., and Brumell, J.H. (2008). *Salmonella*-containing vacuoles: directing traffic and nesting to grow. *Traffic* 9, 2022-2031.
- Bakowski, M.A., Cirulis, J.T., Brown, N.F., Finlay, B.B., and Brumell, J.H. (2007). SopD acts cooperatively with SopB during *Salmonella enterica* serovar Typhimurium invasion. *Cell Microbiol* 9, 2839-2855.
- Barlag, B., and Hensel, M. (2015). The giant adhesin SiiE of *Salmonella enterica*. *Molecules* 20, 1134-1150.
- Bartfeld, S. (2016). Modeling infectious diseases and host-microbe interactions in gastrointestinal organoids. *Dev Biol* 420, 262-270.
- Bartfeld, S., and Clevers, H. (2015). Organoids as Model for Infectious Diseases: Culture of Human and Murine Stomach Organoids and Microinjection of Helicobacter Pylori. *J Vis Exp*.
- Baxter, M.A., and Jones, B.D. (2015). Two-component regulators control hilA expression by controlling fimZ and hilE expression within *Salmonella enterica* serovar Typhimurium. *Infect Immun* 83, 978-985.
- Bayer-Santos, E., Durkin, C.H., Rigano, L.A., Kupz, A., Alix, E., Cerny, O., Jennings, E., Liu, M., Ryan, A.S., Lapaque, N., *et al.* (2016). The *Salmonella* Effector SteD Mediates MARCH8-Dependent Ubiquitination of MHC II Molecules and Inhibits T Cell Activation. *Cell Host Microbe* 20, 584-595.

- Bente, K., Mohammadinejad, S., Charsooghi, M.A., Bachmann, F., Codutti, A., Lefevre, C.T., Klumpp, S., and Faivre, D. (2020). High-speed motility originates from cooperatively pushing and pulling flagella bundles in bilophotrichous bacteria. *Elife* 9.
- Beuzon, C.R., Meresse, S., Unsworth, K.E., Ruiz-Albert, J., Garvis, S., Waterman, S.R., Ryder, T.A., Boucrot, E., and Holden, D.W. (2000). *Salmonella* maintains the integrity of its intracellular vacuole through the action of SifA. *EMBO J* 19, 3235-3249.
- Birmingham, C.L., Smith, A.C., Bakowski, M.A., Yoshimori, T., and Brumell, J.H. (2006). Autophagy controls *Salmonella* infection in response to damage to the *Salmonella*-containing vacuole. *J Biol Chem* 281, 11374-11383.
- Boucrot, E., Henry, T., Borg, J.P., Gorvel, J.P., and Meresse, S. (2005). The intracellular fate of *Salmonella* depends on the recruitment of kinesin. *Science* 308, 1174-1178.
- Brumell, J.H., Tang, P., Zaharik, M.L., and Finlay, B.B. (2002). Disruption of the *Salmonella*-containing vacuole leads to increased replication of *Salmonella enterica* serovar typhimurium in the cytosol of epithelial cells. *Infect Immun* 70, 3264-3270.
- Caiazza, C., Parisi, S., and Caiazza, M. (2021). Liver Organoids: Updates on Disease Modeling and Biomedical Applications. *Biology (Basel)* 10.
- Castanheira, S., and Garcia-Del Portillo, F. (2017). *Salmonella* Populations inside Host Cells. *Front Cell Infect Microbiol* 7, 432.
- Cemma, M., Kim, P.K., and Brumell, J.H. (2011). The ubiquitin-binding adaptor proteins p62/SQSTM1 and NDP52 are recruited independently to bacteria-associated microdomains to target *Salmonella* to the autophagy pathway. *Autophagy* 7, 341-345.
- Chan, K., Baker, S., Kim, C.C., Detweiler, C.S., Dougan, G., and Falkow, S. (2003). Genomic comparison of *Salmonella enterica* serovars and *Salmonella bongori* by use of an *S. enterica* serovar typhimurium DNA microarray. *J Bacteriol* 185, 553-563.
- Chang, S.J., Hsu, Y.T., Chen, Y., Lin, Y.Y., Lara-Tejero, M., and Galan, J.E. (2022). Typhoid toxin sorting and exocytic transport from *Salmonella* Typhi-infected cells. *Elife* 11.
- Chang, S.J., Song, J., and Galan, J.E. (2016). Receptor-Mediated Sorting of Typhoid Toxin during Its Export from *Salmonella* Typhi-Infected Cells. *Cell Host Microbe* 20, 682-689.
- Chatterjee, R., Chaudhuri, D., Setty, S.R.G., and Chakravorty, D. (2022). Deceiving The Big Eaters: *Salmonella* Typhimurium SopB subverts host cell Xenophagy through Akt-TFEB axis in macrophages. *bioRxiv* 10.1101/2022.02.03.479023.
- Chaudhuri, R.R., Morgan, E., Peters, S.E., Pleasance, S.J., Hudson, D.L., Davies, H.M., Wang, J., van Diemen, P.M., Buckley, A.M., Bowen, A.J., *et al.* (2013). Comprehensive assignment of roles for *Salmonella* typhimurium genes in intestinal colonization of food-producing animals. *PLoS Genet* 9, e1003456.
- Cheng, S., Wang, L., Liu, Q., Qi, L., Yu, K., Wang, Z., Wu, M., Liu, Y., Fu, J., Hu, M., *et al.* (2017). Identification of a Novel *Salmonella* Type III Effector by Quantitative Secretome Profiling. *Mol Cell Proteomics* 16, 2219-2228.
- Chong, A., Cooper, K.G., Kari, L., Nilsson, O.R., Hillman, C., Fleming, B.A., Wang, Q., Nair, V., and Steele-Mortimer, O. (2021). Cytosolic replication in epithelial cells fuels intestinal expansion and chronic fecal shedding of *Salmonella* Typhimurium. *Cell Host Microbe* 29, 1177-1185 e1176.
- Chong, A., Lee, S., Yang, Y.A., and Song, J. (2017). The Role of Typhoid Toxin in *Salmonella* Typhi Virulence. *Yale J Biol Med* 90, 283-290.
- Choy, A., Dancourt, J., Mugo, B., O'Connor, T.J., Isberg, R.R., Melia, T.J., and Roy, C.R. (2012). The *Legionella* effector RavZ inhibits host autophagy through irreversible Atg8 deconjugation. *Science* 338, 1072-1076.
- Cirillo, D.M., Valdivia, R.H., Monack, D.M., and Falkow, S. (1998). Macrophage-dependent induction of the *Salmonella* pathogenicity island 2 type III secretion system and its role in intracellular survival. *Mol Microbiol* 30, 175-188.
- Co, J.Y., Margalef-Catala, M., Li, X., Mah, A.T., Kuo, C.J., Monack, D.M., and Amieva, M.R. (2019). Controlling Epithelial Polarity: A Human Enteroid Model for Host-Pathogen Interactions. *Cell Rep* 26, 2509-2520 e2504.

- Co, J.Y., Margalef-Catala, M., Monack, D.M., and Amieva, M.R. (2021). Controlling the polarity of human gastrointestinal organoids to investigate epithelial biology and infectious diseases. *Nat Protoc* 16, 5171-5192.
- Cohen, E., Azriel, S., Auster, O., Gal, A., Zitronblat, C., Mikhlin, S., Scharte, F., Hensel, M., Rahav, G., and Gal-Mor, O. (2021). Pathoadaptation of the passerine-associated *Salmonella enterica* serovar Typhimurium lineage to the avian host. *PLoS Pathog* 17, e1009451.
- Cohen, H., Hoede, C., Scharte, F., Coluzzi, C., Cohen, E., Shomer, I., Mallet, L., Holbert, S., Serre, R.F., Schiex, T., *et al.* (2022). Intracellular *Salmonella* Paratyphi A is motile and differs in the expression of flagella-chemotaxis, SPI-1 and carbon utilization pathways in comparison to intracellular *S. Typhimurium*. *PLoS Pathog* 18, e1010425.
- Connor, M.G., Pulsifer, A.R., Chung, D., Rouchka, E.C., Ceresa, B.K., and Lawrenz, M.B. (2018). *Yersinia pestis* Targets the Host Endosome Recycling Pathway during the Biogenesis of the *Yersinia*-Containing Vacuole To Avoid Killing by Macrophages. *mBio* 9.
- Cooper, S.T., and McNeil, P.L. (2015). Membrane Repair: Mechanisms and Pathophysiology. *Physiol Rev* 95, 1205-1240.
- Cornelis, G.R. (2006). The type III secretion injectisome. *Nat Rev Microbiol* 4, 811-825.
- Cossart, P., and Sansonetti, P.J. (2004). Bacterial invasion: the paradigms of enteroinvasive pathogens. *Science* 304, 242-248.
- Crawford, R.W., Gibson, D.L., Kay, W.W., and Gunn, J.S. (2008). Identification of a bile-induced exopolysaccharide required for *Salmonella* biofilm formation on gallstone surfaces. *Infect Immun* 76, 5341-5349.
- Crawford, R.W., Rosales-Reyes, R., Ramirez-Aguilar Mde, L., Chapa-Azuela, O., Alpuche-Aranda, C., and Gunn, J.S. (2010). Gallstones play a significant role in *Salmonella* spp. gallbladder colonization and carriage. *Proc Natl Acad Sci U S A* 107, 4353-4358.
- Creasey, E.A., and Isberg, R.R. (2014). Maintenance of vacuole integrity by bacterial pathogens. *Curr Opin Microbiol* 17, 46-52.
- Crosnier, C., Stamatakis, D., and Lewis, J. (2006). Organizing cell renewal in the intestine: stem cells, signals and combinatorial control. *Nat Rev Genet* 7, 349-359.
- Crump, J.A., Luby, S.P., and Mintz, E.D. (2004). The global burden of typhoid fever. *Bull World Health Organ* 82, 346-353.
- D'Costa, V.M., Braun, V., Landekic, M., Shi, R., Proteau, A., McDonald, L., Cygler, M., Grinstein, S., and Brumell, J.H. (2015). *Salmonella* Disrupts Host Endocytic Trafficking by SopD2-Mediated Inhibition of Rab7. *Cell Rep* 12, 1508-1518.
- de Lau, W., Kujala, P., Schneeberger, K., Middendorp, S., Li, V.S., Barker, N., Martens, A., Hofhuis, F., DeKoter, R.P., Peters, P.J., *et al.* (2012). Peyer's patch M cells derived from Lgr5(+) stem cells require SpiB and are induced by RankL in cultured "miniguts". *Mol Cell Biol* 32, 3639-3647.
- Deiwick, J., Nikolaus, T., Erdogan, S., and Hensel, M. (1999). Environmental regulation of *Salmonella* pathogenicity island 2 gene expression. *Mol Microbiol* 31, 1759-1773.
- Deiwick, J., Salcedo, S.P., Boucrot, E., Gilliland, S.M., Henry, T., Petermann, N., Waterman, S.R., Gorvel, J.P., Holden, D.W., and Meresse, S. (2006). The translocated *Salmonella* effector proteins SseF and SseG interact and are required to establish an intracellular replication niche. *Infect Immun* 74, 6965-6972.
- Del Bel Belluz, L., Guidi, R., Pateras, I.S., Levi, L., Mihaljevic, B., Rouf, S.F., Wrande, M., Candela, M., Turrone, S., Nastasi, C., *et al.* (2016). The Typhoid Toxin Promotes Host Survival and the Establishment of a Persistent Asymptomatic Infection. *PLoS Pathog* 12, e1005528.
- Deng, Y., Rivera-Molina, F.E., Toomre, D.K., and Burd, C.G. (2016). Sphingomyelin is sorted at the trans Golgi network into a distinct class of secretory vesicle. *Proc Natl Acad Sci U S A* 113, 6677-6682.
- Di Domenico, E.G., Cavallo, I., Pontone, M., Toma, L., and Ensoli, F. (2017). Biofilm Producing *Salmonella* Typhi: Chronic Colonization and Development of Gallbladder Cancer. *Int J Mol Sci* 18.
- Didelot, X., Achtman, M., Parkhill, J., Thomson, N.R., and Falush, D. (2007). A bimodal pattern of relatedness between the *Salmonella* Paratyphi A and Typhi genomes: convergence or divergence by homologous recombination? *Genome Res* 17, 61-68.

- Dikic, I., and Elazar, Z. (2018). Mechanism and medical implications of mammalian autophagy. *Nat Rev Mol Cell Biol* *19*, 349-364.
- Dortet, L., Mostowy, S., Samba-Louaka, A., Gouin, E., Nahori, M.A., Wiemer, E.A., Dussurget, O., and Cossart, P. (2011). Recruitment of the major vault protein by InlK: a *Listeria monocytogenes* strategy to avoid autophagy. *PLoS Pathog* *7*, e1002168.
- Dougan, G., and Baker, S. (2014). *Salmonella enterica* serovar Typhi and the pathogenesis of typhoid fever. *Annu Rev Microbiol* *68*, 317-336.
- Dumont, A., Boucrot, E., Drevensek, S., Daire, V., Gorvel, J.P., Pous, C., Holden, D.W., and Meresse, S. (2010). SKIP, the host target of the *Salmonella* virulence factor SifA, promotes kinesin-1-dependent vacuolar membrane exchanges. *Traffic* *11*, 899-911.
- Dutta, D., and Clevers, H. (2017). Organoid culture systems to study host-pathogen interactions. *Curr Opin Immunol* *48*, 15-22.
- Eckmann, L., Kagnoff, M.F., and Fierer, J. (1993). Epithelial cells secrete the chemokine interleukin-8 in response to bacterial entry. *Infect Immun* *61*, 4569-4574.
- Edsall, G., Gaines, S., Landy, M., Tigertt, W.D., Sprinz, H., Trapani, R.J., Mandel, A.D., and Benenson, A.S. (1960). Studies on infection and immunity in experimental typhoid fever. I. Typhoid fever in chimpanzees orally infected with *Salmonella typhosa*. *J Exp Med* *112*, 143-166.
- Elhadad, D., Desai, P., Grassl, G.A., McClelland, M., Rahav, G., and Gal-Mor, O. (2016). Differences in Host Cell Invasion and *Salmonella* Pathogenicity Island 1 Expression between *Salmonella enterica* Serovar Paratyphi A and Nontyphoidal *S. Typhimurium*. *Infect Immun* *84*, 1150-1165.
- Elhadad, D., Desai, P., Rahav, G., McClelland, M., and Gal-Mor, O. (2015a). Flagellin Is Required for Host Cell Invasion and Normal *Salmonella* Pathogenicity Island 1 Expression by *Salmonella enterica* Serovar Paratyphi A. *Infect Immun* *83*, 3355-3368.
- Elhadad, D., McClelland, M., Rahav, G., and Gal-Mor, O. (2015b). Feverlike Temperature is a Virulence Regulatory Cue Controlling the Motility and Host Cell Entry of Typhoidal *Salmonella*. *J Infect Dis* *212*, 147-156.
- Ellermeier, C.D., and Slauch, J.M. (2003). RtsA and RtsB coordinately regulate expression of the invasion and flagellar genes in *Salmonella enterica* serovar Typhimurium. *J Bacteriol* *185*, 5096-5108.
- Ellermeier, J.R., and Slauch, J.M. (2007). Adaptation to the host environment: regulation of the SPII type III secretion system in *Salmonella enterica* serovar Typhimurium. *Curr Opin Microbiol* *10*, 24-29.
- Ellison, C.J., Kukulski, W., Boyle, K.B., Munro, S., and Randow, F. (2020). Transbilayer Movement of Sphingomyelin Precedes Catastrophic Breakage of Enterobacteria-Containing Vacuoles. *Curr Biol* *30*, 2974-2983 e2976.
- Elpers, L., Deiwick, J., and Hensel, M. (2022). Effect of environmental temperatures on proteome composition of *Salmonella enterica* serovar Typhimurium. *Mol Cell Proteomics*, 100265.
- Eriksson, S., Lucchini, S., Thompson, A., Rhen, M., and Hinton, J.C. (2003). Unravelling the biology of macrophage infection by gene expression profiling of intracellular *Salmonella enterica*. *Mol Microbiol* *47*, 103-118.
- Ettayebi, K., Crawford, S.E., Murakami, K., Broughman, J.R., Karandikar, U., Tenge, V.R., Neill, F.H., Blutt, S.E., Zeng, X.L., Qu, L., *et al.* (2016). Replication of human noroviruses in stem cell-derived human enteroids. *Science* *353*, 1387-1393.
- Fattinger, S.A., Sellin, M.E., and Hardt, W.D. (2021). Epithelial inflammasomes in the defense against *Salmonella* gut infection. *Curr Opin Microbiol* *59*, 86-94.
- Feng, Y., Johnston, R.N., Liu, G.R., and Liu, S.L. (2013). Genomic comparison between *Salmonella Gallinarum* and *Pullorum*: differential pseudogene formation under common host restriction. *PLoS One* *8*, e59427.
- Feng, Z.Z., Jiang, A.J., Mao, A.W., Feng, Y., Wang, W., Li, J., Zhang, X., Xing, K., and Peng, X. (2018). The *Salmonella* effectors SseF and SseG inhibit Rab1A-mediated autophagy to facilitate intracellular bacterial survival and replication. *J Biol Chem* *293*, 9662-9673.
- Figueira, R., and Holden, D.W. (2012). Functions of the *Salmonella* pathogenicity island 2 (SPI-2) type III secretion system effectors. *Microbiology* *158*, 1147-1161.

- Figueira, R., Watson, K.G., Holden, D.W., and Helaine, S. (2013). Identification of *Salmonella* pathogenicity island-2 type III secretion system effectors involved in intramacrophage replication of *S. enterica* serovar typhimurium: implications for rational vaccine design. *MBio* 4, e00065.
- Finkbeiner, S.R., Zeng, X.L., Utama, B., Atmar, R.L., Shroyer, N.F., and Estes, M.K. (2012). Stem cell-derived human intestinal organoids as an infection model for rotaviruses. *mBio* 3, e00159-00112.
- Finn, C.E., Chong, A., Cooper, K.G., Starr, T., and Steele-Mortimer, O. (2017). A second wave of *Salmonella* T3SS1 activity prolongs the lifespan of infected epithelial cells. *PLoS Pathog* 13, e1006354.
- Fiskin, E., Bhogaraju, S., Herhaus, L., Kalayil, S., Hahn, M., and Dikic, I. (2017). Structural basis for the recognition and degradation of host TRIM proteins by *Salmonella* effector SopA. *Nat Commun* 8, 14004.
- Foley, S.L., Johnson, T.J., Ricke, S.C., Nayak, R., and Danzeisen, J. (2013). *Salmonella* pathogenicity and host adaptation in chicken-associated serovars. *Microbiol Mol Biol Rev* 77, 582-607.
- Forbester, J.L., Goulding, D., Vallier, L., Hannan, N., Hale, C., Pickard, D., Mukhopadhyay, S., and Dougan, G. (2015). Interaction of *Salmonella enterica* Serovar Typhimurium with Intestinal Organoids Derived from Human Induced Pluripotent Stem Cells. *Infect Immun* 83, 2926-2934.
- Forest, C.G., Ferraro, E., Sabbagh, S.C., and Daigle, F. (2010). Intracellular survival of *Salmonella enterica* serovar Typhi in human macrophages is independent of *Salmonella* pathogenicity island (SPI)-2. *Microbiology* 156, 3689-3698.
- Friebel, A., Ilchmann, H., Aepfelbacher, M., Ehrbar, K., Machleidt, W., and Hardt, W.D. (2001). SopE and SopE2 from *Salmonella typhimurium* activate different sets of RhoGTPases of the host cell. *J Biol Chem* 276, 34035-34040.
- Fu, Y., and Galan, J.E. (1999). A salmonella protein antagonizes Rac-1 and Cdc42 to mediate host-cell recovery after bacterial invasion. *Nature* 401, 293-297.
- Fulde, M., van Vorst, K., Zhang, K., Westermann, A.J., Busche, T., Huei, Y.C., Welitschanski, K., Froh, I., Pagelow, D., Plendl, J., *et al.* (2021). SPI2 T3SS effectors facilitate enterocyte apical to basolateral transmigration of *Salmonella*-containing vacuoles in vivo. *Gut Microbes* 13, 1973836.
- Furter, M., Sellin, M.E., Hansson, G.C., and Hardt, W.D. (2019). Mucus Architecture and Near-Surface Swimming Affect Distinct *Salmonella* Typhimurium Infection Patterns along the Murine Intestinal Tract. *Cell Rep* 27, 2665-2678 e2663.
- Gal-Mor, O. (2019). Persistent Infection and Long-Term Carriage of Typhoidal and Nontyphoidal Salmonellae. *Clin Microbiol Rev* 32.
- Gal-Mor, O., Suez, J., Elhadad, D., Porwollik, S., Leshem, E., Valinsky, L., McClelland, M., Schwartz, E., and Rahav, G. (2012). Molecular and cellular characterization of a *Salmonella enterica* serovar Paratyphi a outbreak strain and the human immune response to infection. *Clin Vaccine Immunol* 19, 146-156.
- Galan, J.E. (2001). *Salmonella* interactions with host cells: type III secretion at work. *Annu Rev Cell Dev Biol* 17, 53-86.
- Galan, J.E. (2016). Typhoid toxin provides a window into typhoid fever and the biology of *Salmonella* Typhi. *Proc Natl Acad Sci U S A* 113, 6338-6344.
- Galan, J.E., Lara-Tejero, M., Marlovits, T.C., and Wagner, S. (2014). Bacterial type III secretion systems: specialized nanomachines for protein delivery into target cells. *Annu Rev Microbiol* 68, 415-438.
- Galan, J.E., and Wolf-Watz, H. (2006). Protein delivery into eukaryotic cells by type III secretion machines. *Nature* 444, 567-573.
- Garcez, P.P., Loiola, E.C., Madeiro da Costa, R., Higa, L.M., Trindade, P., Delvecchio, R., Nascimento, J.M., Brindeiro, R., Tanuri, A., and Rehen, S.K. (2016). Zika virus impairs growth in human neurospheres and brain organoids. *Science* 352, 816-818.
- Geiger, T., Lara-Tejero, M., Xiong, Y., and Galan, J.E. (2020). Mechanisms of substrate recognition by a typhoid toxin secretion-associated muramidase. *Elife* 9.

- Gerlach, R.G., Claudio, N., Rohde, M., Jackel, D., Wagner, C., and Hensel, M. (2008). Cooperation of *Salmonella* pathogenicity islands 1 and 4 is required to breach epithelial barriers. *Cell Microbiol* 10, 2364-2376.
- Gerlach, R.G., and Hensel, M. (2007). *Salmonella* pathogenicity islands in host specificity, host pathogen-interactions and antibiotics resistance of *Salmonella enterica*. *Berl Munch Tierarztl Wochenschr* 120, 317-327.
- Gerlach, R.G., Jackel, D., Geymeier, N., and Hensel, M. (2007). *Salmonella* pathogenicity island 4-mediated adhesion is coregulated with invasion genes in *Salmonella enterica*. *Infect Immun* 75, 4697-4709.
- Gibani, M.M., Jones, E., Barton, A., Jin, C., Meek, J., Camara, S., Galal, U., Heinz, E., Rosenberg-Hasson, Y., Obermoser, G., *et al.* (2019). Investigation of the role of typhoid toxin in acute typhoid fever in a human challenge model. *Nat Med* 25, 1082-1088.
- Glynn, J.R., Hornick, R.B., Levine, M.M., and Bradley, D.J. (1995). Infecting dose and severity of typhoid: analysis of volunteer data and examination of the influence of the definition of illness used. *Epidemiol Infect* 115, 23-30.
- Godlee, C., Cerny, O., Liu, M., Blundell, S., Gallagher, A.E., Shahin, M., and Holden, D.W. (2022). The *Salmonella* transmembrane effector SteD hijacks AP1-mediated vesicular trafficking for delivery to antigen-loading MHCII compartments. *PLoS Pathog* 18, e1010252.
- Gonzalez-Escobedo, G., and Gunn, J.S. (2013). Gallbladder epithelium as a niche for chronic *Salmonella* carriage. *Infect Immun* 81, 2920-2930.
- Gonzalez-Escobedo, G., Marshall, J.M., and Gunn, J.S. (2011). Chronic and acute infection of the gall bladder by *Salmonella* Typhi: understanding the carrier state. *Nat Rev Microbiol* 9, 9-14.
- Goser, V., Kehl, A., Roder, J., and Hensel, M. (2020). Role of the ESCRT-III complex in controlling integrity of the *Salmonella*-containing vacuole. *Cell Microbiol* 22, e13176.
- Gram, A.M., Wright, J.A., Pickering, R.J., Lam, N.L., Booty, L.M., Webster, S.J., and Bryant, C.E. (2021). *Salmonella* Flagellin Activates NAIP/NLRC4 and Canonical NLRP3 Inflammasomes in Human Macrophages. *J Immunol* 206, 631-640.
- Guiney, D.G., Fang, F.C., Krause, M., Libby, S., Buchmeier, N.A., and Fierer, J. (1995). Biology and clinical significance of virulence plasmids in *Salmonella* serovars. *Clin Infect Dis* 21 Suppl 2, S146-151.
- Guiney, D.G., and Lesnick, M. (2005). Targeting of the actin cytoskeleton during infection by *Salmonella* strains. *Clin Immunol* 114, 248-255.
- Gunn, J.S., Marshall, J.M., Baker, S., Dongol, S., Charles, R.C., and Ryan, E.T. (2014). *Salmonella* chronic carriage: epidemiology, diagnosis, and gallbladder persistence. *Trends Microbiol* 22, 648-655.
- Gunster, R.A., Matthews, S.A., Holden, D.W., and Thurston, T.L.M. (2017). SseK1 and SseK3 Type III Secretion System Effectors Inhibit NF-kappaB Signaling and Necroptotic Cell Death in *Salmonella*-Infected Macrophages. *Infect Immun* 85.
- Haegebarth, A., and Clevers, H. (2009). Wnt signaling, *lgr5*, and stem cells in the intestine and skin. *Am J Pathol* 174, 715-721.
- Haghjoo, E., and Galan, J.E. (2004). *Salmonella typhi* encodes a functional cytolethal distending toxin that is delivered into host cells by a bacterial-internalization pathway. *Proc Natl Acad Sci U S A* 101, 4614-4619.
- Haglund, C.M., and Welch, M.D. (2011). Pathogens and polymers: microbe-host interactions illuminate the cytoskeleton. *J Cell Biol* 195, 7-17.
- Haraga, A., Ohlson, M.B., and Miller, S.I. (2008). Salmonellae interplay with host cells. *Nat Rev Microbiol* 6, 53-66.
- Hart, P.J., O'Shaughnessy, C.M., Siggins, M.K., Bobat, S., Kingsley, R.A., Goulding, D.A., Crump, J.A., Reyburn, H., Micoli, F., Dougan, G., *et al.* (2016). Differential Killing of *Salmonella enterica* Serovar Typhi by Antibodies Targeting Vi and Lipopolysaccharide O:9 Antigen. *PLoS One* 11, e0145945.
- Hautefort, I., Thompson, A., Eriksson-Ygberg, S., Parker, M.L., Lucchini, S., Danino, V., Bongaerts, R.J., Ahmad, N., Rhen, M., and Hinton, J.C. (2008). During infection of epithelial cells *Salmonella enterica* serovar Typhimurium undergoes a time-dependent transcriptional

- adaptation that results in simultaneous expression of three type 3 secretion systems. *Cell Microbiol* 10, 958-984.
- He, Z., Gharaibeh, R.Z., Newsome, R.C., Pope, J.L., Dougherty, M.W., Tomkovich, S., Pons, B., Mirey, G., Vignard, J., Hendrixson, D.R., *et al.* (2019). *Campylobacter jejuni* promotes colorectal tumorigenesis through the action of cytolethal distending toxin. *Gut* 68, 289-300.
- Henry, T., Couillault, C., Rockenfeller, P., Boucrot, E., Dumont, A., Schroeder, N., Hermant, A., Knodler, L.A., Lecine, P., Steele-Mortimer, O., *et al.* (2006). The *Salmonella* effector protein PipB2 is a linker for kinesin-1. *Proc Natl Acad Sci U S A* 103, 13497-13502.
- Hensel, M. (2004). Evolution of pathogenicity islands of *Salmonella enterica*. *Int J Med Microbiol* 294, 95-102.
- Hensel, M., Shea, J.E., Waterman, S.R., Mundy, R., Nikolaus, T., Banks, G., Vazquez-Torres, A., Gleeson, C., Fang, F.C., and Holden, D.W. (1998). Genes encoding putative effector proteins of the type III secretion system of *Salmonella* pathogenicity island 2 are required for bacterial virulence and proliferation in macrophages. *Mol Microbiol* 30, 163-174.
- Heo, I., Dutta, D., Schaefer, D.A., Iakobachvili, N., Artegiani, B., Sachs, N., Boonekamp, K.E., Bowden, G., Hendrickx, A.P.A., Willems, R.J.L., *et al.* (2018). Modelling *Cryptosporidium* infection in human small intestinal and lung organoids. *Nat Microbiol* 3, 814-823.
- Hindle, Z., Chatfield, S.N., Phillimore, J., Bentley, M., Johnson, J., Cosgrove, C.A., Ghaem-Maghani, M., Sexton, A., Khan, M., Brennan, F.R., *et al.* (2002). Characterization of *Salmonella enterica* derivatives harboring defined *aroC* and *Salmonella* pathogenicity island 2 type III secretion system (*ssaV*) mutations by immunization of healthy volunteers. *Infect Immun* 70, 3457-3467.
- Hirose, K., Ezaki, T., Miyake, M., Li, T., Khan, A.Q., Kawamura, Y., Yokoyama, H., and Takami, T. (1997). Survival of Vi-capsulated and Vi-deleted *Salmonella typhi* strains in cultured macrophage expressing different levels of CD14 antigen. *FEMS Microbiol Lett* 147, 259-265.
- Hiyoshi, H., Tiffany, C.R., Bronner, D.N., and Baumler, A.J. (2018a). Typhoidal *Salmonella* serovars: ecological opportunity and the evolution of a new pathovar. *FEMS Microbiol Rev* 42, 527-541.
- Hiyoshi, H., Wangdi, T., Lock, G., Saechao, C., Raffatellu, M., Cobb, B.A., and Baumler, A.J. (2018b). Mechanisms to Evade the Phagocyte Respiratory Burst Arose by Convergent Evolution in Typhoidal *Salmonella* Serovars. *Cell Rep* 22, 1787-1797.
- Ho, T.D., Figueroa-Bossi, N., Wang, M., Uzzau, S., Bossi, L., and Slauch, J.M. (2002). Identification of GtgE, a novel virulence factor encoded on the Gifsy-2 bacteriophage of *Salmonella enterica* serovar Typhimurium. *J Bacteriol* 184, 5234-5239.
- Hofer, M., and Lutolf, M.P. (2021). Engineering organoids. *Nat Rev Mater* 6, 402-420.
- Hoffman, P.S. (1997). Invasion of eukaryotic cells by *Legionella pneumophila*: A common strategy for all hosts? *Can J Infect Dis* 8, 139-146.
- Holt, K.E., Thomson, N.R., Wain, J., Langridge, G.C., Hasan, R., Bhutta, Z.A., Quail, M.A., Norbertczak, H., Walker, D., Simmonds, M., *et al.* (2009). Pseudogene accumulation in the evolutionary histories of *Salmonella enterica* serovars Paratyphi A and Typhi. *BMC Genomics* 10, 36.
- Hornick, R.B., Greisman, S.E., Woodward, T.E., DuPont, H.L., Dawkins, A.T., and Snyder, M.J. (1970a). Typhoid fever: pathogenesis and immunologic control. *N Engl J Med* 283, 686-691.
- Hornick, R.B., Greisman, S.E., Woodward, T.E., DuPont, H.L., Dawkins, A.T., and Snyder, M.J. (1970b). Typhoid fever: pathogenesis and immunologic control. 2. *N Engl J Med* 283, 739-746.
- Hu, X., Chen, Z., Xiong, K., Wang, J., Rao, X., and Cong, Y. (2017). Vi capsular polysaccharide: Synthesis, virulence, and application. *Crit Rev Microbiol* 43, 440-452.
- Isberg, R.R., and Falkow, S. (1985). A single genetic locus encoded by *Yersinia pseudotuberculosis* permits invasion of cultured animal cells by *Escherichia coli* K-12. *Nature* 317, 262-264.
- Isberg, R.R., and Leong, J.M. (1990). Multiple beta 1 chain integrins are receptors for invasin, a protein that promotes bacterial penetration into mammalian cells. *Cell* 60, 861-871.
- Isberg, R.R., Voorhis, D.L., and Falkow, S. (1987). Identification of invasin: a protein that allows enteric bacteria to penetrate cultured mammalian cells. *Cell* 50, 769-778.



- Janis, C., Grant, A.J., McKinley, T.J., Morgan, F.J., John, V.F., Houghton, J., Kingsley, R.A., Dougan, G., and Mastroeni, P. (2011). In vivo regulation of the Vi antigen in *Salmonella* and induction of immune responses with an in vivo-inducible promoter. *Infect Immun* 79, 2481-2488.
- Jennings, E., Thurston, T.L.M., and Holden, D.W. (2017). *Salmonella* SPI-2 Type III Secretion System Effectors: Molecular Mechanisms And Physiological Consequences. *Cell Host Microbe* 22, 217-231.
- Jepson, M.A., and Clark, M.A. (1998). Studying M cells and their role in infection. *Trends Microbiol* 6, 359-365.
- Jepson, M.A., and Clark, M.A. (2001). The role of M cells in *Salmonella* infection. *Microbes Infect* 3, 1183-1190.
- Johansson, M.E., and Hansson, G.C. (2016). Immunological aspects of intestinal mucus and mucins. *Nat Rev Immunol* 16, 639-649.
- Johnson, R., Byrne, A., Berger, C.N., Klemm, E., Crepin, V.F., Dougan, G., and Frankel, G. (2017). The Type III Secretion System Effector SptP of *Salmonella enterica* Serovar Typhi. *J Bacteriol* 199.
- Johnson, R., Mylona, E., and Frankel, G. (2018). Typhoidal *Salmonella*: Distinctive virulence factors and pathogenesis. *Cell Microbiol* 20, e12939.
- Kamanova, J., Sun, H., Lara-Tejero, M., and Galan, J.E. (2016). The *Salmonella* Effector Protein SopA Modulates Innate Immune Responses by Targeting TRIM E3 Ligase Family Members. *PLoS Pathog* 12, e1005552.
- Kaniga, K., Tucker, S., Trollinger, D., and Galan, J.E. (1995). Homologs of the Shigella IpaB and IpaC invasins are required for *Salmonella typhimurium* entry into cultured epithelial cells. *J Bacteriol* 177, 3965-3971.
- Kaniga, K., Uralil, J., Bliska, J.B., and Galan, J.E. (1996). A secreted protein tyrosine phosphatase with modular effector domains in the bacterial pathogen *Salmonella typhimurium*. *Mol Microbiol* 21, 633-641.
- Karlinsey, J.E., Stepien, T.A., Mayho, M., Singletary, L.A., Bingham-Ramos, L.K., Brehm, M.A., Greiner, D.L., Shultz, L.D., Gallagher, L.A., Bawn, M., et al. (2019). Genome-wide Analysis of *Salmonella enterica* serovar Typhi in Humanized Mice Reveals Key Virulence Features. *Cell Host Microbe* 26, 426-434 e426.
- Kellermann, M., Scharte, F., and Hensel, M. (2021). Manipulation of Host Cell Organelles by Intracellular Pathogens. *Int J Mol Sci* 22.
- Khan, M.I., Soofi, S.B., Ochiai, R.L., Khan, M.J., Sahito, S.M., Habib, M.A., Puri, M.K., Von Seidlein, L., Park, J.K., You, Y.A., et al. (2012). Epidemiology, clinical presentation, and patterns of drug resistance of *Salmonella* Typhi in Karachi, Pakistan. *J Infect Dev Ctries* 6, 704-714.
- Kim, J., Koo, B.K., and Knoblich, J.A. (2020). Human organoids: model systems for human biology and medicine. *Nat Rev Mol Cell Biol* 21, 571-584.
- Knodler, L.A. (2015). *Salmonella enterica*: living a double life in epithelial cells. *Curr Opin Microbiol* 23, 23-31.
- Knodler, L.A., Finlay, B.B., and Steele-Mortimer, O. (2005). The *Salmonella* effector protein SopB protects epithelial cells from apoptosis by sustained activation of Akt. *J Biol Chem* 280, 9058-9064.
- Knodler, L.A., Nair, V., and Steele-Mortimer, O. (2014). Quantitative assessment of cytosolic *Salmonella* in epithelial cells. *PLoS One* 9, e84681.
- Knodler, L.A., Vallance, B.A., Celli, J., Winfree, S., Hansen, B., Montero, M., and Steele-Mortimer, O. (2010). Dissemination of invasive *Salmonella* via bacterial-induced extrusion of mucosal epithelia. *Proc Natl Acad Sci U S A* 107, 17733-17738.
- Kocks, C., Marchand, J.B., Gouin, E., d'Hauteville, H., Sansonetti, P.J., Carlier, M.F., and Cossart, P. (1995). The unrelated surface proteins ActA of *Listeria monocytogenes* and IcsA of *Shigella flexneri* are sufficient to confer actin-based motility on *Listeria innocua* and *Escherichia coli* respectively. *Mol Microbiol* 18, 413-423.
- Kreibich, S., Emmenlauer, M., Fredlund, J., Ramo, P., Munz, C., Dehio, C., Enninga, J., and Hardt, W.D. (2015). Autophagy Proteins Promote Repair of Endosomal Membranes Damaged by the *Salmonella* Type Three Secretion System 1. *Cell Host Microbe* 18, 527-537.

- Krieger, V., Liebl, D., Zhang, Y., Rajashekar, R., Chlanda, P., Giesker, K., Chikkaballi, D., and Hensel, M. (2014). Reorganization of the endosomal system in *Salmonella*-infected cells: the ultrastructure of *Salmonella*-induced tubular compartments. *PLoS Pathog* 10, e1004374.
- Kucharzik, T., Lugerling, N., Rautenberg, K., Lugerling, A., Schmidt, M.A., Stoll, R., and Domschke, W. (2000). Role of M cells in intestinal barrier function. *Ann N Y Acad Sci* 915, 171-183.
- Kumar, M.S., and Philominathan, P. (2010). The physics of flagellar motion of *E. coli* during chemotaxis. *Biophys Rev* 2, 13-20.
- Lamers, M.M., van der Vaart, J., Knoops, K., Riesebosch, S., Breugem, T.I., Mykytyn, A.Z., Beumer, J., Schipper, D., Bezstarosti, K., Koopman, C.D., *et al.* (2021). An organoid-derived bronchioalveolar model for SARS-CoV-2 infection of human alveolar type II-like cells. *EMBO J* 40, e105912.
- Langridge, G.C. (2010). Metabolic capability in host-restricted serovars of *Salmonella enterica*. In Darwin College (University of Cambridge).
- Lara-Tejero, M., Kato, J., Wagner, S., Liu, X., and Galan, J.E. (2011). A sorting platform determines the order of protein secretion in bacterial type III systems. *Science* 331, 1188-1191.
- Lau, N., Haerberle, A.L., O'Keeffe, B.J., Latomanski, E.A., Celli, J., Newton, H.J., and Knodler, L.A. (2019). SopF, a phosphoinositide binding effector, promotes the stability of the nascent *Salmonella*-containing vacuole. *PLoS Pathog* 15, e1007959.
- Lawhon, S.D., Maurer, R., Suyemoto, M., and Altier, C. (2002). Intestinal short-chain fatty acids alter *Salmonella typhimurium* invasion gene expression and virulence through BarA/SirA. *Mol Microbiol* 46, 1451-1464.
- Lee, S., Yang, Y.A., Milano, S.K., Nguyen, T., Ahn, C., Sim, J.H., Thompson, A.J., Hillpot, E.C., Yoo, G., Paulson, J.C., *et al.* (2020). *Salmonella* Typhoid Toxin PltB Subunit and Its Non-typhoidal *Salmonella* Ortholog Confer Differential Host Adaptation and Virulence. *Cell Host Microbe* 27, 937-949 e936.
- Lemarignier, M., and Pizarro-Cerda, J. (2020). Autophagy and Intracellular Membrane Trafficking Subversion by Pathogenic Yersinia Species. *Biomolecules* 10.
- Leslie, J.L., Huang, S., Opp, J.S., Nagy, M.S., Kobayashi, M., Young, V.B., and Spence, J.R. (2015). Persistence and toxin production by *Clostridium difficile* within human intestinal organoids result in disruption of epithelial paracellular barrier function. *Infect Immun* 83, 138-145.
- Levine, M.M., Ferreccio, C., Black, R.E., Lagos, R., San Martin, O., and Blackwelder, W.C. (2007). Ty21a live oral typhoid vaccine and prevention of paratyphoid fever caused by *Salmonella enterica* Serovar Paratyphi B. *Clin Infect Dis* 45 Suppl 1, S24-28.
- Liao, A.P., Petrof, E.O., Kuppireddi, S., Zhao, Y., Xia, Y., Claud, E.C., and Sun, J. (2008). *Salmonella* type III effector AvrA stabilizes cell tight junctions to inhibit inflammation in intestinal epithelial cells. *PLoS One* 3, e2369.
- Liss, V., and Hensel, M. (2015). Take the tube: remodelling of the endosomal system by intracellular *Salmonella enterica*. *Cell Microbiol* 17, 639-647.
- Liss, V., Swart, A.L., Kehl, A., Hermanns, N., Zhang, Y., Chikkaballi, D., Bohles, N., Deiwick, J., and Hensel, M. (2017). *Salmonella enterica* Remodels the Host Cell Endosomal System for Efficient Intravacuolar Nutrition. *Cell Host Microbe* 21, 390-402.
- Liu, Y., Mi, Y., Mueller, T., Kreibich, S., Williams, E.G., Van Drogen, A., Borel, C., Frank, M., Germain, P.L., Bludau, I., *et al.* (2019). Multi-omic measurements of heterogeneity in HeLa cells across laboratories. *Nat Biotechnol* 37, 314-322.
- Liu, Y., Yu, K., Zhou, F., Ding, T., Yang, Y., Hu, M., and Liu, X. (2017). Quantitative Proteomics Charts the Landscape of *Salmonella* Carbon Metabolism within Host Epithelial Cells. *J Proteome Res* 16, 788-797.
- Liu, Y., Zhang, Q., Hu, M., Yu, K., Fu, J., Zhou, F., and Liu, X. (2015). Proteomic Analyses of Intracellular *Salmonella enterica* Serovar Typhimurium Reveal Extensive Bacterial Adaptations to Infected Host Epithelial Cells. *Infect Immun* 83, 2897-2906.
- Lober, S., Jackel, D., Kaiser, N., and Hensel, M. (2006). Regulation of *Salmonella* pathogenicity island 2 genes by independent environmental signals. *Int J Med Microbiol* 296, 435-447.
- Lopez-Jimenez, A.T., Cardenal-Munoz, E., Leuba, F., Gerstenmaier, L., Barisch, C., Hagedorn, M., King, J.S., and Soldati, T. (2018). The ESCRT and autophagy machineries cooperate to repair

- ESX-1-dependent damage at the *Mycobacterium*-containing vacuole but have opposite impact on containing the infection. *PLoS Pathog* 14, e1007501.
- Lorkowski, M., Felipe-Lopez, A., Danzer, C.A., Hansmeier, N., and Hensel, M. (2014). *Salmonella enterica* invasion of polarized epithelial cells is a highly cooperative effort. *Infect Immun* 82, 2657-2667.
- Lou, L., Zhang, P., Piao, R., and Wang, Y. (2019). *Salmonella* Pathogenicity Island 1 (SPI-1) and Its Complex Regulatory Network. *Front Cell Infect Microbiol* 9, 270.
- Malik-Kale, P., Winfree, S., and Steele-Mortimer, O. (2012). The bimodal lifestyle of intracellular *Salmonella* in epithelial cells: replication in the cytosol obscures defects in vacuolar replication. *PLoS One* 7, e38732.
- Mathur, R., Oh, H., Zhang, D., Park, S.G., Seo, J., Koblansky, A., Hayden, M.S., and Ghosh, S. (2012). A mouse model of *Salmonella typhi* infection. *Cell* 151, 590-602.
- Mazurkiewicz, P., Thomas, J., Thompson, J.A., Liu, M., Arbibe, L., Sansonetti, P., and Holden, D.W. (2008). SpvC is a *Salmonella* effector with phosphothreonine lyase activity on host mitogen-activated protein kinases. *Mol Microbiol* 67, 1371-1383.
- McClelland, M., Sanderson, K.E., Clifton, S.W., Latreille, P., Porwollik, S., Sabo, A., Meyer, R., Bieri, T., Ozersky, P., McLellan, M., *et al.* (2004). Comparison of genome degradation in Paratyphi A and Typhi, human-restricted serovars of *Salmonella enterica* that cause typhoid. *Nat Genet* 36, 1268-1274.
- McLaughlin, K.J., Nash, R.P., and Redinbo, M.R. (2014). Unique helicase determinants in the essential conjugative TraI factor from *Salmonella enterica* serovar Typhimurium plasmid pCU1. *J Bacteriol* 196, 3082-3090.
- Mesquita, F.S., Thomas, M., Sachse, M., Santos, A.J., Figueira, R., and Holden, D.W. (2012). The *Salmonella* deubiquitinase SseL inhibits selective autophagy of cytosolic aggregates. *PLoS Pathog* 8, e1002743.
- Miller, R.A., Betteken, M.I., Guo, X., Altier, C., Duhamel, G.E., and Wiedmann, M. (2018). The Typhoid Toxin Produced by the Nontyphoidal *Salmonella enterica* Serotype Javiana Is Required for Induction of a DNA Damage Response In Vitro and Systemic Spread In Vivo. *mBio* 9.
- Miller, R.A., and Wiedmann, M. (2016). The Cytolethal Distending Toxin Produced by Nontyphoidal *Salmonella* Serotypes Javiana, Montevideo, Oranienburg, and Mississippi Induces DNA Damage in a Manner Similar to That of Serotype Typhi. *MBio* 7.
- Mills, D.M., Bajaj, V., and Lee, C.A. (1995). A 40 kb chromosomal fragment encoding *Salmonella typhimurium* invasion genes is absent from the corresponding region of the *Escherichia coli* K-12 chromosome. *Mol Microbiol* 15, 749-759.
- Mirold, S., Rabsch, W., Rohde, M., Stender, S., Tschape, H., Russmann, H., Igwe, E., and Hardt, W.D. (1999). Isolation of a temperate bacteriophage encoding the type III effector protein SopE from an epidemic *Salmonella typhimurium* strain. *Proc Natl Acad Sci U S A* 96, 9845-9850.
- Misselwitz, B., Barrett, N., Kreibich, S., Vonaesch, P., Andritschke, D., Rout, S., Weidner, K., Sormaz, M., Songhet, P., Horvath, P., *et al.* (2012). Near surface swimming of *Salmonella Typhimurium* explains target-site selection and cooperative invasion. *PLoS Pathog* 8, e1002810.
- Moran, G.W., Leslie, F.C., Levison, S.E., Worthington, J., and McLaughlin, J.T. (2008). Enteroendocrine cells: neglected players in gastrointestinal disorders? *Therap Adv Gastroenterol* 1, 51-60.
- Moreau, K., Lacas-Gervais, S., Fujita, N., Sebbane, F., Yoshimori, T., Simonet, M., and Lafont, F. (2010). Autophagosomes can support *Yersinia pseudotuberculosis* replication in macrophages. *Cell Microbiol* 12, 1108-1123.
- Niekamp, P., Scharte, F., Sokoya, T., Vittadello, L., Kim, Y., Deng, Y., Sudhoff, E., Hilderink, A., Imlau, M., Clarke, C.J., *et al.* (2022). Ca(2+)-activated sphingomyelin scrambling and turnover mediate ESCRT-independent lysosomal repair. *Nat Commun* 13, 1875.
- Noel, G., Baetz, N.W., Staab, J.F., Donowitz, M., Kovbasnjuk, O., Pasetti, M.F., and Zachos, N.C. (2017). A primary human macrophage-enteroid co-culture model to investigate mucosal gut physiology and host-pathogen interactions. *Sci Rep* 7, 45270.

- Nord, A.L., Biquet-Bisquert, A., Abkarian, M., Pigaglio, T., Seduk, F., Magalon, A., and Pedaci, F. (2022). Dynamic stiffening of the flagellar hook. *Nat Commun* 13, 2925.
- Noster, J., Chao, T.C., Sander, N., Schulte, M., Reuter, T., Hansmeier, N., and Hensel, M. (2019). Proteomics of intracellular *Salmonella enterica* reveals roles of *Salmonella* pathogenicity island 2 in metabolism and antioxidant defense. *PLoS Pathog* 15, e1007741.
- Nunez-Hernandez, C., Tierrez, A., Ortega, A.D., Pucciarelli, M.G., Godoy, M., Eisman, B., Casadesus, J., and Garcia-del Portillo, F. (2013). Genome expression analysis of nonproliferating intracellular *Salmonella enterica* serovar Typhimurium unravels an acid pH-dependent PhoP-PhoQ response essential for dormancy. *Infect Immun* 81, 154-165.
- Ochman, H., Soncini, F.C., Solomon, F., and Groisman, E.A. (1996). Identification of a pathogenicity island required for *Salmonella* survival in host cells. *Proc Natl Acad Sci U S A* 93, 7800-7804.
- Ogawa, M., Mimuro, H., Yoshikawa, Y., Ashida, H., and Sasakawa, C. (2011). Manipulation of autophagy by bacteria for their own benefit. *Microbiol Immunol* 55, 459-471.
- Ogawa, M., Yoshimori, T., Suzuki, T., Sagara, H., Mizushima, N., and Sasakawa, C. (2005). Escape of intracellular *Shigella* from autophagy. *Science* 307, 727-731.
- Oliva, G., Sahr, T., and Buchrieser, C. (2018). The Life Cycle of *L. pneumophila*: Cellular Differentiation Is Linked to Virulence and Metabolism. *Front Cell Infect Microbiol* 8, 3.
- Otten, E.G., Werner, E., Crespillo-Casado, A., Boyle, K.B., Dharamdasani, V., Pathe, C., Santhanam, B., and Randow, F. (2021). Ubiquitylation of lipopolysaccharide by RNF213 during bacterial infection. *Nature* 594, 111-116.
- Pakkanen, S.H., Kantele, J.M., and Kantele, A. (2012). Cross-reactive gut-directed immune response against *Salmonella enterica* serovar Paratyphi A and B in typhoid fever and after oral Ty21a typhoid vaccination. *Vaccine* 30, 6047-6053.
- Pakkanen, S.H., Kantele, J.M., and Kantele, A. (2014). Cross-reactive immune response induced by the Vi capsular polysaccharide typhoid vaccine against *Salmonella* Paratyphi strains. *Scand J Immunol* 79, 222-229.
- Parkhill, J., Dougan, G., James, K.D., Thomson, N.R., Pickard, D., Wain, J., Churcher, C., Mungall, K.L., Bentley, S.D., Holden, M.T., *et al.* (2001). Complete genome sequence of a multiple drug resistant *Salmonella enterica* serovar Typhi CT18. *Nature* 413, 848-852.
- Pickard, D., Li, J., Roberts, M., Maskell, D., Hone, D., Levine, M., Dougan, G., and Chatfield, S. (1994). Characterization of defined *ompR* mutants of *Salmonella typhi*: *ompR* is involved in the regulation of Vi polysaccharide expression. *Infect Immun* 62, 3984-3993.
- Pickard, D., Wain, J., Baker, S., Line, A., Chohan, S., Fookes, M., Barron, A., Gaora, P.O., Chabalgoity, J.A., Thanky, N., *et al.* (2003). Composition, acquisition, and distribution of the Vi exopolysaccharide-encoding *Salmonella enterica* pathogenicity island SPI-7. *J Bacteriol* 185, 5055-5065.
- Prouty, A.M., and Gunn, J.S. (2000). *Salmonella enterica* serovar typhimurium invasion is repressed in the presence of bile. *Infect Immun* 68, 6763-6769.
- Prouty, A.M., Schwesinger, W.H., and Gunn, J.S. (2002). Biofilm formation and interaction with the surfaces of gallstones by *Salmonella* spp. *Infect Immun* 70, 2640-2649.
- Pui, C.F., Wong, W. C., Chai, L. C., Tunung, R., Jeyaletchumi, P., Noor Hidayah, M. S., Ubong, A., Farinazleen, M. G., Cheah, Y. K. and Son, R (2011). *Salmonella*: A foodborne pathogen. *International Food Research Journal* 18, 465-473.
- Raffatellu, M., Wilson, R.P., Chessa, D., Andrews-Polymenis, H., Tran, Q.T., Lawhon, S., Khare, S., Adams, L.G., and Baumler, A.J. (2005). SipA, SopA, SopB, SopD, and SopE2 contribute to *Salmonella enterica* serotype typhimurium invasion of epithelial cells. *Infect Immun* 73, 146-154.
- Rajashekar, R., Liebl, D., Chikkaballi, D., Liss, V., and Hensel, M. (2014). Live cell imaging reveals novel functions of *Salmonella enterica* SPI2-T3SS effector proteins in remodeling of the host cell endosomal system. *PLoS One* 9, e115423.
- Ramsden, A.E., Holden, D.W., and Mota, L.J. (2007). Membrane dynamics and spatial distribution of *Salmonella*-containing vacuoles. *Trends Microbiol* 15, 516-524.
- Ranganathan, S., Doucet, M., Grassel, C.L., Delaine-Elias, B., Zachos, N.C., and Barry, E.M. (2019). Evaluating *Shigella flexneri* Pathogenesis in the Human Enteroid Model. *Infect Immun* 87.

- Ray, K., Marteyn, B., Sansonetti, P.J., and Tang, C.M. (2009). Life on the inside: the intracellular lifestyle of cytosolic bacteria. *Nat Rev Microbiol* 7, 333-340.
- Reuter, T., Scharte, F., Franzkoch, R., Liss, V., and Hensel, M. (2021). Single cell analyses reveal distinct adaptation of typhoidal and non-typhoidal *Salmonella enterica* serovars to intracellular lifestyle. *PLoS Pathog* 17, e1009319.
- Ribet, D., and Cossart, P. (2015). How bacterial pathogens colonize their hosts and invade deeper tissues. *Microbes Infect* 17, 173-183.
- Rios, A.C., and Clevers, H. (2018). Imaging organoids: a bright future ahead. *Nat Methods* 15, 24-26.
- Roder, J., Felgner, P., and Hensel, M. (2021a). Comprehensive Single Cell Analyses of the Nutritional Environment of Intracellular *Salmonella enterica*. *Front Cell Infect Microbiol* 11, 624650.
- Roder, J., Felgner, P., and Hensel, M. (2021b). Single-cell analyses reveal phosphate availability as critical factor for nutrition of *Salmonella enterica* within mammalian host cells. *Cell Microbiol* 23, e13374.
- Roder, J., and Hensel, M. (2020). Presence of SopE and mode of infection result in increased *Salmonella*-containing vacuole damage and cytosolic release during host cell infection by *Salmonella enterica*. *Cell Microbiol* 22, e13155.
- Rodriguez-Colman, M.J., Schewe, M., Meerlo, M., Stigter, E., Gerrits, J., Pras-Raves, M., Sacchetti, A., Hornsveld, M., Oost, K.C., Snippert, H.J., *et al.* (2017). Interplay between metabolic identities in the intestinal crypt supports stem cell function. *Nature* 543, 424-427.
- Rolando, M., Escoll, P., Nora, T., Botti, J., Boitez, V., Bedia, C., Daniels, C., Abraham, G., Stogios, P.J., Skarina, T., *et al.* (2016). *Legionella pneumophila* SIP-lyase targets host sphingolipid metabolism and restrains autophagy. *Proc Natl Acad Sci U S A* 113, 1901-1906.
- Roodsant, T., Navis, M., Aknouch, I., Renes, I.B., van Elburg, R.M., Pajkrt, D., Wolthers, K.C., Schultsz, C., van der Ark, K.C.H., Sridhar, A., *et al.* (2020). A Human 2D Primary Organoid-Derived Epithelial Monolayer Model to Study Host-Pathogen Interaction in the Small Intestine. *Front Cell Infect Microbiol* 10, 272.
- Ruiz-Albert, J., Yu, X.J., Beuzon, C.R., Blakey, A.N., Galyov, E.E., and Holden, D.W. (2002). Complementary activities of SseJ and SifA regulate dynamics of the *Salmonella typhimurium* vacuolar membrane. *Mol Microbiol* 44, 645-661.
- Sabbagh, S.C., Forest, C.G., Lepage, C., Leclerc, J.M., and Daigle, F. (2010). So similar, yet so different: uncovering distinctive features in the genomes of *Salmonella enterica* serovars Typhimurium and Typhi. *FEMS Microbiol Lett* 305, 1-13.
- Salcedo, S.P., Noursadeghi, M., Cohen, J., and Holden, D.W. (2001). Intracellular replication of *Salmonella typhimurium* strains in specific subsets of splenic macrophages in vivo. *Cell Microbiol* 3, 587-597.
- Sato, T., Vries, R.G., Snippert, H.J., van de Wetering, M., Barker, N., Stange, D.E., van Es, J.H., Abo, A., Kujala, P., Peters, P.J., *et al.* (2009). Single Lgr5 stem cells build crypt-villus structures in vitro without a mesenchymal niche. *Nature* 459, 262-265.
- Schneider, W.R., and Doetsch, R.N. (1974). Effect of viscosity on bacterial motility. *J Bacteriol* 117, 696-701.
- Schreurs, R., Baumdick, M.E., Drewniak, A., and Bunders, M.J. (2021). In vitro co-culture of human intestinal organoids and lamina propria-derived CD4(+) T cells. *STAR Protoc* 2, 100519.
- Schroeder, N., Henry, T., de Chastellier, C., Zhao, W., Guilhon, A.A., Gorvel, J.P., and Meresse, S. (2010). The virulence protein SopD2 regulates membrane dynamics of *Salmonella*-containing vacuoles. *PLoS Pathog* 6, e1001002.
- Schroeder, N., Mota, L.J., and Meresse, S. (2011). *Salmonella*-induced tubular networks. *Trends Microbiol* 19, 268-277.
- Schulte, M., and Hensel, M. (2016). Models of intestinal infection by *Salmonella enterica*: introduction of a new neonate mouse model. *F1000Res* 5.
- Schulte, M., Olschewski, K., and Hensel, M. (2021). The protected physiological state of intracellular *Salmonella enterica* persists reduces host cell-imposed stress. *Commun Biol* 4, 520.
- Sellin, M.E., Muller, A.A., Felmy, B., Dolowschiak, T., Diard, M., Tardivel, A., Maslowski, K.M., and Hardt, W.D. (2014). Epithelium-intrinsic NAIP/NLRC4 inflammasome drives infected enterocyte expulsion to restrict *Salmonella* replication in the intestinal mucosa. *Cell Host Microbe* 16, 237-248.

- Sepe, L.P., Hartl, K., Iftekhar, A., Berger, H., Kumar, N., Goosmann, C., Chopra, S., Schmidt, S.C., Gurumurthy, R.K., Meyer, T.F., *et al.* (2020). Genotoxic Effect of *Salmonella* Paratyphi A Infection on Human Primary Gallbladder Cells. *mBio* *11*.
- Shea, J.E., Hensel, M., Gleeson, C., and Holden, D.W. (1996). Identification of a virulence locus encoding a second type III secretion system in *Salmonella* typhimurium. *Proc Natl Acad Sci U S A* *93*, 2593-2597.
- Shivaprasad, H.L. (2000). Fowl typhoid and pullorum disease. *Rev Sci Tech* *19*, 405-424.
- Smith, A.C., Cirulis, J.T., Casanova, J.E., Scidmore, M.A., and Brumell, J.H. (2005). Interaction of the *Salmonella*-containing vacuole with the endocytic recycling system. *J Biol Chem* *280*, 24634-24641.
- Smith, A.C., Heo, W.D., Braun, V., Jiang, X., Macrae, C., Casanova, J.E., Scidmore, M.A., Grinstein, S., Meyer, T., and Brumell, J.H. (2007). A network of Rab GTPases controls phagosome maturation and is modulated by *Salmonella enterica* serovar Typhimurium. *J Cell Biol* *176*, 263-268.
- Snoeck, V., Goddeeris, B., and Cox, E. (2005). The role of enterocytes in the intestinal barrier function and antigen uptake. *Microbes Infect* *7*, 997-1004.
- Song, J., Gao, X., and Galan, J.E. (2013). Structure and function of the *Salmonella* Typhi chimaeric A(2)B(5) typhoid toxin. *Nature* *499*, 350-354.
- Spano, S., and Galan, J.E. (2012). A Rab32-dependent pathway contributes to *Salmonella* typhi host restriction. *Science* *338*, 960-963.
- Spano, S., Liu, X., and Galan, J.E. (2011). Proteolytic targeting of Rab29 by an effector protein distinguishes the intracellular compartments of human-adapted and broad-host *Salmonella*. *Proc Natl Acad Sci U S A* *108*, 18418-18423.
- Spano, S., Ugalde, J.E., and Galan, J.E. (2008). Delivery of a *Salmonella* Typhi exotoxin from a host intracellular compartment. *Cell Host Microbe* *3*, 30-38.
- Spellberg, B., and Edwards, J.E., Jr. (2001). Type 1/Type 2 immunity in infectious diseases. *Clin Infect Dis* *32*, 76-102.
- Spinosa, M.R., Progidia, C., Tala, A., Cogli, L., Alifano, P., and Bucci, C. (2007). The *Neisseria meningitidis* capsule is important for intracellular survival in human cells. *Infect Immun* *75*, 3594-3603.
- Spring, I., Martinez, V.A., Hotz, C., Schwarz-Linek, J., Grady, K.L., Nava-Sedeno, J.M., Vissers, T., Singer, H.M., Rohde, M., Bourquin, C., *et al.* (2018). Hook length of the bacterial flagellum is optimized for maximal stability of the flagellar bundle. *PLoS Biol* *16*, e2006989.
- Stecher, B., Hapfelmeier, S., Muller, C., Kremer, M., Stallmach, T., and Hardt, W.D. (2004). Flagella and chemotaxis are required for efficient induction of *Salmonella enterica* serovar Typhimurium colitis in streptomycin-pretreated mice. *Infect Immun* *72*, 4138-4150.
- Steele-Mortimer, O., Meresse, S., Gorvel, J.P., Toh, B.H., and Finlay, B.B. (1999). Biogenesis of *Salmonella* typhimurium-containing vacuoles in epithelial cells involves interactions with the early endocytic pathway. *Cell Microbiol* *1*, 33-49.
- Stein, M.A., Leung, K.Y., Zwick, M., Garcia-del Portillo, F., and Finlay, B.B. (1996). Identification of a *Salmonella* virulence gene required for formation of filamentous structures containing lysosomal membrane glycoproteins within epithelial cells. *Mol Microbiol* *20*, 151-164.
- Straley, S.C., and Harmon, P.A. (1984). *Yersinia pestis* grows within phagolysosomes in mouse peritoneal macrophages. *Infect Immun* *45*, 655-659.
- Sun, H., Kamanova, J., Lara-Tejero, M., and Galan, J.E. (2016). A Family of *Salmonella* Type III Secretion Effector Proteins Selectively Targets the NF-kappaB Signaling Pathway to Preserve Host Homeostasis. *PLoS Pathog* *12*, e1005484.
- Taelman, J., Diaz, M., and Guiu, J. (2022). Human Intestinal Organoids: Promise and Challenge. *Front Cell Dev Biol* *10*, 854740.
- Tartera, C., and Metcalf, E.S. (1993). Osmolarity and growth phase overlap in regulation of *Salmonella* typhi adherence to and invasion of human intestinal cells. *Infect Immun* *61*, 3084-3089.
- Tattoli, I., Philpott, D.J., and Girardin, S.E. (2012). The bacterial and cellular determinants controlling the recruitment of mTOR to the *Salmonella*-containing vacuole. *Biol Open* *1*, 1215-1225.

- Thiennimitr, P., Winter, S.E., Winter, M.G., Xavier, M.N., Tolstikov, V., Huseby, D.L., Sterzenbach, T., Tsolis, R.M., Roth, J.R., and Baumber, A.J. (2011). Intestinal inflammation allows *Salmonella* to use ethanolamine to compete with the microbiota. *Proc Natl Acad Sci U S A* *108*, 17480-17485.
- Thomson, N.R., Clayton, D.J., Windhorst, D., Vernikos, G., Davidson, S., Churcher, C., Quail, M.A., Stevens, M., Jones, M.A., Watson, M., *et al.* (2008). Comparative genome analysis of *Salmonella* Enteritidis PT4 and *Salmonella* Gallinarum 287/91 provides insights into evolutionary and host adaptation pathways. *Genome Res* *18*, 1624-1637.
- Thurston, T.L., Wandel, M.P., von Muhlinen, N., Foeglein, A., and Randow, F. (2012). Galectin 8 targets damaged vesicles for autophagy to defend cells against bacterial invasion. *Nature* *482*, 414-418.
- Trombert, A.N., Berrocal, L., Fuentes, J.A., and Mora, G.C. (2010). *S. Typhimurium sseJ* gene decreases the *S. Typhi* cytotoxicity toward cultured epithelial cells. *BMC Microbiol* *10*, 312.
- Trombert, A.N., Rodas, P.I., and Mora, G.C. (2011). Reduced invasion to human epithelial cell lines of *Salmonella enterica* serovar Typhi carrying *S. Typhimurium sopD2*. *FEMS Microbiol Lett* *322*, 150-156.
- Tse, C.M., In, J.G., Yin, J., Donowitz, M., Doucet, M., Foulke-Abel, J., Ruiz-Perez, F., Nataro, J.P., Zachos, N.C., Kaper, J.B., *et al.* (2018). Enterohemorrhagic *E. coli* (EHEC)-Secreted Serine Protease EspP Stimulates Electrogenic Ion Transport in Human Colonoid Monolayers. *Toxins (Basel)* *10*.
- Tsolis, R.M., Young, G.M., Solnick, J.V., and Baumber, A.J. (2008). From bench to bedside: stealth of enteroinvasive pathogens. *Nat Rev Microbiol* *6*, 883-892.
- Utley, M., Franklin, D.P., Krogfelt, K.A., Laux, D.C., and Cohen, P.S. (1998). A *Salmonella typhimurium* mutant unable to utilize fatty acids and citrate is avirulent and immunogenic in mice. *FEMS Microbiol Lett* *163*, 129-134.
- von Moltke, J., Ji, M., Liang, H.E., and Locksley, R.M. (2016). Tuft-cell-derived IL-25 regulates an intestinal ILC2-epithelial response circuit. *Nature* *529*, 221-225.
- Wagner, C., and Hensel, M. (2011). Adhesive mechanisms of *Salmonella enterica*. *Adv Exp Med Biol* *715*, 17-34.
- Walawalkar, Y.D., Vaidya, Y., and Nayak, V. (2016). Response of *Salmonella Typhi* to bile-generated oxidative stress: implication of quorum sensing and persister cell populations. *Pathog Dis* *74*.
- Wandel, M.P., Kim, B.H., Park, E.S., Boyle, K.B., Nayak, K., Lagrange, B., Herod, A., Henry, T., Zilbauer, M., Rohde, J., *et al.* (2020). Guanylate-binding proteins convert cytosolic bacteria into caspase-4 signaling platforms. *Nat Immunol* *21*, 880-891.
- Welch, M.D., and Way, M. (2013). Arp2/3-mediated actin-based motility: a tail of pathogen abuse. *Cell Host Microbe* *14*, 242-255.
- WHO (2008). The global burden of disease: 2004 update.
- WHO (2014). Antimicrobial resistance: global report on surveillance 2014.
- WHO (2018a). *Salmonella* (non-typhoidal) - Fact sheet.
- WHO (2018b). Typhoid - Fact sheet.
- Wong, K.K., McClelland, M., Stillwell, L.C., Sisk, E.C., Thurston, S.J., and Saffer, J.D. (1998). Identification and sequence analysis of a 27-kilobase chromosomal fragment containing a *Salmonella* pathogenicity island located at 92 minutes on the chromosome map of *Salmonella enterica* serovar typhimurium LT2. *Infect Immun* *66*, 3365-3371.
- Wood, M.W., Jones, M.A., Watson, P.R., Siber, A.M., McCormick, B.A., Hedges, S., Rosqvist, R., Wallis, T.S., and Galyov, E.E. (2000). The secreted effector protein of *Salmonella dublin*, SopA, is translocated into eukaryotic cells and influences the induction of enteritis. *Cell Microbiol* *2*, 293-303.
- Xing, Z., Gauldie, J., Cox, G., Baumann, H., Jordana, M., Lei, X.F., and Achong, M.K. (1998). IL-6 is an antiinflammatory cytokine required for controlling local or systemic acute inflammatory responses. *J Clin Invest* *101*, 311-320.
- Xu, Y., Zhou, P., Cheng, S., Lu, Q., Nowak, K., Hopp, A.K., Li, L., Shi, X., Zhou, Z., Gao, W., *et al.* (2019). A Bacterial Effector Reveals the V-ATPase-ATG16L1 Axis that Initiates Xenophagy. *Cell* *178*, 552-566 e520.

- Yang, Z., Soderholm, A., Lung, T.W., Giogha, C., Hill, M.M., Brown, N.F., Hartland, E., and Teasdale, R.D. (2015). SseK3 Is a *Salmonella* Effector That Binds TRIM32 and Modulates the Host's NF-kappaB Signalling Activity. *PLoS One* *10*, e0138529.
- Ye, Z., Petrof, E.O., Boone, D., Claud, E.C., and Sun, J. (2007). *Salmonella* effector AvrA regulation of colonic epithelial cell inflammation by deubiquitination. *Am J Pathol* *171*, 882-892.
- Yoshikawa, Y., Ogawa, M., Hain, T., Yoshida, M., Fukumatsu, M., Kim, M., Mimuro, H., Nakagawa, I., Yanagawa, T., Ishii, T., *et al.* (2009). *Listeria monocytogenes* ActA-mediated escape from autophagic recognition. *Nat Cell Biol* *11*, 1233-1240.
- Yu, X.J., Liu, M., and Holden, D.W. (2016). *Salmonella* Effectors SseF and SseG Interact with Mammalian Protein ACBD3 (GCP60) To Anchor *Salmonella*-Containing Vacuoles at the Golgi Network. *MBio* *7*.
- Zhang, Y., Higashide, W.M., McCormick, B.A., Chen, J., and Zhou, D. (2006). The inflammation-associated *Salmonella* SopA is a HECT-like E3 ubiquitin ligase. *Mol Microbiol* *62*, 786-793.
- Zhou, D., Mooseker, M.S., and Galan, J.E. (1999). An invasion-associated *Salmonella* protein modulates the actin-bundling activity of plastin. *Proc Natl Acad Sci U S A* *96*, 10176-10181.
- Zomer-van Ommen, D.D., Pukin, A.V., Fu, O., Quarles van Ufford, L.H., Janssens, H.M., Beekman, J.M., and Pieters, R.J. (2016). Functional Characterization of Cholera Toxin Inhibitors Using Human Intestinal Organoids. *J Med Chem* *59*, 6968-6972.
- Zoppino, F.C., Militello, R.D., Slavin, I., Alvarez, C., and Colombo, M.I. (2010). Autophagosome formation depends on the small GTPase Rab1 and functional ER exit sites. *Traffic* *11*, 1246-1261.



## VIII. List of Abbreviations

3-MA	3-methyladenine
AdSC	adult stem cells
AHT	anhydrotetracycline
Ap	apical
ATCC	american type culture collection
B1g	bacterial immunoglobulin
Bl	basolateral
BMP	bone morphogenetic protein
Ca <sup>2+</sup>	calcium
CBC	crypt based columnar
Cer	ceramide
CFU	colony forming units
CLEM	correlative light and electron microscopy
CLSM	confocal laser-scanning microscopy
DEG	differently expressed genes
DMEM	Dulbecco's modified Eagles medium
DMSO	dimethyl sulfoxide
EEC	enteroendocrine cells
ENA	European Nucleotide Archive
EqSM	engineered sphingomyelin-binding equinatoxin II
ESCRT	endosomal sorting complex required for transport
FACS	fluorescence-activated cell sorting
Factin	filamentous actin
FC	flow cytometry
FP	fluorescent protein
G3P	sn-Glycerol-3-phosphate
G6P	glucose-6-phosphate
GA	glutaraldehyde
Gal	galectin

## LIST OF ABBREVIATIONS

---

GAP	GTPase-activating protein
GEF	guanine exchange factor
GPN	glycyl-L-phenylalanine 2-naphtylamide
HeLa	Henrietta Lacks
HESI	heated electrospray ionization
HMDS	hexamethyldisilazane
iFCS	inactivated fetal calf serum
IFN- $\gamma$	interferon $\gamma$
IL	interleukin
IM	imaging medium
Inl	internalin
iPSC	induced pluripotent stem cells
IR	infrared
<i>L.m.</i>	<i>Listeria monocytogenes</i>
LAMP1	lysosomal-associated membrane protein 1
LB	Luria-Bertani
LCI	live cell imaging
LCV	<i>Listeria</i> -containing vacuole
LLO	listeriolysin O
LLOMe	L-leucyl-L-leucine O-methyl ester
LPS	lipopolysaccharide
LT	lysotracker
ManNAc	N-acetylmannosamine
M-cell	Microfold cell
MDCK	Madin-Darby canine kidney
MH	Mueller-Hinton II
MHC	major histocompatibility complex
MIP	maximum intensity projection
MOI	multiplicity of infection
MVP	major vault protein
Neu5Ac	<i>N</i> -acetylneuramic acid

---

NTS	non-typhoidal <i>Salmonella</i>
OPA	optical parametric amplifier
PAMPs	pathogen-associated molecular patterns
PAS	periodic acid-Schiff
PCA	principal component analysis
PCN	phosphate, carbon, nitrogen
PCV	pathogen-containing vacuole
PE	phosphatidylethanolamine
PEC	polarized epithelial cells
PFA	paraformaldehyde
PMA	phorbol-12-myristate-13-acetate
PS	phosphatidylserine
RANKL	receptor activator of NF- $\kappa$ B Ligand
RNF213	ring finger protein 213
ROCK	Rho-associated coiled-coil containing kinases
RT	room temperature
<i>S. enterica</i>	<i>Salmonella enterica</i>
<i>S. enterica</i> serovar Paratyphi A	SPA
<i>S. enterica</i> serovar Tphi	STY
<i>S. enterica</i> serovar Typhimurium	STM
SCV	<i>Salmonella</i> containing vacuole
SDCM	spinning disc confocal microscopy
SEM	scanning electron microscopy
SIF	<i>Salmonella</i> -induced filaments
SIT	<i>Salmonella</i> -induced tubules
SLO	streptolysin O
SM	sphingomyelin
SMS	sphingomyelin synthase
SPI	<i>Salmonella</i> pathogenicity island
T1SS	type 1 secretion system
T3SS	type 3 secretion system

## LIST OF ABBREVIATIONS

---

TCS	two component system
TCV	typhoid conjugate vaccine
TEER	transepithelial electrical resistance
TEM	transmission electron microscopy
TNF- $\alpha$	tumor necrosis factor alpha
TPM	transcripts per kilobase million
TS	typhoidal <i>Salmonella</i>
TT	typhoid toxin
WGA	wheat germ agglutinin
WHO	World Health Organization
WT	wild-type
<i>Y.p.</i>	<i>Yersinia pseudotuberculosis</i>
YCV	<i>Yersinia</i> -containing vacuole
ZEN	ZEISS Efficient Navigation

## IX. List of Publications

(\* authors contributed equally)

### Single molecule analyses of *Salmonella enterica* translocated effector proteins reveal dynamics and targeting to host endosomal membranes

Vera Göser, Marc Schulte\*, [Felix Scharte\\*](#), Rico Franzkoch\*, Viktoria Liss, Olympia E. Psathaki, Michael Hensel

*under review at Nat Commun* <https://doi.org/10.1101/2022.05.16.492065>

### Ca<sup>2+</sup>-activated sphingomyelin scrambling and turnover mediate ESCRT-independent lysosomal repair

Patrick Niekamp, [Felix Scharte](#), Tolulope Sokoya, Laura Vittadello, Yeongho Kim, Yongqiang Deng, Elisabeth Südhoff, Angelika Hilderink, Mirco Imlau, Christopher J. Clarke, Michael Hensel, Christopher G. Burd, Joost C. M. Holthuis

*Nat Commun* 13, 1875 (2022). <https://doi.org/10.1038/s41467-022-29481-4>

### Intracellular *Salmonella Paratyphi A* is motile and differs in the expression of flagella-chemotaxis, SPI-1 and carbon utilization pathways in comparison to intracellular *S. Typhimurium*

(highlighted as cover image in PLoS Pathogens; DGHM Paper of the Month)

Helit Cohen\*, Claire Hoede\*, [Felix Scharte\\*](#), Charles Coluzzi, Emiliano Cohen, Inna Shomer, Ludovic Mallet, Sébastien Holbert, Remy Felix Serre, Thomas Schiex, Isabelle Virlogeux-Payant, Guntram A. Grassl, Michael Hensel, Hélène Chiapello, Ohad Gal-Mor

*PLoS Pathog*, 2022, 18(4): e1010425. <https://doi.org/10.1371/journal.ppat.1010425>

### Single cell analyses reveal distinct adaptation of typhoidal and non-typhoidal *Salmonella enterica* serovars to intracellular lifestyle

Tatjana Reuter\*, [Felix Scharte\\*](#), Rico Franzkoch, Viktoria Liss, Michael Hensel

*PLoS Pathog*, 2021, 17(6): e1009319. <https://doi.org/10.1371/journal.ppat.1009319>

### Manipulation of Host Cell Organelles by Intracellular Pathogens

Malte Kellermann, [Felix Scharte](#), Michael Hensel

*Int. J. Mol. Sci.* 2021, 22(12), 6484; <https://doi.org/10.3390/ijms22126484>

### Pathoadaptation of the passerine-associated *Salmonella enterica* serovar Typhimurium lineage to the avian host

Emiliano Cohen, Shalevet Azriel, Oren Auster, Adiv Gal, Carmel Zitronblat, Svetlana Mikhlin, [Felix Scharte](#), Michael Hensel, Galia Rahav, Ohad Gal-Mor

*PLoS Pathog*, 2021, 17(3): e1009451. <https://doi.org/10.1371/journal.ppat.1009451>

## X. *Curriculum Vitae*

### Personal Data

Name: Felix Scharte  
Date of Birth: May 2<sup>nd</sup> 1993 in Gütersloh, Germany

### Professional Experience

02/2022 - to date **Scientific Coordinator** of the graduate school 'IRTG' of the CRC 944  
'Physiology and Dynamics of Cellular Microcompartments' in the department of Biology/Chemistry at the University of Osnabrück

06/2018 - 09/2021 **Scientific Employee** in the microbiology division in the department of Biology/Chemistry at the University of Osnabrück

02/2014 - 02/2017 **IT-Support** in the divisions of animal physiology and microbiology in the department of Biology/Chemistry at the University of Osnabrück

### Education

06/2018 - to date **PhD Student** in Microbiology in the department of Biology/Chemistry at the University of Osnabrück  
Doctoral Thesis: 'Single cell biology of typhoidal *Salmonella*: heterogeneity of intracellular *Salmonella* and the unique cytosolic lifestyle of *S. Paratyphi A*' Supervisor: Prof. Dr. rer. nat. Michael Hensel

10/2015 - 05/2018 **Master of Science** in Life Sciences (Molecular and Cell Biology) in the department of Biology/Chemistry at the University of Osnabrück  
Master's Thesis: 'Functional Analysis of Virulence Factors of Typhoidal *Salmonella enterica* Serovars' in Microbiology  
Supervisor: Prof. Dr. rer. nat. Michael Hensel

10/2012 - 10/2015 **Bachelor of Science** in Life Sciences in the department of Biology/Chemistry at the University of Osnabrück  
Bachelor's Thesis: 'Gewebespezifische Expression von Rab-GTPasen in *Drosophila melanogaster* im Hinblick auf eine potenzielle Kolokalisation mit Vps8' in Zoology/Developmental Biology,  
Supervisor: Prof. Dr. rer. nat. Achim Paululat

08/2003 - 06/2012 **'Abitur'**, Städtisches Gymnasium Harsewinkel

## Voluntary Commitment

- 01/2019 - 08/2021 Elected student representative of the graduate school 'IRTG' of the CRC 944 'Physiology and Dynamics of Cellular Microcompartments' in the department of Biology/Chemistry at the University of Osnabrück
- 11/2012 - 06/2018 Elected student representative of the student body of the faculty of Biology/Chemistry at the University of Osnabrück.

## Awards & Scholarships

- 11/2021 - 02/2022 Graduation Scholarship of the Hans Mühlenhoff-Stiftung
- 09/2021 ibidi Photo Contest  
Publication of a stunning microscopy image in the ibidi calendar 2022
- 07/2021 Poster Award for an Exceptional Presentation titled:  
'From Vacuole to Cytosol - Cytosolic motility of intracellular *Salmonella* Paratyphi A in host cells' at the FASEB Science Research Conference 'The Microbial Pathogenesis Conference: Mechanisms of Infectious Disease'
- 12/2018 Award from the department of Biology/Chemistry at the University of Osnabrück for outstanding commitment and constructive collaboration as member of the student body of the faculty of Biology/Chemistry and student representative in university committees and appointment commissions

## Attendances at Conferences

- 07/2022 EMBO|EMBL Symposium: 'Innate immunity in host-pathogen interactions' (Heidelberg)  
*Poster:* Error-prone trigger invasion releases *Salmonella* Paratyphi A into host cell cytosol and cytosolic motility favors evasion of xenophagy (with flash talk)
- 11/2021 CRC 944 IRTG Retreat (Borkum)  
*Poster:* From Vacuole to Cytosol - Cytosolic motility of *Salmonella enterica* Paratyphi A and its role in autophagy (with flash talk)
- 09/2021 CRC 944 International Symposium: 'Cellular Microcompartments and their Physiology in Organelle and Cell Function' (Osnabrück)  
*Poster:* From Vacuole to Cytosol - Cytosolic motility of *Salmonella enterica* Paratyphi A and its role in autophagy

- 07/2021 Federation of American Societies for Experimental Biology (FASEB) Science Research Conference ‘The Microbial Pathogenesis Conference: Mechanisms of Infectious Disease’ (Virtual)  
*Poster:* From Vacuole to Cytosol – Cytosolic motility of *Salmonella* Paratyphi A in host cells (Poster Award)
- 10/2019 CRC 944 IRTG Retreat (Langwedel)  
*Talk:* Organoids, a suitable *ex vivo* model to study *Salmonella* pathogenesis? Imaging *Salmonella* infection in 3D & 2D Enteroids  
*Poster:* Uncovering Features of the Typhoidal *Salmonella* Serovar Paratyphi A
- 07/2019 Summer School ‘Biomembranes & Cellular Microcompartments’ (Osnabrück)  
*Poster:* The Intracellular Lifestyle of the Typhoidal *Salmonella enterica* Serovar Paratyphi A
- 02/2019 71th Annual Conference of the German Association for Hygiene and Microbiology (DGHM) (Göttingen)  
*Talk:* The Many-Faced Pathogen: Intracellular Phenotypes of *Salmonella* Paratyphi A
- 10/2018 *Salmonella* Meeting (Dorfweil-Schmitten)  
*Talk:* The Many-Faced Pathogen: Intracellular Phenotypes of *Salmonella* Paratyphi A  
*Poster:* The Intracellular Lifestyle of the Typhoidal *Salmonella enterica* Serovar Paratyphi A
- 09/2018 CRC 944 IRTG Retreat (Osnabrück)  
*Poster:* The Intracellular Lifestyle of the Typhoidal *Salmonella enterica* Serovar Paratyphi A
- 09/2018 EMBO|EMBL Symposium: ‘Organoids: Modelling Organ Development and Disease in 3D Culture’ (Heidelberg)
- 07/2018 Summer School ‘Biomembranes & Cellular Microcompartments’ (Osnabrück)  
*Poster:* Intracellular phenotypes of *Salmonella enterica* Serovar Typhi and Paratyphi A (with flash talk)
- 11/2017 *Salmonella* Meeting (Freiburg im Breisgau)  
*Talk:* The Intracellular Lifestyle of *Salmonella enterica* Serovar Typhi and Paratyphi A



## XI. Danksagung

An dieser Stelle möchte ich mich bei allen bedanken, die mich auf meinem Weg bis hierhin unterstützt haben.

Zunächst möchte ich mich bei Professor Dr. Michael Hensel dafür bedanken, dass ich nach meiner Masterarbeit während meiner Promotion weiter an dem Paratyphi-Projekt und auch an vielen weiteren spannenden Projekten mitarbeiten durfte. Vielen Dank für Ihre Unterstützung und Betreuung, sowie die Möglichkeit für diverse Konferenzbesuche und das Korrekturlesen dieser Arbeit.

Professor Dr. Guntram Graßl möchte ich für die tolle Zusammenarbeit im Organoid-Projekt und im SHT-Konsortium, sowie für die Erstellung des Zweitgutachtens danken.

Vielen Dank an Professor Dr. Joost Holthuis und Dr. Rainer Kurre für die Bereitschaft Teil meiner Prüfungskommission zu sein. Besonders möchte ich mich bei Rainer dafür bedanken, dass ich ihn mit Fragen zur Mikroskopie und Auswertung löchern konnte und auch bei Reparaturen am Leica und dem SD über die Schulter schauen durfte.

Bei der gesamten Arbeitsgruppe Mikrobiologie bedanke ich mich für die schöne Zeit mit euch. Angefangen mit dem HiWi Job (den ich nie so richtig losgeworden bin) über die Masterarbeit, bis zum Ende meiner Promotion. Danke an Nathy, Lena, Pascal, Viktoria, Laura, Rico, Leo, Tatjana und Malte. Wir haben zusammen das Beste aus der Corona-Zeit gemacht und uns gegenseitig bei unseren Problemen zur Seite gestanden und gute, sowie schlechte Zeiten überwunden. Vielen Dank, dass ihr mich in diversen Diskussionen ausgehalten und auf mich gewartet habt, wenn meine innere Uhr mal wieder falsch ging. Nathy, wir haben die meiste Zeit zusammen in der Abteilung verbracht und nun auch dieses Kapitel abgeschlossen, vielen Dank für die gemeinsame Zeit. Auch bei den Mibis, die nicht mehr vor Ort sind, darunter ganz besonders Tatjana, Vera, Jenne, Marc, Carina und Alex, möchte ich mich an dieser Stelle noch einmal bedanken. Ihr habt hier definitiv eine Lücke zurückgelassen. Die lustigen Momente mit lauten Lachern, die Comic- und Filmdrehs und die gemeinsame Zeit, die ich mit euch bei unseren Treffen und *Salmonella* Meetings verbringen durfte, werden mir noch lange im Gedächtnis bleiben. Tatjana, vielen Dank für die gemeinsame Zeit und Unterstützung im S3\*\*-Labor. Einige Lieder werden untrennbar mit unseren Gesangseinlagen verbunden bleiben. Alex, vielen Dank, dass du mich damals so gut eingearbeitet hast und dass wir auch heute noch unsere Gedanken in langen Sprachnachrichten oder Texten austauschen können. Monika, Monika, Ulla und Jörg darf ich an dieser Stelle natürlich nicht vergessen. Ihr haltet den Laden zusammen, wisst wo alles zu finden ist und steht allen mit unendlicher Geduld und Hilfsbereitschaft zur Seite.

Danke auch an die KollegInnen in der Biophysik, Zoologie, Neurobiologie und der Fachschaft, dass ich immer wieder mal auf einen Tee, Kakao ein Bier oder auch zum Grillen vorbeikommen durfte.

Zu guter Letzt möchte ich mich bei meinen Freunden und meiner Familie bedanken. Ohne eure Unterstützung und Entbehrungen hätte ich es nicht bis hierhin geschafft. Danke Mama und Papa, dass ihr mir stets den Rücken freigehalten und mir die Möglichkeit gegeben habt, das zu tun was mir am meisten Spaß macht. Damit geht der größte Dank an euch.

Juliane, dich habe ich natürlich nicht vergessen. Fast von Beginn an warst du in Osnabrück an meiner Seite und ich hoffe, dass du wir auch weiterhin unser Leben gemeinsam verbringen. Ich danke dir von Herzen, dass du immer für mich da bist und mich auch daran erinnerst mal eine Pause einzulegen. Ich freue mich nach diesem großen Stück Arbeit auf die gemeinsame Zeit und darauf weitere Abenteuer mit dir zu erleben.

– Danke! –

## **XII. Erklärung über die Eigenständigkeit der erbrachten wissenschaftlichen Leistungen**

Ich erkläre hiermit, dass ich die vorliegende Arbeit ohne unzulässige Hilfe Dritter und ohne Benutzung anderer als der angegebenen Hilfsmittel angefertigt habe. Die aus anderen Quellen direkt oder indirekt übernommenen Daten und Konzepte sind unter Angabe der Quelle gekennzeichnet.

Bei der Auswahl und Auswertung haben die unter V.6. ‚Contributions of co-authors‘ aufgeführten Personen in der jeweils beschriebenen Weise unentgeltlich mitgewirkt.

Weitere Personen waren an der inhaltlichen und materiellen Erstellung der vorliegenden Arbeit nicht beteiligt. Insbesondere habe ich hierfür nicht die entgeltliche Hilfe von Vermittlungs- bzw. Beratungsassistenten (Promotionsberater oder andere Personen) in Anspruch genommen. Niemand hat von mir unmittelbar oder mittelbar geldwerte Leistungen für Arbeiten erhalten, die im Zusammenhang mit dem Inhalt der vorgelegten Dissertation stehen.

Die Arbeit wurde bisher weder im In- noch im Ausland in gleicher oder ähnlicher Form einer anderen Prüfungsbehörde vorgelegt.

(Ort, Datum)

(Unterschrift)

### **XIII. Supplementary Information on DVD**

- PDF file of PhD thesis “Single cell biology of typhoidal *Salmonella*: heterogeneity of intracellular *Salmonella* and the unique cytosolic lifestyle of *S. Paratyphi A*”
- PDF file and supporting information of publication “Single cell analyses reveal distinct adaptation of typhoidal and non-typhoidal *Salmonella enterica* serovars to intracellular lifestyle” in folder “Reuter et al. 2021”
- PDF file and supplementary information of publication “Ca<sup>2+</sup>-activated sphingomyelin scrambling and turnover mediate ESCRT-independent lysosomal repair” in folder “Niekamp et al. 2022”
- PDF file and supporting information of publication “Intracellular *Salmonella Paratyphi A* is motile and differs in the expression of flagella-chemotaxis, SPI-1 and carbon utilization pathways in comparison to intracellular *S. Typhimurium*” in folder “Cohen et al. 2022
- Supplementary information of manuscript “From vacuole to cytosol – Disruptive invasion triggers cytosolic release of *Salmonella Paratyphi A* and subsequent cytosolic motility favors evasion of xenophagy” in folder “Scharte et al. 2022”